THE UNIVERSITY OF CHICAGO

THE ROLE OF THE *TBX5* PARALOGUES DURING PECTORAL FIN DEVELOPMENT IN ZEBRAFISH

A DISSERTATION SUBMITTED TO
THE FACULTY OF THE DIVISION OF THE BIOLOGICAL SCIENCES
AND THE PRITZKER SCHOOL OF MEDICINE
IN CANDIDACY FOR THE DEGREE OF
DOCTOR OF PHILOSOPHY

COMMITTEE ON DEVELOPMENT, REGENERATION AND STEM CELL BIOLOGY

BY
ERIN ALANA THORPE BOYLE ANDERSON

CHICAGO, ILLINOIS
MARCH 2019

Table of Contents

List of Figures

List of Tables

ACKNOWLEDGMENTS

I want to thank everyone who has been involved in this process of getting a Ph.D. First, thank you to my advisor, Robert Ho, for all your guidance and help on this project. I also want to thank you for all the freedom provided in my scientific endeavors. One amazing benefit of being in the Ho lab is that you also get all the guidance of Vicky Prince and the Prince lab, and I want to thank Vicky for all the support and input she has provided over the years. Thank you also to the members of my committee, Cliff Ragsdale, Sally Horne-Badovinac and Jill de Jong for all the help and guidance you have provided in challenging me to have the best project and dissertation possible.

I want to thank all the members of the Prince and Ho labs for the countless hours spent together and all the advice and suggestions they have given me throughout my time in graduate school. Thank you Noor, Kamil, and Manny for all the science chats and for letting me in to borrow your keys whenever I lock myself in the hallway. Thank you to everyone for keeping me company late at night in lab, especially Alana, Chris and Stephanie (you nocturnal people). Thank you to Qiyan, for the time lapse data which was the starting point for much of this dissertation. Thank you to Adam for keeping the fish alive and the microscopes working. Thank you to Haley for teaching me beads and timelapses, and for general life advice given while during those experiments in that ridiculously hot microscope room. Especially thank you to Ana and Lindsey, for being my 2013 DRSB friends. I'm so glad we all ended up in Culver. Thank you for all the time spent going through grad school together, whether writing NSF grants or quals together or planning experiments. Lindsey, thank you for being my science twin, and going through every class and lab together. It will be truly weird when we leave and no longer see each other almost every single day.

I also want to thank my Molecular Biosciences cohort; Chris K., Phil, Katherine, Alyssa, Sahar, Lindsey M, Chris C., Katie, Kevin and Beth; and Anna Chen, for all the support and advice while we were figuring out grad school together. I'd also like to thank the older

DRSB students for all your advice and help and excellent journal club presentations to give us something to aspire to. Thank you to the Coates lab for all our lunchroom conversations and puzzle time.

I also want to thank everyone who encouraged me to study biology and go get a Ph.D. Thank you to Mr. Rauch, my high school biology teacher, for starting my interest in biology. As an undergraduate, there were also several people who were very important in encouraging me to pursue research and graduate school. I want to especially thank Dr. Michelle Whaley and Dr. Dawn Hopkins for all the time and effort they put into helping me pursue my undergraduate research goals and apply for graduate school.

Finally, I want to thank my family. I want to thank my sisters, my parents, and my cousins, for listening to all of my grad school stories and science talk and generally being supportive. Thank you to my excellent husband, Dan. You are very awesome and have made my time in graduate school so much better. Thank you for all of your support and help, and especially for providing the perspective of someone who is not in graduate school. Thank you for providing a connection to the outside world and making sure that sometimes I go do social things or go on vacation. I appreciate all the time you have spent listening to me talk about fish that I have not paid back by listening to you talk about accounting, although perhaps I have paid it back in listening to you talk about baseball. And finally, thank you to Rocket for making sure I get outside and stop worrying about science at least two times a day, because sometimes there are more important things to worry about, like squirrels.

ABSTRACT

The transcription factor *Tbx5* is necessary for development of the forelimb and closely linked with the evolution of this limb. Loss of just one copy of *TBX5* in humans is associated with Holt-Oram Syndrome (HOS), which manifests as defects in both the forelimb and the heart. In zebrafish, *tbx5* was duplicated during the teleost specific whole-genome duplication, and zebrafish therefore have two copies of *tbx5*: *tbx5a* and *tbx5b*. In the pectoral fins of wildtype embryos, the cells of the fin field migrate away from the somites along the mediolateral (ML) axis and converge along the anterio-posterior (AP) axis. Tbx5a regulates the AP convergence of these cells during fin field migration by controlling expression of *fgf24* in a subset of the fin field cues. Therefore, loss of Tbx5a results in embryos lacking pectoral fins. Tbx5b-deficient embryos form small pectoral fins, through unknown mechanisms. In this dissertation, I aim to characterize the role of *tbx5b* during zebrafish development, particularly during pectoral fin development, and compare to the known functions of *tbx5a*. These comparisons will provide insight into the fate of duplicated genes in the zebrafish.

All previous work on the role of *tbx5b* has been performed in Tbx5b-deficient embryos generated via morpholino. In order to confirm that the morpholino accurately recapitulates the mutant phenotype, I first created and characterized a mutant for *tbx5b*. The *tbx5b -/-* embryos phenocopy the previously described Tbx5b-deficient embryos in both the heart and the pectoral fin defects. Further analysis of *tbx5b -/-* pectoral fins reveals that in addition to the small size when compared to same-stage wildtype fins, *tbx5b -/-* pectoral fins lack some anterior structures of the fin, which is similar to the limb defects seen in HOS patients.

In order to identify the different transcriptional networks of embryos deficient in the *tbx5* paralogues, whole-embryo RNA sequencing was performed in wildtype embryos and embryos lacking the *tbx5* paralogues during the stages of pectoral fin development. Loss of the *tbx5* paralogues, in particular *tbx5b*, resulted in changes to gene expression in the intermediate mesoderm, the somites, and the yolk syncytial layer, which may be sources of signaling cues

during the migration processes of the cells of the fin field, due to their proximity to the migrating cells. Furthermore, loss of the *tbx5* paralogues produced morphological changes in both the vasculature and the somites.

To understand how loss of *tbx5b* could result in a small fin, I performed cell tracking analysis in the fin field of Tbx5b-deficient embryos and compared this data to previously collected data on the dynamics of the cells of the fin field in both wildtype and Tbx5a-deficient embryos. Normal fin field migration involves both an AP convergence movement and a ML migration. In Tbx5a-deficient embryos, the signaling molecule Fgf24 is no longer present, resulting in a lack of AP convergence, although ML migration is unaffected. In Tbx5b-deficient embryos, there are mild defects in AP convergence, likely due to a decrease in the levels of *fgf24* expression. The anterior cells are most strongly affected by loss of Tbx5b, which may explain the anterior defects seen in Tbx5b-deficient fins. Additionally, in Tbx5b-deficient embryos, there is no net ML migration of the fin field. Furthermore, the double-deficient embryos display defects in both AP convergence and ML migration.

Overall, this dissertation expands the knowledge on the role of the *tbx5* paralogues in zebrafish during migration of the cells of the fin field. Loss of the *tbx5* paralogues results in changes in surrounding tissues, illustrating the complex interactions and signaling that occur between tissues. Likewise, tissues such as the intermediate mesoderm and yolk syncytial layer have the ability to impact the development of the fin. Additionally, both *tbx5* paralogues regulate the migration of the cells of the fin field, with *tbx5a* primarily responsible for regulating AP convergence and *tbx5b* primarily responsible for regulating the ML migration movements. The genetic association of these movements along orthogonal axes suggests that subfunctionalization of these movements has occured. Furthermore, this data suggests that in tetrapods, the ancestral *Tbx5* regulates both migration movements, such that loss of *Tbx5* would result in cells that fail to migrate, therefore explaining the lack of forelimb in Tbx5-deficient tetrapods.

CHAPTER 1

INTRODUCTION

Paired limbs are one of the characteristics of the vertebrate body plan. The gene *Tbx5* plays an essential role in the evolution and development of the forelimb (i.e. the anterior set of paired limbs). In zebrafish, *tbx5* has duplicated into two paralogues: *tbx5a* and *tbx5b*. In this dissertation, I characterize the roles that these two genes play during development of zebrafish, particularly during pectoral fin development. In this chapter, I briefly describe the evolution of limbs in vertebrates as well as some of the molecular underpinnings of this evolution. Next, the developmental mechanisms involved in the formation and patterning of the limbs will be discussed. This chapter concludes with a review of the role of *Tbx5* during development of the limbs and a discussion of both the duplication of *tbx5* in zebrafish and the implications of this duplication on pectoral fin development.

1.1 The evolution of paired limbs in vertebrates

Most vertebrates possess two sets of paired limbs, the forelimbs and the hindlimbs. In fish, these structures are homologous to the pectoral and pelvic fins, respectively (Figure 1.1) [1]. Amphioxus, a chordate that is sister to vertebrates, lacks paired fins. Paired fins are also lacking in lamprey and hagfish, the two extant agnathans (jawless vertebrates). However, all extant gnathostomes either possess two sets of paired fins or have lost them secondarily. In both chondrichthyans and actinoptergyians, these limbs are present as pectoral and pelvic fins. In tetrapods, including mammals and birds, the two representatives of tetrapods that I will focus on in this dissertation, these limbs are present as a forelimb and hindlimb, or a wing and leg, respectively. Additionally, it appears that pectoral fins evolved prior to pelvic fins, as fossils show that the extinct group of osteostracans contain only pectoral fins, not pelvic fins and there are no known fossils that contain only pelvic fins [2].

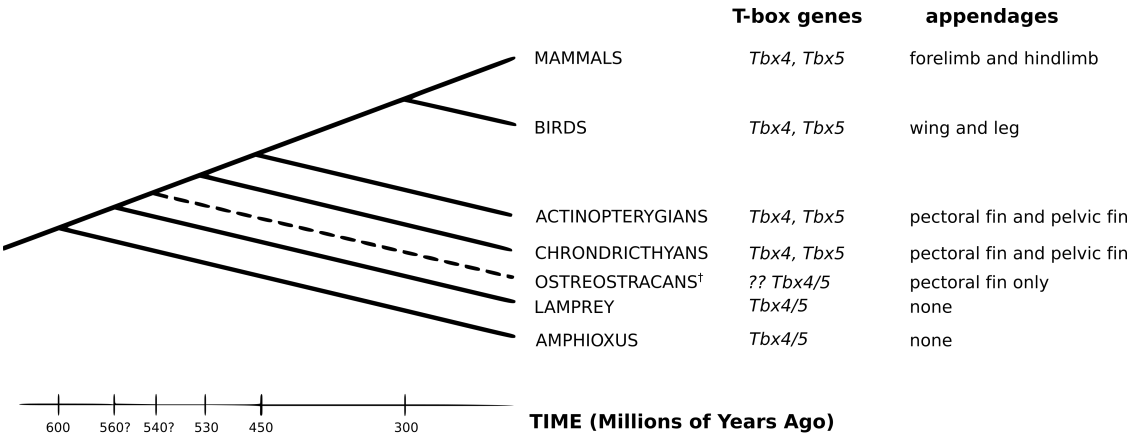

Figure 1.1: Phylogenetic analysis of paired limb evolution. Figure is modified from [3]. The tree shows the relationship between chordates. The dotted line represents extinct groups. The column describing T-box genes describes the condition of the *Tbx4/5* genes in these animals. Appendages lists the paired limbs are present in the given animal.

The two T-box genes *Tbx4* and *Tbx5* are closely associated with the evolution of the paired limbs in vertebrates. *Tbx4* and *Tbx5* formed from a duplication of an ancestral *Tbx4/5* gene [4]. While jawed vertebrates possess both *Tbx4* and *Tbx5*, jawless vertebrates possess only the ancestral *Tbx4/5* gene [3]. Lampreys, which possess the ancestral *Tbx4/5*, do not have paired fins [3] (Figure 1.1). Because of this relationship, it is hypothesized that the evolution of the paired limbs is tightly associated with co-opting the *Tbx4/5* genes to produce these novel structures [5].

In amphioxus, the ancestral *Tbx4/5* gene is expressed in the mesoderm that gives rise to the heart [6, 7]. Likewise, in lampreys, *Tbx4/5* is expressed in the lateral plate mesoderm in regions that contribute to the heart [8]. In addition to expression in the heart, *Tbx4* and *Tbx5* are expressed specifically in the hindlimbs and forelimbs, respectively [5, 9]. Furthermore, *Tbx5* is essential for development of the forelimb, as deletion of this gene results in failure to form a forelimb [10, 11, 12]. In zebrafish, *tbx5* has been duplicated into two paralogues, *tbx5a* and *tbx5b*. These paralogues will be described more thoroughly in Section 1.3.4. Later chapters will attempt to understand the separate roles of these two paralogues and how they have functionally evolved post-duplication.

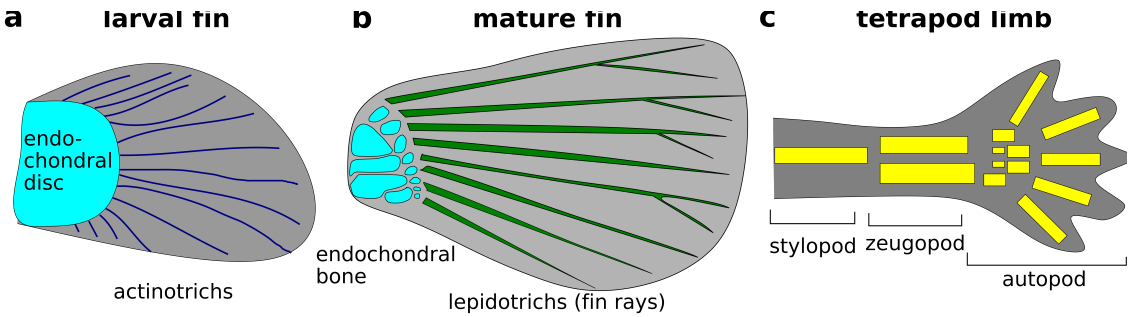

Figure 1.2: Structures of a tetrapod limb compared to that of a larval and adult pectoral fin. (a) Larval fins consist of endochondral discs (light blue) and more distal structures called actinotrichs (dark blue). (b) Adult fins have endochondral bone (light blue) and structures called lepidotrichs (green) supporting the larger fin. (c) Tetrapod limbs can be divided into three parts: the stylopod, zeugopod and autopod. Structures not to scale.

How has the fin evolved into the tetrapod limb? In order to answer this question, I will first describe the components of both fins and tetrapod limbs. Because this dissertation focuses on development of the fins in zebrafish, I will specifically describe the structures of zebrafish fins. Furthermore, because of the delay in pelvic fin development (pelvic fin buds appears at approximately 3 weeks post fertilization), most work on the development of paired fins in zebrafish and in this dissertation focuses on the pectoral fins. Zebrafish pectoral fins have two functional phases of development: the larval phase and the adult phase. Larval fins consist of an endochrondral disc and an apical fin fold, which contains supporting extracellular matrix structures called actinotrichs (Figure 1.2a) [13]. Larval fins last until approximately 3 weeks post fertilization, at which point these fins begin to transform into adult fins (Figure 1.2b) [13]. In this process, the endochrondral disc begins to separate into smaller structures and the fin as a whole rotates so that it has a horizontal rather than a vertical orientation [13]. In the distal fin, cells migrate between the actinotrichs and the basement membrane and begin to ossify, forming lepidotrichs (fin rays). As the fin rays form, the actinotrichs begin to disappear [13].

Tetrapod limbs can be divided into three regions along the proximal-distal axis: the stylopod (humerus), the zeugopod (radius and ulna) and the autopod (hand) (Figure 1.2c).

The stylopod and zeugopod are homologous to the bones derived from the endochondral discs [14, 15]. The relationship between the fin rays and the autopod is less clear, as the fin rays are formed through different processes than the digits or bones of the autopod. However, recent work has suggested that there may be more similarities at the molecular level between the fin rays and the tetrapod autopod than previously thought [16, 17, 18].

1.2 Limb and fin development

This dissertation focuses on the embryonic development of the pectoral fin. This section will review the developmental processes involved in formation of the limb and fin, of which most of the early processes are conserved between the fin and the limb. First, I briefly discuss the specification of the cells that will become the limb. I then review the processes by which those cells form a limb bud and discuss signaling centers involved in the growth and patterning of the limb bud. I conclude with a discussion of the late stages of development in the pectoral fin, which differs from the development of the tetrapod forelimb.

1.2.1 Limb field cells in the lateral plate mesoderm are specified early in development

In order to discuss the formation of the **limb field**, which consists of the cells that will contribute to the limb bud, it is first necessary to describe the tissue from which the majority of these cells derive. Most of the mesenchymal core of the limb bud is derived from the **lateral plate mesoderm** (LPM). The LPM is a thin layer of tissue that lies just laterally to the somites and over the yolk syncytial layer (Figure 1.3a-b). In zebrafish, the LPM is present as a single layer of cells at the location that the pectoral fin forms, although the LPM anterior to the pectoral fin consists of two separate single-cell layers (Figure 1.3a-b). Early in development, by 14 hpf in zebrafish, the LPM can be identified by expression of

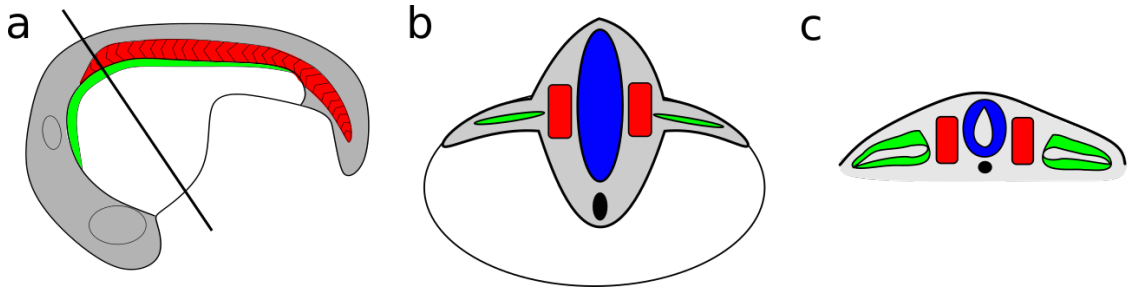

Figure 1.3: The lateral plate mesoderm in zebrafish and tetrapods(a) Lateral view of a schematic of a zebrafish embryo during somitogenesis. Black line indicates where the cross section is (b) Cross section of an embryo during somitogenesis. (c) Cross section of a generic vertebrate during embryogenesis. Red marks the somites, green marks the lateral plate mesoderm, blue marks the neural tube, black marks the notochord, white marks the yolk, gray marks all other embryonic tissues.

hand2, which is present throughout the LPM. In mammals and chick, the LPM is present in two multi-cell layers of tissue, generally separated by a cavity. The more dorsal layer is the somatic (parietal) mesoderm and the ventral layer is the splanchic (visceral) mesoderm (Figure 1.3c).

Tbx5 is the earliest marker of the the limb field. Many signaling pathways and transcription factors are involved in the initiation and maintenance of *Tbx5*. In the following paragraphs, I will describe three factors known to play a significant role in establishing *Tbx5* expression at the level of the forelimb: the *Hox* transcription factors, retinoic acid (RA) signaling, and Wnt/β-catenin signaling. Inputs from all three of these factors act to establish appropriate expression of *Tbx5* [19].

In mice, 6 *Hox* genes are expressed at the level of *Tbx5* expression in the limb field: *Hoxa4*, *Hoxa5*, *Hoxb4*, *Hoxb5*, *Hoxc4*, and *Hoxc5* [20]. All 6 of these *Hox* genes can activate expression of a Tbx5 reporter when co-electroporated in chick [20]. These proteins directly bind to *Hox* binding sites in a conserved intron 2 enhancer of *Tbx5* to activate expression. Furthermore, *Hox* genes expressed at other locations in the embryo, such as *Hoxc9*, have the ability to repress activation of *Tbx5* in the LPM, suggesting that the *Hox* genes limit expression of *Tbx5* to the limb field through a combination of activation and repression [21].

RA signaling during gastrulation is required for initiation of *Tbx5* expression and loss of RA results in loss of limbs in fish, mouse and chick embryos [22, 23]. However, these phenotypes can be rescued in zebrafish by overexpression of dominant-negative *fgfr1*; this along with other evidence suggests that the limits of *Tbx5* expression are controlled by opposing gradients of RA and FGF [24]. There is some debate over whether RA signaling directly activates expression of *Tbx5* in the limb field as found in chick [19] or indirectly by repression of *Fgf8* as found in mice and zebrafish [24]. Despite these disrepencies between model systems, it is clear that RA is involved in establishing *Tbx5* expression. Furthermore, RA signaling acts in conjunction with *Tbx5* in a feedforward loop in establishing limb development; RA promotes expression both of *Tbx5* as well as promoting *Fgf* expression in the developing limb directly [19].

RA signaling from the somites regulates expression of *Tbx5* at least partially by regulating expression of *Wnt2b* in the intermediate mesoderm [25]. Normally, *WNT2B* is expressed at the level of the forelimb in chick [26]. *WNT2B* expression can induce an ectopic limb bud in chick, in part by inducing expression of *FGF10* in the mesoderm and *FGF8* in the ectoderm [26]. Expressing a dominant-negative TBX5 in the forelimb field results in downregulation of *WNT2B*, *FGF10*, and *FGF8* in the limb bud, suggesting that *Tbx5* is important in regulating this interaction [27]. Interestingly, when an ectopic limb bud is induced by ectopic *WNT2B* expression, this also induces *TBX5* expression, suggesting a feedback loop between *TBX5* and *WNT2B* [28]. Furthermore, β-catenin signaling can directly activate *Tbx5* expression in chick [19]. However, in zebrafish, knockdown of Wnt2ba results in loss of *tbx5a* expression, while knockdown of Tbx5a does not result in loss of *wnt2b* expression, suggesting that in zebrafish, *wnt2b* may be upstream of *tbx5a* and not subject to a feedback loop [29]. In mice, *Wnt2b* does not appear to be expressed in the limb prior to digit formation [30].

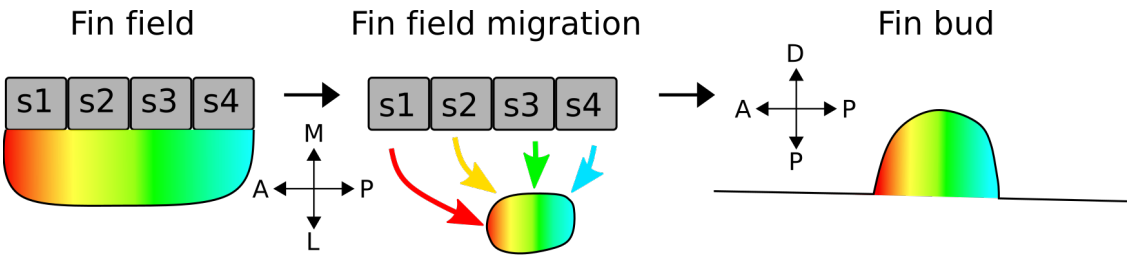

Figure 1.4: Cells in the fin field migrate to form a fin bud. Cells are originally located in the fin field. These cells undergo a stereotypic migration process to form the fin bud. Anterior cells migrate farther than more posterior cells. Cells maintain their same relative positions. Gray blocks are somites, rainbow tissue is the fin field/fin bud. Axes: A-anterior,P-posterior, M-medial, L-lateral, P-proximal, D-distal.

1.2.2 The cells of the fin field migrate to form a fin bud

The process by which the cells of the limb field form a limb bud has been most comprehensively studied in the pectoral fin of zebrafish. Therefore, I will first describe the processes of fin field migration in zebrafish, then compare with the current information available on this process in tetrapods. In zebrafish, the pectoral fin field consists of the cells of the LPM located adjacent to somites 1-4 [31]. At 18 hpf, these cells migrate and begin to converge [31]. Cells maintain the same relative positions during this migration process, so that anterior cells remain anterior at the end of migration and posterior cells remain posterior at the end of the migration process [31]. This process is summarized in Figure 1.4, where the fin field is color coded based on the somite that the LPM cells are located adjacent to, such that cells adjacent to somite 1 are red, cells adjacent to somite 2 are yellow, cells adjacent to somite 3 are green and cells adjacent to somite 4 are blue. This migration consists of two simultaneous processes: a convergence movement along the AP axis and a ML migration away from the somites [31]. The more anterior cells adjacent to somites 1 and 2 migrate farther than the posterior cells adjacent to somites 3 and 4 in the same amount of time, and therefore migrate with an increased speed and persistence (Figure 1.4) [31]. By 30 hpf, a visible three-dimensional fin bud can be detected (Figure 1.4).

In zebrafish, *fgf24* is necessary for the AP convergence [31, 32]. Either directly or indirectly, Tbx5a activates *fgf24*, a zebrafish specific member of the Fgf8/17/18 subfamily, in the mesenchyme (Figure 1.5a) [32]. Loss of either Tbx5a or Fgf24 results in a failure of the AP convergence movements responsible for formation of a fin bud [32, 31]. Rather than converging to form a fin bud, both Tbx5a-deficient and Fgf24-deficient cells migrate laterally across the embryo past the site of the future limb bud to produce embryos with no fins (Figure 1.5b,c) [31]. Chapter 5 of this dissertation will discuss the regulation of the ML migration movements.

In tetrapods, the *TBX5+* cells in the limb field will contribute to the limb. However, the precise dynamics of how these cells contribute to the limb, whether through migration or through epithelial to mesenchymal transition, as proposed by Gros et al. [33] is unknown, as there have been no studies tracking the initial cellular dynamics of these cells prior to limb bud formation. Once the limb bud has formed, however, there is evidence from Wyndengaarden et al. that cells from the surrounding LPM migrate to contribute to the limb bud [34]. Specifically, imaging in mice at embryonic day 9 (E9.0) when the limb field has started to thicken between somites 8 and 12 shows that the cells are moving caudally and contributing to the limb bud [34]. By E9.25, cells from the LPM can be seen to enter the limb bud both moving laterally from the LPM immediately adjacent to the limb bud and moving caudally (anteriorly) from LPM located posterior to the limb bud [34]. Although this data does not demonstrate how the limb bud initially forms, it does show that cells migrate into the limb bud from the surrounding LPM once a limb bud has formed. This suggests that cells also migrate to form the initial limb bud in mice, although there have been no studies directly analyzing the dynamics of the limb field prior to limb bud formation in mice. Furthermore, this paper shows that, in chick, labelled LPM also migrates caudally and laterally into the wing bud, which additionally suggests that migration of the LPM to form a limb bud may be a general feature of tetrapods [34]. However, mapping of the cell migration of the limb

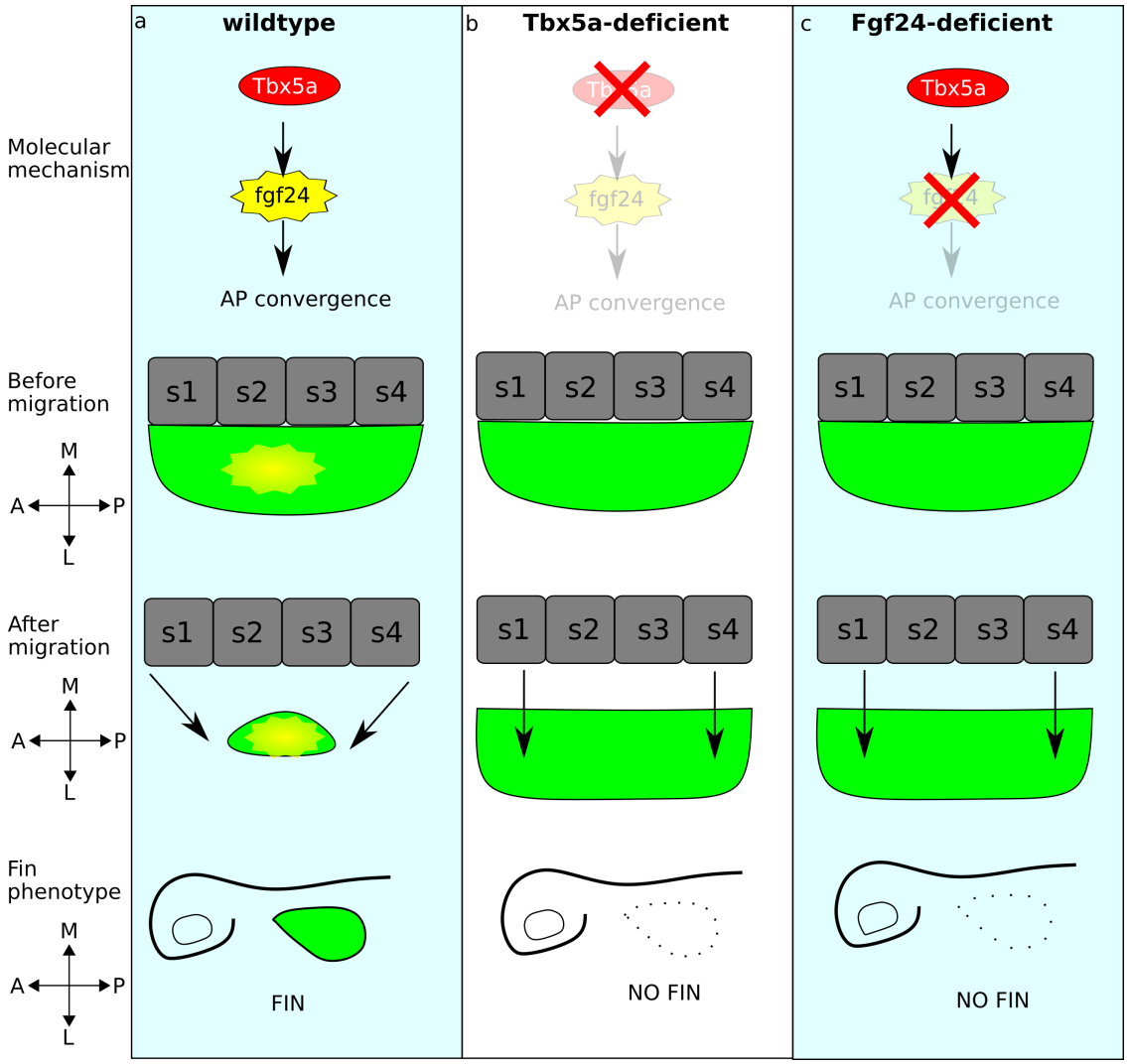

Figure 1.5: *tbx5a* and *fgf24* are necessary for regulating the migration of the fin field cells into the fin bud. (a) In wildtype embryos, Tbx5a activates Fgf24 in a subset of the cells of the fin field. The cells migrate laterally and converge along the AP axis and a fin is formed. (b) In embryos lacking Tbx5a, Fgf24 is not expressed and the cells migrate laterally but do not converge along the AP axis and no fin is formed. (c) In embryos lacking Fgf24, the cells migrate laterally but do not converge along the AP axis and no fin is formed. Gray blocks are somites, labelled s1-s4, green is the cells of the fin field. Yellow is the Fgf24 signal. Axes: A-anterior, P-posterior, M-medial, L-lateral.

field is needed in tetrapods to determine if migration occurs prior to formation of the limb bud in a similar mechanism as in zebrafish.

1.2.3 Signaling centers pattern the limb bud along multiple axes

A morphologically distinct limb bud is visible by 30 hpf in zebrafish, by E9 in mice, and by 52-56 hpf in chick. By the time a morphologically distinct limb bud is detectable, signaling centers are present which are responsible for determining the different axes within the bud. The main signaling centers are the Apical Ectodermal Ridge (AER), which secretes FGFs and is involved in proximal distal patterning and outgrowth, and the Zone of Polarizing Activity (ZPA), which secretes Sonic hedgehog (SHH) is involved in AP patterning. These two centers also interact through a complex series of signaling feedback loops (Figure 1.6). Most experiments on the patterning of these signaling centers has been performed in chick and mice embryos, but these signaling centers are also present in the fin bud of zebrafish.

As the limb bud is forming, the FGF10 signal within the cells of the limb mesenchyme induces formation of the AER [35]. The AER is an ectodermal ridge along the distal end of the limb bud that runs along the anterior-posterior axis. It is both morphologically and molecularly distinct in early limbs. Signaling from the AER via secreted FGF8 protein is important not only in regulating outgrowth but also in controlling the proximal-distal patterning of the limb bud [35, 36]. The cells closest to the AER are maintained in an undifferentiated state due to FGF signaling. As the limb grows, the cells exit the undifferentiated zone and differentiate [37]. Based on a proximal signal from the flank, most probably RA, and the distal signal from the AER, the cells assume a fate based on their location along the proximal-distal axis [37]. *fgf24* is upstream of *fgf10* in the FGF signaling cascade in the fin field of zebrafish [32].

The ZPA regulates AP polarity in the limb via Sonic Hedgehog (SHH) signaling in the posterior domain, which promotes posterior fates [38]. *Shh* expression is restricted to the

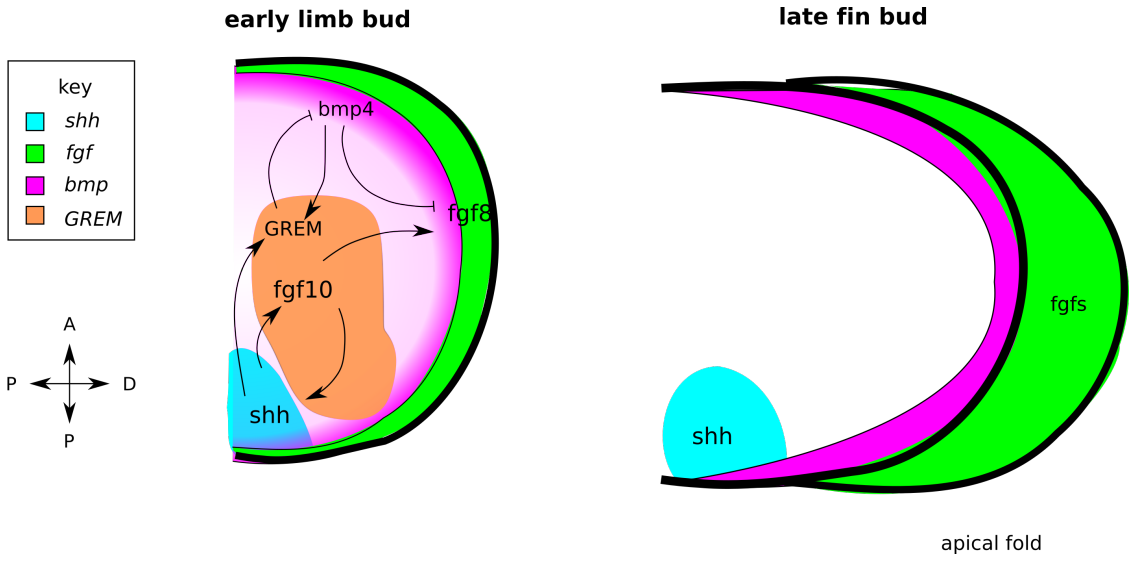

Figure 1.6: Signaling centers in the developing limb bud. *fgf8* (green) expression in the AER is activated by *fgf10* expression in the mesenchyme, which also interacts with *shh* expression in a positive feedback loop. *shh* (blue) is expressed in the ZPA in the posterior of the limb bud. This signaling promotes *GREM* (orange) adjacent to the *shh* expression, which represses signaling of *bmp4* (pink), restricting expression towards the periphery. *bmp4* likewise restricts expression of *fgf8* to the AER by repressing expression of *fgf8*.

posterior domain of the limb bud through interactions between *HOX* transcription factors, *Hand2*, and *Gli1* [39, 40]. Furthermore, SHH in the ZPA and mesenchymal FGF10 signal to each other in a reinforcing feedback loop, maintaining expression throughout limb development [41, 42]. This is one of the many examples of interactions that occur between different signaling centers in limb development.

*Bmp*s, particularly *Bmp4*, play roles in AER formation and during the beginning of limb bud outgrowth in mice [43]. *Bmp4* is expressed both in the mesoderm and in the ventral ectoderm [44]. At later stages, by 10.5 dpf in mice, *Bmp4* is found in the mesoderm directly adjacent to the AER as well as in the AER. [44]. However, expression of *GREM* upregulated by SHH then restricts the expression of the *Bmp*s towards the outer limits of the limb bud, which allows for a feedback loop to form between the *Fgf*, *Shh* and *Bmp*s [45]. Conditional loss of *Bmp4* in the limb mesenchyme results in severely delayed formation of the AER, as well as expanded expression of *Fgf8* in the AER [44]. The BMP4 signal is received by

BMPR1A in the ectoderm, and loss of BMPR1A from the ectoderm interferes with formation of the AER, resulting in loss of *Fgf* expression and other molecular markers in the AER [46]. *Bmp* mutants also show defects in DV patterning of the limb, suggesting that *Bmps* may play a role in patterning this axis [46].

Once the limb bud has been formed, proximal-distal patterning and outgrowth is promoted by both oriented cell motility and directed growth. In the limb bud, the cells are oriented with the long axis of the cell aligned with the proximal-distal axis of the limb bud and with their Golgi bodies oriented distally, indicating migration towards the distal end of the limb (i.e. towards the AER). Furthermore, live imaging has shown that these mesenchymal cells migrate anteriorly [47]. The polarity of this migration appears to be mediated by *Wnt5*, not by FGF signaling. Loss of *Wnt5* in mouse forelimbs results in a loss of polarization of these cells along the proximal-distal axis and a decreased velocity of migration towards the AER. Introducing a source of WNT5 rescues the loss of polarization seen in these *Wnt5* -/- embryos, while introducing a source of FGFs was not able to rescue the cell orientation [47]. This shows that once a limb bud has already formed, FGFs do not directly influence directed migration or oriented cell division but can change the velocity of a cell, allowing for an overall net movement towards the source of FGF [48].

The dorsal-ventral (DV) axis of the limb is patterned by the ectoderm [49, 50]. *Wnt7a* expression in the dorsal ectoderm produces a gradient that promotes dorsal fates while *Engrailed* expression in the ventral ectoderm represses *Wnt7a* and promotes ventral fates [51, 52]. The signaling involved in this patterning interacts with and is affected by the other signaling centers present in the limb at this time. WNT7A plays a minor role in AP patterning by regulation of SHH signaling and BMP signaling affects expression of *Engrailed* [51, 53].

1.2.4 In fish, the AER transforms into the Apical Fin Fold

In the pectoral fin buds of zebrafish, the AER converts into the apical fin fold (AF) around 32-36 hpf [54]. The AF is a folded epithelial tissue at the most distal part of the developing fin [55]. The AF is not initially filled with the mesenchymal cells present in the rest of the fin, although the actinotrichia, and later lepidotrichia, will form in the AF to provide structure and support [55]. Although the AER continues to promote outgrowth of the mesenchymal cells in the limb bud, which will then become endoskeletal components, the AF extends beyond the AER and is important for patterning and growth of the more distal part of the fin that will contain the fin rays [54]. *bmp4* expression is present in the AF by 36-40 hpf [56]. This expression of *bmp4* is presumably carried over from the initial expression of *bmp4* in the AER.

The actinotrichia are extracellular structures derived both from the ectoderm and the mesoderm: early actinotrichia development is due to synthesis from ectodermal cells while growth of the actinotrichia is due to protein synthesis from mesenchymal (presumably mesodermal) cells that migrate into the fin fold [57]. These actinotrichias are composed of collagens and the proteins *actinodin 1* and *actinodin 2*. Loss of both of these proteins, but not either individually, results in a loss of actinotrichia in pectoral and median fin folds [58]. Furthermore, pectoral fin bud patterning and growth signals are affected by loss of the actinotrichia proteins compared to control siblings, with a decrease in both *fgf8a* expression and downstream *fgf* signaling factors in the AER and a corresponding delay in overall growth of the pectoral fin bud [58]. There are also defects in AP patterning, with expansion of posterior genes *ssha* and *hoxd13a* into more anterior domains [58]. This suggests a role of these proteins prior to the formation of visible actinotrichia.

1.2.5 Other tissues contribute to the pectoral fin

Although the LPM contributes significantly to the development of the pectoral fin, other tissues also contribute to the functioning fin. Endothelial cells form the vasculature of the fin. At least some of the pectoral fin muscles are derived from somitic mesoderm cells that migrate from somites 4-7 between 24 and 33 hpf [59]. Furthermore, ablation of these somitic-derived AER cells results in a decrease in fin fold length, as well as a specific decrease in the size of actinotrichia, suggesting that these somitic cells play an important role in the development of these fin-specific structures, beyond just formation of the pectoral fin muscles [59]. There is also evidence that cells of the neural crest may migrate into the fins and surround the developing lepidotrichia (fin rays) [60]. However, some studies indicate that the neural crest contributes to the lepidotrichia of the caudal and dorsal fins, but not of the pectoral fin [61].

1.3 The roles of *Tbx5* during development

In this section, I describe the role that *Tbx5* plays during development. Because this dissertation is primarily focused on limb development, I emphasize the role that *Tbx5* plays in forelimb and pectoral fin development. I also specifically discuss the roles of the two paralogues of *tbx5* in zebrafish development.

1.3.1 TBX5 is a transcription factor that directly binds DNA and interacts with other proteins

The TBX5 protein is a transcription factor containing a T-box domain, which directly binds DNA and is highly conserved between Tbx5 and the other T-box proteins. The T-box domain in TBX5 is a 7 stranded beta barrel [62]. This site binds to the consensus site (A/G)GGTGT (C/G/T)(A/G) with no preference between the different variations [63]. There are also two

known and highly conserved nuclear localization sequences (NLS) domains in TBX5, one within the T-box and one located after the T-box. TBX5 is capable of binding DNA both as a monomer and as a homodimer [62, 64].

TBX5 also directly binds with many other transcription factors to synergistically regulate transcription and morphogenesis during development, such as NKX2.3, GATA4, GATA6, MYOCARDIN, and TBX20 in the heart, and SALL4 in both the heart and limb [65, 66, 67, 68, 69, 70]. As most of the work of the molecular function of TBX5 has focused on its role in heart development, direct binding partners of TBX5 specific to limb development are unknown.

PDLIM7, a scaffolding protein, is also expressed in the heart and limb fields as well as the eye, overlapping with expression of *TBX5*, and appears to regulate the subcellular localization of TBX5 [71]. Addition of PDLIM7 results in localization of TBX5 (and TBX4) to the actin filaments as well as in the nucleus—in the absence of PDLIM7, TBX5 is localized primarily in the nucleus [71]. This localization may serve to sequester TBX5, thereby regulating levels of transcription [71]. During normal development, the proportion of TBX5 that is localized to the nucleus varied across cells both in the heart and the limb [72]. Interestingly, TBX5 appears to shuttle between the nucleus and the cytoplasm in the presence of PDLIM7, rather than remaining primarily in one localization, suggesting that this is an active method of regulating TBX5 localization [72]. Camarata et al. suggest that TBX5 plays a function in the cytoplasm as well as in the nucleus; however there is no further information on what this role could be.

1.3.2 TBX5 mutations are associated with Holt-Oram syndrome in humans

In humans, Holt-Oram syndrome (HOS) is associated with mutations in a single copy of *TBX5* [73], which has a rate of 0.7 in 100,000 live births [74]. It manifests as a series of combined arm and heart defects. The heart defects include septation defects and cardiac

conduction syndrome [73]. The limb defects tend to be more severe on the anterior part of the limb and have a range of severity, from minor defects in the thumb, to truncation of the entire limb [73]. In human embryos, *TBX5* is expressed in both the heart and developing forelimbs, as well as other tissues including the retina, lungs, and trachea [75].

HOS can be caused by mutations in several regions of the *TBX5* gene, with some cases having more severe heart defects and others have relatively mild heart defects but more severe limb defects. Some studies have suggested that the location of these different mutations can correlate with the phenotype. Basson et al. have suggested that the different locations of missense mutations which differentially affect either heart or limb development more severely can be used to identify different sites on the TBX5 protein that are important in regulating either heart or limb development, respectively [76]. Specifically, they find that in the patients they examined, mutations near the beginning of the T-box are correlated with strong heart and mild limb phenotypes while mutations near the end of the T-box show the reverse correlation [76]. However, other studies have not found this correlation, leaving these issues up to debate [77].

1.3.3 Tbx5 is involved in limb identity, initiation, and patterning in tetrapods

Tbx5 was first identified as a T-box gene expressed specifically in the limbs of mouse embryos in 1996, along with *Tbx4* [4, 9]. These initial studies led to the hypothesis that *Tbx4* and *Tbx5* were identity genes. In other words, expression of *Tbx5* would cause a limb to become a forelimb while expression of *Tbx4* would cause a limb to become a hindlimb. Supporting this idea, ectopic expression of *TBX5* in the hindlimb in chick is sufficient to convert the identity of the hindlimb to grow feathers (i.e appear more wing-like) [12, 78].

Later studies in chick found that ectopic TBX5 could induce formation of a limb bud in a region of the LPM outside of the limb field, suggesting that *TBX5* is involved in more

than identity, but may also be involved in induction of the limb bud. This was further confirmed in zebrafish, where loss of *tbx5a* results in fish that fail to form a pectoral fin [10]. Consistent with this data, deletion of *Tbx5* from the limb forming region of the LPM in mice also results in failure to form a limb [11]. This data suggests that not only is *Tbx5* involved in determining the identity of a limb, but it may also play a role in initiation of limb development.

Conditional deletions of *Tbx5* in mice has shown that *Tbx5* also plays a role in later patterning of the forelimb. Deletion of *Tbx5* after a limb bud has formed results in mild patterning defects in the skeleton, which are primarily on the anterior end of the limb [79]. Furthermore, deletion of *Tbx5* in the limbs also causes significant mispatterning of the muscles and tendons of the forelimbs [80]. Deletion of *Tbx5* from exclusively the myoblasts in the limb does not result in mispatterning of these muscles, suggesting that *Tbx5* expression in the surrounding cells is sufficient for patterning of the myoblasts [80]. Chapter 4 of this dissertation reveals additional examples in which the *tbx5* paralogues affects the patterning of adjacent tissues.

1.3.4 Zebrafish have two tbx5 paralogues

This dissertation primarily deals with the role that *tbx5* plays in zebrafish development. There has been a whole genome duplication in the lineage leading to the teleost fish [81, 82]. Due to this duplication, zebrafish have two copies of *tbx5*: *tbx5a* and *tbx5b* [83]. There are high levels of conservation in the T-box domain between the paralogues and tetrapod Tbx5 proteins but low levels of conservation throughout the rest of the protein [84]. *tbx5a* is expressed in both the heart field and the limb field of the LPM, as well as the retina [85]. *tbx5b* is expressed in both the retina and the heart field [83]. Expression in the heart is similar for both paralogues until 36 hpf, when *tbx5b* expression is restricted to the ventricle, whereas *tbx5a* expression remains in both chambers of the heart [83]. Additionally, while

tbx5a is detectable through *in situ* hybridization as early as 14 hpf in the LPM, *tbx5b* is not detectable until 17 hpf [83]. Some studies report that there does not appear to be detectable expression of *tbx5b* distinct from background in the pectoral fin bud [83], while others have reported low levels of *tbx5b* expression in the pectoral fins at 36 hpf [84]. Despite this, Tbx5b-deficient embryos display clear phenotypes in fin bud formation and fin development, indicating it is very likely to function in the developing fin field. In Chapter 5, I will describe how *tbx5b* affects the migration of the fin field cells during fin bud formation.

tbx5a -/- mutants undergoes normal heart jogging—the first break in right-left asymmetry—at 24 hpf [86]. However, the heart fails to loop in these mutants [86]. By 3 days post fertilization (dpf), the linear heart has become elongated and a pericardial edema forms, which gives rise to the name of the mutant, *heartstrings*. By 5 dpf, most embryos die due to lack of circulation [86]. Fish heterozygous for *heartstrings* show no heart defects, unlike patients with Holt-Oram syndrome. This may be either due to the presence of two *tbx5* paralogues in zebrafish or the fact that *heartstrings* may be a hypomorph rather than a null allele, as the mutation is located after the T-box domain. Therefore the Heartstrings mutant protein should still be capable of binding DNA, suggesting that there is some uncharacterized essential function or domain in Tbx5a located past the T-box.

Tbx5b-deficient embryos display defects in heart development as early as 24 hpf. Heart jogging often fails to occur correctly, resulting in a heart at the midline rather than on the left—although occasionally heart jogging does occur, in what appears to be a random manner, with hearts jogging either to the left or to the right [87]. Heart looping also fails to occur in Tbx5b-deficient embryos [87].

The *tbx5* paralogues do not regulate gene expression within the heart in the same manner. Specifically, expression of both *hand2* and *versican a* showed expanded expression in the heart of both Tbx5a-deficient and Tbx5b-deficient embryos compared to wildtype embryos, while expression of both *bmp4* and *natriuretic peptide A* showed changes in expression in

only Tbx5a-deficient embryos compared to wildtype [84]. This suggests that although the two paralogues may have overlapping roles, they also have the ability to affect different transcriptional pathways within the heart.

Neither the *heartstrings -/-* mutants nor Tbx5a-deficient embryos develop a fin bud or pectoral fins [10, 86]. Tbx5b-deficient embryos show a milder defect in the pectoral fin than do Tbx5a-deficient embryos. A pectoral fin forms, although formation of this fin bud is delayed, with 70% of embryos lacking a visible fin bud at 30 hpf [84]. By 3 dpf, all Tbx5b-deficient embryos have fins, although 85% of these fins are small [84]. In addition to their reduced size, these fins are often misshapen and some are upturned [84]. Furthermore, Tbx5b-deficient embryos display changes in some genes involved in patterning the pectoral fin bud [84, 87], in contrast to Tbx5a-deficient embryos which exhibit a complete loss of gene expression associated with the pectoral fin bud [10]. Tbx5b-deficient embryos show proportional expression of *hand2* (consistent with the smaller fin size) compared to wildtype. However Tbx5b-deficient fins display almost complete absence of *vcana*, a marker for the AF [84]. Expression of *bmp4*, an early marker of the AER, is expanded beyond the AER into the mesenchyme of the fins of Tbx5b-deficient embryos at 36 hpf [84]. Because expression of the early fin mesenchyme gene *hand2* is still present, but there are defects in expression of genes patterning the AF, Parrie et al. suggest that Tbx5b-deficient pectoral fins have a defect in the differentiation of the AF, which could be responsible for the small and misshapen fins [84]. However, Parrie et al. do not assay for gene expression in other signaling centers of the fin bud, such as the ZPA and AER. In Chapter 3, I will provide a more detailed analysis on the role of Tbx5b on the early signaling centers of the pectoral fin bud.

One reason for the lack of pectoral fin development in Tbx5a-deficient embryos is loss of *fgf24*, which is responsible for the AP convergence movements of the cells of the fin field, as discussed in Section 1.2.2 [31, 32]. Tbx5b-deficient embryos express *fgf24* in the LPM at 28 hours, although by 36 hpf, the pattern is altered compared to uninjected controls

[87]. Specifically, at 36 hpf, expression of *fgf24* has switched from the mesenchyme to the ectoderm in wildtype embryos but not in Tbx5b-deficient embryos [87]. However, expression of *fgf24* was not analyzed during the stages of fin field migration, when it acts as a migration cue.

Development of the pectoral fins appears to be delayed as the 48 hpf pectoral fins of Tbx5b-deficient embryos appear similar in size and shape to 36 hpf control embryo's fins [87]. Pi-Roig et al. hypothesize that *tbx5a* initiates fin outgrowth while *tbx5b* is required later in pectoral fin development to maintain this growth [87]. However, the small fin bud phenotype of Tbx5b-deficient embryos suggests that *tbx5b* does not exclusively function late in fin development, as otherwise it should not produce fin buds that are delayed and small. Chapter 5 will provide further insight into the role of Tbx5b during fin bud formation and a detailed analysis of the dynamics of Tbx5b-deficient cells during fin bud formation.

1.3.5 Implications of the duplication of the tbx5 genes in zebrafish

Because *tbx5* has duplicated in zebrafish, I will briefly review common implications of gene duplication. Post gene duplication, both copies of the duplicated gene are less constrained as initially there are two functional copies [88]. Often, one copy may accumulate mutations, lose function, and become a pseudogene through a process known as **nonfunctionalization** [88]. Alternatively, **neofunctionalization** may occur, where one copy maintains the original function but the other paralogue acquires novel functions through mutations [88]. Another possible result of gene duplication is **subfunctionalization**. In this process, each paralogue accumulates mutations, resulting in divergence in the function of each individual copy; however, each paralogue maintains a specific subset of the original functions and therefore the organism maintains the complete function of the ancestral gene [88].

Subfunctionalization commonly occurs by changes in the spatial or temporal expression of a gene, often by mutation of regulatory regions, so that each duplicated gene is expressed only

in a subset of the expression patterns of the original gene. Examples of subfunctionalization have been shown to occur multiple times in the zebrafish, perhaps most notably in the case of the *hoxB5* paralogues in zebrafish. HoxB5a and HoxB5b are proteins with similar functions and are expressed in overlapping but non-identical patterns both temporally and spatially. However, the sum of the two expressions of *hoxB5a* and *hoxB5b* in zebrafish is equivalent to the expression of the non-duplicated *Hoxb5* in chick, mouse, and frog embryos, indicating that these genes have subfunctionalized in zebrafish [89].

Although morpholino injections of either *tbx5* paralogue produce both heart and fin defects, injected mRNA can only rescue the cognate phenotype, but not that of its paralogue [84], supporting the hypothesis that there are functional differences between the two proteins. Further supporting this hypothesis, loss of either of the two paralogues results in different patterns of gene expression in both the heart and fin, suggesting that *tbx5a* and *tbx5b* may act within different transcriptional networks. The data in this dissertation further supports the hypothesis that Tbx5a and Tbx5b have functional differences during the development of zebrafish.

In this dissertation, I examine the roles of the two *tbx5* paralogues in zebrafish. Although many studies have been performed on the role of *tbx5a* in zebrafish, far fewer studies have examined the role of *tbx5b* or of the combined paralogues. My work will characterize the role of *tbx5b* in zebrafish and compare and contrast it to what is known about *tbx5a*.

In chapter 3, I describe the creation and characterization of a mutant for *tbx5b*. The *tbx5b -/-* embryos phenocopy the previously described Tbx5b-deficient phenotype in both the heart and the limb defects, validating the use of the morpholino in the following experiments. *tbx5b -/-* mutants also display gene expression indicating that the ZPA and AER have formed properly, although the AF may be delayed. Analysis of skeletal components of the fin reveals that anterior elements of the fin are more affected in *tbx5b -/-* mutants than the posterior elements of the fin. Finally, I find that *tbx5b -/-* mutants and Tbx5b-deficient embryos also

exhibit previously unreported defects in the head and jaw.

In chapter 4, I describe a whole embryo RNA sequencing experiment performed to better understand the broader transcriptional networks of the *tbx5* paralogues. This work reveals that loss of the *tbx5* paralogues results in changes to tissues outside of the LPM. Specifically, loss of Tbx5b results in changes in vasculature gene expression and patterning. Additionally, there are several other tissues that show changes in gene expression when either or both Tbx5 paralogue is lost, most notably the somites.

In chapter 5, I specifically examine the effect of loss of Tbx5b on the cellular dynamics of the LPM during fin field migration and compare it to previously characterized data on the loss of Tbx5a during these stages. Tbx5b-deficient embryos have reduced AP convergence movements, which may be due to decreased levels of *fgf24* expression. The most anterior cells are most affected by loss of Tbx5b and are less likely to contribute to the fin bud in Tbx5b-deficient embryos. Additionally, Tbx5b-deficient embryos fail to migrate along the ML axis, suggesting that the migration dynamics of the cells of the fin field are jointly controlled by both *tbx5* paralogues such that *tbx5a* is primarily responsible for mediating the AP convergence of the fin field and *tbx5b* is primarily responsible for migration along the ML axis. This may imply that *tbx5* has subfunctionalized, at least in its role controlling fin bud formation in zebrafish. Correspondingly, in the double-deficient embryos, there is a loss of migration along both the AP and the ML axes.

CHAPTER 2

METHODS AND MATERIALS

Zebrafish embryos and morpholino injections

Zebrafish were maintained under standard laboratory conditions [90]. Morpholino injections were performed as described by Nasevicius and Ekker [91]. 3.7 ng of Tbx5a morpholino (5- CCTGTACGATGTCTACCGTGAGGC-3) [84] and 5 ng of Tbx5b translation blocking morpholino (5-GGATTCGCCATATTCCCGTCTGAGT-3) [10] was injected per embryo. These amouns were chosen by injecting embryos with a range of doses as the lowest amounts which result in complete pentrance of the respective phenotypes. Morpholinos were diluted from the 25 µM stock concentration in 0.2 M KCl with 10% of either fast green or rhodamine red used for visual confirmation of injections.

The following transgenic strains of zebrafish were used in this thesis: *Tg(fli1a:GFP)*, *Et(hand2:eGFP)ch2* [31], *Tg(h2afx:h2afv-mCherry)mw3*, and *Tg(tbx5a::GFP)* [92]. The following mutant strains of zebrafish were used in this thesis: *heartstrings* mutants [86] and $tbx5b^{ch2}$.

Imaging and analysis

Embryos imaged using the confocal were imaged at either 20x or 40x magnification using a Zeiss Laser Scanning Microscope 710. Whole mount *in situ* imaging and live embryo bright-field imaging was performed on a Zeiss Axioplan microscope. Specific mounting conditions will be described below.

Somite measurements

Live embryos were mounted laterally in 3% methylcellulose and imaged at 5x on a Zeiss Axioplan microscrope. Somites were measured and counted manually in FIJI [93]. Statistical significance was calculated using ANOVA and TukeyHSD tests in R.

XCentrin::Cherry localization

100 ng of *Xcentrin::Cherry* RNA and 20 ng of *H2B::CFP* RNA were injected into single-cell embryos [94]. Embryos were mounted at 18 hpf and 22 hpf in 0.8% agarose in a glass-bottomed dish and imaged with the 40x objective. Images were imported to FIJI for analysis. The angle between the nucleus and the XCentrin::RFP fluorescence was measured using FIJI for each spot located within the lateral plate mesoderm. The angles were plotted using the ggplot2 package in R [95].

Tbx5a::GFP quantification

Tg(tbx5a::GFP) embryos were injected with Tbx5b morpholino at the single-cell stage. Embryos were raised to 30 hpf under standard conditions, then mounted dorsally in 0.5% agarose. A Z-stack was taken using the 40x objective through through all stacks that contained fluorescence. If necessary, tiling was used to capture the complete extent of fluorescence near the limb bud. The images were imported into FIJI for analysis.

The images were transformed into a maximum intensity projection and the dorsal area of the limb bud was measured using a best fit ellipse. The images were transformed into binary images by setting a threshold with an upper limit of 255 and a lower limit of 20. The total size of GFP fluorescence was measured using Analyze Particles in FIJI. The area of cells outside of the limb bud was calculated by subtracting the area of the limb bud from the total area of GFP. Regions anterior, adjacent and posterior to the limb bud were measured by selecting regions anterior, adjacent, or posterior to the limb bud on the thresholded image

and analyzing particles. Statistics were calculated using a t-test in R.

Cell tracking and analysis

Embryos were imaged at intervals of 8 minutes on a 20x objective using a heated stage for a minimum of 6 hours. Images were imported into FIJI for analysis. Cell tracking was performed on the maximum intensity projections using the Manual Tracking plugin on FIJI. In addition to tracking cells in the LPM adjacent to somites 1 through 5, a separate file was tracked for drift correction for each embryo. This drift correction file contained tracks for 3-5 nuclei of midline cells.

Data was imported into R for analysis. Embryo registration and drift correction were performed using the custom R package CellTrackingEBA (available on github at erinboyle-anderson/CellTrackingEBA) and custom R scripts (available as a Supplemental File). This calculated measurements for displacement, compaction factor, scatter, tracklength, speed, persistence, and log mean square displacement. Plots were generated using the R package ggplot2 [95].

RNA sequencing and analysis

For the preliminary RNA sequencing experiment, embryos were injected with Tbx5a morpholino or Tbx5b morpholino. Both uninjected siblings and injected embryos were raised to 18 hpf and 21 hpf. 10 embryos were pooled per genotype and RNA was extracted using Trizol. RNA libraries were submitted to the sequencing core and single end 50 bp oligo dT libraries were generated. Illumina high throughput sequencing was performed with the samples from 18 hpf sequenced in one lane and the samples from 21 hpf sequenced in another lane.

For the complete experiment, embryos were injected with either Tbx5a morpholino, Tbx5b morpholino or both morpholinos at the single-cell stage. Uninjected siblings and

injected embryos were raised to 18 hpf or 21 hpf. Eyes were removed using forceps and 10 embryos were pooled per genotype. RNA was extracted using Trizol. Three biological replicates were performed for each genotype, on three seperate days. RNA libraries were submitted to the sequencing core and single-end 50 bp oligo dT cDNA libraries were generated. Illumina high throughput sequencing was performed, with all samples run on 2 lanes.

Differential gene expression was analyzed using 3 methods to identify significant differential gene expression. In all cases TopHat (v2.1.0) was used to align the RNA sequencing reads to the zebrafish genome (Zv9). Differential gene expression was identified Cufflinks (v2.2.1) and Cuffdiff (v3.1.2); EdgeR [96]; or Cufflinks then the HOLT method [97]. Default parameters were used for all conditions. Preliminary gene expression was analyzed using only the Cufflinks suite. The Cufflinks suite was performed using the Galaxy interface [98]. The RNA sequencing data has been deposited in NCBIs Gene Expression Omnibus [99] and are accessible through GEO Series accession number GSE115640 (https://www.ncbi.nlm.nih.gov/geo/query/acc.cgi?acc=GSE115640).

CRISPR mutant creation and gRNA screen

gRNAs for CRISPR were generated using CHOPCHOP [100]. Cas9 was generated from a plasmid from the Jao lab [101]. gRNAs and *Cas9* mRNAs were transcribed using the methods previously described [102].

To generate the *tbx5b -/-* mutant, the specific variable sequenced used was GAGCTGAGTTTGTAGTGGCG which targeted the first exon prior to the start of the TBOX domain. 100 ng of Cas9 mRNA and 150 ng of Tbx5b gRNA were injected into F0 embryos. 30% showed phenotypes consistent with the Tbx5b mutant phenotype and died at 6 dpf. Surviving siblings were grown to adulthood, then outcrossed to *AB fish to generate stable F1 lines. These F1 lines were genotyped by tail clipping, amplifying the first two exons of Tbx5b using the primers ztbx5bATGfwd [83] and 5 CCATGCATAAATACCAGCCG 3',

followed by TA cloning using pMD20 (Clontech) and Sanger sequencing.

For the gRNA screen, the variable sequences in Table 2.1 were used to generate gRNA using the protocols described above. 185 ng of *Cas9* mRNA, 100 ng of gRNA and 1.8 ng of Tbx5b MO were injected into the embryo. The embryos were screened daily from 1-3 dpf to identify changes in limb size and shape.

Table 2.1: gRNA sequences used to generate CRISPR mutants

gene	sequence
aimp1	GGGACTGGAACAGAAGGCCG
cpt1b	GGGTGACATCATGGAAGAAA
cyp1b1	GGACGCGGAGTTCCAGCAGG
hsp90aa1.2	GGTCTGTGAGACTTTCATAG
krt91	GGCAGTGTGCACGGAGGAGC
mybphb	GGCCGGCTCCTCCTTCTTCG
obsl1a	GGTTATCGTATTACCCAAGA
phlda2	GGGTCTTCCTCTTCCAGAAT
pvalb2	GGCCTTGAGAATTCCAGCAA
si:dkey-4p15.3	GGAATTGCAGAGGCATACCT
ctsc	GGCGTTTATAGCCGGGTTTT
ryr1b	GGACACCGTGGACATGACGG

in situ hybridizations

DIG-labelled antisense probes were generated from plasmids for *sox7* provided by Dr. Brant Weinstein [103] and *hhex* provided by Dr. Chong Shin [104] using the methods described below. The probes for *shha* and *notch1a* was generated from lab stocks. The remaining probes were transcribed directly from PCR products (refer to Table B.1 for primer sequences)

generated using cDNA produced using the iScript cDNA synthesis kit (Biorad). *In situ* hybridizations were performed as described by Ahn et al [10].

PCR template generation

38.75 µl	nfH_20
5 µl	buffer
2 µl	F primer
2 µl	R primer
1 µl	10 mM dNTPs
0.25 µl	Taq
1 µl	cDNA (18+21 hpf embryos)
30 µl	

The cycling conditions were as follows: 95° C for 30 seconds, followed by 40 cycles of 95° C for 30 seconds, annealing at 57° C for 60 seconds, then extension at 68° C for 60 seconds. This was followed by 5 minutes at 68° C after which the reaction was held at 12° C indefinitely. The reactions were then purified using PCR Purification columns (Quiagen).

Transcription reaction

-	template DNA
-	nfH_20
6 µl	5x transcription buffer (NEB)
3 µl	DTT
2 µl	DIG
2 µl	RNAsin
2 µl	T7 enzyme (NEB)
30 µl	

For the template DNA, either 100-200 ng of PCR product or 1 µg of linearized plasmid was added. The reaction was incubated at 37° C for 3 hours, 1 µl DNAse H was added. The reaction was incubated for 15 minutes at 37° C, then precipitated with LiCl. The pellet was resuspended in 100 µl nfH_2O and 1 µl RNAsin. Probes were tested via *in situ* to determine the best concentration to use to promote maximum signal with minimum background. Probes were generally diluted to concentrations between 1:20 and 1:100.

qPCR analysis

cDNA was produced using the iScript cDNA synthesis kit (Biorad) and then diluted to a concentration of 1/5 the original concentration. The primer mix was produced by combining 1 µl forward primer and 1 µl reverse primer (at 100 mM each) with 98 µl nfH_2O.

10 µl	SYBR green
5 µl	cDNA
5 µl	primer mix
20 µl	

qPCR analysis was performed using a DNA engine/Opticon 2 qPCR machine. The following cycling conditions were used: incubate 95° C for 15 minutes, followed by 40 cycles of 95° C for 15 seconds, 58° C for 20 seconds and 72° C for 20 seconds. A melting curve analysis was performed following amplification. C_t values were determined using the Opticon 2 software.

Histology

Alcian blue staining and Alizarin red staining were performed using a protocol provided by Jared Talbot [105]. Embryos were fixed for at least an hour in 2% PFA. Following a 10 minute rinse in 50% rthanol, embryos were incubated for 2 days in Double Stain (see below). Embryos were then washed in 80% ethanol/10 mM $MgCl_2$ for 30 minutes, then rinsed in 50% ethanol and 25% rthanol for 5 minutes per wash. They were bleached for 10 minutes in a mixture of 3% H_2O_2/0.1% KOH, then rinsed with 25% glycerol/0.1% KOH twice for at least 10 minutes each. Embryos were then combined with 25% glycerol/0.5% KOH overnight at 4° C, then imaged on a Zeiss axioplan compound scope. Pectoral fins were dissected using forceps.

Double Stain

32.6 ml	95% Ethanol
5.9 ml	H_2O
500 µm	1 M $MgCl_2$
1 ml	0.5% Alizarin red (in H_2O)
10 ml	0.2% Alcian blue (in 90% Ethanol)
50 ml	

CHAPTER 3

CREATION AND CHARACTERIZATION OF A *TBX5B* MUTANT ZEBRAFISH

3.1 PREFACE

Parts of this chapter are derived from a publication in *PLoS ONE* with the following citation:

Boyle Anderson, E. A. T. & Ho, R. K. A transcriptomics analysis of the *tbx5* paralogues in zebrafish. *PLoS ONE* 13, e0208766 (2018).

The *in situ* characterization of the signaling centers of the fin buds and the analysis of the cartilage components of the larval fin are unpublished experiments.

3.2 Abstract

Through the use of morpholinos, *tbx5b* has been found to be involved in development of both the heart and the pectoral fin. However, the phenotypes of Tbx5b-deficient embryos have not been validated in a *tbx5b* -/- mutant. In this chapter, I describe the creation and characterization of a *tbx5b* mutant generated using CRISPR-Cas9 mutagenesis. The $tbx5b^{ch2}$ mutation is a 4 base pair insertion in the 1st intron, which results in a protein truncation prior to the T-box domain. This mutant phenocopies the Tbx5b-deficient embryo, displaying defects in both the heart and pectoral fin. Markers for both the AER and the ZPA are present in *tbx5b* -/- mutant fin buds. In addition to generating a novel resource for studying this phenotype, this validates use of the morpholino in the following studies. Furthermore, newly identified phenotypes in both the *tbx5b* -/- mutant and the Tbx5b-deficient embryos in the head and jaw, which are formed from tissues derived neither from the retina nor the LPM, suggest that *tbx5b* may be having a broader impact on the embryo beyond the limits of its expression.

3.3 INTRODUCTION

In zebrafish, *tbx5b* is primarily expressed in both the retina and in the heart-forming region of the lateral plate mesoderm (LPM) during somitogenesis, with low levels of expression detected in the pectoral fins at later stages of development [83]. Expression remains in the heart from 17 hpf throughout development, although at 60 hpf, *tbx5b* expression becomes restricted primarily to the ventricle [83]. The presence of expression in the pectoral fin forming regions is less clear: Albalat et al. report no *tbx5b* expression in either the pectoral fin field or the pectoral fin, while Pi-Roig et al. report faint expression of *tbx5b* in the pectoral fin at 36 hpf [83, 87].

Tbx5b-deficient embryos fail to undergo heart looping. Furthermore, these embryos display defects in heart development as early as heart jogging—the first break in asymmetry in heart development [87]. Additionally, Tbx5b-deficient embryos were reported to exhibit delayed fin bud development, as 70% of embryos lacked fin buds at 30 hpf, although small fin buds were present in the majority of embryos by 36 hpf. By 72 dpf, 86% of embryos displayed small fins, while a smaller percentage (6.2%) displayed upturned fins [84].

Examining the Fgf signaling cascade in the fins of Tbx5b-deficient embryos implies that there is misregulation of signaling pathways during fin development. Both Parrie et al. and Pi-Roig et al. suggest that the primary cause of the fin phenotype of Tbx5b-deficient embryos is a delay in fin bud formation, citing both the delayed transition of *fgf24* from the mesenchyme to the epithelium and the delay in apical fold (AF) specification indicated by expression patterns of *bmp4* [84, 87]. However, neither Parrie et al. nor Pi-Roig et al. address the effect of loss of Tbx5b on the Apical Ectodermal Ridge (AER) or the Zone of Polarizing activity (ZPA). As previously discussed, these two signaling centers are involved in regulating proximal-distal and AP patterning, respectively (Figure 1.6).

Although both Parrie et al. and Pi-Roig et al. provide an initial overview of the role of *tbx5b* during heart and pectoral fin development, these studies were both performed in

Tbx5b-deficient embryos, rather than in *tbx5b* -/- mutants. While morpholinos are an important tool in studying the effects of specific genes, they have several key limitations. First, they have the possibility of producing off-target, non-specific phenotypes [106]. Second, they may not produce a complete knockdown [106]. Because of these concerns, the Tbx5b-phenotypes should be validated in a mutant to ensure they are indeed representative of loss of Tbx5b.

Despite the problems associated with morpholinos, there are also many advantages to utilizing morpholinos. With morpholinos, it is possible to generate a dose-curve that will allow study of differing levels of the gene of action, something especially useful in the study of dose-sensitive genes, such as the T-box genes. The use of morpholinos also allows for the assaying of single gene effects without paralogous gene compensation, which is a particular problem in zebrafish due to the teleost-specific whole-genome duplication [107]. Morpholinos are also extremely helpful for practical concerns, such as when studying effects of a gene before a visible phenotype is present—otherwise, to test if *tbx5b* affects early fin field migration, a process that occurs before it is morphologically possible to distinguish *tbx5b* -/- embryos from wildtype siblings, one would need to test four times as many embryos, as only 25% of them would be homozygous for the mutation.

For these reasons, the best method of studying the effects of *tbx5b* in pectoral fin development may be to initially use a combined approach, where the phenotype is tested both in *tbx5b* -/- mutants and in Tbx5b-deficient embryos to ensure that the phenotype is consistent in both cases. This is especially important in this case, as duplicates such as the *tbx5* paralogues are more likely to show compensation [84]. Once a morpholino and mutant have been found to produce similar phenotypes, the appropriate tool can be selected depending on experimental parameters.

In this chapter, I describe the creation and characterization of a *tbx5b* mutant produced using CRISPR Cas9 mutagenesis. Using both morphological and molecular methods, I report

that the *tbx5b -/-* mutant and the Tbx5b-deficient embryos display similar phenotypes in both heart and fin development. This suggests that the Tbx5b-deficient phenotype accurately recapitulates the effects of loss of Tbx5b and the phenotypes are not due to off-target effects. The fin buds of *tbx5b -/-* mutants possess both ZPAs and AERs. The larval fins of *tbx5b -/-* mutants display defects in the internal structural components, with a bias towards defects at the anterior end of the fin. Furthermore, defects in head development—a previously unreported phenotype—are present in both *tbx5b -/-* mutants and Tbx5b-deficient embryos.

3.4 RESULTS

3.4.1 tbx5b -/- mutants phenocopy the morpholino-induced phenotype of Tbx5b-deficient embryos

Tbx5b-deficient embryos display early defects in fin bud size, despite the lack of reported expression in the early fin field. This could be due to previously unreported expression of *tbx5b* in the fins of wildtype embryos. Nevertheless, consistent with earlier studies [83, 84, 87], I report that *tbx5b* is expressed in the retina (Figure 3.1a, star) and in the anterior region of the LPM (Figure 3.1a, arrowhead) of embryos during somitogenesis stages, with no detectable expression in the fin field at 24 hpf or at other stages tested prior to fin bud formation (data not shown). However, this does not eliminate the possibility that *tbx5b* could be expressed in the fin field prior to 36 hpf at levels undetectable by *in situ* hybridization. As probes for *tbx5b* often produce relatively faint staining of *tbx5b* or high levels of background staining, this may provide further evidence for the presence of *tbx5b* in the fin field below the levels detectable by *in situ* hybridization.

To ensure that the previously characterized defects found in Tbx5b-deficient embryos were indeed representative of loss of Tbx5b, and not due to off-target morpholino effects such as partial knockdown of Tbx5a, CRISPR Cas9 directed mutagenesis was used to generate a

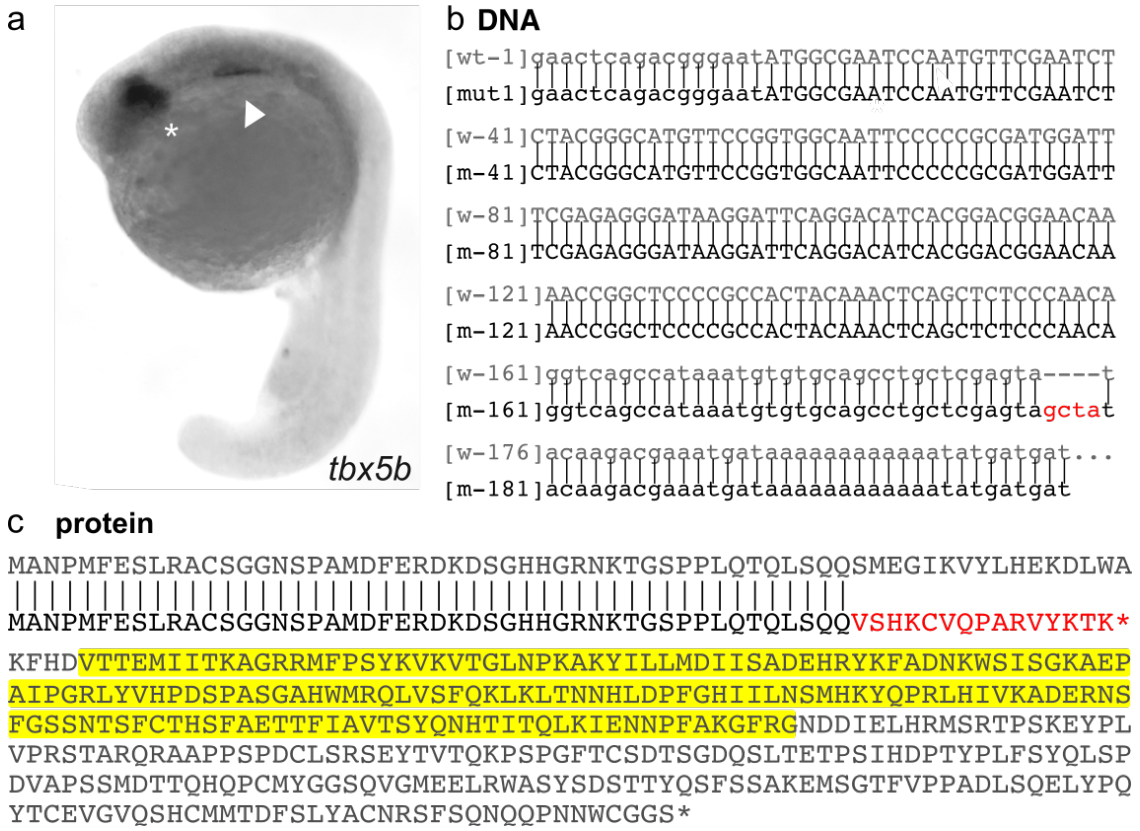

Figure 3.1: Analysis of *tbx5b* expression and the *tbx5b*^{ch2} mutant. (a) *tbx5b* is expressed in the eye (star) and in the anterior LPM (arrowhead) in a wildtype embryo at 21 hpf (b) *tbx5b*^{ch2} mutants have a 4 base insertion in the first intron. Capital letters are the ORF, lowercase letters are the 3'UTR and the first intron. Red letters are the indel (c) The 4 bp insertion disrupts splicing, which would result in a RNA transcript containing the first intron, therefore producing a protein with a premature stop codon (*). The T-box is highlighted yellow.

mutation in *tbx5b*. The specific gRNA sequence used was GAGCTGAGTTTGTAGTGGCG which targeted the first exon prior to the start of the T-box domain, in order to increase the chances of generating a null allele. 30% of the F0 injected embryos displayed phenotypes consistent with the characteristics exhibited by Tbx5b-deficient embryos, including hearts that failed to loop and small, malformed pectoral fins. Unaffected injected siblings were raised to adulthood and screened by in-crossing to identify mutant carriers. Once mutants had been identified by the phenotypes produced in the offspring, mutant F0 fish were out-crossed to produce stable F1 mutants. Sequencing identified a 4 base pair insertion (GCTA) in the first intron (Figure 3.1b). This insertion presumably acts by disrupting splicing. This would result in mutant mRNA that incorrectly retains the first intron. The resulting protein would contain the first 49 appropriate amino acids, after which the inclusion of the intron would result in an incorrect protein sequence and a stop codon after 16 incorrect amino acids (Figure 3.1c). Furthermore, since the T-box domain begins at amino acid 56 in Tbx5b (Figure 3.1c, highlighted in yellow), the resulting mutants should possess no Tbx5b that is capable of directly binding to DNA, and therefore the resulting protein should be nonfunctional. However, multiple attempts to amplify and sequence *tbx5b* cDNA to confirm this missplicing event were unsuccessful, both in the wildtype and in *tbx5b* -/- mutant embryos. These attempts included attempts to optimize the PCR amplification conditions through changing the reagents concentrations, annealing temperatures and testing multiple primer pairs, including previously published primers [83]. Forward primers tested were located throughout the 5' UTR and the first exon, reverse primers were located throughout the rest of the gene, at locations from the second exon to the final exon.

Heterozygous *tbx5b* +/- fish do not display defects in fin or heart development. However, the *tbx5b* -/- mutants produce similar phenotypes as the reported Tbx5b-deficient embryos [84, 87]. Specifically, the heart fails to loop and a pericardial edema is formed (arrowheads, Figure 3.2b,c). This edema will continue to grow as the embryo ages and the *tbx5b* -/-

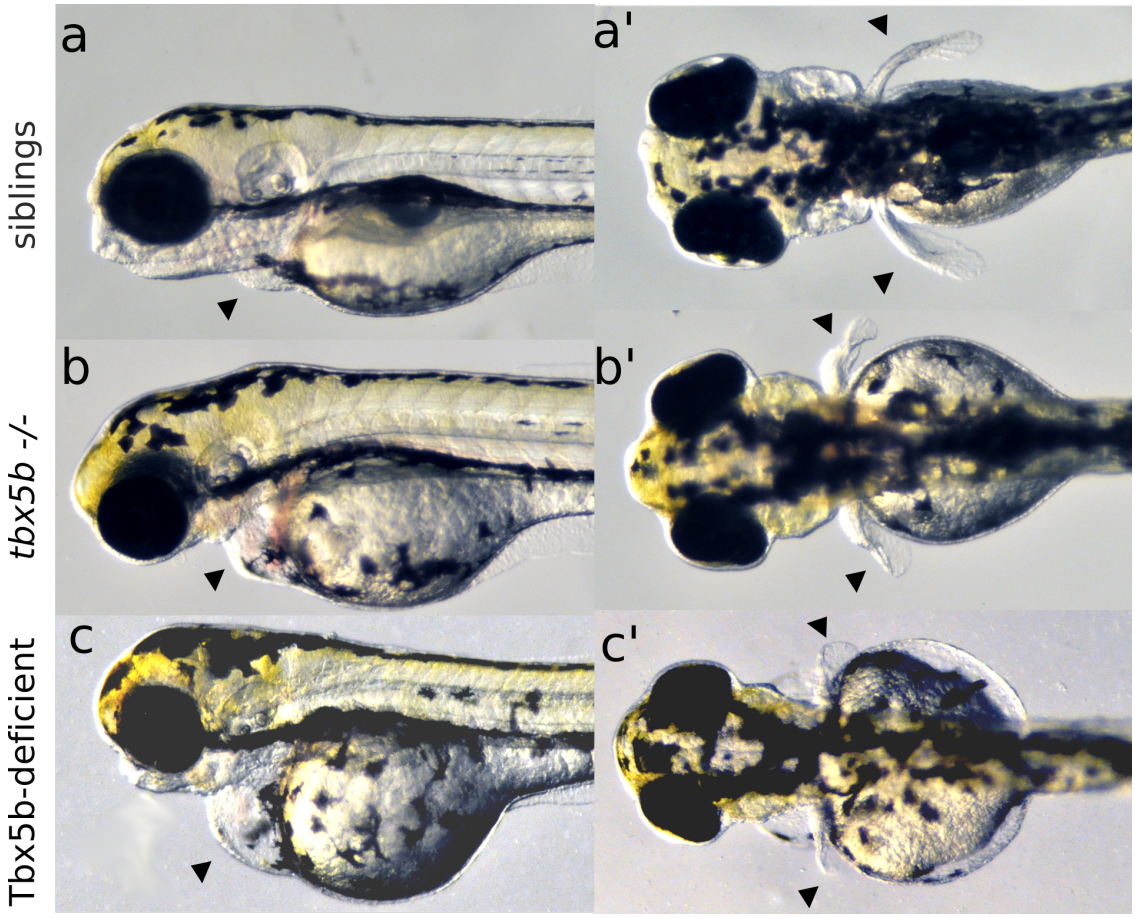

Figure 3.2: *tbx5b -/-* mutants phenocopy Tbx5b-deficient embryos. (a-c) Embryos at 3 dpf. Siblings from a *tbx5b +/-* in-cross display normal heart (a) and fin (a') development while *tbx5b -/-* mutant siblings have affected hearts (b) and fins (b') which phenocopy the defects seen in the heart (c) and fins (c') of embryos injected with a Tbx5b morpholino. Arrowheads indicate heart (a-c) and pectoral fins (a'-c')

mutant embryos die between 5 and 6 dpf. The *tbx5b -/-* mutants also exhibit similar fin defects to the Tbx5b-deficient embryos. Although pectoral fin buds initially form, these fin buds tend to be smaller than same-stage wildtype fin buds [84] and eventually develop malformed pectoral fins. At 3 dpf, when the pectoral fins of the wildtype embryo have elongated to cover approximately half the length of the yolk (Figure 3.2a', arrowheads) both the *tbx5b -/-* mutants and the Tbx5b-deficient embryos have significantly shorter, misshapen pectoral fins (Figure 3.2b',c', arrowheads). However, the upturned fins reported in a small percentage of Tbx5b-deficient embryos by Parrie et al. were not detected in any of the *tbx5b -/-* mutants or in Tbx5b-deficient embryos examined. In their studies, Parrie et al. use a different strain of wildtype zebrafish (WIK instead of *AB), which could account for the differences in phenotypes, as I also did not detect upturned fins in Tbx5b-deficient embryos. Alternatively, Parrie et al. may have been using an incomplete dose of morpholino as they report small fins in only 85% of embryos injected, while I find all embryos injected with 5 ng of morpholino produce small fins. Parrie et al. do not report the total amount of morpholino injected.

3.4.2 tbx5b -/- mutants display defects both in early and late fin development

Both Parrie et al. and Pi-Roig et al. report that Tbx5b-deficient embryos display small and delayed fin buds as well as later defects in fin development. Parrie et al. report that some markers in the early fin bud are normal, such as *hand2* expression, while other markers of fin development, such as *versican a*, are defective [84]. Likewise, Pi-Roig et al. report that the Fgf signaling cascade involved in fin patterning is still present in Tbx5b-deficient fin buds, although there are some delays and misregulations, notably that *fgf24* remains expressed in the fin mesenchyme of Tbx5b-deficient embryos longer than in wildtype embryos [87]. However, the effect of loss of Tbx5b on the ZPA and the AER, two key signaling centers,

has not been previously reported.

Shha signaling from posterior of the ZPA is essential for the AP patterning of the fin [38]. *shha* expression is present in the posterior mesenchyme of the fin buds of wildtype siblings at 32 hpf (arrow, Figure 3.3a). At 32 hpf, the fin buds of both the Tbx5b-deficient and the *tbx5b -/-* mutants are notably smaller, however *shha* expression is still present in the posterior region of the fin bud (arrows, Figure 3.3a',a"). Expression of *shha* appears to be proportional with the reduced size of the fin bud, suggesting that the ZPA is appropriately established in the fin buds of both Tbx5b-deficient and *tbx5b -/-* mutants.

The AER is necessary for outgrowth and proximal-distal patterning of the fin bud [108]. *dlx2* is expressed in the AER of developing fin buds, but lost in Tbx5a-deficient embryos [46]. At 32 hpf, *dlx2* expression is present in the overlying ectoderm of the fin bud of wildtype siblings (arrows, Figure 3.3b). This expression is maintained in the ectoderm of the smaller fin buds of both *tbx5b -/-* mutants and Tbx5b-deficient embryos (Figure 3.3b',b"), suggesting that the AER is patterned appropriately in both the *tbx5b -/-* mutants and Tbx5b-deficient embryos.

bmp4 is initially expressed in the mesenchyme and essential for formation of the AER, and is also essential for later development of the AF [109]. At 48 hpf, *bmp4* is expressed throughout the mesenchyme of the fin with the highest concentrations at the periphery of the fin, closest to the overlying ectoderm and the AF (arrows, Figure 3.3c). The fin bud is much smaller and appears delayed in both the *tbx5b -/-* mutant and the Tbx5b-deficient embryos at this time. The expression of *bmp4* is present at higher relative levels throughout the entire mesenchyme of the fin buds of both *tbx5b -/-* mutants and Tbx5b-deficient embryos, although it is still expressed at higher levels at the periphery (arrows) than in the center of the fin bud (Figure 3.3c',c"). Consistent with Parrie et al.'s interpretation of *bmp4* expression, this data suggests that AF specification is delayed in both *tbx5b -/-* mutants and Tbx5b-deficient embryos.

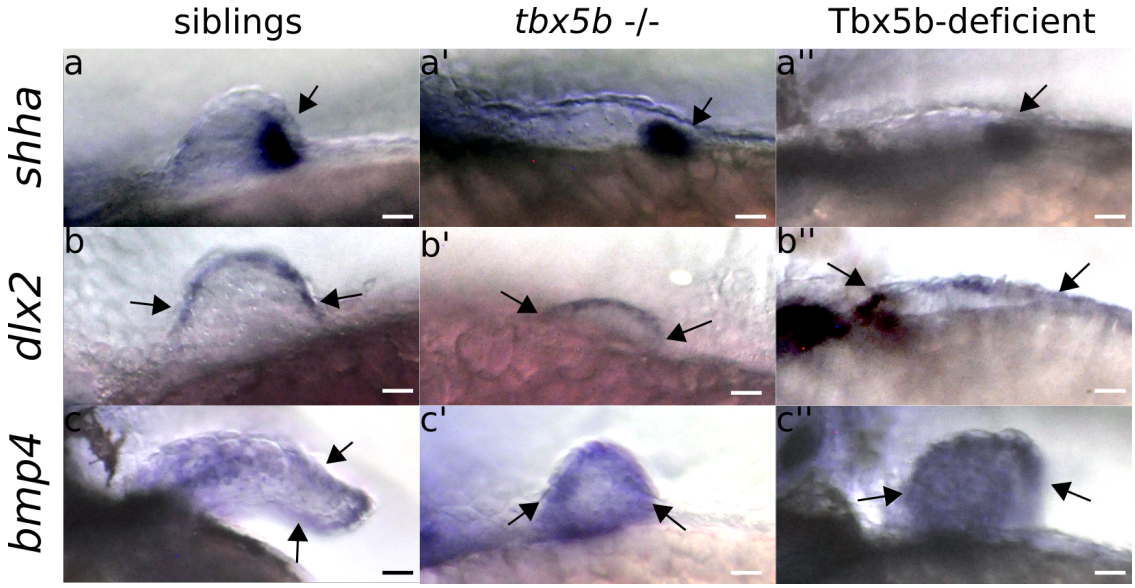

Figure 3.3: *tbx5b* -/- mutants and Tbx5b-deficient embryos display gene expression associated with early signaling centers. (a-a") arrows indicate expression of *shha* in the posterior region (ZPA) of 32 hpf wildtype siblings (a), *tbx5b* -/- (a') and Tbx5b-deficient (a") embryos. (b-b") Arrows indicate expression of *dlx2* in the AER of 32 hpf wildtype siblings (b), *tbx5b* -/- (b') and Tbx5b-deficient (b") embryos. (c-c") Arrows indicate *bmp4* expression adjacent to the AF of 48 hpf wildtype siblings (c) *tbx5b* -/- (c'), and Tbx5b-deficent (c") embryos. Scale bars are 10 µm.

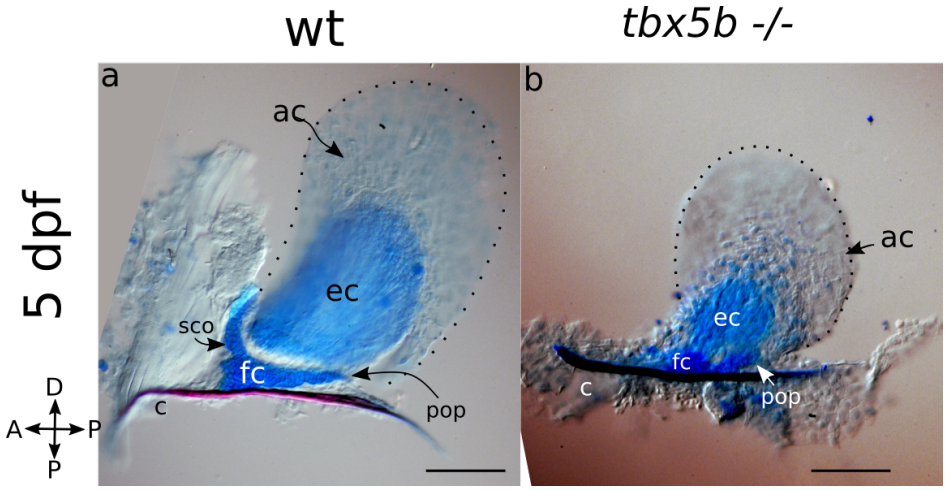

Figure 3.4: Alcian Blue and Alizarin Red staining of the larval fin at 5 dpf. Alcian Blue staining indicates the cartilage staining and Alizarin Red detects bone. Dotted lines indicate the total extent of the fin (a) wildtype fin (b) *tbx5b -/-* fin. Scalebars are 100 µm. ac-actinotrich, ec-endochondral disc, c-cleithrum, sc-scopulocoracoid, fc-foramen coracoid, pop-postcoracoid process

Although the fins of *tbx5b -/-* embryos have been shown to be small and misshapen throughout development, the underlying structural components of the fins have not yet been analyzed. To fully understand the defects present in the fin, Alcian Blue and Alizarin Red staining was performed on both wildtype and *tbx5b -/-* embryos at 5 dpf, in order to identify the structures present at this stage. Alcian Blue stains cartilage blue while Alizarin Red stains bone red. At this stage, several structures are present in the wildtype fin and pectoral girdle, which will first be described in the wildtype embryos. The cleithrum, the homologous structure to the collarbone, has ossified at this stage and is present in both the wildtype and the *tbx5b -/-* mutants (Figure 3.4a,b). The coracoid processes are a cartilaginous c-shaped structure supporting the fin which can be divided into three regions: the scopulocoracoid, the foramen coracoid and the postcoracoid process, listed in order from anterior to posterior (Figure 3.4a). The fin itself consists of an endochondral disc which is composed of cartilage at this stage and a distal AF, also known as a fin fold. The AF is filled with supporting structures called actinotrichs. In Figure 3.4a, one of the many actinotrichs is labelled.

As expected, the most noticeable difference is that the fin of the *tbx5b -/-* mutant is smaller than the wildtype fin. Both the endochondral disc and the AF are reduced in size. Most of the components of the fin are present in the *tbx5b -/-* mutant, although some are mispatterned. The boundary between the endochondral disc and the coracoid processes as well as the boundary between the endochondral disc and the AF is not as well defined in *tbx5b -/-* fins as in wildtype (Figure 3.4b). Notably, in the second case, cartilage staining is scattered into the AF (Figure 3.4b). The AF in the *tbx5b -/-* mutants is smaller than the AF in wildtype embryos (outlined in dotted lines, Figure 3.4b). The *tbx5b -/-* fins still contain many actinotrichia (Figure 3.4, ac labels one of several actinotrichs present in the fin). Defects in the patterning of the cartilage appear to be more severe in the anterior region of the fin than in more posterior regions, which can most clearly be seen by the loss of the scopulocoracoid in *tbx5b -/-* mutants (Figure 3.4b).

3.4.3 tbx5b -/- mutants display defects in the head in addition to the defects in the heart and pectoral fins

Both *tbx5b -/-* mutants and Tbx5b-deficient embryos exhibit defects in tissues beyond the heart and the pectoral fin. The heads of both the Tbx5b-deficient and *tbx5b -/-* mutant embryos appear to be reduced in size compared to wildtype siblings (Figure 3.2b,c). Overall head shape is truncated and rounder than wildtype embryos and the eyes appear to be slightly smaller. The jaws of affected embryos do not project as far anteriorly as do the jaws of similarly-stage wildtype embryos (Figure 3.5). Notably, from the ventral view of the jaw, the Meckel's cartilage extends anterior to the eyes in wildtype embryos (Figure 3.5a', arrow), while in *tbx5b -/-* mutant embryos, the Meckel's cartilage does not extend anterior to the eyes (Figure 3.5b'). Additionally, the overall length of the head and jaw structures along the AP axis is noticeably shorter in *tbx5b -/-* mutant embryos compared to wildtype embryos.

tbx5b -/- mutants appear to also exhibit slight defects or delays in pigmentation, although

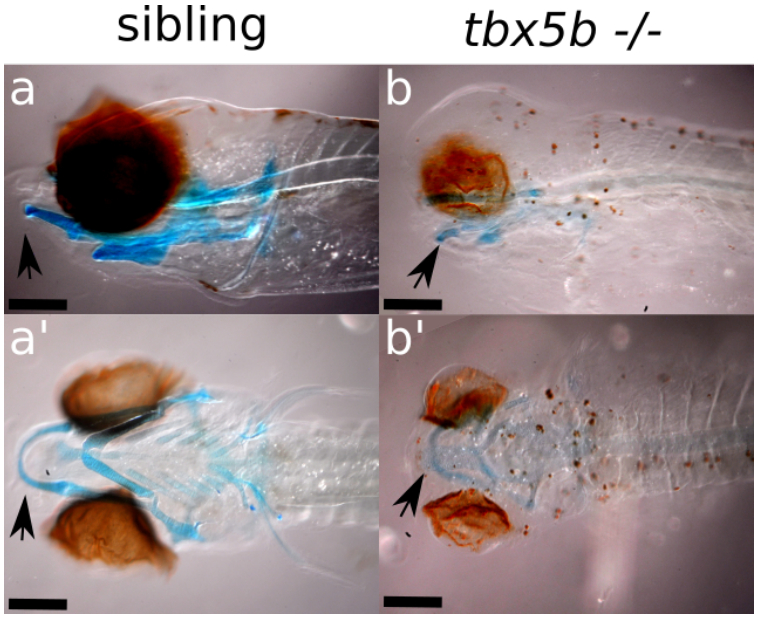

Figure 3.5: *tbx5b -/-* mutants display defects in the cartilage of the head. Alcian Blue staining in the jaw at 6 dpf. Wildtype siblings display a more protruding lower law that extends beyond the eye as can be seen both from a lateral (a) and ventral (a') view. Affected *tbx5b -/-* embryos have a rounder head and a jaw that does not protrude beyond the eyes, as seen from both a lateral (b) and ventral (b') view. Scalebar is 100 µm.

this phenotype has not been comprehensively analyzed. Additionally, unlike their wildtype siblings, the swim bladder of Tbx5b-deficient embryos does not inflate, although it does otherwise form appropriately [110]. As previously mentioned, both *tbx5b -/-* mutants and Tbx5b-deficient embryos die by 6 dpf, presumably due to circulation issues caused by the non-functioning heart.

3.5 DISCUSSION

3.5.1 tbx5b -/- mutants and Tbx5b-deficient embryos display similar phenotypes during heart and fin development

In this chapter, I described a *tbx5b -/-* mutant that produced similar phenotypes in both the heart and fin as those generated with morpholinos. Because morpholinos accurately

recapitulate the homozygous mutant phenotypes for both *tbx5a* and *tbx5b* and because the homozygous mutant phenotypes cannot be identified during the stages of fin field migration, in the following chapters morpholinos will be used to create embryos deficient in either of the Tbx5 paralogues as well as in both. When necessary, new phenotypes can also be validated in the mutant in order to more fully capture the true role of *tbx5b* during the development of the zebrafish.

Although earlier studies have reported that the fin bud develops normally in Tbx5b-deficient embryos [84, 87], these studies have not explicitly examined the signaling centers present in the fin bud, although the later stages of the Fgf signaling cascade have been examined in detail. In this chapter, I report that both the AER and ZPA are present in the fin bud of Tbx5b-deficient and *tbx5b -/-* mutant embryos. This suggests that although the fin bud is small, the early signaling centers are present. This is in contrast to the Tbx5a-deficient embryos, which fail to form these signaling centers [10].

The *tbx5b -/-* mutant embryos, while they have smaller fin buds than same stage wildtype embryos, maintain expression of *dlx2* in the AER (Figure 3.3), consistent with the data reported by Pi-Roig et al. suggesting Tbx5b-deficient embryos establish expression of normal AER patterning genes [87]. Parrie et al. suggest that the AF is not correctly specified in Tbx5b-deficient embryos due to the fact that at 46 hpf, *bmp4* is not expressed in the AF but expressed uniformly throughout the fin bud, unlike the restricted expression in same-stage wildtype embryos [84]. However, in later stage embryos (48 hpf, Figure 1.6c), this expression no longer appears to be uniform across the fin, suggesting that there may only be a delay in specification of the AF, rather than a total failure of specification. Additionally, the AF continues to expand *in tbx5b -/-* mutants, such that by 5 dpf, although smaller than the fins of same-stage wildtype embryos, the size is significantly larger than it was at 48 hpf. Furthermore, actinotrichia form in the AF of both the wildtype and *tbx5b -/-* fins, implying that some functions of the AF are intact. Combined, this supports the hypothesis

that the AF is specified at some point in *tbx5b -/-* embryos, although there may be a delay in specification. Due to the fact that the *tbx5b -/-* embryos die at 5 dpf, it cannot be conclusively determined if the size defects in the AF are exclusively due to a delay.

Loss of Tbx5b appears to have a weaker effect on the skeletal and cartilage components of the fins than loss of Tbx5a. Both Tbx5a-deficient and *heartstrings -/-* mutants exhibit an almost complete loss of elements of the fin, with only a small cleithrum present in these embryos some of these embryos at 5 dpf [10, 86]. However, partial Tbx5a-deficient embryos display a similar phenotype to *tbx5b -/-* embryos, producing fins containing most cartilage components, but with defects in the anterior structure, with the severity varying with the dose [10]. This suggests that in some cases, Tbx5b may be acting similarly to a partial dose of Tbx5a. Furthermore, the anterior bias of these defects resembles the anterior bias of defects seen in the forelimbs of Holt-Oram patients [73] .

Although the ZPA contains proportional expression of *shha*, suggesting that AP patterning in the fin bud is established appropriately, there are still anterior defects seen in the cartilage patterning of the fin bud. One possible explanation for these defects is that some elements of the fin are pre-patterned early in development—prior to fin bud formation. If the anterior cells do not manage to contribute to the fin field, this may result in deletions to anterior structures. Chapter 5 analyzes the migration dynamics of the fin field prior to fin bud formation and will further discuss this hypothesis. Another explanation for loss of anterior structures in *tbx5b -/-* fins is that although AP patterning appears to be established normally at 32 hpf, Tbx5b is also affecting patterning at a later stage in development, as proposed by both Parrie et al. and Pi-Roig et al.

3.5.2 tbx5b appears to have effects on tissues outside of the lateral plate mesoderm

Additionally, this work provides insight into the role of *tbx5b* beyond fin development. Notably, both *tbx5b -/-* mutants and Tbx5b-deficient embryos displayed defects in tissues outside of the LPM, particularly in the head. How is this possible? One such possibility is that *tbx5b* expression in the retina is having an effect on surrounding tissues. Interestingly, in mice *Tbx5* expression has been detected in the mesenchyme of the mandibular arch [9]. It may be possible that *tbx5b* is directly expressed in the jaw or precursor cells at low levels not detected by *in situ* hybridization. Alternatively, the *tbx5* paralogues, and especially *tbx5b*, may have a broader ability to act indirectly on the multiple tissues outside of the LPM. The effect of the *tbx5* paralogues on tissues outside of the LPM will be explored further in Chapter 4.

A third possibility is that *tbx5b* could be influencing the behavior of pharyngeal arch progenitor cells while they are present in the LPM; these cells will then give rise to much of the jaw. There are multiple sources of evidence that suggest that cells from the LPM, particularly the secondary heart field, migrate to the pharyngeal arches and contribute to the head mesoderm [111, 112, 113]. As *tbx5b* is expressed in the region of the LPM that contributes to the secondary heart field, this provides a route by which *tbx5b* could be directly affecting development in the jaw.

A final possibility is that the defects in the jaw may be a byproduct of the pericardial edema. Many phenotypes that cause pericardial edema also produce corresponding jaw phenotypes. For instance, *silent heart* mutants do not have heart beats due to failure to express *cardiac troponin T* [114, 115]. Similar to *tbx5b -/-* mutants, these embryos also have reduced growth both in the eye and in the jaw [116]. Likewise, treating zebrafish embryos with the polycyclic aromatic hydrocarbon phenathrene also produces a pericardial edema followed by reduced jaw and eye growth, suggesting that cardiac function and pericardial

edema may be somehow linked to the final growth and development of the jaw throughout the embryo, although the mechanism for this link is unknown [116]. Minimally, the link between mutants with both cardiac edemas and jaw defects is not exclusive to these *tbx5b* deficient embryos. Interestingly, although *heartstrings* -/- mutants display similar cardiac phenotypes to *tbx5b* -/- mutants, they do not display this jaw phenotype [46, 86].

CHAPTER 4

A SCREEN FOR THE EFFECTS OF THE *TBX5* PARALOGUES DURING LIMB MIGRATION

4.1 PREFACE

This chapter is derived from a publication in *PLoS ONE* with the following citation:

Boyle Anderson, E. A. T. & Ho, R. K. A transcriptomics analysis of the *tbx5* paralogues in zebrafish. *PLoS ONE* 13, e0208766 (2018).

It contains an extended description of preliminary RNA sequencing data (Figure 4.1).

4.2 ABSTRACT

Tbx5 is essential for limb and heart development. Mutations in *TBX5* are associated with Holt-Oram syndrome in humans. Due to the teleost specific genome duplication, zebrafish have two copies of *tbx5*: *tbx5a* and *tbx5b*. Both of these genes are expressed in regions of the lateral plate mesoderm and retina. In this chapter, I describe a comparative RNA sequencing analysis on zebrafish embryos during the stages of lateral plate mesoderm migration. This work reveals that knockdown of the *tbx5* paralogues results in altered gene expression in many tissues outside of the lateral plate mesoderm, especially in the somitic mesoderm and the intermediate mesoderm. Specifically, knockdown of *tbx5b* results in changes in the differentiation of vasculature progenitors, in later patterning of trunk blood vessels, and in somite size.

4.3 INTRODUCTION

Tbx5 in amniotes is a T-box gene that plays a role in development of both heart and limb. It is expressed in a territory of the lateral plate mesoderm (LPM), a thin tissue lying lateral

to the somitic mesoderm, as well as in the eye. The more anterior *Tbx5*-positive cells in the LPM contribute to the secondary heart field and other tissues, while the more posterior *Tbx5*-positive LPM cells contribute to the forelimb. In humans, mutation of just one copy of *TBX5* is associated with Holt-Oram syndrome, in which heart and forearm defects occur in 1 in 100,000 live births [117]. These heart defects include septation defects and cardiac conduction syndrome. The limb defects have a range of severity, from minor defects in the thumb, to truncations of large parts of the arm, with a reported bias towards more prevalent defects on the anterior part of the limb [118].

Mice that are haploinsufficient for *Tbx5* mimic the Holt-Oram syndrome phenotype, having both defective heart and forelimb tissues [11]. Mice completely lacking *Tbx5* die early due to implantation defects caused by *Tbx5*'s role in extraembryonic tissues. However when Cre-mediated deletion is used to remove *Tbx5* from later-staged embryos, mice survive until embryonic day 10.5, although development stalls at day 9.5 [11]. The heart tube of these mutant mice fails to undergo looping and forms only one atrium, rather than the normal two atria which should be present at this stage [11]. When *Tbx5* is removed selectively from tissue that will become the forelimbs allowing the mouse to continue development past embryonic day 9.5, those mice fail to form forelimb buds, leading to the complete lack of forelimbs in the perinatal mouse [119].

Due to the whole genome duplication in the lineage leading to teleost fish, zebrafish have two paralogous gene copies of *tbx5*: *tbx5a* and *tbx5b* [83]. In the zebrafish, *tbx5a* is expressed in both the heart and fin field regions of the LPM, as well as the retina [85]. The sister paralogue *tbx5b* is expressed in both the retina and the heart field, a subset of where *tbx5a* is expressed [83]. While *tbx5a* is detectable through *in situ* hybridization as early as 14 hpf in the LPM, *tbx5b* is not detectable until 17 hpf [83]. Some studies report that there does not appear to be detectable expression of *tbx5b* distinct from background in the pectoral fin bud [83], while others have reported low levels of *tbx5b* expression in the resulting pectoral

fins at later stages in development [84]. Despite this, Tbx5b-deficient embryos and *tbx5b -/-* mutants exhibit clear phenotypes in fin bud formation and fin development, indicating that it may function at some point in the developing fin field or surrounding tissues.

Early heart development occurs normally for *heartstring -/- (tbx5a)* mutants, with heart jogging occurring correctly at around 24 hpf [86]. However, heart looping does not occur in these embryos, which die at 5 dpf [86]. Tbx5b-deficient embryos display earlier and more severe heart defects than *heartstring -/-* mutants. Tbx5b-deficient embryos display defects in heart development as early as 24 hours, as heart jogging fails to occur correctly, often resulting in a heart at the midline rather than on the left—although occasionally heart jogging occurs to the right [87]. Heart looping also fails to occur in Tbx5b-deficient embryos [87].

Heartstring -/- mutants do not develop a pectoral fin bud or pectoral fins. This is due to downstream loss of *fgf24* expression, which is regulated by Tbx5a and required for the migrating LPM cells to converge and form a fin bud [31, 32]. Unlike Tbx5a-deficient embryos, Tbx5b-deficient embryos form pectoral fin buds and fin, although they exhibit delayed fin bud formation with the resulting pectoral fins often small or misshapen [84]. Fin development appears to be delayed as the 48 hpf pectoral fins of Tbx5b morpholino-injected embryos appear morphologically similar to 36 hpf control embryos fins [87]. Pi-Roig et al. hypothesize that *tbx5a* initiates fin outgrowth while *tbx5b* is required later in pectoral fin development to maintain this growth [87]. However, the delay in fin bud development in Tbx5b-deficient embryos can be seen as early as 30 hpf, when the fin bud first becomes morphologically distinct in wildtype embryos [84]. This suggests that *tbx5b* may function early in fin bud formation as well as in later stages of fin bud development.

Although morpholino injections for either *tbx5* paralogue produce both heart and fin defects in zebrafish, injected mRNA can rescue the cognate phenotype, but not that of its paralogue [84], suggesting that there are functional differences between the two paralogues.

Additionally, the *tbx5* paralogues differentially affect gene expression during development of both the heart and fins. Specifically, Tbx5a-deficient embryos lose expression of *fgf24* in the fin field while Tbx5b-deficient embryos maintain expression of *fgf24*, but exhibit a delay in switching expression of *fgf24* from mesenchymal tissue to ectodermal tissue at 36 hpf [87]. In the heart, expression of *vcana* is expanded in embryos deficient in either Tbx5a or Tbx5b, but expression of *bmp4* is only restricted in embryos deficient in Tbx5a, not in embryos deficient in Tbx5b [84]. These changes, as well as changes in expression of other molecular markers, suggest that *tbx5a* and *tbx5b* may act within different transcriptional networks.

As previously stated, *tbx5a* and *tbx5b* result from a duplication event during the teleost specific genome duplication [84]. How have they evolved to have the possibly non-overlapping functions they have today, implied by the different effects of depletion and the fact that they cannot rescue their paralogue? As transcription factors, it is possible to gain insight into how the *tbx5* paralogues are functioning by understanding the transcriptional networks that they affect. In this chapter, I perform comparative RNA sequencing experiments between the *tbx5* paralogues. In order to target genes that might play a role in the migration of fin bud and heart precursors, I collected embryos at 18 hpf and 21 hpf, during the time that the cells in the LPM are migrating. This screen identified genes that are expressed and differentially regulated outside of the LPM, with two tissues of note being the vasculature and the somites.

4.4 RESULTS

4.4.1 RNA sequencing to identify differences between the transcriptional networks of tbx5 paralogues

Whole embryo RNA sequencing was performed at both 18 hpf and 21 hpf. These time points were chosen as they represent the beginning and a midpoint of LPM migration in

the fin field, respectively [31]. Because both Tbx5a and Tbx5b morpholinos accurately recapitulate the homozygous mutant phenotypes (Figure 3.2) and because the homozygous mutant phenotypes cannot be identified during the stages of fin field migration, morpholinos were used to create embryos deficient in either of the Tbx5 paralogues as well as in both. The use of morpholinos also allows for the assaying of single gene effects without paralogous gene compensation [107].

Preliminary experiments were first performed on pooled embryos at both 18 and 21 hpf. Only single Tbx5a-deficient and Tbx5b-deficient embryos were tested and compared to wildtype embryos at these time points using the Tophat/Cufflinks suite (Figure 4.1a-d). Specifically, there were 64 genes upregulated at 18 hpf and 132 genes downregulated in Tbx5a-deficient embryos compared to wildtype embryos at 18 hpf (Figure 4.1a, Table B.2). There were 89 genes upregulated and 125 genes downregulated when comparing Tbx5b-deficient embryos to wildtype embryos at 18 hpf (Figure 4.1b, Table B.2). At 21 hpf, there were 91 genes significant upregulated and 92 genes downregulated in Tbx5a-deficient embryos compared to wildtype (Figure 4.1c, Table B.3). There were 98 genes upregulated and 86 genes downregulated in Tbx5b-deficient embryos compared to wildtype at 21 hpf (Figure 4.1d, Table B.3). Because some genes are differentially regulated in both time points or by both paralogues, this produced a list of 494 differentially regulated genes. Genes were identified by alignment to the Zv9 genome.

In order to understand what kinds of genes were being detected in this preliminary experiment, I then searched ZFIN [120] for known expression data of the genes found to be differentially regulated in either Tbx5a or Tbx5b-deficient embryos compared to wildtype embryos at these time points. Overall, I found that 54 of these genes were expressed in the eye, 23 genes were expressed in the fin, 9 genes were expressed in the heart, 22 genes were expressed in both the fin and the heart and 45 genes were expressed in other tissues, including the nervous system, liver, yolk syncytial layer (YSL), gills, jaw, neural crest, pharyngeal

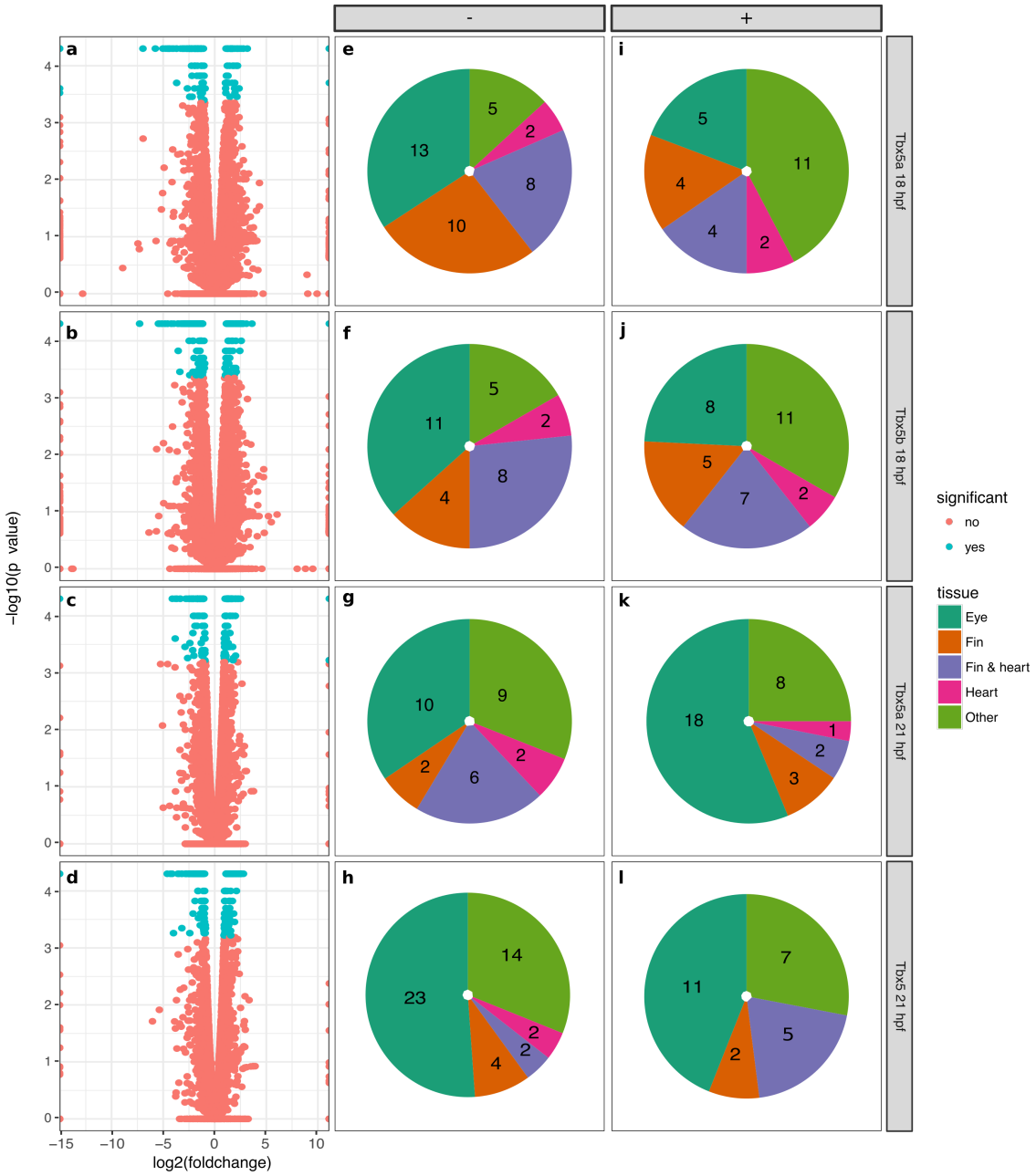

Figure 4.1: The preliminary RNA sequencing experiments reveals that many genes are expressed in tissues outside of the lateral plate mesoderm. These charts represent the differential gene expression information of the preliminary RNA sequencing experiments. (a-d) Volcano plots display differential gene expression of Tbx5a-deficient and Tbx5b-deficient embryos compared to wildtype at both 18 hpf and 21 hpf. Red dots are genes that do not exhibit significant differential change in expression and blue dots are genes that exhibit significant differential gene expression. (e-l) The pie charts display the expression information of genes that are either downregulated (e-h) or upregulated (i-l) and have expression information available on ZFIN. (continued on following page)

Figure 4.1: (Continued) Teal represents expression in the eye, orange represents expression in the fin, purple represents expression in both the fin and heart, pink represents expression in the heart and green represents expression in any other tissue.

arches, blood or kidney. Notably, this gives expression data for 153 of the 494 differentially expressed genes or 31%. I then compared expression of genes in the different tissues among the different time points and genotypes to try and identify any pattern in tissue expression.

At 18 hpf, the genes that were downregulated in Tbx5a-deficient embryos compared to wildtype embryos had 13 genes expressed in the eyes, 10 genes, expressed in the fin, 8 genes expressed in the fin and heart, 2 genes expressed in the heart, and 5 genes expressed in other tissues (Figure 4.1e). Similarly, the genes that were downregulated at 18 hpf in Tbx5b-deficient embryos compared to wildtype had 23 genes expressed in the eye, 4 genes expressed in the fin, 2 genes expressed in both the fin and the heart, 2 genes expressed in the heart and 14 genes expressed in other tissues (Figure 4.1f). The genes that were upregulated at this time in Tbx5a-deficient embryos compared to wildtype had 5 genes expressed in the eye, 4 genes expressed in the fin, 4 genes expressed in both the fin and heart, 2 genes expressed in the heart and 11 genes expressed in other tissues (Figure 4.1i). The genes that were upregulated at this time in Tbx5b-deficient embryos compared to wildtype embryos had 8 genes expressed in the eye, 5 genes expressed in the fin, 7 genes expressed in the fin and heart, 2 genes expressed in the heart and 11 genes expressed in other tissues (Figure 4.1j).

At 21 hpf, the genes that were downregulated in Tbx5a compared to wildtype had 10 genes expressed in the eye, 2 genes expressed in the fin, 6 genes expressed in the fin and heart, 2 genes expressed in the heart and 9 genes expressed in other tissues (Figure 4.1g). In the list of genes that were downregulated in Tbx5b-deficient embryos compared to wildtype at 21 hpf, there were 23 genes expressed in the eye, 4 genes expressed in the fin, 2 genes expressed in the fin and heart, 2 genes expressed in the heart, and 14 genes expressed in other tissues (Figure 4.1h). In the list of genes that were upregulated at 21 hpf in Tbx5a-deficient embryos compared to wildtype embryos, there were 18 genes expressed in the eye,

3 genes expressed in the fin, 2 genes expressed in the fin and heart, 1 gene expressed in the heart and 8 genes expressed in other tissues (Figure 4.1k). In the list of genes that were downregulated at 21 hpf in Tbx5b-deficient embryos compared to wildtype, there were 11 genes expressed in the eye, 2 genes expressed in the fin, 5 genes expressed in the fin and heart, 0 genes expressed in the heart and 7 genes expressed in other tissues (Figure 4.1l).

Because these preliminary results found many of the genes differentially expressed were expressed primarily in the eye (54 of 153 genes with known expression) and in an attempt to limit the differentially expressed targets to genes that may play a role in either heart or fin development, the eyes were removed before cDNA extraction for all subsequent experiments, although some comparisons include the preliminary sequencing data performed using complete embryos (Table B.2, Table B.3). In addition, for these experiments, 3 separate samples of 10 pooled embryos were used for each condition. Furthermore, I also added a new morpholino condition to the experiment, that of embryos injected concurrently with Tbx5a and Tbx5b morpholinos (henceforth referred to as double-deficient embryos).

To create lists of differential gene expression for each genotype, differential expression was compared between deficient and wildtype embryos at the same time point. As described in Chapter 2, three different procedures for identifying differential gene expression were used in this study, which produced distinctive lists of differentially expressed genes. The preliminary experiment produced 632 million reads and a list of 494 differentially expressed genes (detected using Cuffdiff), of which 454 were unique. This final triplicate sequencing gave 309.4 million reads. When using Cuffdiff to produce differential gene expression lists, a list of 162 differentially expressed genes were identified (Figure 4.2a, Table B.4, Table B.5). Of these genes, 111 were unique to this method of analysis. Of note, only 13 genes were detected as differentially expressed between both the preliminary and triplicate experiment, despite the fact that the only difference between them is number of replicates and removal of the eyes. EdgeR identified the greatest number of differentially expressed genes in this

dataset, identifying 1561 differentially expressed genes, of which 1515 were unique to this dataset (Figure 4.2b, Table B.6, Table B.7). The HOLT method identified the fewest number of differentially expressed genes, identifying 61 differentially expressed genes, of which 31 were unique to this method (Figure 4.2c, Table B.8, Table B.9). These results are consistent with other studies finding that different methods of identifying differential gene expression can produce relatively different lists of differential gene expression [121].

In order to select a smaller subset of these results for further screening, a list was created of genes that had been detected as differentially regulated by at least two methods of the analyses outlined above (Figure 4.2d). This produced a list of 78 genes that were differentially expressed in Tbx5a-deficient, Tbx5b-deficient or double-deficient embryos (Figure 4.3). However, not all expression changes were significant for each comparison for each gene. This is because the list was compiled of genes that had at least one significant differential expression change for any condition, not of genes that had significant differential expression changes for all conditions. When clustering the lists generated by differential gene expression for all conditions, the two separate time points first cluster together, suggesting that the largest difference in significant differential gene expression is temporal (Figure 4.3). Next, for both time points, Tbx5a-deficient and double-deficient target genes cluster together, suggesting that in general the list of Tbx5a targets is more similar to the double-deficient target list than it is to Tbx5b list (Figure 4.3).

4.4.2 Candidate gene identification and in situ hybridization

To understand spatiotemporal information about the results of this whole-embryo RNA-sequencing experiment, *in situ* hybridizations were performed for the 78 genes on the combined list. This provided information about the tissue in which a target gene was located in and if there were any detectable changes in expression levels or patterning in Tbx5a-deficient, Tbx5b-deficient, or double-deficient embryos at different time points.

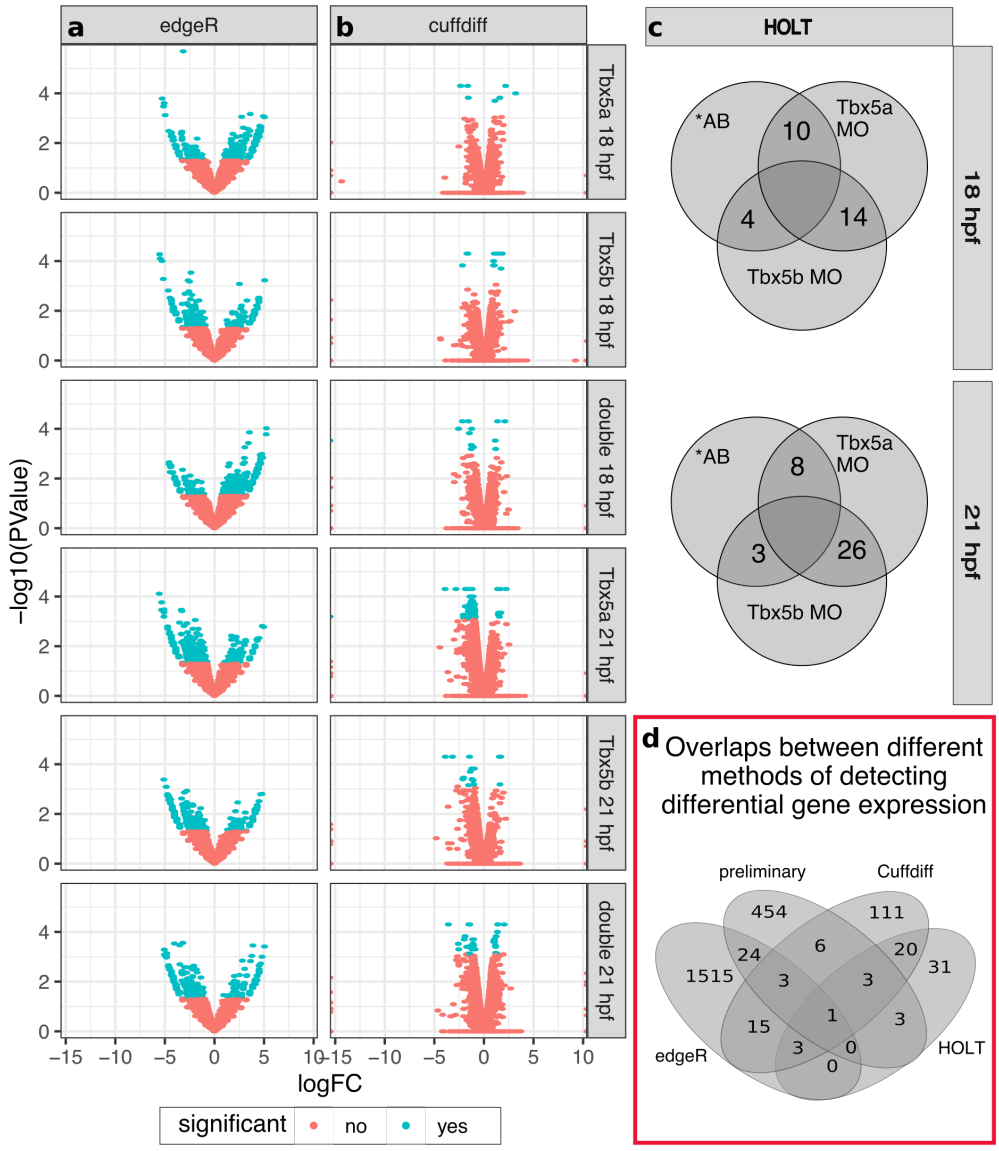

Figure 4.2: Differential expression across Cuffdiff, edgeR and the HOLT method. (a-c) The diagrams display the number of genes enriched at least 2 fold in the respective comparisons. (a) edgeR-identified gene expression. (b) Cuffdiff-identified gene expression. (c) HOLT-identified gene expression by sequential comparisons. (d) Venn diagram displaying the overlapping gene expression values comparing these three methods of identifying differential gene expression and the preliminary experiments.

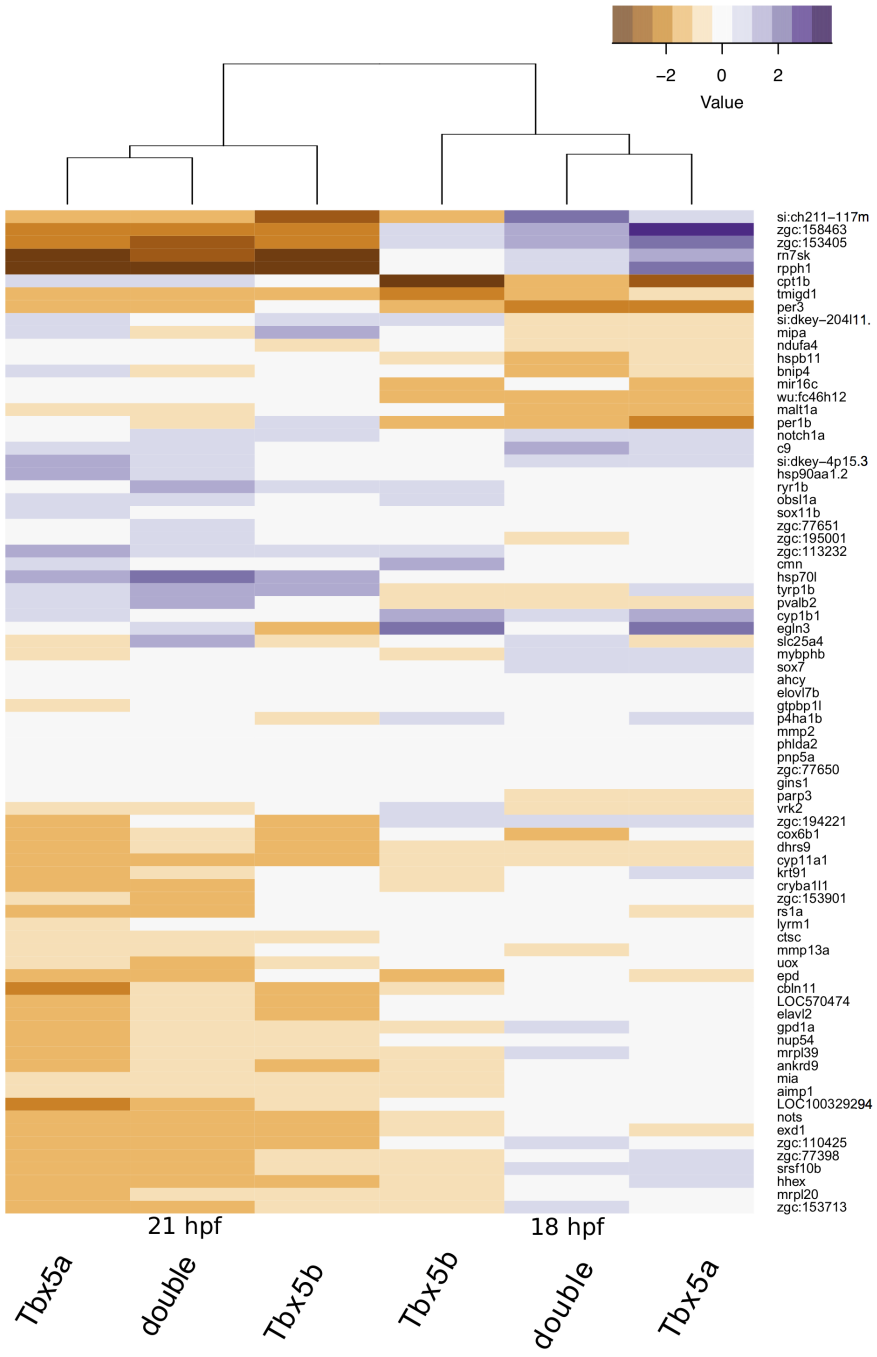

Figure 4.3: Heatmap visualizing differential expression of all overlapping 78 genes. This figure displays the logfold2 gene expression changes compared to wildtype embryos at each time point for all genes that were identified using 2 or more differential gene expression methods. Orange genes are downregulated compared to wildtype while purple genes are upregulated compared to wildtype. The differential expression values used to generate this are based on the values generated in the triplicate cuffdiff experiment. The genotypes are clustered based on similarity.

Of the 78 candidate genes, 18 were confirmed to have specific changes in expression that was detectable by *in situ* expression changes. These genes were expressed in a variety of tissues (Figure 4.4a-b). Nine genes were identified as being differentially expressed in the somites, three genes were identified as being expressed in the intermediate mesoderm, two genes were identified as being expressed in the YSL, two genes were identified as being differentially expressed in the eye, one gene was identified as being differentially expressed in the periderm, and one gene was identified as being differentially expressed in epidermal tissue (a full list is provided in Figure 4.4c).

4.4.3 Loss of the tbx5 paralogues causes changes in expression in the vasculature

Three of the genes were expressed in the intermediate mesoderm, a tissue which lies immediately medially to the LPM and differentiates into blood/endothelial precursors and the pronephric tubules. Both *sox7* and *hhex* are expressed primarily in endothelial precursors [122, 123], while *cox6b1* is expressed in the developing pronephros. Vasculature and endothelial precursors originate in the LPM and then migrate to the midline during somitogenesis [122]. *sox7* in particular exhibits a distinctive change in both Tbx5b and double-deficient embryos, which appears to correspond with a disrupted or disorganized migration of angioblasts migrating to the dorsal aorta (Figure 4.5a).

Of the two genes mis-regulated in the vasculature, *sox7* displays the most striking effect. In wildtype embryos, the vasculature precursors are arranged in a regular fashion on both sides of the midline at 18 hpf (Figure 4.5a). In Tbx5a-deficient embryos, there is an increased disorganization of these precursor cells (Figure 4.5a'). Both Tbx5b-deficient and double-deficient embryos exhibit a strong decrease in organization of these cells, as well as an apparent decrease in the number of expressing cells present (Figure 4.5a"-a''').

The gene *hhex* appears misexpressed at 21 hpf by *in situ* hybridization. In wildtype

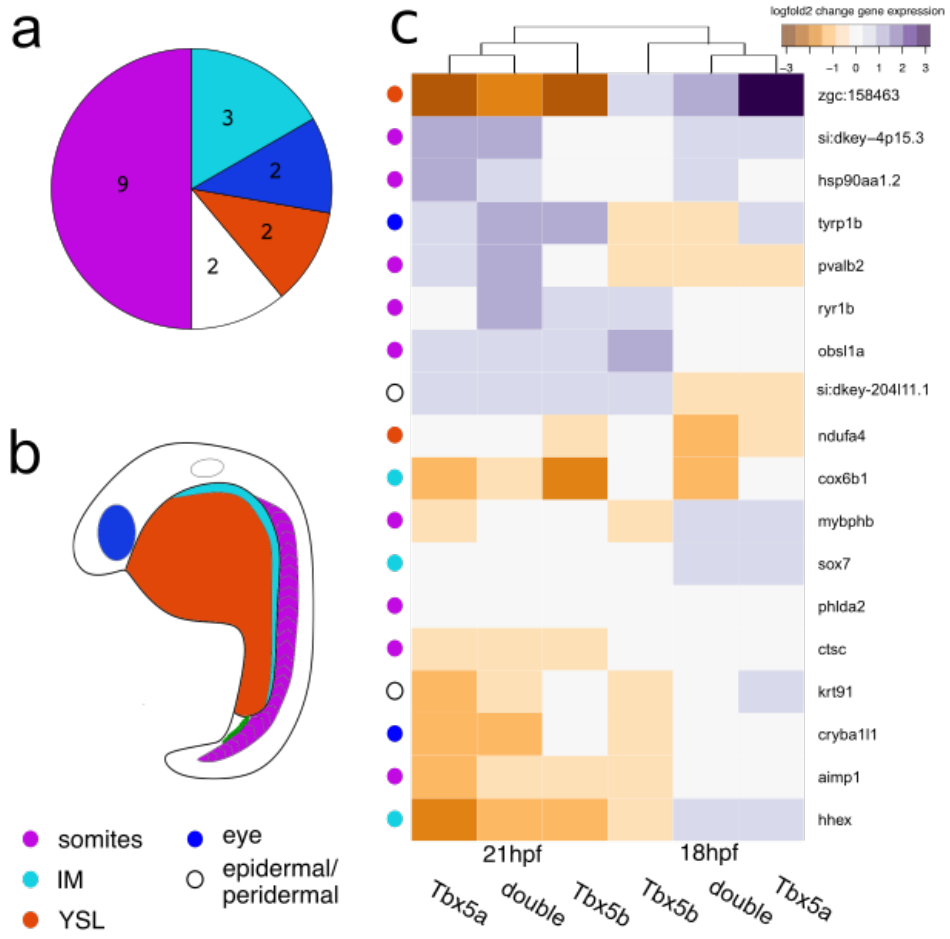

Figure 4.4: *in situ* validated changes in gene expression reveal changes in many tissues. (a) Tissue of expression of genes with validated changes in expression. (b) Schematic diagram of an embryo displaying the different tissues where affected genes were expressed. (c) Heatmap of differential gene expression in the confirmed genes. Colors are based on the fold change values generated in the triplicate Cuffdiff differential expression. The colored dot to the left of the each column corresponds with the main tissue of expression of the gene. White is epidermal or peridermal expression, blue is eye expression, orange is expression in the yolk syncytial later (YSL), light blue is expression in the intermediate mesoderm (IM) and purple is somitic expression.

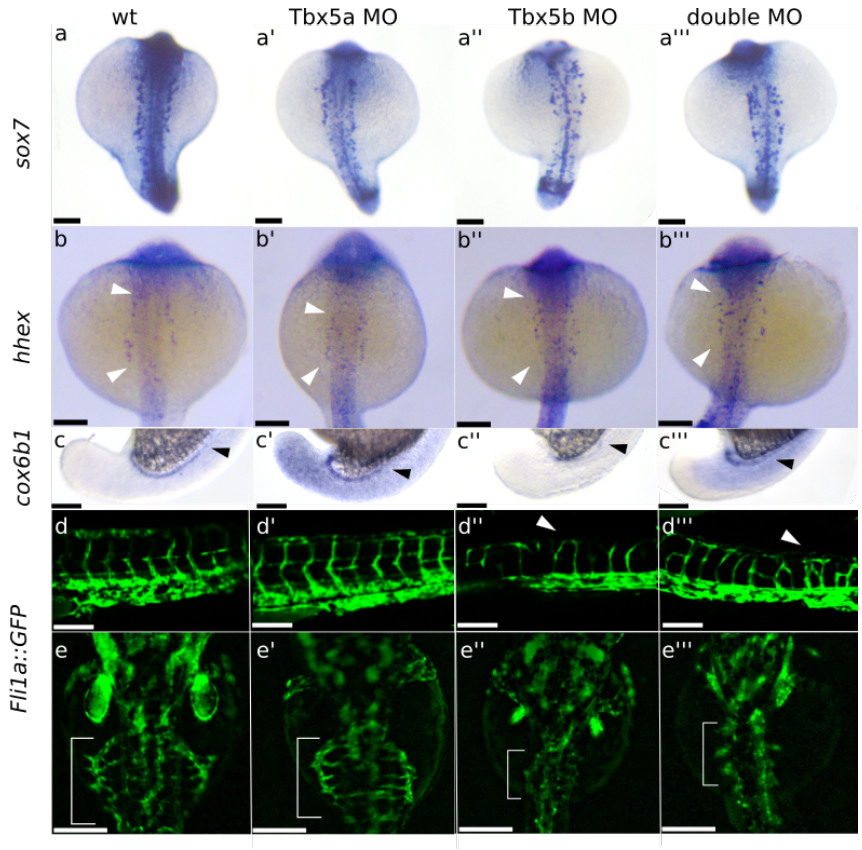

Figure 4.5: Vasculature changes in Tbx5-deficient embryos. (a-a’’’) Dorsal view of *sox7* expression at 18 hpf displaying misexpression in Tbx5a-deficient embryos (a’), Tbx5b-deficient embryos (a”) and double-deficient embryos (a’’’) compared to normal wildtype expression (a). (b-b’’’) Dorsal view of *hhex* expression at 21 hpf displaying mild misexpression in Tbx5a-deficient embryos (b’) and more severe misexpression in Tbx5b-deficient embryos (b”) and double-deficient embryos (b’’’) compared to wildtype (b) (c-c’’’) Lateral view of *cox6b1* expression in the posterior intermediate cell mass at 18 hpf in the developing pronephric duct. Arrowheads mark the anterior limit of expression. Expanded expression is present in the surrounding tissue of Tbx5a-deficient (c’) and double-deficient (c’’’) embryos, while expression is decreased throughout the embryo in Tbx5b-deficient embryos (c”). (d-d’’’) Lateral view of the *fli1a::GFP* line displays increased branching in the intersomitic vessels of both Tbx5b (d”) and double morphants (d’’’) (see arrowheads) compared to either wildtype (d) or Tbx5a morphants (d’). (e-e’’’) Dorsal view of the *fli1a::GFP* line. The subintenstinal vessels are marked with a bracket in 3 dpf embryos. There is a decrease in size of the subintestinal vasculature in Tbx5b-deficient (e”) and double-deficient (e’’’) embryos compared to either wildtype (e) or Tbx5a-deficient embryos (e’). Scale bars are 100 µm.

embryos, *hhex* is expressed in vasculature precursors as well as in the intermediate cell mass located post yolk-extension (Figure 4.5b), which will contribute to either the pronephros or blood/endothelium. The wildtype expression is present in two orderly stripes on both sides of the embryo (Figure 4.5b, see arrowheads marking the extent of the expression). In Tbx5a-deficient embryos the extent of this expression is slightly decreased compared to wildtype embryos (Figure 4.5b', see arrowheads marking the extent of expression), although the expression is still located in two orderly stripes. However, both Tbx5b-deficient and double-deficient embryos exhibit scattered expression of these cells, including expression closer to the midline than in either wildtype or Tbx5a-deficient embryos (Figure 4.5b-b'''). This is consistent with the *sox7* data suggesting that there is both a strong downregulation and mis-expression of vasculature precursors in Tbx5b and double-deficient embryos.

The gene *cox6b1* is expressed in the developing pronephros (Figure 4.5c, arrowhead marks the anterior extent). In Tbx5a-deficient embryos, there is ectopic *in situ* expression present in the surrounding tissue of the embryo, as well as an increased level of expression in the pronephros (Figure 4.5c). However, Tbx5b-deficient embryos exhibit a decrease in *in situ* levels of expression, with only faint levels of *cox6b1* expression remaining in the pronephros (Figure 4.5c). This downregulation is consistent with the significant differential gene expression data, which found that *cox6b1* was significantly downregulated in Tbx5b-deficient embryos compared to wildtype embryos at 18 hpf (Table B.2). Interestingly, *cox6b1* expression in the double-deficient embryos is also expanded and appears more similar to Tbx5a-deficient embryos (Figure 4.5c). The RNA sequencing data only detected a significant change in differential gene expression at 18 hpf in Tbx5b-deficient embryo in both the preliminary and the triplicate experiments (Table B.2, Table B.4).

To test if there are any underlying defects in the vasculature, the *Tg(fli1a::EGFP)y1* transgenic line was used to examine the structure of the vasculature [124]. The intersomitic vessels ("ISV") of normal embryos are present in a clear "V shape" pattern as these vessels

form between the somites (Figure 4.5c). Notably, these vessels are patterned prior to fluid flow, so the patterning of the ISV should not be affected by possible changes in fluid flow due to the defective hearts of Tbx5-deficient embryos. Tbx5a-deficient embryos exhibit normal branching in the ISV (Figure 4.5d'). However, Tbx5b-deficient embryos display minor defects in the ISV with additional ectopic branching (arrowhead, Figure 4.5d"). Double-deficient embryos display an even stronger defect in the structure of the ISV, exhibiting an increase in ectopic branching points (arrowhead, Figure 4.5d"').

The subintestinal vessels (SIV) of embryos at 3 dpf were also examined for patterning defects. In wildtype embryos the SIV spreads out over the yolk with small vessels leading back to the midline along the length of the SIV (Figure 4.5e, in brackets). Tbx5a-deficient embryos in general display an overall SIV morphology that is relatively normal sized and shaped (Figure 4.5e'). However, the size of the SIV is largely decreased in Tbx5b-deficient embryos (Figure 4.5e") and almost completely missing in double-deficient embryos (4.5e"'). This suggests that the *tbx5* paralogues may be playing a role in vasculogenesis.

4.4.4 Somitic genes are the largest category of differentially expressed genes in Tbx5-deficient embryos

The largest category of differentially expressed genes were those expressed in the somites. Although all of these genes were misexpressed in the affected embryos, three of these genes, *hsp90aa1.2*, *mybphb*, and *phlda2*, exhibited misexpression patterns most strongly at 18 hpf (Figure 4.6, Figure 4.7). Six genes, *obsl1a*, *pvalb2*, *si:dkey-4p15.3*, *ctsc*, *aimp1*, and *ryr1b*, exhibited misexpression patterns most strongly at 21 hpf (Figure 4.6, Figure 4.7).

The gene *hsp90aa1.2* is a heat shock protein and upregulated in all morphant conditions at 18 hpf (Figure 4.6a-a"'). Wildtype embryos display *hsp90aa1.2* expression clearly expressed within somites (Figure 4.6a). In Tbx5a-deficient embryos, *hsp90aa1.2* expression is upregulated especially in the anterior somites (Figure 4.6a'). In Tbx5b-deficient embryos,

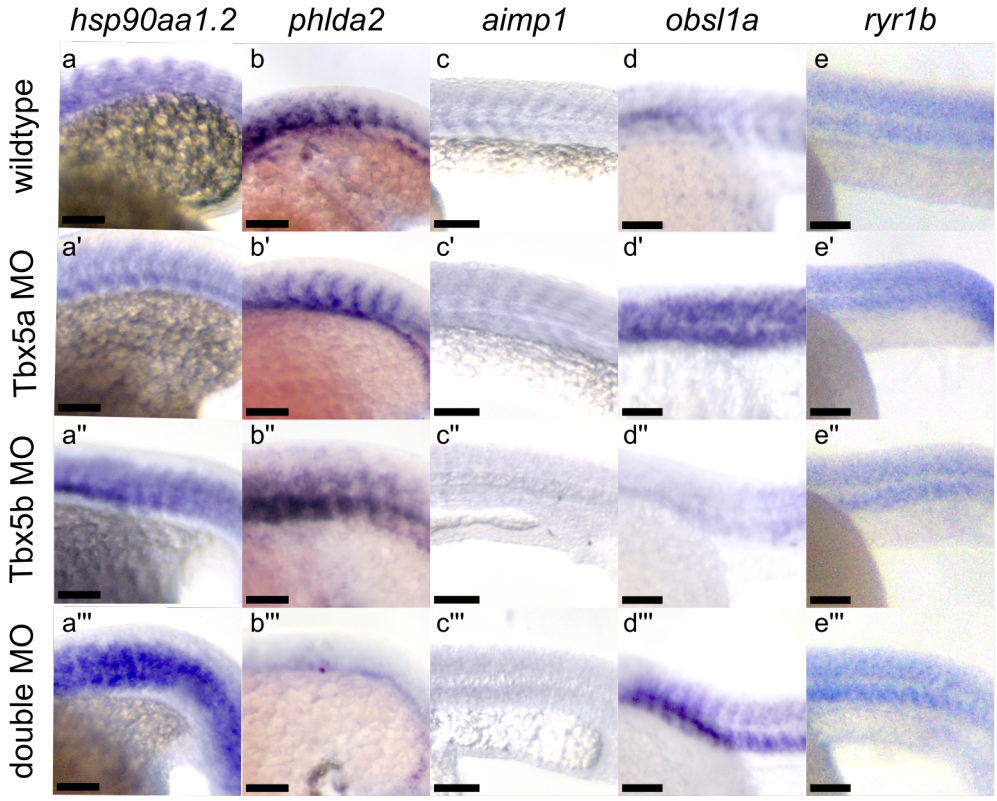

Figure 4.6: Changes in somitic gene expression consistent with the RNA sequencing analysis. All views are lateral, see text for details. *hsp90aa1.2* expression at 18 somite stage is expanded in Tbx5b-deficient (a"), double-deficient (a"') embryos compared to wildtype (a). *phlda2* expression at 18 hpf is consistent in the somites in wildtype (b), Tbx5a-deficient (b') and Tbx5b-deficient (b") embryos, but mostly absent in double-deficient embryos (b"'). Expression of *aimp1* at the 21 hpf stage is decreased in Tbx5a-deficient (c'), Tbx5b-deficient (c") and double-deficient (c"') embryos compared to wildtype embryos (c). In 21 hpf embryos, *obsl1a* expression is increased in the somites of Tbx5a-deficient (d') and double-deficient (d"') embryos compared to wildtype (d) embryos. Tbx5b-deficient embryos exhibit a decrease in expression in the trunk somites (d") but an increase in the more posterior somites (Figure 4.7f") compared to wildtype embryos. Expression of *ryr1b* is increased slightly in the Tbx5a-deficient (e') embryos compared to wildtype embryos (e) and most strongly in the double-deficient embryos especially in the ventral somites (e"'). Expression of *ryr1b* in the Tbx5b-deficient embryos (e"') is more similar to wildtype than to Tbx5a-deficient embryos. Scale bar is 100 µm.

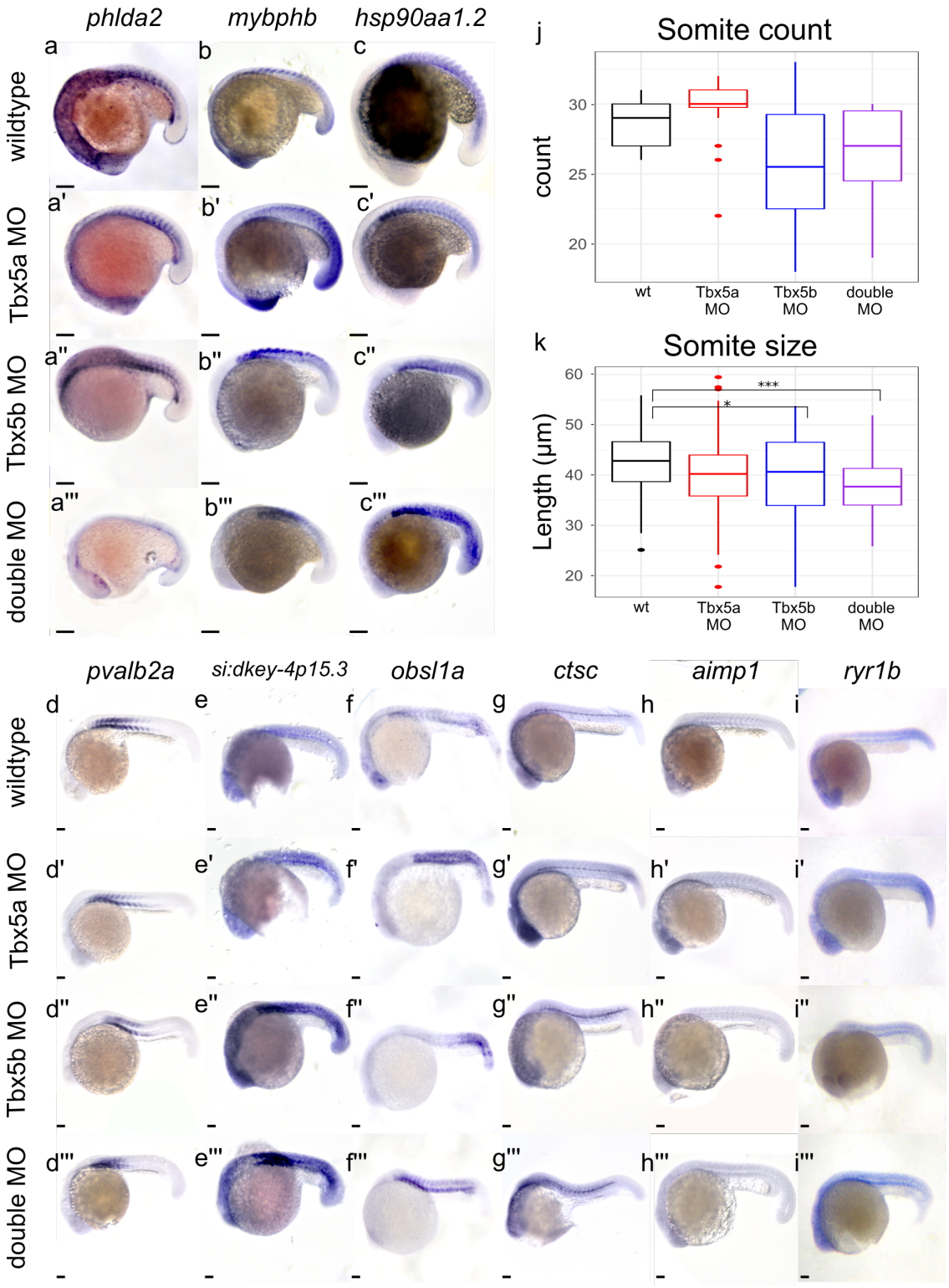

Figure 4.7: *in situ* hybridization of all genes differentially expressed in the somites. (continued on following page)

Figure 4.7: (Continued) (a-a''') At 18 hpf, *phlda2* is upregulated in Tbx5a (a') and Tbx5b (a") deficient embryos compared to wildtype embryos (a'), but downregulated in the double-deficient embryos (a'''). At 18 hpf, *mybphb* exhibits upregulation in Tbx5a (b') and double (b''') deficient embryos compared to wildtype embryos (b). At 18hpf, *hsp90aa1.2* is upregulated in Tbx5a (c'), Tbx5b (c") and double (c''') deficient embryos compared to wildtype (c) embryos, especially in the anterior somites. At 21 hpf, *pvalb2* expression is increased in Tbx5b (d") and double (d''') deficient embryos compared to wildtype (d) but not Tbx5a-deficient embryos (d'). At 21 hpf, *si:dkey-4p:15.3* expression is increased in Tbx5a (e'), Tbx5b (e") and double (e''') deficient embryos. At 21 hpf, *obsl1a* expression is upregulated in Tbx5a (f'), Tbx5b (f") and double (f''') deficient embryos compared to wildtype (f) embryos. At 21 hpf, *ctsc* expression is expanded in Tbx5a (g') and Tbx5b (g") deficient embryos compared to wildtype (g) embryos. At 21 hpf, *aimp1* expression is decreased in Tbx5a (h'), Tbx5b (h") and double (h''') deficient embryos compared to wildtype embryos (h). At 21 hpf, *ryr1b* expression is increased in both Tbx5a (i') and double (i''') deficient embryos compared to wildtype (i) embryos. (j) Somite count of embryos at 25 hpf. Tbx5a-deficient (n=16), Tbx5b-deficient (n=12), and double-deficient (n=15) exhibit no significant difference in somite count compared to wildtype (n=15). (k) Somite length measured along the AP axis of wildtype (n=104), Tbx5a-deficient (n=110), Tbx5b-deficient (n=66) and double-deficient (n=96). Both Tbx5b-deficient and double-deficient embryos have a significant decrease in somite size compared to wildtype embryos. (j-k) significance was tested using ANOVA and Tukey HSD test, *$p<0.05$, ***$p<0.0001$ Scale bar is 100 µm.

hsp90aa1.2 is also upregulated in the anterior somites but additionally appears to be misexpressed throughout the entire somite structure as well, as compared to either the wildtype or the Tbx5a-deficient embryos (Figure 4.7c") in which boundaries of expression between somites can be seen more clearly (Figure 4.7a'''). The gene *phlda2* is also expressed in the somites at 18 hpf, as well as in more anterior head mesenchyme (Figure 4.6b, Figure 4.7a). Both the *in situ*s and the RNA sequencing data exhibit a decrease in embryo-wide expression of *phlda2* in single-deficient embryos at 18 hpf compared to wildtype embryos (Figure 4.7a'-a"), although the levels of expression specifically in the somites appear consistent for both Tbx5a-deficient and Tbx5b-deficient embryos. However, *in situ* expression in the anterior regions of the embryo outside of the somites is specifically decreased in wildtype compared to either Tbx5a-deficient or Tbx5b-deficient embryos which may explain the RNA sequencing results (Figure 4.7 a-a"). The double-deficient embryos display a strong loss of expression both in the somites and throughout the whole embryo (Figure 4.6b''', Figure 4.7a''').

The gene *aimp1* is expressed in all somites at 21 hpf (Figure 4.6c, Figure 4.7h). Consistent with the whole-embryo differential expression data, the level of expression appears to be decreased in all morphant embryos at 21 hpf, most notably in the Tbx5b-deficient and double-deficient embryos (Figure 4.7c'-c''', Figure 4.7h'-h'''). Expression for *obsl1a* expression at 21 hpf resides both in the eye and in the somites (Figure 4.6d, Figure 4.7f). Consistent with the RNA sequencing differential expression levels, *obsl1a* expression appears to be upregulated in Tbx5a-deficient embryos in the somites at 21 hpf, although expression in the eye appears to be lost in these embryos (Figure 4.7b', Figure 4.6'). Tbx5b-deficient embryos display decreased expression of *obsl1a* in the trunk somites but an increased expression level compared to wildtype embryos in the more posterior somites (Figure 4.7f", Figure 4.6d"). This is consistent with the RNA sequencing data as the Tbx5b-deficient embryos display a less strong upregulation than Tbx5a-deficient embryos, which could be due to the uneven upregulation throughout the body of the embryo. Additionally, rather than being upregulated throughout all somites, only posterior somites appear to exhibit an upregulation in *obsl1a* (Figure 4.7f", Figure 4.6d'''). Double-deficient embryos exhibit a general increase in expression of *obsl1a* throughout all the somites, although this upregulation appears to be stronger in the ventral half of the somites than in the dorsal half (Figure 4.7f'''). At 21 hpf, *ryr1b* is expressed broadly throughout the somitic mesoderm (Figure 4.6e, Figure 4.7i). The whole embryo RNA sequencing data finds a trend towards upregulation in all deficient conditions, although this change is only significant in the double morphant compared to wildtype condition. This is consistent with the *in situ* expression data, in which an increase in expression of *ryr1b* in the double-deficient embryos (most strongly in the dorsal somites) is observed (Figure 4.6e''', Figure 4.7i'''). There is also a potentially a slight increase in expression in the Tbx5a-deficient embryos compared to wildtype, especially in the more posterior somites (Figure 4.6e', Figure 4.7i'). Expression of *ryr1b* in the Tbx5b-deficient embryos (Figure 4.6e") is more similar to wildtype than to Tbx5a-deficient embryos. Since

the RNA sequencing data found no significant change in differential gene expression in the Tbx5b-deficient embryo, this *in situ* data is consistent with the RNA sequencing data.

However, the remaining expression by *in situ* hybridization for the somite specific genes does not perfectly correspond with the whole embryo differential expression data. The following genes are either partially consistent or inconsistent between the RNA sequencing data and the *in situ* hybridization data. These genes may represent false positives or they may represent the limitations of using *in situ* hybridizations as a quantitative measurement. At 18 hpf, *mybphb* is expressed only in the dorsal half of the somites in wildtype embryos. It is upregulated in Tbx5a-deficient embryos, with the upregulation most strongly seen in the somites but also in the head of the embryo (Figure 4.7b-b'). The Tbx5b-deficient embryos display an expansion of expression in the somites compared to wildtype, with expression detectable in both the dorsal and ventral half of the somites, with a loss of expression in the head (Figure 4.7b"). The double-deficient embryos exhibit an increase in levels of expression of *mybphb* in the anterior somites, but a decrease in expression of *mybphb* in the posterior somites and the head, making it difficult to compare levels of expression with wildtype (Figure 4.7b'''). This is mismatched with the RNA sequencing data which finds significant downregulation only in the Tbx5a-deficient embryos compared to wildtype at this time.

The gene *pvalb2* is upregulated in all morphant conditions at 21 hpf by RNA sequencing, although it is not significantly upregulated in the Tbx5a-deficient embryos by *in situ* (Figure 4.7d-d'''). The *in situ* expression changes for *pvalb2* display a change in pattern at both the Tbx5b-deficient and double-deficient embryos, with expression appearing to be stronger, but limited to more anterior somites when compared to wildtype, which makes it difficult to conclusively determine if the levels of *pvalb2* are differentially regulated on a whole-embryo level. Expression levels of *sidkey-4p15.3* appear to be upregulated and expanded throughout the somites in all deficient cases by *in situ*, however it is only significantly upregulated in the RNA sequencing data in the Tbx5a-deficient condition (Figure 4.7e-e'''). Furthermore,

there is a discrepancy in *sidkey-4p15.3* levels in Tbx5b-deficient embryos which appear to be differentially downregulated by the EdgeR comparison at 21 hpf, despite apparent increase in expression as seen by *in situ.* The gene *ctsc* is expressed specifically at the middle of the somite and found to be significantly downregulated by RNA sequencing in both the Tbx5a-deficient and Tbx5b-deficient embryos at 21 hpf (Table B.7); in contrast the *in situ* expression in embryos appears to be expanded (Figure 4.7g-g'').

Despite the large number of somite-specific genes differentially expressed in this study, gross somite morphology appears similar in wildtype and Tbx5-deficient embryos (Figure 3.2), as well as in *tbx5a -/-* mutants or Tbx5a-deficient embryos [86, 10]. To test if the size or number of somites was different, I measured somite size and counted somite number in embryos deficient in the Tbx5 paralogues at 25 hpf, one hour after the end of somitogenesis [125]. There were no significant changes in somite count in the Tbx5a-deficient embryos compared to wildtype (Figure 4.7j). There was a significant decrease in length of the somites in both the Tbx5b-deficient and double-deficient embryos compared to wildtype, but no decrease in somite length in Tbx5a-deficient embryos compared to wildtype (Figure 4.7k).

4.4.5 Other tissues display changes in expression in Tbx5-deficient embryos

The retina is another site of expression of both *tbx5* paralogues. Both *cryba1l1* and *tyrp1b* are primarily expressed in the eye and exhibit the largest differential expression changes there. The gene *cryba1l1* is expressed in the wildtype eye at 21 hpf (Figure 4.8a). In Tbx5a-deficient embryos, *cryba1l1* expression is reduced to a smaller region of the eye (arrowhead), consistent with the significant downregulation at this phase (Figure 4.8a'). The expression also appears to be decreased in both Tbx5b-deficient and double-deficient embryos, despite no significant change in gene expression as detected by whole embryo RNA sequencing (Figure 4.8a"). The gene *tyrp1b* is expressed in the dorsal-posterior part of the developing eye at 21 hpf, and is

expressed at higher levels in all Tbx5 deficient embryos, consistent with the whole embryo RNA sequencing data (Figure 4.8 b-b'''). Notably, *tyrp1b* expression in the Tbx5a-deficient embryos appears stronger in the eye than in the wildtype embryos (Figure 4.8b-b'). While Tbx5b-deficient and double-deficient embryos display a strong increase in staining intensity, the expression is reduced to a smaller portion of the eye, especially in the Tbx5b-deficient embryos (expression boundaries marked by arrowheads, Figure 4.8 b"-b''').

Two genes were expressed in the YSL, *zgc:158643* and *ndufa4*. Expression of *ndufa4* was increased in the double-deficient embryos at 18 hpf (Figure 4.8c-c'''); however the triplicate Cuffdiff data found that *ndufa4* was significantly downregulated in the double-deficient compared to wildtype (Figure 4.3, Table B.4). The gene *zgc:158643* is expressed in the YSL, in an expression pattern that appears to mimic the position of the yolk granule cells, as well as in the tail (Figure 4.8d). Expression of *zgc:158643* in Tbx5a-deficient embryos appears to be expanded along the yolk, while in both Tbx5b-deficient and double-deficient embryos, expression is expanded to cover the entire yolk, as well as expanded expression in the tail and body of the embryo (Figure 4.8d'-d''').

Two genes, *si:dkey-204l11.1* and *krt91*, were differentially expressed in the periderm or epidermis of the embryo. The gene *si:dkey-204l11.1* appears to be downregulated in Tbx5a-deficient and double-deficient embryos, consistent with the differential expression detected by RNA sequencing (Figure 4.8e-e'''). *in situ* expression of *krt91* appears to be greatly downregulated in only the double-deficient embryos at 21 hpf, although the RNA sequencing data finds a significant change in differential gene expression in Tbx5a-deficient embryos compared to wildtype (Figure 4.8f-f''').

4.5 DISCUSSION

An RNA-sequencing analysis comparing the transcriptomes of Tbx5 deficient embryos identified 78 genes with differential gene expression that was corroborated by *in situ* hybridization.

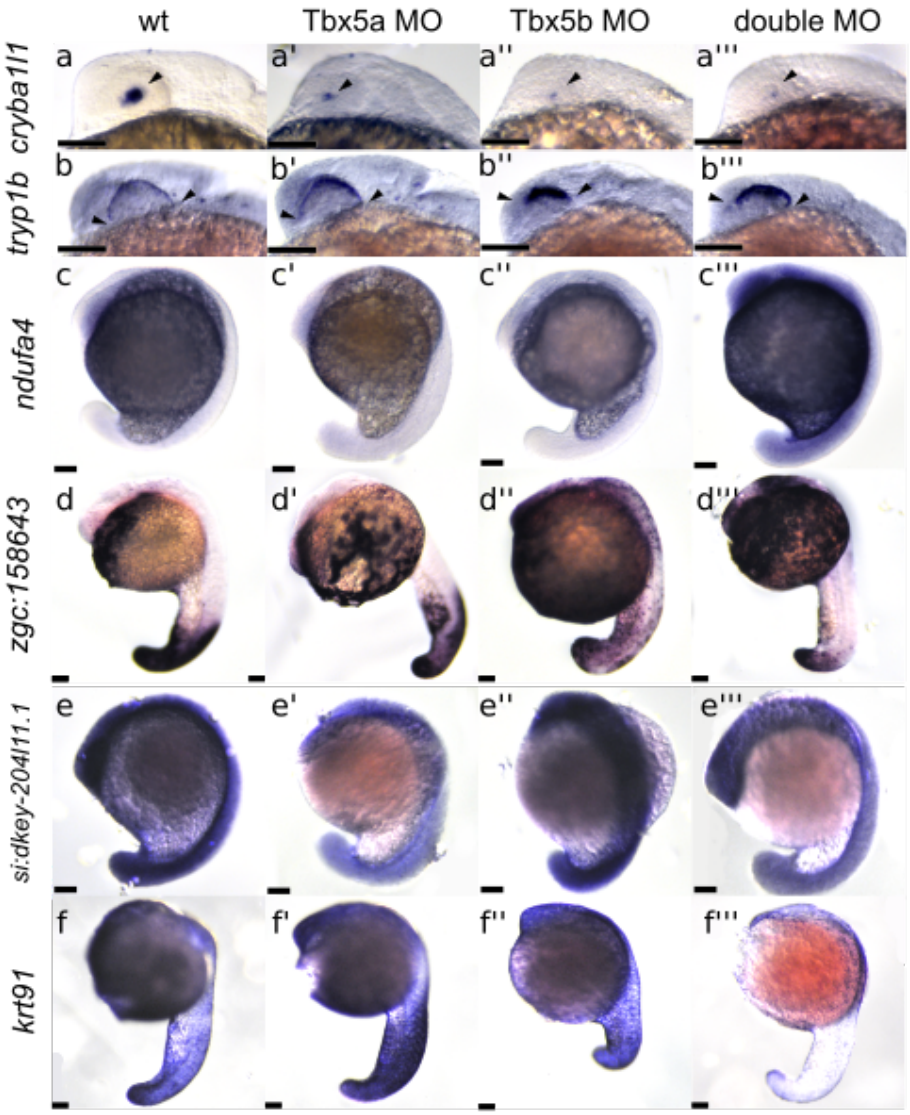

Figure 4.8: Expression of genes differentially regulated by the *tbx5* paralogues in the eye, yolk syncytial layer, and epidermis. At 21 hpf, *cryba1l1* is downregulated in Tbx5a (a') and Tbx5b (a") deficient embryos compared to wildtype (a) embryos in the eye. At 21 hpf, *tyrp1b* expression is expressed at higher levels in Tbx5a (b'), Tbx5b (b") and double (b"') deficient eyes compared to wildtype (b) eyes. At 18 hpf, *ndufa4* is upregulated in the double-deficient embryo (c"') compared to wildtype (c) embryos. Expression of *zgc:158642* at 21 hpf is upregulated in Tbx5b (d") and double (d"') deficient embryos compared to wildtype embryos (d). At 18 hpf, *si:dkey-204l11.1* expression is downregulated in Tbx5a (e') and double (e"') deficient embryos compared to wildtype (e) embryos. At 21 hpf, expression of *krt91* is downregulated in double-deficient embryos (f"') compared to wildtype embryos (f). Note f" has normal tail length, but it is bent out of focus of this image. All views are lateral. Scale bars are 100 µm.

Most of these identified targets were not expressed in the LPM, but were expressed in surrounding tissues. Two of the larger classes of differentially expressed genes were found to be specific to either the vasculature or somitic tissues. Notably, the two gene expression changes I found in the vasculature correlate with morphological defects in Tbx5b-deficient and double-deficient embryos. There were also nine genes misexpressed in the somites of Tbx5-deficient embryos, suggesting possible changes in somitic cell-derived functions, although overall patterning and development of the early somites in Tbx5b-deficient embryos display only minor differences compared to wild-type siblings.

Tbx5b appears to be regulating vasculature formation, with possible contribution from Tbx5a as Tbx5a-deficient embryos do not display a vasculature phenotype, but double-deficient embryos exhibit a worse phenotype than single Tbx5b knockdown. The observation that Tbx5 paralogues affect vasculature development is novel. Interestingly, I observed both an increase of branching and vasculature formation in the ISV and a decrease in branching and vasculature formation in the SIV (Figure 4.5-e'''). How can these opposite effects in the vasculature be reconciled? This may be due to the different methods of formation of these tissues. The SIV is a flow-dependent tissue—its growth and patterning is at least partially dependent on the existence of fluid flow [123]. Therefore, the decrease in SIV size and branching could be partially explained by the loss or decrease of fluid flow due to the heart defects in Tbx5b-deficient embryos. Although this does not fully explain why Tbx5a-deficient embryos appear to have normal SIV, it could indicate that the similar Tbx5b-deficient heart phenotype actually results in a less effective circulation than the Tbx5a -deficient hearts. In comparison, the ISV are patterned prior to the establishment of fluid flow in those vessels, so ISV should not be affected directly by pressure differences due to the heart defects. The defects observed in ISV may therefore be due to more direct functional effects of loss of the Tbx5 genes.

The decrease in *sox7* expression is particularly noteworthy because it suggests interaction

between *tbx5* genes with the VEGF/Notch signaling pathways that are known to control vasculature branching. Patterning of the vasculature depends partially on a balance between VEGF and Notch signaling [126]. Overexpression of VEGF signaling results in ectopic branching while overexpression of Notch signaling leads to a decrease in branching. Extra branching in the ISV is also seen in double Sox7/Sox18-deficient embryos, although not in either single-deficient embryos or the *sox7* -/- mutants [123, 127]. Furthermore, *sox7* expression is dependent on Shh and VEGF signaling but is upstream of Notch signaling [128]. This increased branching is consistent with a reduction of Notch signaling, which would be consistent with a decrease in *sox7* expression seen in Tbx5b-deficient and double-deficient embryos.

As the ISVs are patterned between the somites, there could also be a connection between the differential target gene expression in the somites and the mispatterning in the vasculature. The gene *hsp90aa1.2* has been found to promote both VEGF and Notch signaling via HIF1 as an intermediary [129]. *hsp90aa1.2* also has three T-BOX consensus sites located in its introns. It is upregulated in both the Tbx5b and double-deficient embryos compared to wildtype, which correlates with the increased branching seen in the vasculature. Another target in the somites is *aimp1*, which is secreted and inhibits angiogenesis by affecting endothelial migration and adhesion [130]. Since *aimp1* appears to be downregulated in both the Tbx5b-deficient and double-deficient embryos, this downregulation of *aimp1* at the somite boundaries could potentially be partially responsible for the increased branching of the ISV.

Interestingly, in regards to the genes expressed in the vasculature, Tbx5b-deficient embryos and double-deficient embryos exhibited more similar phenotypes compared to Tbx5a-deficient embryos (Figure 4.5a-b'''). However for the pronephros gene *cox6b1*, the opposite was observed, i.e. the Tbx5a-deficient phenotype was more similar to the double-deficient (Figure 4.5c-c'''). This may indicate that the *tbx5* paralogues differentially affect separate components of the intermediate mesoderm through downstream signaling pathways.

How can Tbx5b be affecting tissues that it does not appear to be expressed in? For instance, although expression in the fin can be seen by 36 hpf [84], mutant phenotypes appear earlier, with noticeable delays and decreased size of the fin bud visible as early as 30 hpf. One possible answer is that, perhaps at least in the fin, *tbx5b* is present prior to 36 hpf, but at a level lower than that detectable by *in situ* hybridizations. However, the RNA sequencing also identified effects of Tbx5b in many additional tissues, including the vasculature and the somites. Another explanation for how Tbx5b is affecting tissues that it is not expressed in is that Tbx5 paralogues may be acting non-cell autonomously. This has been previously described in mice, where TBX5 knockdown was found to have a non-cell-autonomous action in muscle patterning in the forelimb [80]. However, RNA sequencing alone cannot determine whether a transcription factor is directly or indirectly affecting the expression levels of a specific gene, as the change in expression levels could also be due to other genes affected elsewhere in the transcriptional network.

Furthermore, this data finds that both *tbx5* paralogues are involved in a wide range of transcriptional networks that extend beyond the tissue that these genes are expressed in. This work has allowed for an examination of the embryo-wide changes in gene expression and characterization of the environment through which the cells of the LPM are migrating. The fact that this screen did not recover any significant network of genes that appear to be exclusively expressed in the LPM could be due to the relative tissue size. The LPM is a relatively small tissue at 18 and 21 hpf, consisting of approximately 300 cells per embryo. Therefore, it is perhaps not too surprising that so many genes recovered in this experiment were misexpressed in the somites, one of the largest components of embryonic mesoderm. Another possibility is that of the 78 genes found to be differently expressed via RNA sequencing, many of them may have been differentially regulated in the LPM, but not at a level or pattern detectable by *in situ* hybridization.

One may question why there have not been somite or vasculature defects previously

associated with HOS patients or in *Tbx5* mutant mice. One possible reason is that this study allows a higher level of resolution than available in other organisms, particularly in humans. These are subtle defects that may not be assayed as easily in other animals. For instance, although the ISV was mispatterned in the double-deficient embryos, it was still present and appeared functional (i.e. blood flow was present in the ISV). Furthermore, because these are subtle phenotypes, they may not be present in Holt-Oram patients, who still have one functioning copy of *Tbx5*. Additionally, zebrafish also are able to reach a more mature stage of development when lacking the *tbx5* paralogues than mice embryos, as mice embryos lacking *Tbx5* stall in development at embryonic day 9.5 due to heart defects [11], which may prevent these phenotypes from being detected.

In conclusion, this chapter summarizes an RNA sequencing experiment performed on the *tbx5a* and *tbx5b* paralogues in zebrafish. It found that gene expression levels were affected in many different tissues, notably the vasculature and the somites. These changes in gene expression are also reflected morphologically in the affected tissues, with changes occurring both in the vasculature and the somites of Tbx5a-deficient and Tbx5b-deficient embryos.

CHAPTER 5

THE *TBX5* PARALOGUES ACT IN COMBINATION TO CONTROL THE DIFFERENT DIRECTIONS OF MIGRATION IN THE FIN FIELD OF ZEBRAFISH

5.1 PREFACE

This chapter contains currently unpublished work as well as a reanalysis of data previously published. The tracking of wildtype and Tbx5a-deficient cells was collected by Qiyan Mao and published with the following citation:

Mao, Q., Stinnett, H. K. & Ho, R. K. Asymmetric cell convergence-driven zebrafish fin bud initiation and pre-pattern requires Tbx5a control of a mesenchymal Fgf signal. *Development* 142, 43294339 (2015).

I performed the time lapse experiments and tracking for Tbx5b-deficient and double-deficient embryos, as well as analysis of all four genotypes using custom R scripts. Furthermore, I performed all remaining experiments reported in this chapter.

5.2 ABSTRACT

Zebrafish deficient in *tbx5a* lack pectoral fin buds, whereas zebrafish deficient in *tbx5b* exhibit misshapen pectoral fins, supporting the hypothesis that both paralogues function in fin development. The mesenchymal cells of the fin bud are derived from the Lateral Plate Mesoderm (LPM). Previous work utilizing transgenic GFP expression in the LPM has found that wildtype fin field cells are initially located adjacent to somites 1-4. The wildtype fin field cells migrate along the mediolateral (ML) axis away from the midline and converge along the anterior-posterior (AP) axis to form a fin bud located adjacent to somites 2 and 3. To better characterize the functions of the *tbx5* paralogues in zebrafish, I time-lapse analyzed

the migrations of fin bud precursors in Tbx5b-deficient and double-deficient embryos and compared to previously collected data on the dynamics of migration in wildtype and Tbx5a-deficient embryos. As previously reported, in Tbx5a-deficient embryos, the cells of the fin field migrate normally along the ML axis but display a complete loss of AP convergence. In Tbx5b-deficient embryos, the cells of the fin field display a reduced AP convergence compared to wildtype embryos which may be responsible for the small fin of Tbx5b-deficient embryos. However, more strikingly, Tbx5b-deficient embryos display a complete loss of ML migration, although the effect of this migration on fin positioning is unclear. This suggests that zebrafish *tbx5a* and *tbx5b* regulate separable migration direction vectors that, when combined, recapitulate the migration of the wildtype fin field. Furthermore, fin field cells in the double-deficient zebrafish do not engage in directed migrations along either the ML or AP axis. Thus together, these two paralogues may be acting to instruct separate vectors of fin field migration in order to direct proper fin bud formation.

5.3 INTRODUCTION

Both *tbx5b -/-* mutants and Tbx5b-deficient embryos display small fin buds and delayed pectoral fin bud formation, suggesting that these phenotypes may be due to defects in the migration of the pectoral fin field. In zebrafish, fate mapping revealed that the pectoral fin field is located adjacent to somites 1-4 in the LPM [31]. Detailed analysis of the cellular dynamics of the fin field has reveals that these cells migrate to form the fin bud [31]. Starting at 18 hours post fertilization (hpf), the cells migrate laterally away from the midline along the mediolateral (ML) axis and converge along the anterior-posterior axis (AP) to form a fin bud adjacent to somites 2 and 3. Because of the location of the fin bud, the most anterior cells must migrate a greater distance than the more posterior cells, and therefore migrate with a slightly increased speed and in a more persistent manner [31]. During this migration, the cells of the fin field maintain their nearest neighbor relationships [31].

Previously reported data has found that in Tbx5a-deficient embryos, the cells of the LPM do not converge along the AP axis [31]. Instead these cells travel laterally along the yolk and disperse, failing to form a fin bud [31]. Migration away from the midline is not affected, as the cells continue to migrate laterally away from the midline past the time and location when the cells would normally converge and form a fin bud [31]. Further work has found that Tbx5a regulates AP convergence by regulating expression of *fgf24* in a subset of cells of the fin field [31, 32]. Fgf24, a zebrafish specific FGF, acts as a convergence cue during this migration process [31, 32]. In Fgf24-deficient embryos, the cells of the fin field fail to converge and instead migrate laterally past the site where a fin bud would normally form. Furthermore, ectopic application of FGF protein through microbead implantation can partially rescue the convergence defects of both Tbx5a-deficient and Fgf24-deficient embryos [31]. This suggests that Fgf24 is the convergence cue responsible for the AP convergence of the cells in the fin field [31].

In this chapter, I analyze the cellular dynamics of the cells of the fin field in Tbx5b-deficient embryos and compare to previously published data on the effects of loss of Tbx5a on the cellular dynamics of the fin field. Unlike Tbx5a-deficient embryos, these cells converge along the AP axis, although the convergence movements are decreased compared to wildtype embryos. Notably, Tbx5b-deficient embryos also display a significant defect in migration along a novel dimension—unlike both wildtype and Tbx5a-deficient embryos, the cells of the Tbx5b-deficient embryos do not migrate laterally away from the midline. This suggests that in zebrafish, the *tbx5* paralogues may be working combinatorially in order to produce the full dynamics of wildtype fin development. Further supporting this, embryos deficient in both paralogues of Tbx5 display a general loss of directed migration with an increased randomness of migration, suggesting that both paralogues are required for directed migration of the cells in the fin field.

5.4 RESULTS

5.4.1 The cells of the fin field migrate in Tbx5b-deficient embryos

The gene *tbx5a* has been found to be expressed in the LPM in the cells that will form the mesenchymal core of the pectoral fin bud [31] and observation of this expression pattern provides information on the location of fin field cells at a given time. In wildtype embryos at 16 hpf, the precursor cells of the fin field, as marked by *tbx5a*, are present in two bilateral stripes (Figure 5.1a). At 18 hpf, *tbx5a* expression is separated between the anterior heart-contributing cells and the posterior fin field cells (Figure 5.1b, limits indicated with arrowheads). At later stages, the *tbx5a* expression is present in a smaller domain of the embryo, and at 20.5 hpf, the AP extent of this domain is beginning to decrease while the ML extent of this domain is increasing (Figure 5.1c). At 22 hpf, a circular expression domain is detectable at the site of the future fin bud (Figure 5.1d). At 30 hpf, a three-dimensional fin bud is present; *tbx5a* is primarily expressed within the fin bud, although there is a small domain of expression anterior to the fin bud (Figure 5.1f).

In Tbx5a-deficient embryos, *tbx5a*-expressing cells are present in bilateral stripes at 16 and 18 hpf (Figure 5.1a'-b'). However, in 22 hpf embryos, *tbx5a* expression is present in a broad region across the embryo, rather than concentrated at the site of the future fin bud (Figure 5.1d') [10]. At 25 hpf, *tbx5a*-positive cells are scattered across a broad region of the yolk (Figure 5.1e'). As these images suggest, these embryos do not form fin buds [10, 86].

Examination of *tbx5a* expression in Tbx5b-deficient embryos reveals a different pattern than either wildtype or Tbx5a-deficient embryos. At both 16 and 18 hpf, *tbx5a* expression in Tbx5b-deficient embryos appears similar to wildtype with expression primarily in two bilateral stripes (Figure 5.1a",b"). However, at 22 hpf, the pattern of *tbx5a* expression in the Tbx5b-deficient embryos is different than in wildtype embryos, such that the expression is more similar to the lateral stripe at 18 hpf in wildtype embryos than the circle at the future

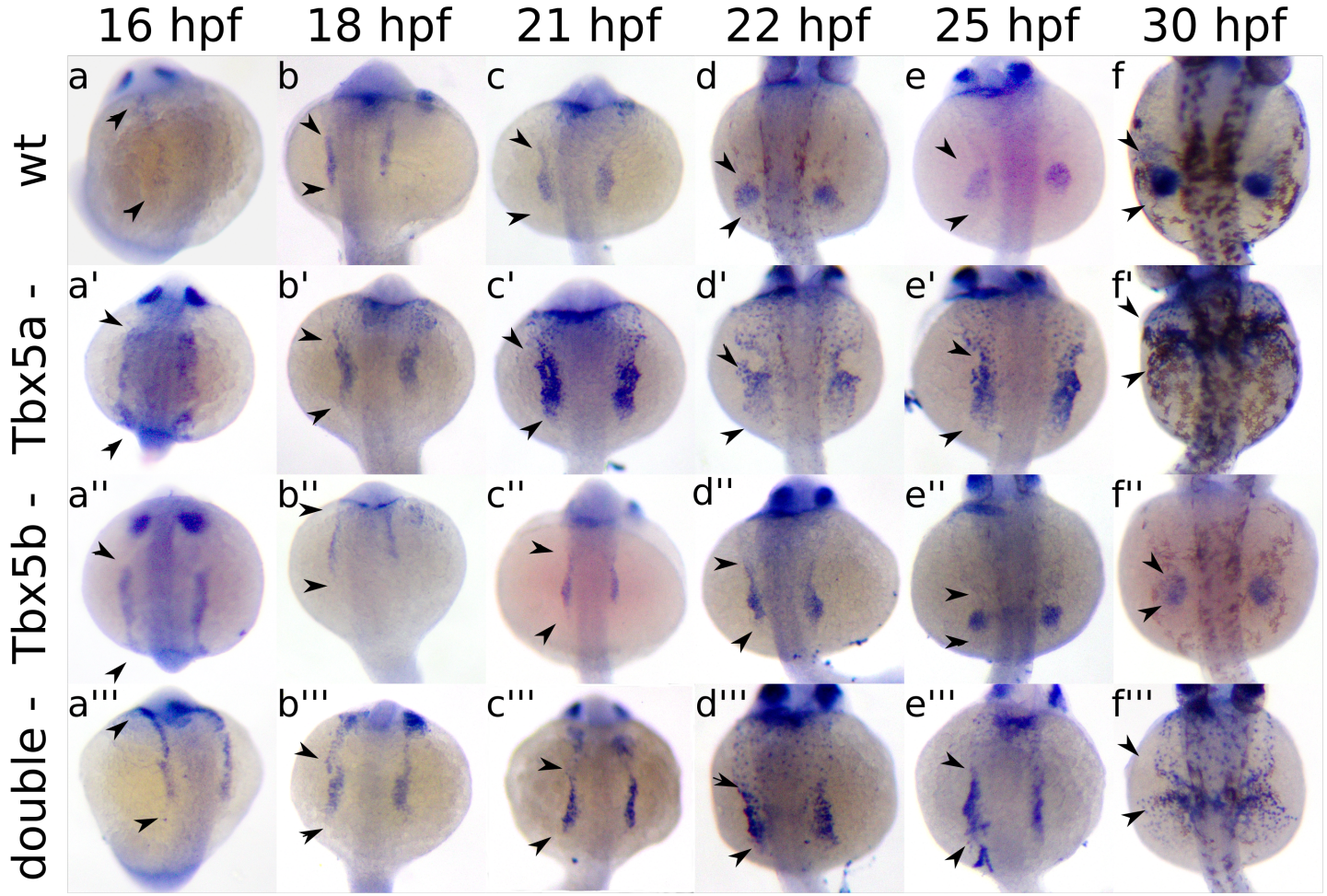

Figure 5.1: *tbx5a* expression in embryos deficient in the Tbx5 paralogues. Embryos are shown in a dorsal view with anterior facing up. Embryos shown are at 16 hpf (a, a', a", a'''), 18 hpf (b, b', b", b'''), 20 hpf (c, c', c", c'''), 22 hpf (d, d', d", d'''), 25 hpf (e, e', e", e'''), and 30hpf (f,f',f",f'''). Embryos are either wildtype (a), injected with a control morpholino (b-f), Tbx5a-deficient (a'-f') and Tbx5b-deficient (a"-f"). Arrowheads mark the extent of *tbx5a* expression

site of the fin bud in wildtype (Figure 5.1e'''). Consistent with the fact that Tbx5b-deficient embryos form fin buds [84, 87], by 25 hpf expression of *tbx5a* is localized to a circle at the site of the future fin bud (Figure 5.1e''').

5.4.2 Analysis of the migration dynamics of Tbx5b-deficient cells

To compare the migration dynamics of the fin field in Tbx5b-deficient embryos to wildtype and Tbx5a-deficient embryos, I analyzed newly acquired data from Tbx5b-deficient embryos as well as previously published data sets on wildtype and Tbx5a-deficient embryos originally reported in Mao et al. [31]. For these studies, doubly transgenic *Et(hand2:GFP)ch2; Tg(h2afx:h2afv-mCherry)mw3* embryos were used as described in Mao et al. (2015). *Et (hand2:GFP)ch2* marks the cells of the LPM while *Tg(h2afx:h2afv-mCherry)mw3* is a nuclear marker used for cell tracking [31]. Embryos were imaged at 8 minute intervals for 6 hours starting at 18 hpf, the time at which migration begins in the fin field [31].

In wildtype embryos, the cells of the fin field are located between somites 1 and 4, a region that is also marked by *tbx5a* expression [31]. At 18 hpf, the GFP+ cells are present as two stripes on either side of the midline (Figure 5.2a). As migration initiates, these cells move away from the dorsal midline in a ML direction and converge along the AP axis (Figure 5.2a'). By 23 hpf, a cluster of cells has formed that will become the mesenchymal core of the future fin bud (Figure 5.2a") [31]. The overall movements of these cells can also be visualized in Figure 5.2 a''', which displays the tracks of 60 cells overlaid on the nuclear channel. These tracks illustrate the movement of the cells both away from the midline and along the AP axis.

At 18 hpf, the fin field cells of Tbx5a-deficient embryos are distributed similarly to wildtype embryos (Figure 5.2b). However, at 21 hpf, the LPM cells in Tbx5a-deficient embryos appear to continue migrating laterally without displaying any AP convergence movements, unlike same-stage wildtype embryos (Figure 5.2b'). By 23 hpf, the Tbx5a-deficient cells have

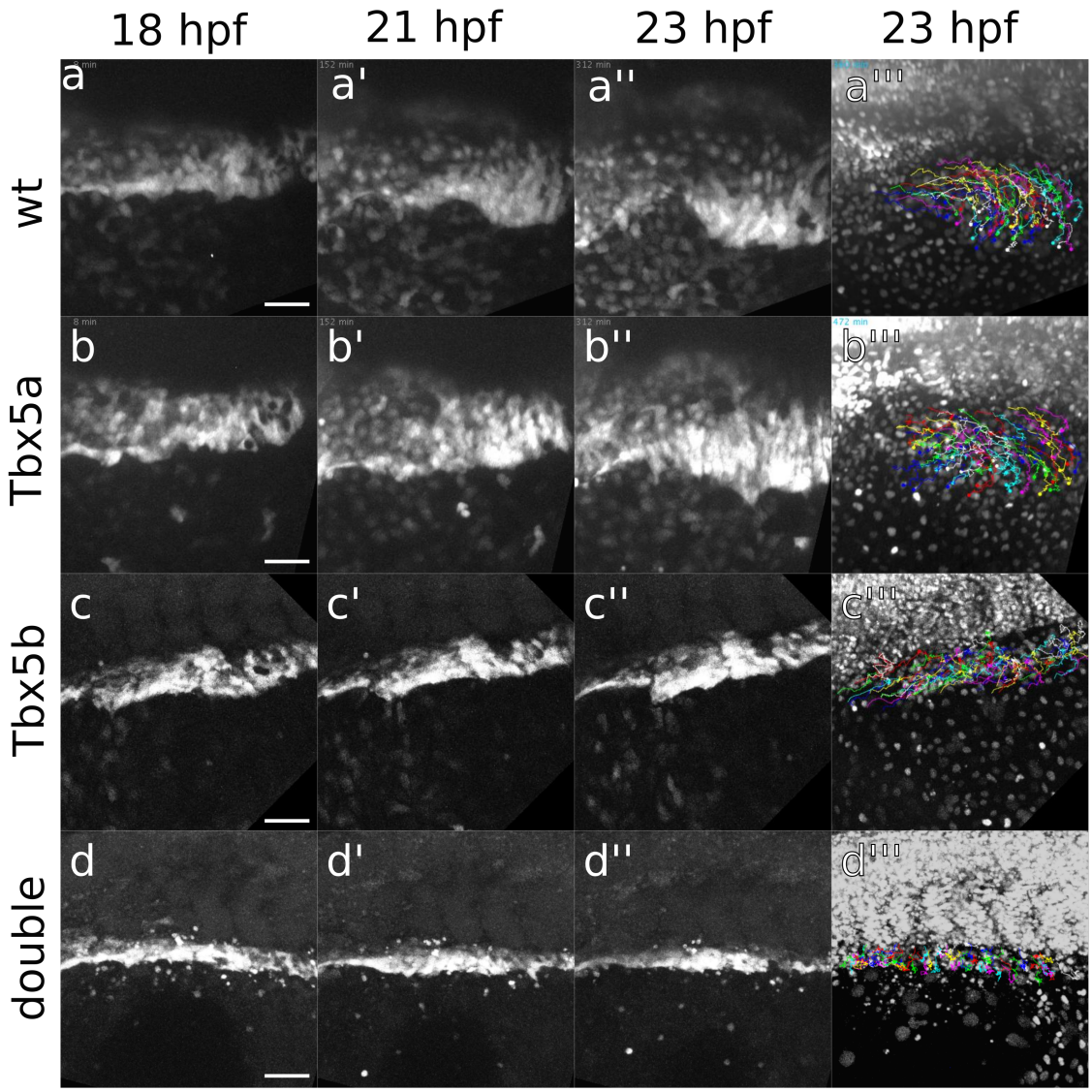

Figure 5.2: *hand2::eGFP* expression in the fin field during the tracked time in the movies. Scale bar is 50 µm. (a-a’’’) The cells of the fin field converge along the AP axis and migrate along the ML axis to condense at the site of the fin bud. (b-b’’’) Tbx5a-deficient embryos migrate laterally but do not converge along the AP axis. (c-c’’’) Tbx5b-deficient embryos converge along the AP axis but do not migrate laterally. (d-d’’’) Double-deficient embryos appear to neither migrate laterally nor converge along the AP axis. a’’’, b’’’, c’’’, d’’’ shows the tracks overlaid over the nuclei at the final frame tracked for each movie.

Table 5.1: Number of cells tracked for each embryo and each genotype

	genotype			
Embryo	wildtype	Tbx5a -	Tbx5b -	double -
1	60	60	72	66
2	60	60	69	42
3	60	60	69	48
4	60	60	65	60
5	60	60	74	60
6	60	60	77	49
7	60	60	63	51
8	60	60	60	60

continued to migrate in the ML direction and eventually migrate past the usual position of the fin bud without forming a condensation of cells (Figure 5.2b"). The loss of AP convergence can be visualized in Figure 5.2b"', where the parallel tracks indicate migration along only the ML axis while the cells maintain their relative AP positions.

In Tbx5b-deficient embryos, the fin field cells do not initially migrate in the ML direction and appear to undergo less AP convergence compared to wildtype embryos. At 18 hpf, the fin field cells are organized in a stripe along the ML axis (Figure 5.2c). By 21 hpf, these cells as a group condense along the AP axis (Figure 5.2 c') and by 23 hpf, they have formed a defined cluster of cells (Figure 5.2c"). However the Tbx5b-deficient cells do not appear to make appreciable migration movements in the ML direction during the time visualized, unlike both wildtype and Tbx5a-deficient embryos (Figure 5.2 c"').

To identify the behavior of the individual cells in the LPM, cell tracking analysis was performed on 8 embryos per genotype. A minimum of 42 and a maximum of 77 cells were tracked for each embryo, with 549 cells followed over all Tbx5b-deficient embryos (Table 5.1). These tracks were compared to the previously published data on wildtype and Tbx5a-deficient cells in the fin field in which 8 embryos were analyzed per genotype with 60 cells tracked per embryo [31].

Figure 5.3a displays all drift-corrected tracks for each embryo. The AP axis is arranged such that 0 is the anterior edge of somite 1 with increasing numbers representing more

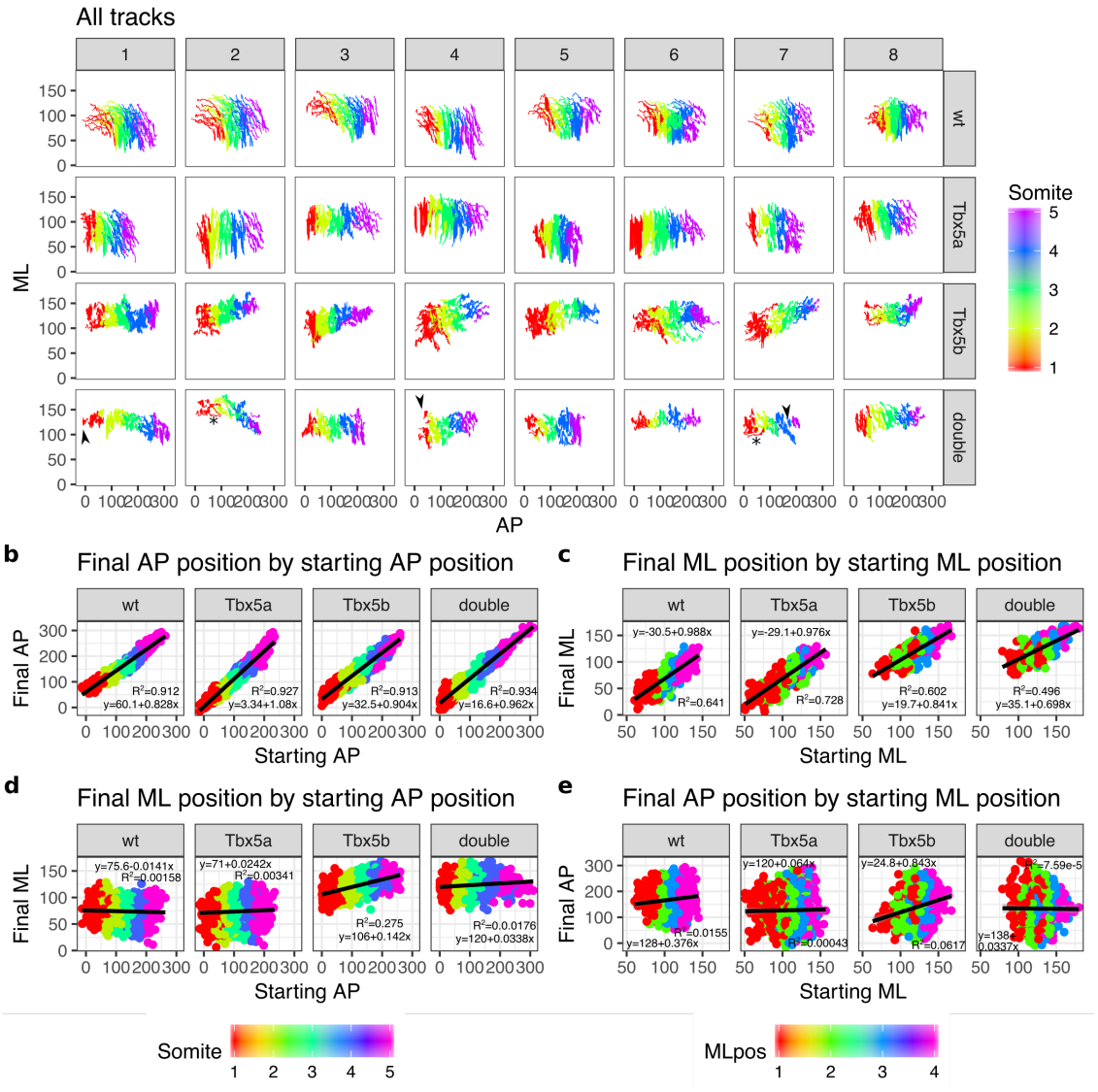

Figure 5.3: Correlation between AP and ML positions over time. All units are in µm. Color coding by position along the AP axis is red is for cells that started migrating adjacent to somite 1, yellow for cells that started migrating adjacent to somite 2, green for cells that started migrating adjacent to somite 3, blue for cells that started migrating adjacent to somite 4 and purple for cells that started migrating adjacent to somite 5. Color for position along the ML axis is red for quartile 1, green for quartile 2, blue for quartile 3 and purple for quartile 5. (a) Tracks for each embryo over time, colored by starting AP position. (b) Correlation between starting AP position and final AP position, colored by AP position and separated by genotype. (c) Correlation between starting AP position and final AL position colored by ML position and separated by genotype. (d) Final ML position by starting AP position colored by AP position and separated by genotype. (e) Final ML position by starting ML position, colored by ML position and separated by genotype. Arrowheads indicate especially short tracks while * indicates long tracks in double-deficient embryos.

posterior positions; the ML axis is arranged such that the medial edge of the LPM is roughly located at 150, with decreasing numbers representing more lateral positions. Each track represents the movement of a single cell from 18 hpf to 23 hpf. The tracks are color-coded based on the somite that each cell is adjacent to at 18 hpf. In wildtype embryos, the tracks of the fin field cells (cells adjacent to somites 1-4) indicate that cells migrate along the ML axis as well as converging along the AP axis (Figure 5.3a). The cells that begin migration adjacent to somite 5, which do not contribute to the fin field [31], also undergo migration movements along both the AP and the ML axes. Furthermore, the tracks appear to maintain the same relative positions throughout the course of migration; tracks that begin migration adjacent to somite 1 (i.e. red tracks) remain anterior throughout the course of migration while more posterior tracks (i.e. blue tracks adjacent to somite 4) remain posterior throughout migration. As previously found by Mao et al., the anterior cells of the fin field migrate with different properties than the more posterior cells. Consistent with that data, the tracks of the more anterior wildtype cells (i.e. red tracks) appear to be migrating farther than the more posterior tracks (compare red tracks to blue tracks, Figure 5.3a).

In Tbx5a-deficient embryos, the tracks of the cells of the fin field are parallel along the ML axis, indicating ML migration is occurring and that AP convergence movements are reduced or lost (Figure 5.3a) [31]. The cells located adjacent to somite 5 (i.e. purple tracks) appear to migrate both along the ML axis and the AP axis with different behaviors than the fin field cells. The Tbx5a-deficient cells appear to maintain the same relative positions–anterior cells still remain anterior and posterior cells remain posterior; however, convergence along the AP axis appears to have been lost (Figure 5.3a). Migration along the ML axis appears to be unaffected, as the tracks appear to cover approximately the same distance over the ML axis. This is consistent with the known behavior of Tbx5a in regulating the AP convergence movements of the fin field [31]. Additionally, all tracks of the fin field appear to be similar lengths regardless of the initial AP position of a cell (Figure 5.3a).

The tracks of Tbx5b-deficient embryos reveal separate behaviors than those of either wildtype of Tbx5a-deficient embryos. Unlike either wildtype of Tbx5a-deficient embryos, the ML extent of these tracks is reduced. In both wildtype and Tbx5a-deficient embryos, the tracks extend approximately 100 µm while in Tbx5b-deficient embryos, the ML extent of the tracks appears to be reduced to only 50 µm. The cells appear to maintain some AP movements, as many of the tracks appear to be oriented laterally (Figure 5.3a). This data suggests that Tbx5b may be playing a role in regulating ML migration movements, although it is unclear if Tbx5b is involved in regulating AP migration movements.

Figure 5.3b compares the initial position of each cell along the AP axis to the final position of each cell along the AP axis. The X-axis (Starting AP Position) and the Y-axis (Final AP Position) are arranged so that 0 is the anterior boundary of somite 1. Each point represents a single cell that is color-coded by its AP position at 18 hpf. Examining the plot for the wildtype embryos reveals a consistent relationship between the starting AP and final AP position. The black line is a linear regression for these points with a slope of 0.828 and a y-intercept of 60.1. Furthermore, the R^2 value of the best fit line is 0.912, suggesting that over 90% of the variation can be predicted by this line. The final position of each cell along the AP axis can be predicted accurately by the starting position, across all positions on the AP axis.

Plotting the AP position of Tbx5a-deficient cells at 18 hpf against the AP position of that cell at 23 hpf produces a similar plot as the plot for wildtype cells. The best-fit line has a slope of 1.08 and a y-intercept of 3.34, with an R^2 value of 0.927. There is a tight correlation between the initial and final AP position of a given cell, as indicated by the high R^2 value. The slope is similar to that of the plot for wildtype embryos. However, the entire plot has been shifted down compared to the wildtype plot, as illustrated by the decreased value for the y-intercept, which is consistent with an overall reduction in AP movements.

Plotting the AP position of a Tbx5b-deficient cell at 18 hpf against its position at 23 hpf

also reveals a similar correlation between AP values over time as wildtype embryos. A linear regression on this data gives an intercept of 32.5 and a slope of 0.904, with an R^2 value of 0.913. The linear regression can therefore predict a high proportion of the variability in the data. As the slopes are similar, this suggests that the AP position of a cell in any given position is approximately 30 µm posterior to its initial starting position. As the y-intercept is approximately half of the value seen in wildtype embryos, this suggests that for any given cell, the final AP position is approximately 30 µm posterior to its initial AP position, which is only half of the distance traveled in wildtype embryos, suggesting a decrease in AP movements

Figure 5.3c compares the initial position of each cell along the ML axis with the final position of each cell along the ML axis. The X and Y axis both represent the positions along the ML axis in µm with lower values representing more lateral values and higher values representing more medial values. In order to differentiate between positions on the ML axis, the lateral extent of the LPM was divided into 4 quartiles at 18 hpf, with quartile 1 being the most lateral and quartile 4 being the most medial. Each point is color-coded according to the starting ML position. In wildtype embryos plotting the starting ML position of cells at 18 hpf against the final ML position of cells at 23 hpf reveals a consistent relationship. Note that the scale for the initial ML position axis begins at 50 while the scale for the final ML position axis begins at 0, suggesting that as a whole, wildtype cells migrate approximately 50 µm laterally across all quartiles. The best-fit line has a slope of 0.988 and a y-intercept of -30.5, with an R^2 value of 0.641. The positive slope implies that cells move more laterally over time along the ML axis. The R^2 value suggests that this can explain 64% of the variation in the data, suggesting that the final position of a cell along the ML axis can be predicted by the initial position of a cell on the ML axis.

A similar pattern is seen in Tbx5a-deficient embryos. The best-fit line has a y-intercept of -29.1 and a slope of 0.976, with a R^2 value of 0.729. The Tbx5a-deficient plot displays

a very similar pattern as the wildtype pattern, suggesting that in Tbx5a-deficient embryos, the final positions of a cell across the ML axis is very similar to that of wildtype embryos.

However, in Tbx5b-deficient embryos, the pattern has shifted. The best fit line has a y-intercept of 19.7 and a slope of 0.841, with an R^2 value of 0.602. The overall position of the points has shifted, so that a cell's initial position is far more similar to its final position. Furthermore, although the colors of the separate quartile remained relatively segregated in both Tbx5a-deficient and wildtype embryos, this is less consistent in Tbx5b-deficient embryos. For instance, several cells from quartile 1 (i.e. red) appear to be located more laterally than other cells from quartile 2 (i.e. green). This is because the mediolateral length varies across the different embryos in Tbx5b-deficient embryos and since the quartiles are assigned per embryo, the positions are not as consistent in size as the divisions along the AP axis, and when comparing points from a single embryo, this mixing of quartiles is mostly lost (data not shown). Overall, Figure 5.3c indicates that in Tbx5b-deficient embryos, the ML position of a cell at 23 hpf can be predicted by the initial ML position of a cell at 18 hpf. Furthermore, the ML position of a cell remains relatively consistent from 18 hpf to 23 hpf, unlike in wildtype and Tbx5b-deficient embryos, suggesting that there may be a defect in ML migration movements in Tbx5b-deficient embryos.

Figure 5.3d plots the AP position of cells at 18 hpf against the ML position of cells at 23 hpf. Each point is colored based on the AP position, such that the color represents the somite the cell was adjacent to at 18 hpf. For any initial AP position in wildtype embryos, there are cells distributed across the entire range of ML positions at 23 hpf. This can also be visualized by the trend line, which is parallel to the AP axis and located centrally in the range of final ML positions; furthermore, the R^2 value is low (0.00158) and therefore this best fit line can explain less than 1% of the variation in the data. This suggests that there is no correlation between the AP position of cells at 18 hpf and the ML position of wildtype cells at 23 hpf. Likewise, Tbx5a-deficient embryos also have no correlation between the AP

position at 18 hpf and the final position of cells at 23 hpf, as evidenced by both the wide spread of data and the low R^2 value.

However, Tbx5b-deficient embryos exhibit mildly different patterns when plotting the AP position at 18 hpf against the ML position at 23 hpf. First, the final ML positions of Tbx5b-deficient are more medial than the final ML positions of wildtype embryos. Second, there is a correlation between the initial AP position and the final ML position of a cell, where more anterior cells have a tendency towards a more lateral position. However, this correlation is not very strong (R^2 value = 0.275), as this trend line can only explain 27.5% of the variation in data, suggesting that the correlation between the AP and ML axes may be biologically irrelevant.

Figure 5.3e plots the ML position of a cell at 18 hpf against the AP position of a cell at 23 hpf. Each point is colored based on the initial ML position. There is no correlation between the initial ML position of a cell and the final AP position of that cell in wildtype embryos, as evidenced by both the large distribution of values of final AP position for any given initial ML position, as well as the flat slope of the trend line and the extremely low R^2 value. This pattern is consistent in Tbx5a-deficient embryos. However, Tbx5b-deficient embryos appear to display an increased slope compared to wildtype or Tbx5a-deficient embryos, although the R^2 value remains low at 0.0617.

Figures 5.3a-e suggest that migration occurs in Tbx5b-deficient embryos and that migration remains **spatiotopic**, i.e. cells maintain the same relative positions in the fin bud as in the fin field, consistent with the data in Mao et al. [31]. These figures also show that there are migration defects in Tbx5b-deficient embryos. In the following sections, I will characterize these defects to understand how they contribute to the small fin bud phenotype.

The underlying cause of this phenotype may be due to defects in the early phases of fin bud formation; therefore I propose two, non-mutually exclusive hypotheses for how different cellular dynamics in the fin field could result in a smaller fin bud, which will be discussed in

the following sections. First, the cells in the Tbx5b-deficient embryos could have an impaired ability to migrate (e.g. migrate at a reduced speed) compared to the cells of the wildtype embryos. This decreased speed could result in the cells reaching the site of the fin bud at a later time, thus resulting in a smaller and delayed fin bud consistent with Parrie et al. and Pi-Roig et al.'s interpretation [84, 87]. Second, there could be an error in the orientation of the migration, such that the cells of the fin field fail to fully converge in order to form a fin bud. This would be a milder version of the defect seen in Tbx5a-deficient embryos, where due to a loss of *fgf24* expression, the cells in the fin field fail to converge and instead migrate laterally past the site of the fin bud [31]. As Tbx5b-deficient embryos maintain expression of *fgf24* [87] and form a fin bud, it is expected that the fin bud cells would still converge, although this movement may be impaired compared to the behavior of wildtype cells.

5.4.3 Tbx5b-deficient embryos are not impaired in their ability to migrate

One hypothesis for the defect in fin bud formation is that the fin field cells migrate at a reduced speed, which could result in a smaller fin bud due to fewer cells reaching the proper location. There is no significant difference between the mean speed of migration of wildtype and Tbx5a-deficient embryos (Figure 5.4a). However, the mean speed of Tbx5b-deficient cells is in fact higher than either wildtype or Tbx5a-deficient cells (350 nm/min in wildtype versus 374 nm/minute in Tbx5b-deficient embryos, p=0.0082). This suggests that a reduced speed of migration cannot be responsible for the smaller size of the fin bud, as the Tbx5b-deficient cells do not migrate slower than the wildtype cells.

Figure 5.4b displays the average speed of each cell plotted against its position on the AP axis at 18 hpf. The AP axis is measured in µm, where 0 µm is the anterior limit of somite 1. The points are color-coded by the somite that the cells are adjacent to at 18 hpf. The black line represents the average speed for each position along the AP axis, divided into 30 bins, and the gray ribbon represents the 95% confidence interval. The speed of a cell in

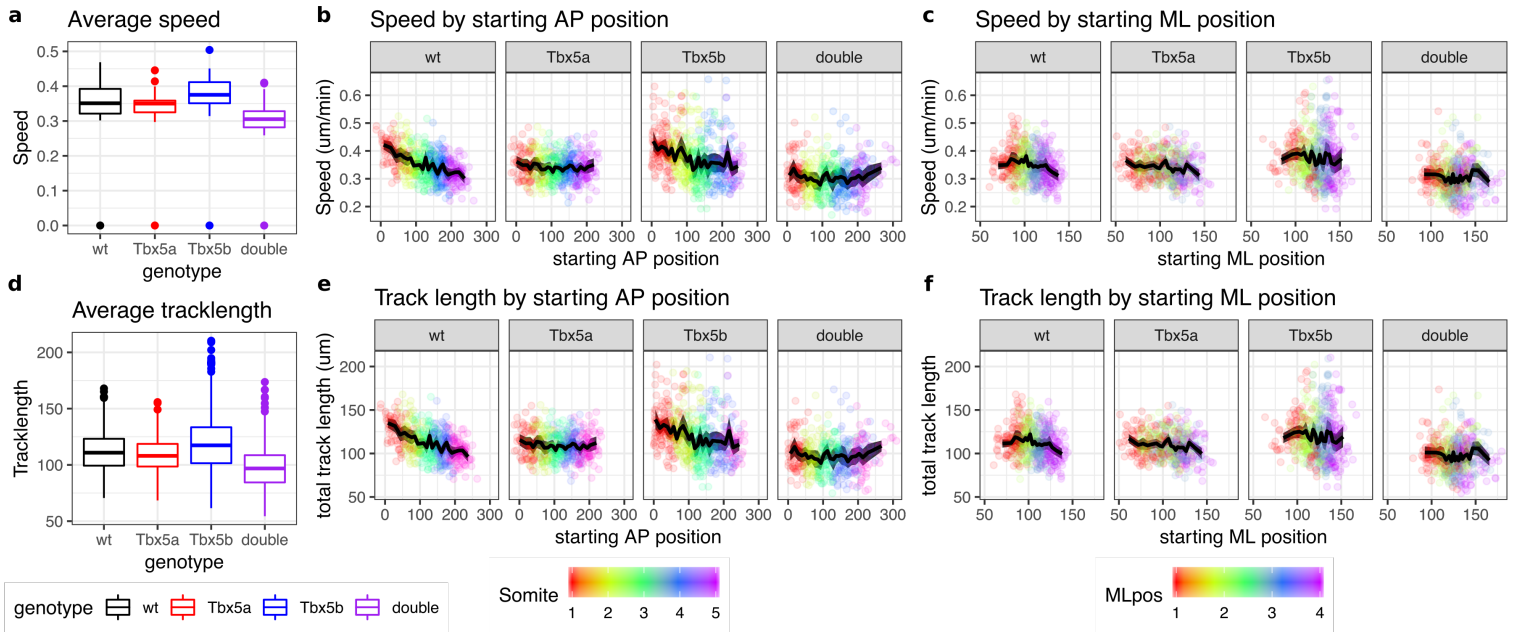

Figure 5.4: Speed and track length of embryos over time. All units of speed are measured in µm/minute and all units of distance are measured in µm. For measurements along the AP axis, red is for cells that started migrating adjacent to somite 1, yellow for cells that started migrating adjacent to somite 2, green for cells that started migrating adjacent to somite 3, blue for cells that started migrating adjacent to somite 4 and purple for cells that started migrating adjacent to somite 5. Color for position along the ML axis is red for quartile 1, green for quartile 2, blue for quartile 3 and purple for quartile 4. (a) Mean speed per genotype over all time points (b) Speed varies along AP position. (c) Speed is relatively constant with respect to starting ML position. (d) Plot of the final track length measurements per genotype. (e) Track length by starting AP position (f) Track length by starting ML position. For b-c, each dot represents the mean speed of a single track against it's position on either the AP or ML axis, colored by the respective position. The black line is the average speed at each position, divided into 30 bins. The gray ribbon is a 95% confidence interval. For d-e, each dot represents the final track length of a single track against its position on either the AP or ML axis, colored by the respective position. The black line is the average track length at each position, divided into 30 bins. The gray ribbon is a 95% confidence interval.

a wildtype embryo varies based on its initial position on the AP axis, with more anterior cells, such as those that begin their migration adjacent to somite 1, migrating with a greater average speed than more posterior cells, such as those that begin their migration adjacent to somite 4. This is consistent with previous interpretations of this data [31]. In Tbx5a-deficient embryos, the average speed of migration does not vary along the AP axis, consistent with previous interpretations of this data [31]. In Tbx5b-deficient embryos, the speed of the cells migrating is highest in the cells that begin their migration adjacent to somite 1 and lowest in the cells that begin their migration adjacent to somites 4, similar to the trends present in wildtype (Figure 5.4b).

In Figure 5.4c, the average speed of a cell over all time points is plotted against its position along the ML axis at 18 hpf. In wildtype embryos, the speed remains relatively consistent across the first three quartiles, although there is a slight decrease in speed in the most lateral cells of quartile 4. In both Tbx5a-deficient and Tbx5b-deficient embryos, the speed remains consistent across all initial ML positions (Figure 5.4c).

There is also a difference in the total track lengths of the Tbx5b-deficient embryos, compared to both wildtype and Tbx5a-deficient embryos. The track length is the total cumulative distance traveled by a cell over the course it is tracked. Similar to the values for speed, the track length is slightly but significantly increased in Tbx5b-deficient cells compared to wildtype cells (Figure 5.4d).

Figure 5.4e displays the track length of each cell plotted against its initial position on the AP axis, colored based on the somite the cell was adjacent to at 18 hpf. In wildtype embryos, the more anterior cells have an increased track length compared to more posterior cells. This suggests that the overall movement of these cells is greater, consistent with previous interpretations of this data [31]. In Tbx5a-deficient embryos, the track length does not vary based on the initial AP position of a cell, consistent with previous analysis of this data (Figure 5.4e) [31]. In Tbx5b-deficient embryos, anterior cells, such as those that begin

migration adjacent to somite 1, exhibit an increased track length compared to more posterior cells (Figure 5.4e). Furthermore, the overall track length is greater at all points along the AP axis compared to wildtype embryos, implying that the increase in overall track length is not due to changes at a specific location along the AP axis, but is increased uniformly across the AP axis.

Figure 5.4f displays the track length of each cell plotted against its initial position along the ML axis, colored by ML quartile. The most medial cells (purple, quartile 4) appear to have a slightly reduced track length when compared to the rest of the embryos, although this difference is slight and may be neither significant nor biologically relevant. There is no correlation between ML position and track length in either Tbx5a-deficient or Tbx5b-deficient embryos (Figure 5.4f).

5.4.4 Tbx5b-deficient embryos display decreased convergence along the AP axis

In Tbx5a-deficient embryos, the fin bud fails to form due to a complete loss of AP convergence [31]. Perhaps the small fin bud in Tbx5b-deficient embryos could be due to a reduction of AP convergence movements. AP convergence can most easily be visualized through use of a spaghetti plot, as in Figure 5.5a, which summarizes the AP trajectories for each embryo over time. Each red line is the average AP position over time of all cells that begin their migration adjacent to somite 1 for each embryo. Similar lines are also plotted in yellow for cells adjacent to somite 2, green for cells adjacent to somite 3 and blue for cells adjacent to somite 4. The black lines are the average AP position for all embryos adjacent to the respective somite. By plotting the movements of the LPM cells relative to the center of mass of the fin bud precursor pool, the plots illustrate that in the wildtype embryos, tracks from somite areas 1-4 converge along the AP axis as time progresses (Figure 5.5a, dashed circles). The purple lines represent the average position of cells adjacent to somite 5; these cells do

not contribute to the fin bud and do not converge (Figure 5.5a) [31].

In Tbx5a-deficient embryos, the trajectories displayed by the spaghetti plots reveal no convergence of the cells of the fin field, consistent with previous interpretations. The parallel trajectories of the fin field indicate that average position of cells adjacent to somites 1-4 remains constant from 18 hpf to 23 hpf. The size of the fin field (indicated with the dotted circle) is roughly the same size at both 18 hpf and 23 hpf (Figure 5.5a). The cells adjacent to somite 5 migrate away from the fin field in Tbx5a-deficient embryos. This is consistent with previous interpretation of this data suggesting that AP convergence is lost in Tbx5a-deficient embryos.

In Tbx5b-deficient embryos, the spaghetti plots reveal that there may be some convergence behaviors. The trajectories, most notably for those cells adjacent to somites 1 and 4, appear to show some AP convergence movements. Unlike in wildtype and Tbx5a-deficient embryos, the average position of cells adjacent to somite 5 also appears to show some slight AP convergence movements, suggesting that there may be overall tissue reduction in the LPM surrounding the fin field at this time. The average width of the fin field (dotted circles, Figure 5.5a) is less at 23 hpf than at 18 hpf, therefore AP convergence occurs, although it appears that the overall level of convergence is less than in wildtype embryos.

The amount of convergence depicted in these spaghetti plots can be quantified by calculating the compaction factor, found by taking the difference of the mean AP location of cells from somite 1 and cells in somite 4. This value is normalized by dividing by the difference at start of the time lapse analysis. A value of 1 would demonstrate no change in the convergence of cells from somite 1 and 4, while a value less than 1 demonstrates that cells from somite 1 are closer to cells from somite 4 than at the start of the tracking. The compaction factor for wildtype embryos decreases over time, consistent with the previously reported AP convergence movements [31], with a final compaction factor of 0.73 (Figure 5.5b). Tbx5a-deficient embryos have a compaction factor of around 1 throughout the whole time period,

consistent with the findings that they do not converge during this migration, with a final value of 1.02 (Figure 5.5b). Tbx5b-deficient embryos exhibit a decrease in the compaction factor over time, suggesting that they converge along the AP axis, with a final compaction factor of 0.88 at 23 hpf (Figure 5.5b) However, when compared to wildtype embryos, the overall compaction is intermediate (difference of 0.15), suggesting that Tbx5b-deficient cells do not converge as completely. One possibility for a reduction on compaction could be that Tbx5b-deficient embryos merely display a delay in convergence. However, if Tbx5b-deficient cells are tracked for an additional 20 time points, the compaction factor does not decrease after 23 hpf, suggesting that this decreased AP convergence is not merely due to a delay in convergence (Figure 5.5b). This suggests that a decreased convergence may be responsible for the small fin bud formed in Tbx5b-deficient embryos.

A similar measure of convergence is scatter, which measures the standard deviation of all cells in the fin field and compares it to the starting value. A scatter value of 1 indicates that the cells remain the same distance apart over time, while a decreasing value suggests that the cells are getting closer together. While compaction factor measures the overall changes in the fin field, by relying on the average position of cells adjacent to only somite 1 and somite 4, scatter accounts for the position of all the cells within the fin field. Consistent with interpretations from Mao et al., scatter decreases in wildtype embryos over time while increasingly slightly over time in Tbx5a-deficient embryos (Figure 5.5c) [31]. For Tbx5b-deficient embryos, scatter also decreases over time. This is consistent with the previous data finding that Tbx5b-deficient embryos display a partial convergence of the fin field.

The decrease in AP convergence in Tbx5b-deficient embryos compared to wildtype could be due to a change in the AP displacement of the cells of the fin field. The cells of wildtype embryos exhibit increasing AP displacement over time, with a final displacement of 37.83 µm during a period of 320 minutes (Figure 5.5d). The Tbx5a-deficient embryos exhibit a lower AP displacement over time (12.40 µm) (Figure 5.5d). The Tbx5b-deficient embryos

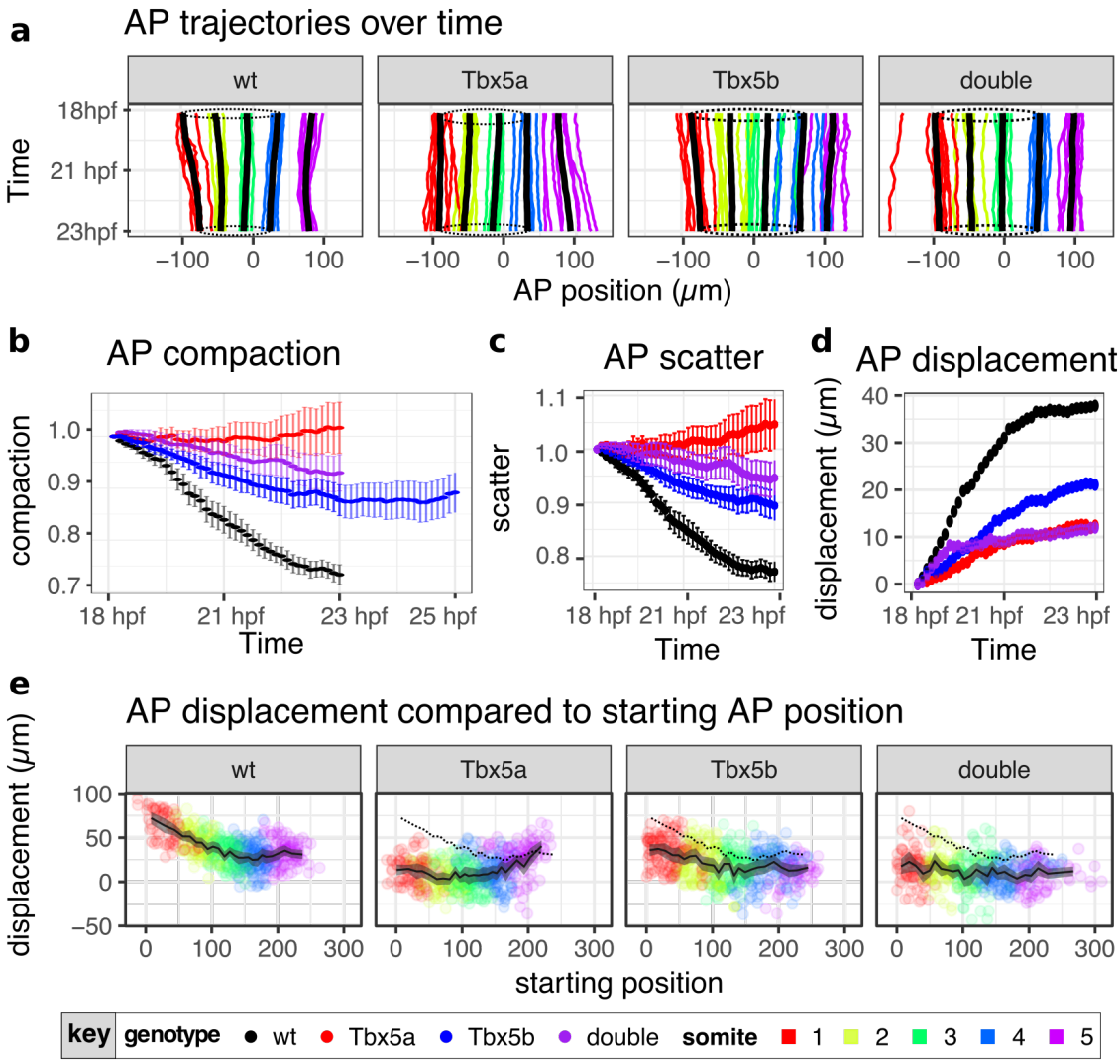

Figure 5.5: AP trajectories and displacement with regards to both time and AP position. (a) The mean AP position of for cells adjacent to somite 1-5, corrected for center of mass. Each colored line represents the mean AP position of the cells adjacent to a somite for each embryo, with the color representing the somite. The black lines represent the mean AP position for cells adjacent to each somite across all embryos of that genotype. (b) AP compaction factor from 18 hpf to 25 hpf. Each point represents the mean compaction factor across all embryos for the respective genotype. Only Tbx5b-deficient embryos were tracked to 25 hpf, all other genotypes were only analyzed until 23 hpf. (c) Average AP scatter over from 18 hpf to 23 hpf. (d) Average AP displacement from 18 hpf to 23 hpf. Each point represents the mean displacement value from starting position for each track at each time point. (e) Each colored point represents the total displacement for a single track with respect to starting position. The black line represents the mean displacement with respect to starting position, binned over 25. The gray ribbon represents the 95% confidence interval. The dotted line is the average displacement for wildtype embryos, plotted to allow easier comparisons. (continued on following page)

Figure 5.5: (Continued) Black is wildtype, red is Tbx5a-deficient, blue is Tbx5b-deficient and purple is double-deficient. Red represents cells adjacent to somite 1, yellow cells adjacent to somite 2, green cells adjacent to somite 3, blue cells adjacent to somite 4 and purple cells adjacent to somite 5. For b-d, error bars represent standard error.

exhibit a final AP displacement of 21.06 µm, approximately half of the total displacement of wildtype embryos along the AP axis (Figure 5.5d).

In Figure 5.5e, the final AP displacement for each cell is plotted against its initial position on the AP axis. As previously found in Mao et al. in wildtype embryos, all LPM cells along the length of the somite 1-4 area, have positive displacement values along the AP axis with the greatest values exhibited by the more anterior regions next to somite 1 and somite 2. In the Tbx5a-deficient embryos, the AP displacement values for the fin field cells is very close to zero across the entire AP axis. In Tbx5b-deficient embryos, most cells display positive displacement values and similar to wildtype embryos, the most anterior groups next to somite 1 and somite 2 display the highest levels of AP displacement. However, despite still displaying an anterior bias, the loss of AP displacement when compared to wildtype is greater among the anterior cells than the more posterior cells, with the difference in displacement of 27.5 µm between wildtype and Tbx5b-deficient cells for cells adjacent to somite 1 compared to a difference of 11.7 µm for cells adjacent to somite 4 (Figure 5.5e, compare to the dotted line).

Tbx5a affects AP convergence by regulating expression of *fgf24*. Is *fgf24* responsible for the reduced convergence seen in Tbx5b-deficient embryos? At 21 hpf, *fgf24* is expressed in a subset of cells in the fin field (Figure 5.6a) [31, 32]. Consistent with previously reported data, Tbx5a-deficient embryos lack *fgf24* in the fin field (Figure 5.6b). Tbx5b-deficient embryos display expression of *fgf24* in the fin field, although expression appears to be reduced compared to wildtype embryos (Figure 5.6c).

Could the decreased convergence contribute to the small fin bud such that not all cells of the fin field are able to contribute to the fin bud in Tbx5b-deficient embryos? In order to identify the cells of the fin field, a *Tg(tbx5a::GFP)* line was used, which marks all Tbx5a+

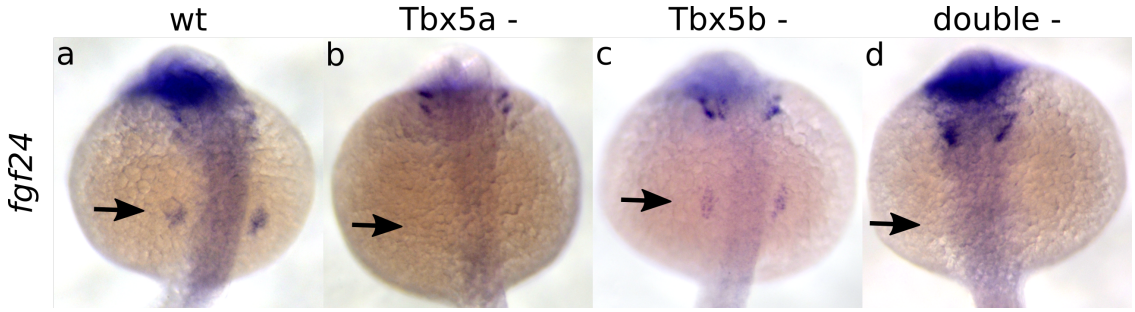

Figure 5.6: *fgf24* expression is reduced in Tbx5b-deficient embryos. (a) *fgf24* is expressed in the fin field of wildtype embryos (b) *fgf24* is lost from the fin field of Tbx5a-deficient embryos (b) *fgf24* expression is decreased in the fin field of Tbx5b-deficient embryos (d) *fgf24* expression is lost in double-deficient embryos. All embryos are shown at 21 hpf in a dorsal view, anterior is oriented towards the top. Arrows indicate the location of *fgf24* expression in the fin field.

cells with GFP [131]. At 30 hpf, the fin field domain is spatially distinct from the heart forming domain and a morphologically-distinct fin bud is present; however, not all Tbx5a+ cells are contributing to the fin bud (Figure 5.7a, fin bud outlined in red). Likewise, in Tbx5b-deficient embryos, a fin bud is present and there are also cells located outside of the fin bud (Figure 5.7b, fin bud outlined in red). To estimate the differences in size between the fin field and fin bud of wildtype and Tbx5b-deficient embryos, the area of Tbx5a/GFP+ cells was measured in 8 embryos of each genotype. The boundaries of the fin bud were identified by visualizing the fin bud in three dimensions, after which the area was estimated using the maximum intensity projection. While this method may underestimate the number of cells within the three-dimensional fin bud, the cells located outside of the fin bud are present as only a single layer of cells, so it should provide an accurate estimate for those cells. There is no significant difference between the total area covered by Tbx5a/GFP+ cells between wildtype and Tbx5b-deficient embryos (Figure 5.7c). However, consistent with the differences in overall size of the fins, the area of fin buds in Tbx5b-deficient embryos displays a significant ($p<0.01$) decrease in area compared to wildtype embryos (Figure 5.7d). Furthermore, the area of the cells outside of the fin is significantly increased ($p<0.05$) in Tbx5b-deficient embryos compared to wildtype embryos (Figure 5.7e). This suggests that

the small fins in Tbx5b-deficient embryos may indeed be smaller because the cells of the fin field fail to make it into the fin bud.

Because cells of the fin field display different amounts of displacement depending on their location on the AP axis (Figure 5.5e) [31], the initial position of a cell could determine if a cell will contribute to the fin bud in a Tbx5b-deficient embryo. In order to test this hypothesis, the Tbx5a/GFP+ domain was divided into three regions: cells anterior to the fin bud, cells adjacent to the fin bud and cells posterior to the fin bud. Cells adjacent to the fin bud are cells that are not within the fin bud but are located neither anterior nor posterior to the fin bud. The surface area of cells anterior to the fin bud was significantly ($p<0.05$) larger than wildtype (Figure 5.7f), while there was no significant difference in area between cells adjacent or posterior to the fin bud (Figure 5.7g-h), suggesting that cells from the anterior regions of the fin field are less able to contribute to the fin bud in Tbx5b-deficient embryos than either cells from posterior regions of the fin field or the anterior regions of wildtype cells. This conclusion can be reached because cells are known to migrate spatiotopically along the AP axis in both wildtype and Tbx5b-deficient embryos (Figure 5.3b) [31].

5.4.5 Tbx5b-deficient embryos display a loss of displacement along the ML axis

Observing the time-lapse images of the Tbx5b-deficient embryos suggested that these embryos exhibit defects in the ML migration process. To differentiate the cells along the ML axis, the trajectories were divided into quartiles based on the ML extent of the GFP-positive cells of each individual *Et(hand2:GFP)ch2* embryo. Each colored line in Figure 5.8a represents the average ML position of all cells in that quartile over time per embryo, and the black line represents the average ML position for all embryos over time in each quartile. Both wildtype and Tbx5a-deficient embryos display a consistent ML migration across all groups, which is visualized by the slope of both the colored and the black lines (Figure 5.8a). How-

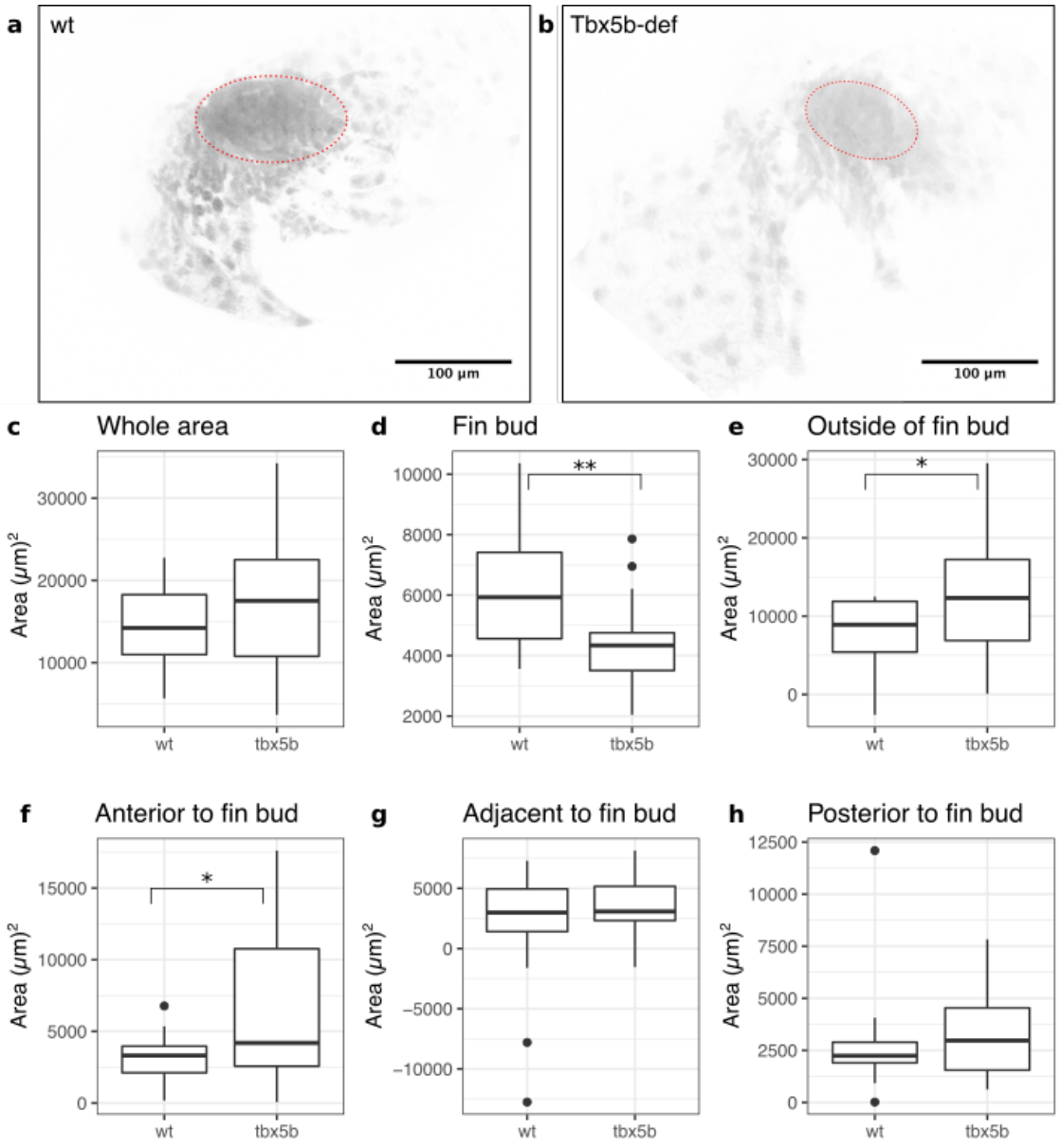

Figure 5.7: Tbx5b-deficient fin buds are small because more cells fail to join the fin bud. (a-b) Max intensity projections of representative fin buds at 30 hpf of *Tg(Tbx5a::GFP)* embryos. The fin bud is outlined in red. Anterior is to the left, the midline is up. Representative images are shown for both (a) uninjected and (b) Tbx5b-deficient embryos. (c-h) Measurements of the area of GFP+ cells in and surrounding the fin buds of these embryos. For both conditions, n=8 embryos and 16 fin buds. (c) There is no significant difference in the total area between wildtype and Tbx5b-deficient embryos. (d) There is a significant ($p<0.01$) difference in the area of wildtype and Tbx5b-deficient fin buds. (e) There is a significant different ($p<0.05$) in the amount of GFP+ expression outside of the fin bud. (f) There is a significant difference ($p<0.05$) in the amount of cells outside the fin bud that are located anterior to the fin bud. There is no significant difference in the amount of cells outside the fin bud located either adjacent (g) or posterior (h) to the fin bud.

ever, Tbx5b-deficient cells display a marked difference in behavior along the ML axis, with essentially no overall change in starting versus final position along the ML axis (Figure 5.8a). The slopes of the both the black and the colored lines are flat, suggesting that the average position of all cells in a given quartile neither moves away from nor towards the midline.

Measuring the ML displacement for each cell also suggests a lack of ML migration in Tbx5b-deficient embryos. Figure 5.8b calculates displacement along the ML axis; both wildtype and Tbx5a-deficient embryos display similar rates of displacement during the first 5 hours of migration. However, Tbx5b-deficient embryos appear to display no net displacement along the ML axis over time (Figure 5.8b). This data implies that ML migration is severely impaired in Tbx5b-deficient embryos, unlike Tbx5a-deficient embryos.

The compaction factor along the ML axis measures the relative distance between cells in the most medial and most lateral quartile over time. There is no significant difference between the final compaction factor of wildtype and Tbx5b-deficient embryos (Figure 5.8c, p=0.37). Likewise, there are no significant difference between any genotype when measuring ML scatter (Figure 5.8d). Unlike AP displacement, ML displacement does not vary along the ML axis (Figure 5.8e). Combined, this data suggests that the ML migration occurs at a consistent rate throughout the fin field.

Since ML migration is strongly reduced in Tb5b-deficient embryos, does this affect fin positioning? In order to test this hypothesis, I measured the distance between the fin buds in *tbx5b -/-* embryos and their wildtype siblings at 30 hpf. Fin buds were first stained with *tbx5a* via *in situ* hybridization, imaged dorsally on the Zeiss Axioplan microscope, then measurements were taken in FIJI. Two measurements were taken: the shortest distance between the two fin buds and the distance between the centers of each fin bud. The distance between the midpoints of wildtype and *tbx5b -/-* siblings showed no significant difference (p=0.705). Likewise, measuring the closest difference between the sites of *tbx5a* expression also found no significant difference (p=0.939).

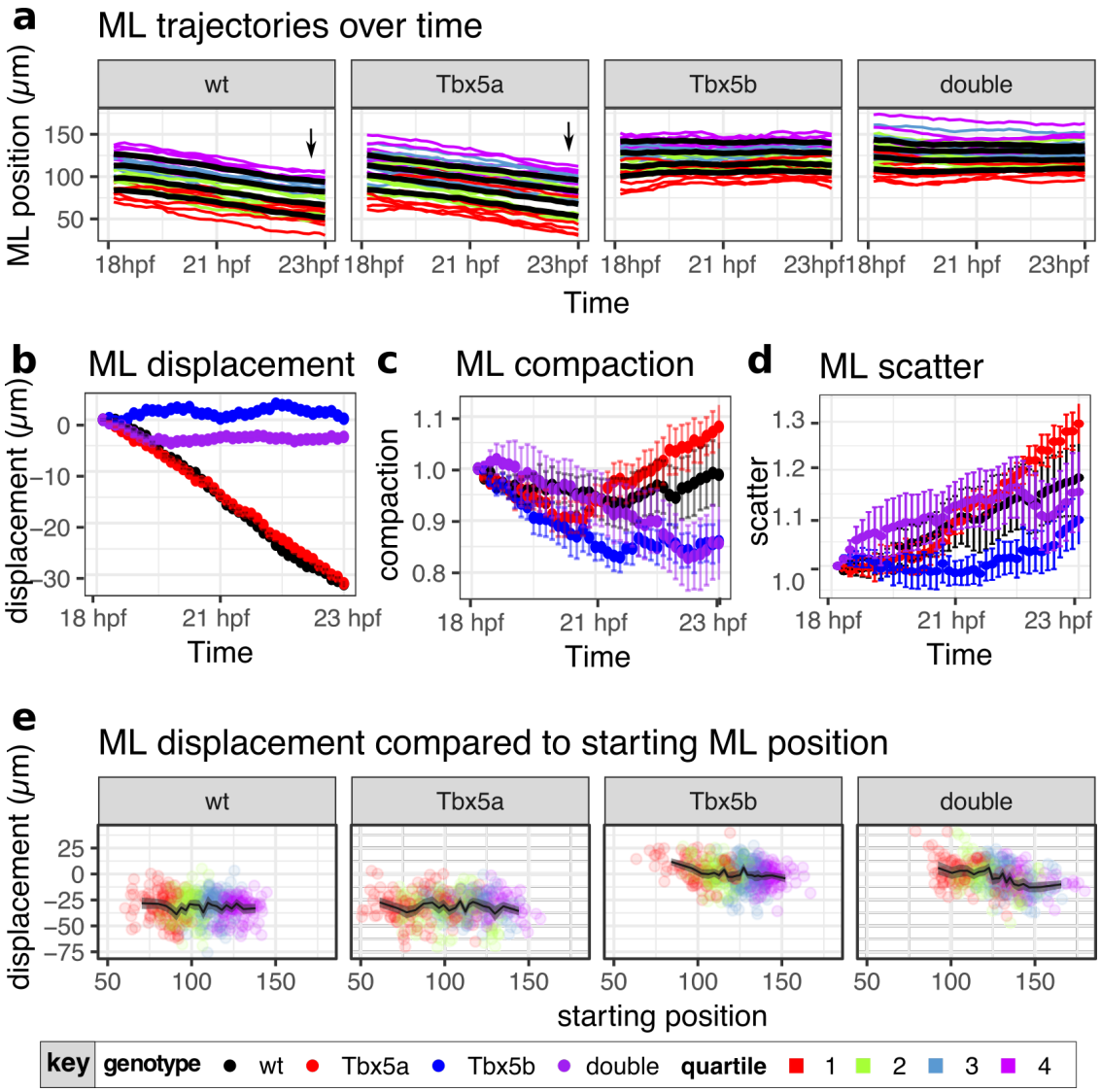

Figure 5.8: ML trajectories and displacement with regards to time and ML position. Black is wildtype, red is Tbx5a-deficient, blue is Tbx5b-deficient and purple is double-deficient. ML quartiles from medial to lateral: red: 1, green:2, blue:3, purple:4. (a) The mean ML position of for embryos divided into 4 quartiles. Each colored line represents the mean ML position per quartile per embryo. The black lines represent the mean ML position for cells adjacent to each somite across all embryos of that genotype. (b) ML displacement from 18 hpf to 23 hpf. Each point represents the mean displacement value from starting position for each track at each time point. (c) ML compaction from 18 hpf to 23 hpf. Each point represents the mean compaction factor across all embryos for the respective genotype. Error bars represent standard error. (d) ML scatter from 18 hpf to 23 hpf. Each point represents the mean scatter across all embryos for the respective genotype. Error bars represent standard error. (e) Each colored point represents the total displacement for a single track with respect to starting position. The black line represents the mean displacement with respect to starting position, binned over 25. The gray ribbon represents the 95% confidence interval.

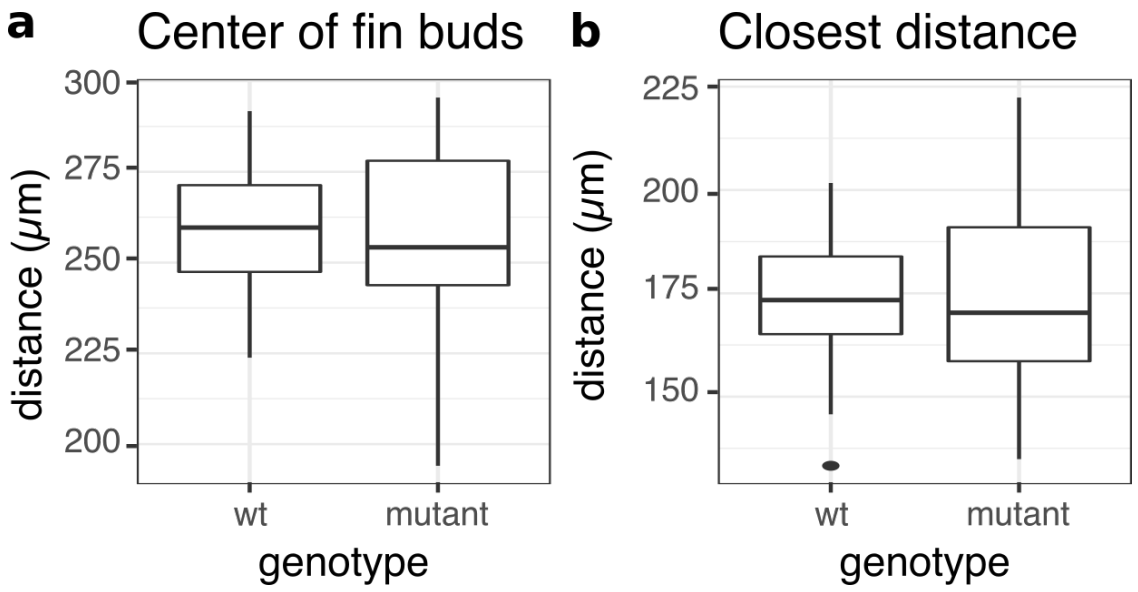

Figure 5.9: ML positioning of the fin buds of *tbx5b* -/- embryos. Distance between fin buds of 30 hpf embryos, n=30 for wildtype siblings and n=15 for *tbx5b* -/- embryos. (a) Distance between the center of the fin bud in wildtype siblings and *tbx5b* -/- embryos at 30 hpf showed no significant difference. (b) Distance between the closest points of the two fin buds was not significantly different between *tbx5b* -/- mutants and wildtype siblings.

5.4.6 Double-deficient embryos display a loss of directional migration and a trend towards more random migration

If Tbx5a and Tbx5b act separately to regulate the AP and ML directions of fin field migration, respectively, then loss of both paralogues should result in cells of the fin field that fail to migrate along both the AP and ML axes. However, another possibility is that Tbx5a and Tbx5b have redundant functions that will be revealed when both paralogues are lost. *in situ* hybridizations were performed to analyze the size and shape of the fin field via *tbx5a* expression at time points throughout fin field migration. If migration is primarily controlled by Tbx5a and Tbx5b across the different axes, *tbx5a* expression marking the fin field should remain relatively consistent over time. Consistent with this hypothesis, examination of the cells of the fin field via *tbx5a* expression reveals expression in two bilateral stripes at 16 hpf, which remains unchanged through 25 hpf (Figure 5.1g-g’’’).

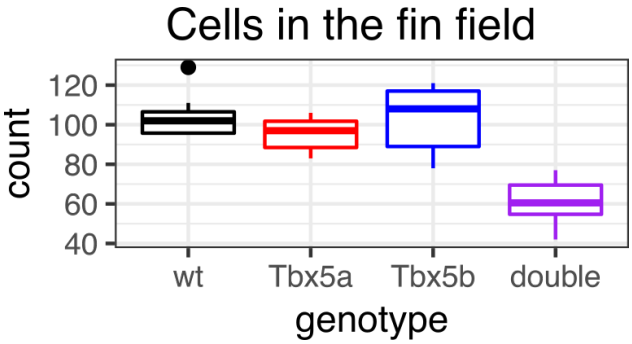

Figure 5.10: Double-deficient embryos have fewer cells in the fin field than wildtype embryos at 18 hpf. This plot shows the number of nuclei located adjacent to somites 1-4 in the LPM of wildtype, Tbx5a-deficient, Tbx5b-deficient and double-deficient embryos.

In order to more fully understand how the *tbx5* paralogues act in combination, cells of the fin field in double-deficient embryos were time-lapsed imaged in the *Et(hand2:GFP)ch2; Tg(h2afx:h2afv-mCherry)mw3* line and their cell movements analyzed as described above. In double-deficient embryos, the cells of the fin field do not make extensive net migration movements in either the ML or AP directions, and the size and shape of the prospective fin field remains relatively constant throughout the course of the movie (Figure 5.1d-d'''). Additionally, the fin field appears smaller in double-deficient embryos. To confirm this observation, the LPM nuclei located between somites 1-4 were counted at 18 hpf, which revealed that there are significantly fewer nuclei present in double-deficient embryos compared to either wildtype or single-deficient embryos (Figure 5.10, p=0.0000015). This is especially notable because loss of a single paralogue does not produce any significant change in the number of nuclei in this region (Figure 5.10).

When the tracks of double-deficient cells are analyzed, they exhibit reduced migration along both axes (Figure 5.3a). Many of the tracks are extremely short with a cell remaining in essentially the same location from 18 hpf to 23 hpf (Figure 5.3a, arrowheads in double-deficient embryo 1, 4, 7) while other tracks are comparatively longer (Figure 5.3a, starred tracks in embryos 2, 7). Some embryos contain both short tracks and longer tracks (i.e. embryo 7). The overall ML extent that these tracks cover is reduced compared to either wildtype of Tbx5a-deficient embryos, suggesting that like Tbx5b-deficient embryos, these tracks display defects in ML migration. It is unclear from the tracks alone how these cells

behave along the AP axis.

Plotting the AP position of a double-deficient cell at 18 hpf against its AP position at 23 hpf reveals a similar pattern to wildtype (Figure 5.3b). The best-fit line has a y-intercept of 16.6 and a slope of 0.962, with an R^2 value of 0.934. This suggests that the final AP position is highly correlated with the initial AP position and that migration along the AP axis remains spatiotopic in double-deficient embryos. Figure 5.3c plots the ML position of double-deficient cells at 18 hpf against the position of the same cell at 23 hpf. The behavior of these cells is spatiotopic, with the final ML position predictable by the ML position at 18 hpf. Furthermore, similar to Tbx5b-deficient embryos, the cells of double-deficient embryos are located at similar positions at both 18 hpf and 23 hpf, suggesting that there may be an impairment in ML migration. Consistent with results for wildtype embryos, double-deficient embryos display neither a correlation between starting AP position and final ML position (Figure 5.3d) nor between the starting ML position and the final ML position (Figure 5.3e).

The double-deficient embryos exhibit less overall movement than either wildtype or single deficient embryos. Notably, the average speed over all time points for double-deficient cells is significantly less than the speed of wildtype cells (difference of 0.30 µm/min, $p<2.2e-16$, Figure 5.4a). Furthermore, the speed remains consistent across both the AP and the ML axis (Figure 5.4b-c). There is also a corresponding decrease in the overall track length of the cells tracked in the double-deficient embryos (97.512 µm versus 112.118 µm, $p<2.2e-16$, Figure 5.4d). The track length does not vary along the AP or the ML axis in double-deficient embryos (Figure 5.4e-f).

The trajectories of the double-deficient cells along the AP axis display a greatly reduced level of AP displacement compared to either wildtype or Tbx5a-deficient embryos (Figure 5.5a), illustrating that in double-deficient embryos, cells do not move as far from their starting points along the AP axis. Furthermore, the AP compaction is also decreased (Figure 5.5b) as reflected in the final AP compaction factor of 0.929. Likewise, the double-

deficient embryos do not exhibit the same decline in AP scatter as seen in wildtype embryos (Figure 5.5c). Similar to Tbx5a-deficient embryos, double-deficient embryos lack any expression of *fgf24* (Figure 5.6d). Combined, this evidence suggests that double-deficient embryos display a general loss of the AP convergence movements seen in wildtype embryos, similar to what is observed in Tbx5a-deficient embryos.

When comparing the ML movement of the double-deficient embryos to wildtype or single-deficient embryos, double-deficient cells behave similarly to Tbx5b-deficient cells. Notably the ML spaghetti plots illustrate that, similar to the Tbx5b-deficient embryos, the double-deficient embryos do not exhibit a concerted ML migration away from the midline over time, as depicted by the flat slopes (Figure 5.8a). Neither the ML compaction factor (Figure 5.8c) nor the ML scatter (Figure 5.8d) is significantly different when compared to wildtype ($p=0.35$, $p=0.99$, respectively). Furthermore, the overall ML displacement is greatly reduced in double-deficient embryos when compared to the ML displacement seen in both wildtype and Tbx5b-deficient embryos (Figure 5.8b). Overall, this data suggests that double-deficient embryos display a general loss of combined ML migration movements, similar to the behavior of Tbx5b-deficient embryos along this axis.

Double-deficient embryos display a general defect in directional migration, as seen by loss of migration movements along both the AP and ML axes. Three separate measures were used to analyze the amount of directional migration behavior present in double-deficient embryos: an overall measure of ballistic movement of the fin field cells (the alpha value), a measure of persistence, and a measurement of the overall angles of migration.

The slope of the log-log plot of mean square displacement versus time, called the alpha value, is a measure of the degree of ballistic versus random movement. An alpha value of 2 represents perfectly ballistic movement while an alpha value of 1 represents perfectly random movement. The alpha value for wildtype cells is 1.72, which is closer to ballistic movement than to random movement (Figure 5.11a). However, both Tbx5a-deficient and

Tbx5b-deficient cells have a decreased alpha value, of 1.51 and 1.35, respectively, thereby suggesting a decreased tendency towards ballistic movement. The alpha value for the double-deficient embryos is 1.11, which is closer to a value of 1 and random migration than the alpha value of either wildtype or single-deficient embryos (Figure 5.11a).

Another measure of the directedness of migration is persistence, which is the ratio of displacement to track length. The higher the persistence value, the more direct the migration is. The Tbx5a-deficient embryos display a decreased persistence compared to wildtype (Figure 5.11b). However, Tbx5b-deficient embryos, in blue, display an even greater decrease in persistence than Tbx5a-deficient embryos, which is the same pattern as seen in comparing alpha values (Figure 5.11b). Double-deficient embryos display the same rates of persistence as Tbx5b-deficient embryos (Figure 5.11b).

Figure 5.11c plots the final persistence value against the position of a cell at 18 hpf, colored by adjacent somite. Previous analysis has found that in wildtype embryos, the cells adjacent to somite 1 and 2 display higher persistence values than cells adjacent to somites 3 and 4 and that this difference in persistence is lost in Tbx5a-deficient embryos [31]. Since Tbx5b-deficient embryos exhibit an overall lower level of persistence, do they lose this correlation with AP position? Although persistence is decreased across the AP axis in Tbx5b-deficient embryos compared to either wildtype or Tbx5a-deficient embryos, the more anterior cells display slightly higher levels of persistence than do the more posterior cells (Figure 5.11c). Although double-deficient embryos display similar trends to Tbx5b-deficient embryo with regards to fin-field wide persistence, unlike Tbx5b-deficient embryos, persistence rates remain uniform across the AP axis (Figure 5.11c).

Figure 5.11d plots persistence against the initial ML position of a cell, color-coded based on initial quartile. There are mild trends in persistence when measured along the ML axis: the cells in quartile 1, which are most lateral, have lower levels of persistence than the cells in quartile 4, which are more medial (Figure 5.11d). This change in persistence along

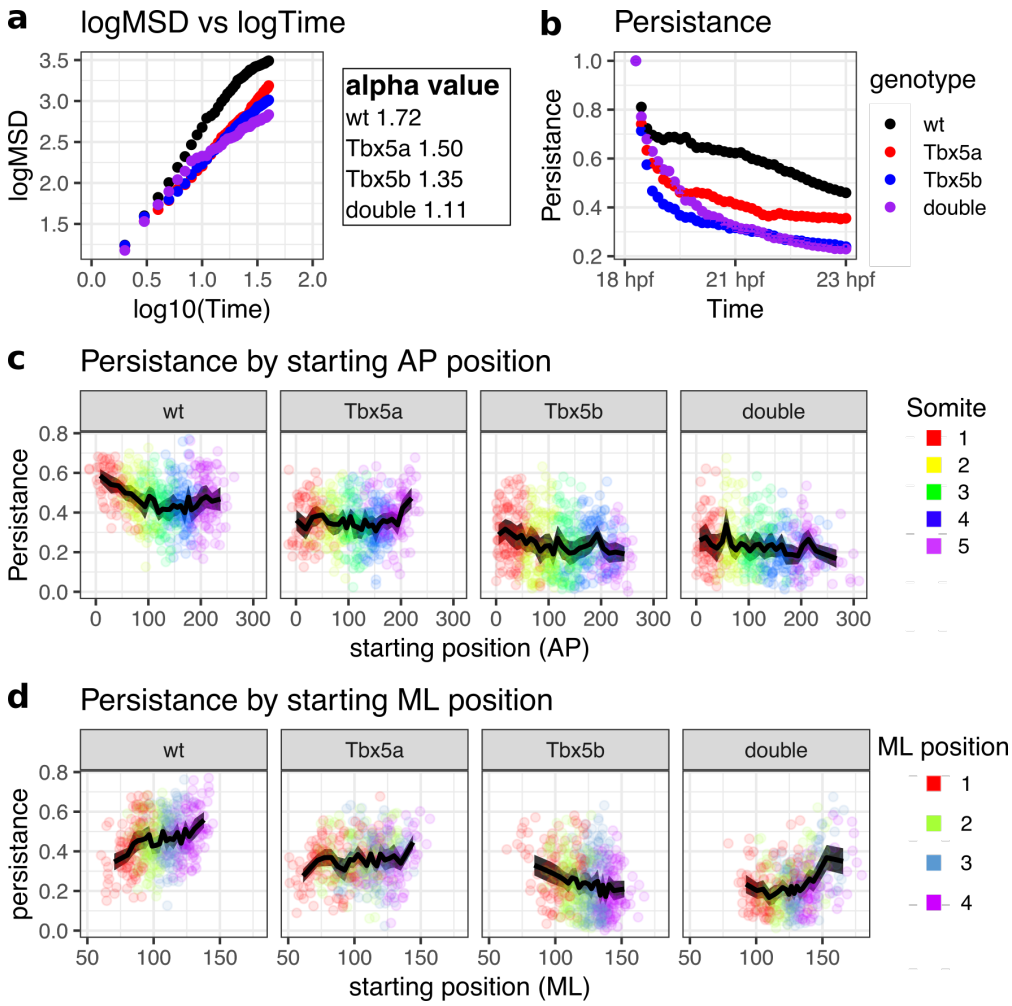

Figure 5.11: Tbx5b and double-deficient cells exhibit less directed migration than either wildtype of Tbx5a-deficient cells. The log-log plot of MSD versus time allows calculation of the alpha values, which is the slope of the line. (b) Persistence for each of the embryos over time. Black is wildtype, red is Tbx5a-deficient, blue is Tbx5b-deficient and purple is double-deficient. (c) Persistence by starting AP position, divided by genotype. Each dot is the mean persistence for each track plotted against the starting AP position. The color represents the somite that the cell was adjacent by at the beginning of migration, red for somite 1, yellow for somite 2, green for somite 3, blue for somite 4 and purple for somite 5. The black line is the mean persistence for all embryos binned into 30 segments. The gray ribbon is the 95% confidence interval. (d) Persistence plotted against starting ML position. Each dot represents the mean persistence values and is colored by the ML position, with red for quartile 1, green for quartile 2, blue for quartile 3 and purple for quartile 4. The ML axis is measured in µm. The black line represents the mean position divided into 30 bins. The gray ribbon is the 95% confidence interval.

the ML axis is lost in Tbx5a-deficient embryos, despite the fact that the movements along the ML axis in Tbx5a-deficient embryos is largely normal (Figure 5.11d). However, the correlation between persistence and ML position is reversed in Tbx5b-deficient embryos, with cells that are more medial displaying lower levels of persistence than cells that are more lateral, indicating that migration is even less directed closer to the midline (Figure 5.11d). Double-deficient embryos display low levels of persistence in quartiles 1-3, with a slight increase in persistence in the most lateral cells of quartile 4 (Figure 5.11d). Overall, the levels of persistence in Tbx5b-deficient and double-deficient embryos are similar, although the trends are distributed differently across the ML axis. The biological impact of these trends is uncertain, especially as no other variables exhibited similar trends across the ML axis.

The third measure of directional migration analyzed was the angle of migration of a cell. In this dissertation, the angle of migration is measured by taking the angle of a cell's displacement trajectory. Figure 5.12 displays the overall angles of migrating LPM fin field cells grouped by adjacent somite. As previously published, when wildtype cells in the fin field converge, they do so topologically, with cells lateral to somite one migrating a different distance and angle than cells lateral to somite four [31]. Therefore measuring the angle of migration reveals information about the regulation of directional migration in the fin field. The migration angle was measured by calculating the displacement of each track relative to the mediolateral axis, which is arbitrarily set to 0 in Figure 5.12. The graphs are oriented such that the AP axis is the X-axis and the ML axis is the Y-axis. Cells that migrate posteriorly will have positive migration angles and cells that migrate anteriorly will have negative migration angles.

In wildtype embryos, the more anterior cells migrate with a positive angle, while the more posterior cells tend to migrate with a negative angle. The cells of the AP axis are divided based on the somite that cell is adjacent to at 18 hpf; cells within a somite group display

similar angles of migration. Overlaying all 4 cell groups displays progression in angles of displacement from somites 1 to 4, as the tracks move along the AP axis (Figure 5.12).

In Tbx5a-deficient embryos, all LPM cells adjacent to somites 1-4 are migrating laterally in the same direction, appearing on the rose diagram with most tracks having a displacement angle close to 0, or pointing laterally (Figure 5.12). This is consistent with the previously shown data indicating that Tbx5a-deficient cells migrate parallel across the ML axis.

When the angles of migration of cells in Tbx5b-deficient embryos are examined, there are several new trends. First, unlike either wildtype or Tbx5a-deficient embryos, a large proportion of Tbx5b-deficient cells are migrating both laterally and medially. These movements may be responsible for the net absence of medio-lateral displacement in the Tbx5b-deficient cells. However, the general AP directions of migration is still preserved. Cells adjacent to somite 1 are still migrating with a primarily positive angle, while cells in somites 3 and 4 are still migrating with a primarily negative angle (Figure 5.12).

For double-deficient embryos, the angles of migration appear to be more uniformly distributed than Tbx5b-deficient embryos (Figure 5.12). For all cells adjacent to somites 1 to 4, the angles of migration appear to be relatively uniform around the plot, suggesting an increased tendency towards random migration in these embryos (Figure 5.12). Overall, this data suggests that while the double-deficient fin field cells still retain the capability for movement, they display a decreased ability to migrate in a directional manner along either axis.

Although the cells appear to have directional migration under which the location determines the overall direction of migration, it is unclear what processes mediate this migration within the cell. Previous studies have used centrosome positioning as a reliable marker for cell-orientation and polarity, as the centrosome is located at the leading edge of cells undergoing migration [94]. Therefore, the angle of the centrosome relative to the nucleus in wildtype embryos was measured, with Xcentrin::RFP RNA used to locate the centrosome.

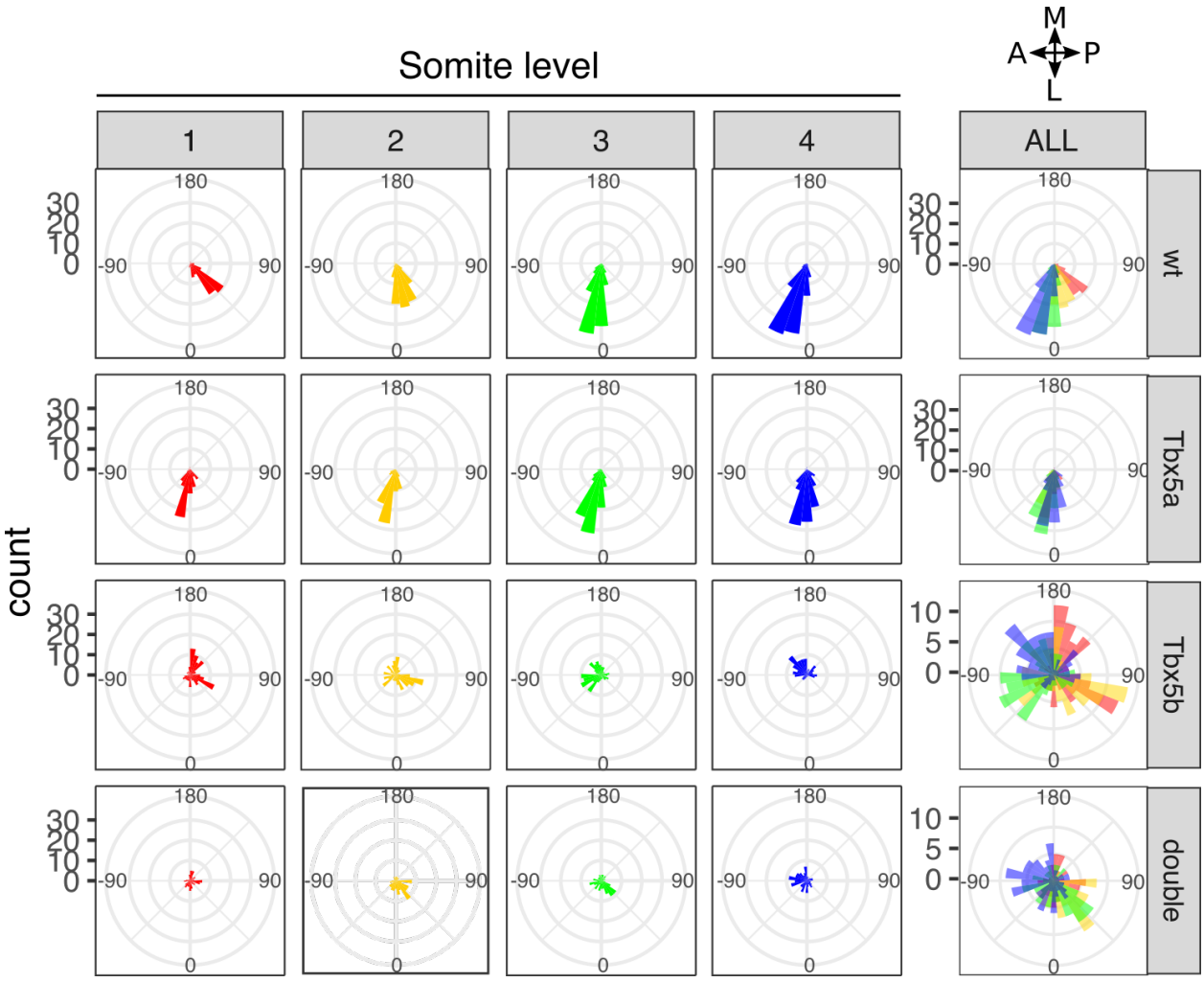

Figure 5.12: Angles of migration by somite level and genotype. The rose diagrams are angular histograms displaying the count of angles binned into 30 groups. Cells adjacent to somite 1 in red, cells adjacent to somite 2 in yellow, cells adjacent to somite 3 in green and cells adjacent to somite 4 in blue. Wildtype deficient embryos display a directed migration, with different angles of migration for somites 1-4. Tbx5a-deficient embryos display similar angles of migration across the AP axis. Tbx5b-deficient embryos display different angles of migration with along the AP axis, but display migration both medially and laterally. double-deficient embryos display random angles of cell migration across all AP positions. The graphs are arranged so that each migration angle is translocated to the origin and arranged so that anterior is to the left, as depicted by the axis in the top right. A-Anterior, P=Posterior, M-Medial, L-Lateral.

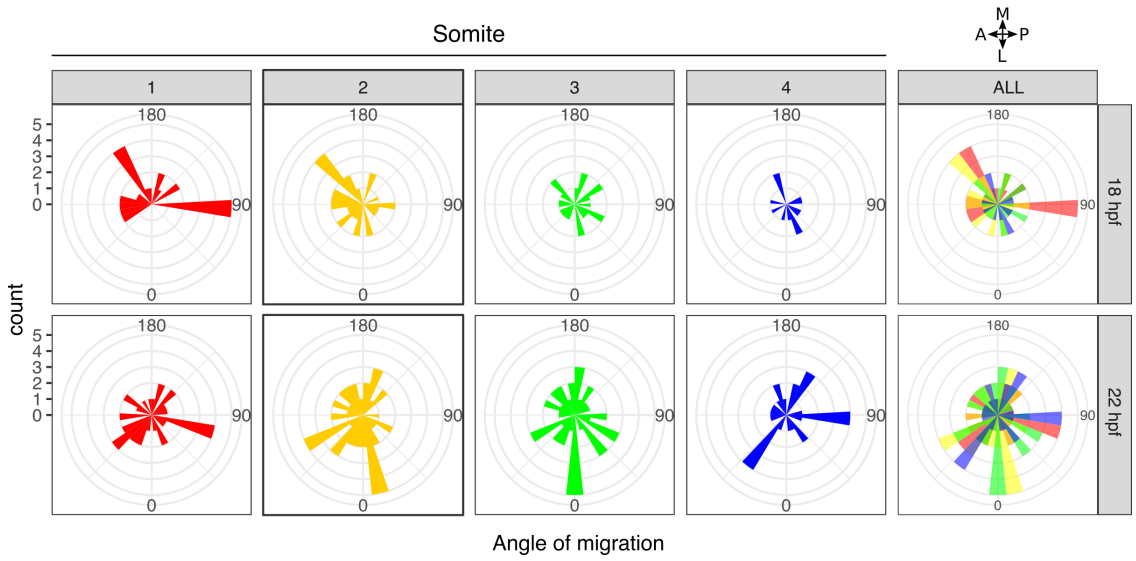

Figure 5.13: xCentrin::RFP localization detects no evidence of polarized migration. The rose diagrams are angular histograms displaying the count of angles binned into 30 groups. At 18 hpf in wildtype embryos, the angle of xCentrin::RFP expression with respect to the nucleus found no significant bias in angle. At 22 hpf, the angle of xCentrin::RFP with respect to the nucleus found no significant bias in angle. The graphs are arranged so that each migration angle is translocated to the origin and arranged so that anterior is to the left, as depicted by the axis in the top right. A-Anterior, P=Posterior, M-Medial, L-Lateral.

At both 18 and 22 hpf, there was no bias in the angles of centrosome migration, either within individual somite groups or across the fin field as a whole (Figure 5.13). This suggests that although directional migration is occurring, the mechanisms regulating this may be different than the mechanisms regulating traditional polarized cells migration seen in fibroblast or neural crest migration.

5.5 DISCUSSION

5.5.1 Decreased convergence along the AP axis may contribute to a small fin bud in Tbx5b-deficient embryos

In this chapter, I have characterized the role of zebrafish *tbx5b* during fin bud formation by comparing the migration dynamics of LPM cells in Tbx5b-deficient embryos to previously published, but contemporaneously re-analyzed, data on wildtype and Tbx5a-deficient embryos. The migration parameters of double-deficient embryos were also analyzed.

Whereas Tbx5a-deficient zebrafish lack fin buds and pectoral fins, Tbx5b-deficient zebrafish form small, misshapen pectoral fins (Figure 3.2) [10, 87]. Tbx5b-deficient fin buds retain early signaling centers, with a small but intact AER and ZPA (Figure 3.3). However, at all stages, the fin buds are smaller than wildtype and I hypothesize that this is due to fewer LPM cells coming to reside within the initial mesenchymal core of the early fin bud. To understand the role *tbx5b* plays prior to fin formation, I examined the underlying dynamics of cell migration in the fin field of Tbx5b-deficient embryos.

The small fin bud appears to be due to defects in the direction of migration rather than defects in the ability of the cells to migrate. In Tbx5b-deficient embryos, the cells of the fin field fail to fully converge along the AP axis when forming a fin bud. Tbx5b-deficient embryos display a final AP compaction factor that is approximately half that of wildtype. This is not a delayed convergence, as extending the cell tracking analyses for another 20 time

points (until 25 hpf) reveals that the compaction factor plateaus at 23 hpf (Figure 5.5b). This is also not due to defects in the ability of the cells to migrate, as LPM cells in Tbx5b-deficient embryos migrate with an increased speed when compared to wildtype (Figure 5.4a). While the compaction factor calculates the size of the fin field over time, the scatter value calculates the space between cells. Similar to compaction factor, the final scatter value in Tbx5b-deficient embryos is approximately half of the final wildtype scatter values, further indicating that the fin field of Tbx5b-deficient embryos partially converges along the AP axis over time.

Furthermore, the small fin bud does not appear to be due to a decrease in the size of the fin field of Tbx5b-deficient embryos. There is no significant difference in the number of cells located in this region between wildtype and Tbx5b-deficient embryos (Figure 5.10). Additionally, the cells adjacent to somites 1-4 still appear to converge suggesting they continue to behave as fin field cells (Figure 5.5).

How could Tbx5b be regulating AP convergence in the fin field? As previously reported [31, 32] the fin field cells are dependent upon a Fgf24 signal in the mesenchyme for the AP convergence movements to occur; knock down or loss of Fgf24 either directly or as a consequence of Tbx5a-deficiency leads to the failure of LPM cells to converge and instead these cells migrate laterally past the site of the fin bud [31]. Mao et al. hypothesized that partial knockdown of Tbx5a led to a decrease in Fgf signaling, particularly in the expression of the Tbx5a dependent target gene *fgf24* resulting in smaller fin buds. At 21 hpf, during the stages of fin field migration, expression of *fgf24* is present in the fin field of Tbx5b-deficient embryos, although expression is reduced compared to wildtype embryos (Figure 5.6), which could be responsible for a reduction in AP convergence of the fin field. This would indicate that although Tbx5b is not necessary for *fgf24* expression, it may be involved in regulating the levels of expression.

Tbx5b-deficient embryos display a bias along the AP axis with regards to many mea-

surements, such as displacement, even when the overall values are reduced with respect to wildtype. However, even in Tbx5b-deficient embryos, the anterior cells adjacent to somite 1 have a greater displacement than the more posterior cells adjacent to somite 4 (Figure 5.5e). Similar to wildtype embryos, these anterior cells are also migrating with a greater speed than more posterior cells. However, the anterior cells are the most affected by loss of Tbx5b, displaying the greatest loss in displacement in Tbx5b-deficient embryos compared to wildtype embryos.

Furthermore, Tbx5b-deficient embryos have a greater proportion of cells outside of the fin bud proper at 32 hpf compared to wildtype, particularly along the anterior border of the fin bud (Figure 5.7). This suggests that the smaller fin bud is a result of a failure of LPM cells to contribute to the fin bud mesenchymal core, most notably at the anterior region of the fin field. Furthermore, anterior cells exhibit a greater decrease in displacement (Figure 5.5c) consistent with measurements reported in Figure 5.7; allowing the conclusion that in Tbx5b-deficient embryos, more anterior LPM cells may fail to enter into the fin bud relative to posterior fin field cells. Notably, Holt-Oram Syndrome patients display an anterior bias in forelimb defects and partial knockdowns of Tbx5a function in zebrafish embryos lead to the preferential mis-migration of anterior fin field cells [10, 73]. As the migration of LPM fin field cells has been reported to be topological along the AP axis, the loss of anterior LPM cells from the fin buds may result in the preferential loss of anterior fin structures contributing to in the small misshapen fins displayed by Tbx5b-deficient and *tbx5b -/-* zebrafish (Figure 3.2).

5.5.2 Tbx5b is necessary for migration of the cells of the fin field along the ML axis

In addition to loss of Tbx5b resulting in a decrease in convergence along the AP axis, Tbx5b-deficient embryos also display an absence of displacement along the ML axis in fin field cells (Figure 5.8). This result was surprising as it suggests that ML migration of the LPM cells

is not a default pathway but under specific genetic control. Other LPM cells, notably those that will form the peritoneum and the second heart field, likewise migrate in a ML direction during development. In both *tbx5a* -/- mutants and Tbx5a-deficient embryos, while AP convergence of the fin field cells fails to occur, these same precursors still exhibit a robust ML movement that is similar in migration dynamics to that of wildtype embryos (Figure 5.5, Figure 5.8 [10, 31]. My data reporting the loss of ML migration in Tbx5b-deficient embryos suggests that Tbx5b may either be playing a direct role in the ability of fin field cells to initiate migration in the ML direction or in the regulation of a signaling molecule that is used as a directional cue. Chapter 6 will propose experiments to further investigate possible sources of the ML cue.

In both wildtype and Tbx5a-deficient embryos, there is a small population of LPM cells that migrates towards the midline. Some of these cells contribute to tissues at the midline rather than to the pectoral fin [31]. I have reported in this chapter that in Tbx5b-deficient embryos, this population of cells migrating towards the midline has increased (Figure 5.12). This increased randomness in migration with respect to the midline may be responsible for the loss of ML migration.

ML migration may be important in regulating the position of the fin bud along the ML axis. However, preliminary experiments appear to suggest that there is no difference in positioning of the fin bud of *tbx5b* -/- mutants, as determined by measuring the distance between the two fin buds (Figure 5.9). There are several explanations for this lack of difference seen in positioning. First, since siblings were measured, there may be some mild phenotype seen in heterozygous siblings which could dilute the statistical power of this test. Second, both measurements include the width of the somites. As Tbx5b-deficient embryos display a decrease in length measured along the AP axis (Figure 4.7j,k), it is possible that *tbx5b* -/- embryos also have a difference in the width of the somites along the ML axis. Therefore, the distance between the somite boundary and the fin field may be different in *tbx5b* -/-

embryos and wildtype siblings, without altering the overall distance between the two fin fields. Alternatively, ML migration may occur in the fin bud between 25 hpf, the last time in which cell tracking was performed in the Tbx5b-deficient embryos, and 30 hpf, when the distance was measured. Future experiments should measure the distance between the fin bud and the boundary of the somite rather than between the two fin buds, as well as at both 25 hpf and 30 hpf, in order to resolve this question.

5.5.3 Double-deficient embryos display reduced migration along both the AP and the ML axis

These studies find that double-deficient embryos exhibit defects in directional migration along both the AP and ML axes. Double-deficient cells still retain the ability to move, albeit at a reduced overall speed compared to wildtype. Double-deficient embryos do not express *fgf24* in the fin field (Figure 5.6d) and exhibit a corresponding loss of AP convergence movements (Figure 5.5). Similarly, analysis of ML migration suggests that double-deficient embryos exhibit significantly impaired ML migration. ML displacement is severely reduced compared to wildtype embryos (Figure 5.8b). Overall, this suggests that the two *tbx5* paralogues act in combination to regulate migration along the separate axes of the fin field.

Furthermore, the movements of double-deficient cells are more random as indicated by changes in the alpha value, persistence measurements, and angles of migration (Figure 5.11, 5.12). The end result of these randomized movements is the lack of any net group movement of the fin field cells away from their initial starting positions to eventually form an operational fin bud. This suggests that the *tbx5* paralogues both play important roles in regulating the direction of migration of the cells of the fin field.

Although both the AP and ML migration movements are reduced compared to wildtype in double-deficient embryos, these embryos do not display the complete loss of directed movements seen in Tbx5a-deficient and Tbx5b-deficient embryos. Along the AP axis, the values

for both the compaction factor and the scatter in double-deficient embryos are intermediate between the Tbx5b-deficient embryos and the Tbx5a-deficient embryos, which display a consistent value of 1 (Figure 5.5b,c). Interestingly, AP displacement plateaus after 8 timepoints. Likewise, double-deficient embryos display normal ML displacement for the first 8 timepoints, at which ML displacement plateaus (Figure 5.8b). The decreased number of cells in the double-deficient embryos may be responsible for the fact that the double-deficient embryos appear to only have partial loss of movement rather than complete loss of movement. Double-deficient embryos have a smaller number of cells in the fin field (Figure 5.10) than either wildtype or single deficient embryos and the fin field as a whole is smaller. Despite the decrease in number of cells, the cells also appear to be organized more densely than wildtype embryos (Figure 5.2), which could be responsible for a reduced movement. Double-deficient cells migrate with decreased speed and tracklength (Figure 5.4), consistent with an overall reduction in the ability of the cells to mgirate.

What could be responsible for the decrease in cell number in the fin field of double-deficient embryos? Previous studies have found that loss of either *tbx5* paralogue, as well as loss of both, did not result in changes in cardiomyocyte number [84], suggesting that the *tbx5* paralogues do not regulate cell number in the anterior LPM. Interestingly, Gros et al. find that the limb field of *Tbx5 -/-* mice contains less cells than that of wildtype embryos [33]. They suggest that this decrease in cell number is not due to changes in either proliferation or cell death, but changes in the epithelial-to-mesenchymal transition [33]. Section 6.2.3 will describe future studies to further elucidate the role of the *tbx5* paralogues in regulating the size of the fin field.

CHAPTER 6

CONCLUSIONS AND FURTHER WORK

In Section 6.1, I summarize the conclusions of this dissertation. In Section 6.2, I discuss remaining questions about the *tbx5* paralogues in zebrafish and propose future directions of study.

6.1 Conclusions

6.1.1 Tbx5b modulates AP convergence in the fin field

tbx5a is expressed in the retina and in regions of the LPM that contribute to the heart and to the pectoral fin, while *tbx5b* is expressed only in the retina and the anterior regions of the LPM that contribute to the heart (Figure 3.1a) [10, 83]. Loss of *tbx5a* results in embryos that completely lack pectoral fins [10, 86]. Interestingly, loss of *tbx5b* produces misshapen fins despite the lack of detectable expression of *tbx5b* in the fin field prior to 26 hpf (Figure 3.2) [84, 87]. Although there is no detectable expression of *tbx5b* in the fin forming region at this time (Figure 3.1a), both Tbx5b-deficient and *tbx5b -/-* mutant embryos display small fin buds at 32 hpf (Figure 3.3). This implies that there are defects in the process of fin bud formation in Tbx5b-deficient embryos.

As described in Mao et al., fin field cells in wildtype embryos both converge along the AP axis and migrate away from the dorsal midline along the ML axis resulting in the formation of the fin bud (Figure 6.1a) [31]. The knockdown of Tbx5a function abrogates AP convergent movements in the fin field while the cells retain the ability to migrate along the ML axis. In the case of Tbx5a, previous authors have found that the signaling molecule Fgf24 is downstream of Tbx5a while functional studies have shown that Fgf24 appears to be the cue for AP convergence movements in the fin field cells (Figure 6.1b) [31, 32]. In the absence of either Tbx5a or Fgf24 function, the fin field cells fail to converge but continue to migrate in

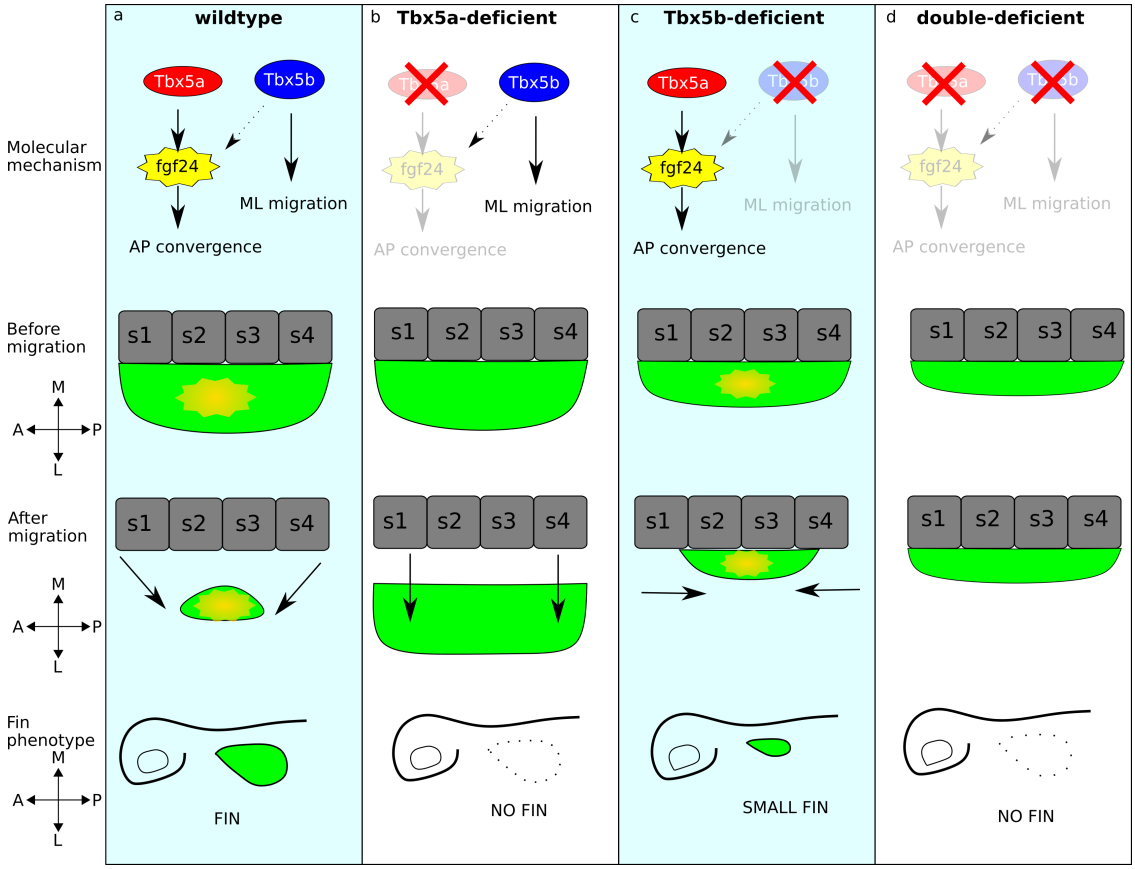

Figure 6.1: Summary of the roles of the *tbx5* paralogues during migration of the limb precursors. (a) In wildtype embryos, Tbx5a promotes AP convergence by regulating expression of *fgf24*, while Tbx5b is necessary for ML migration. This results in the cells of the wildtype fin field migrating along the ML axis and converging along the AP axis to form a fin bud, which will develop into a fin. Tbx5b may play a minor role in regulating *fgf24* levels, indicated by the dotted line. (b) Tbx5a-deficient embryos lacks *fg24* and thus fail to converge, but still migrate laterally, resulting in an embryo with no fin. (c) Tbx5b-deficient embryos do not migrate along the ML axis. Fgf24 levels are reduced by the loss of Tbx5b and AP convergence is also reduced. (d) Double-deficient embryos have cells that do not migrate ML or converge along the AP axis; they form no fin. Cells of the fin field are in green, somites are in gray, Fgf expression is yellow.

the ML direction past the normal position of the fin bud [132].

In Tbx5b-deficient embryos, the ability of the cells to converge along the AP axis is reduced. Both measurements of AP scatter and AP compaction factor find that Tbx5b-deficient embryos exhibit approximately half of the AP convergence movements of wildtype embryos (Figure 5.5). This implies that Tbx5b plays a minor role in regulating the AP convergence movements in the fin. Tbx5b may be affecting AP convergence movements by modulating levels of *fgf24* expression in the fin field. In support of this hypothesis, Tbx5b-deficient embryos exhibit decreased levels of *fgf24* in the fin field at 24 hpf compared to wildtype embryos (Figure 5.6). However, Tbx5b alone is not sufficient for either *fgf24* production or AP convergence movements, as Tbx5a-deficient embryos, which still produce Tbx5b at normal levels (Figure A.3c), show neither AP convergence movements nor expression of *fgf24*. I propose that the small fin buds of Tbx5b-deficient fins are due to some anterior cells in Tbx5b-deficient embryos failing to contribute to the fin bud due to an incomplete AP convergence. The anterior cells must travel a greater distance than more posterior cells; this likely explains their greater sensitivity to changes in levels of *fgf24*.

Furthermore, I have shown that the larval fins of *tbx5b -/-* mutant embryos lack some anterior elements (Figure 3.4). These phenotypes are similar to the phenotypes of partial Tbx5a-deficient and partial Fgf24-deficient embryos [31]. Mao et al. suggests that the defects in anterior structures of these fins, as well as the defects seen in Holt-Oram Syndrome patients, may be explained by a pre-patterning of the fin field prior to migration. In this model of fin development, the fate of the cells within the fin field is specified early and the migration maintains the organization, from which the structures of the fin then form [31]. Therefore, when anterior cells fail to contribute to the fin bud, there are corresponding defects in anterior structures of the fin [31]. The data gathered in this dissertation supports this hypothesis. Furthermore, in addition to analysis of cellular dynamics in the fin field, I find that anterior cells of the fin field, as identified by Tbx5a::GFP expression, are more

likely not to contribute to the fin bud in Tbx5b-deficient embryos than in wildtype embryos (Figure 5.7). This provides another line of evidence indicating that convergence is necessary for fin bud formation and that cells that fail to converge do not contribute to the fin bud.

6.1.2 Tbx5b regulates ML migration in the fin field

In both wildtype and Tbx5a-deficient embryos, the fin field migrates laterally along the ML axis. This early migration is lost in Tbx5b-deficient embryos (Figure 5.8), indicating that Tbx5b regulates ML migration. The role of ML migration in fin development is currently unknown; it may play a role in determining the size or pattern of the fin field, or may primarily be involved in regulating fin position. However, the small size of the fin may be due exclusively to the failure of anterior LPM cells to contribute to the fin bud rather than defects in ML migration. Furthermore, analysis of *tbx5a* expression in 30 hpf embryos reveals that the fin buds of both wildtype and Tbx5b-deficient embryos are positioned similarly with respect to the lateral edge of the somites (Figure 5.1f,f"). Additionally, *tbx5b -/-* embryos do not appear to show defects in the position of the fin buds at 30 hpf (Figure 5.9). As Tbx5b-deficient embryos showed no signs of ML displacement from 18 hpf to 25 hpf (Figure 5.5), this may suggest that additional ML migration occurs between 25 hpf and 30 hpf in Tbx5b-deficient embryos. However, the size and shapes of the somites are also affected in Tbx5b-deficient embryo (Figure 4.7j,k); therefore measuring the distance between the two fin buds may not give accurate information on the positioning of the fin. Future work measuring the distance between the lateral edge of the somites and the fin bud of Tbx5b-deficient embryos may show that ML positioning is indeed altered with respect to the somite boundaries.

How does Tbx5b regulate ML migration in the fin field? Migration may be regulated through cell intrinsic mechanisms, such as changes to cell shape or polarization. Alternatively, migration may be regulated through secreted or extracellular signaling molecules, similar to the role of *fgf24* in regulating the AP convergence movements of the fin field. The

following sections will discuss each of these hypotheses for the role of Tbx5b in regulating ML migration.

Cells do not appear to have polarized centrosomes during fin field migration

Migrating cells are polarized such that the leading edge of the cell is morphologically or molecularly different than the lagging edge of these cell. During the migration of many cell types, the centrosome and the Golgi apparatus are actively positioned at the leading edge of the cell relative to the nucleus [133]. In both neurons and fibroblasts, positioning is maintained through signaling cascades involving the Par proteins [133]. PCP proteins such as Vangl are also involved in regulating the migration of polarized cells including neurons, neural crest cells and mesoderm cells undergoing convergent extension [134]. Polarized migration is also seen in the MESP1+ cells of the first heart field, which display polarized actin polymerization and localization of the Golgi apparatus to the leading edge of the cell [135], indicating that in mice, some LPM cells undergo polarized migrations. However, prior to this dissertation, there have been no analysis of the polarization of cells of the fin field.

Cells of the both the fin bud and the limb bud appear to be polarized. At 42 hpf, fin buds cells in the base of the fin bud are elongated and show concentrations of actin protrusions at the leading end, suggesting polarized migration into the fin bud [34]. In mice, the cells entering the limb bud are elongated and possess polarized Golgi apparatus [34]. This is consistent with work showing that the PCP pathway regulates distal growth of the limb bud [48]. However, the polarization of cells of the fin field has not been previously analyzed.

Cells of the fin field move at a stereotypic angle depending on their AP position. At 22 hpf, the cells of the fin field are actively migrating; if the migration is polarized then centrosome position should correlate with the migration angle at this time. However, I found no correlation between centrosome positioning and migration angle in wildtype cells of the fin field (Figure 5.13). Furthermore, the overall shape of the cells appeared to be

isometric rather than elongated in the direction of migration (Figure 5.2), although this was not comprehensively analyzed. These findings suggest that the cells of the fin field do not undergo a polarized migration as determined by centrosome position. Future studies should analyze the dynamics of actin within the fin field to identify if the cells show a consistent polarization of actin cytoskeletal elements during these migration processes.

In mice, the orientation of the cells of the limb bud can be altered by loss of WNT5 signaling, but not by loss of FGF signaling, leading to the hypothesis that FGF signaling regulates velocity but not polarization [47]. WNT5 has been found to regulate the phosphorylation of the PCP component VANGL2 in the limb bud [136]. Combined, this data suggests that if the cells of the fin field are not polarized, they may become polarized during fin bud development due to Wnt5 signaling once a fin bud has been formed. Consistent with this hypothesis, *wnt5b* is not expressed in the fin field of 24 hpf embryos, but is strongly expressed in the pectoral fin bud by 48 hpf [137]. *wnt5a* does not appear to be expressed in the pectoral fin bud [137].

The somites may be the source of a repulsive cue regulating ML migration

The somites are located adjacent to the fin field and known to be involved in regulating the extent of *tbx5a* expression through retinoic acid signaling [25]. The LPM cells in the fin field normally migrate away from the somites; however, in both Tbx5b-deficient and double-deficient embryos, many cells show a net angle of migration towards the somites (Figure 5.12). Furthermore, many of the genes identified from the whole embryo RNA-sequencing experiment in Chapter 4 were found to be misexpressed in the somites and the intermediate mesoderm. Combined, this data leads to the hypothesis that a repulsive cue from the somites may regulate ML migration. This would imply that in Tbx5b-deficient embryos, the repulsive cue is either lost or no longer detectable, leading to migration that appears random with respect to the midline.

There is precedent for repulsion as a method of guiding cell migration. During the migration of primordial germ cells (PGCs), migration is guided by a combination of a posterior attractive cue and a repulsive cue located in the somites. In zebrafish, the PGCs undergo a migration from two ventral bilateral clusters adjacent to the first 3 somites to a location adjacent to somite 8 [138]. The posterior migration of the PGCs is regulated by signaling from the attractive cue SDF1 at somite 8 [138]. However, there is also a secondary repulsive migration cue. This repulsive cue is mediated by LPP proteins, zebrafish orthologs of the *Drosophila* phospholipase Wunen [139, 140]. There are 6 *LPP* genes, which are expressed in the somitic mesoderm concurrently with the posterior migration of the PGCs [140]. Loss of the LPP proteins alters the migration trajectories of the PCGs, such that migration no longer occurs along the yolk but rather the cells migrate in a more dorsal manner adjacent to the somites [140]. Furthermore, loss of *wunen* in *Drosophila* embryos results in random migration of PGCs [141], similar to the random migration with respect to the midline seen in the fin field cells in Tbx5b-deficient embryos (Figure 5.12).

The migration of the fin field may be regulated through a similar mechanism as PGC migration, such that migration is mediated both by an attractive cue (i.e. *fgf24*) and a as of yet unknown repulsive cue in the somites, regulated by Tbx5b. Section 6.2.1 will discuss methods of identifying the specific molecule(s) involved in this process. However, one limitation of a repulsive signal in regulating migration is the relatively limited effective range of said cue. The fin field cells move 50 µm laterally from 18-23 hpf, and the fin field cells of Tbx5a-deficient embryos continue to move laterally after 23 hpf (Figure 5.8). If the effective range of a repulsive signal from the somites is similar during fin field migration and PGC migration (Paksa et al. calculate a range of 15-30 µm [140]), a repulsive cue may not be sufficient to generate the entire ML migration of the wildtype embryos and may function in conjunction with an attractive cue. Alternatively, the repulsive cue may only be necessary during initiation of migration for determining cell orientation, in which case an effective

range of 30 µm may be sufficient.

Signaling from the YSL may play an instructive role in regulating ML migration

In zebrafish, the cells of the fin field migrate directly over the YSL providing ample opportunity for signaling between the two tissues. Furthermore, signaling from underlying tissue has been shown to directly affect the migration of overlying cells in the LPM. Multiple signaling pathways from the YSL have been implicated in the migration of the anterior myocardial precursors [142, 143], as well as regulating other cell movement processes, such as gastrulation [144]. The most relevant example is the regulation of the cardiac precursors in the LPM by the YSL-specific transcription factor *mxtx1* [142]. In Mxtx1-deficient embryos, cardiac precursors fail to migrate towards the midline and fuse, although anterior migration movements of the cardiac precursors is not affected [142]. This migration defect appears to be specific to signaling from the YSL, as the same phenotype is seen when Mxtx1 is knocked down only in the YSL [142]. Furthermore, only cardiac precursor migration is affected; endoderm development occurs normally [142]. This effect is produced by regulation of the extracellular matrix over which the cardiac precursors migrate primarily by promoting *fibronectin 1* transcription [142].

Similar mechanisms may regulate the ML migration of the fin field, where a signal from the YSL may be required to promote appropriate ML migration, perhaps by altering the underlying extracellular matrix. Consistent with this hypothesis, the RNA sequencing screen identified two genes that were differentially expressed in the YSL: *zgc:158643* and *ndufa4* (Figure 4.8). Furthermore, the preliminary RNA sequencing screen detected multiple extracellular matrix components (Table B.2, Table B.3) that could be involved in this process. These could either be targets of signaling in the YSL, as YSL signaling is involved in regulating the extracellular matrix over which the LPM migrates, or directly regulated by the

cells of the fin field. Section 6.2.1 will propose methods to identify molecules involved in ML migration.

6.1.3 Evolutionary implications of the tbx5 duplication and the role of Tbx5 in tetrapods

As *tbx5a* and *tbx5b* are likely a result of the whole genome duplication event in teleosts, this research addresses how genes may persist after a duplication event resulting in the formation of paralogous sister genes from a single ancestral gene. One possible result of gene duplication is subfunctionalization, a process in which one or both paralogues accumulate mutations which leads to the distribution of the original suite of functions displayed by the single parent gene amongst the two sister genes [88]. Under subfunctionalization, paralogous genes may continue to share some common functions, but have divided others in a complementary fashion.

Subfunctionalization commonly occurs by changes in the spatial or temporal expression of a gene, perhaps by mutation of regulatory regions such that each duplicated gene may be expressed only in a subset of the expression patterns of the original gene. There are several examples of subfunctionalized genes in the zebrafish most notably in the Hox cluster, such as in the *hoxb5* paralogues [89]. Based upon the differing fin phenotypes displayed by Tbx5a- and Tbx5b-deficient embryos, Pi-Roig et al. suggested that the *tbx5* paralogues may have been subfunctionalized in the limb, with Tbx5a acting primarily in early limb development and Tbx5b playing a larger role in late limb development [87]. In this dissertation, I have shown that Tbx5a and Tbx5b mediate different migration parameters of the early fin field LPM cells. My data suggests that the two paralogous zebrafish genes have subfunctionalized different components of the migration pathway mechanisms such that the two vectors of AP and ML movements have been distributed amongst Tbx5a and Tbx5b respectively.

If Tbx5a and Tbx5b have indeed subfunctionalized, then the shared and individual func-

tions of the two paralogues should closely resemble the complete suite of essential functions of the ancestral parent gene. As tetrapods exhibit the ancestral condition of a single *Tbx5* gene, characterization of the phenotypes displayed by zebrafish embryos that are doubly deficient for both Tbx5a and Tbx5b may shed light on the mechanisms leading to the loss of limb phenotype in knock-out mice and possibly on the limb defects observed in Holt-Oram syndrome patients in which early cell migration studies are more difficult to perform.

This dissertation reveals that double-deficient embryos exhibit defects in directional migration along both the AP and ML axes. Double-deficient cells still retain the ability to move, albeit at a reduced overall speed compared to wildtype. However, their movements are more random as indicated by both changes in the alpha value and persistence measurements (Figure 5.11). Cell tracking data also illustrates that groups of cells from all regions of the fin field will migrate in variously distributed directions, with cells from each somite group having migration angles distributed relatively uniformly across a circle (Figure 5.12). The end result of these randomized movements is the lack of any net group movement of the fin field cells away from their initial starting positions to eventually form an operational fin bud.

Overall, this work leads to a hypothesis for a possible role for tetrapod *Tbx5* during formation of the limb bud (Figure 6.2). It had been proposed that the loss of Tbx5 function in tetrapods may be due to a failure of an epithelial to mesenchymal transition (EMT) [33]. The subfunctionalization of separable migration vectors between zebrafish *tbx5a* and *tbx5b* genes, and especially the failure of the double-deficient zebrafish cells to make directional migrations (Figure 5.12, Figure 5.11), suggests that the forelimb bud in tetrapods, which retain the ancestral single *Tbx5* gene configuration, may form through a process where AP convergence and ML migration cues are both regulated by the single *Tbx5* gene. Therefore, in *Tbx5* -/- mice, it could be that rather than a failure of EMT, the mesenchymal cells in the limb field are still capable of movements but failing to make persistent directional net migrations.

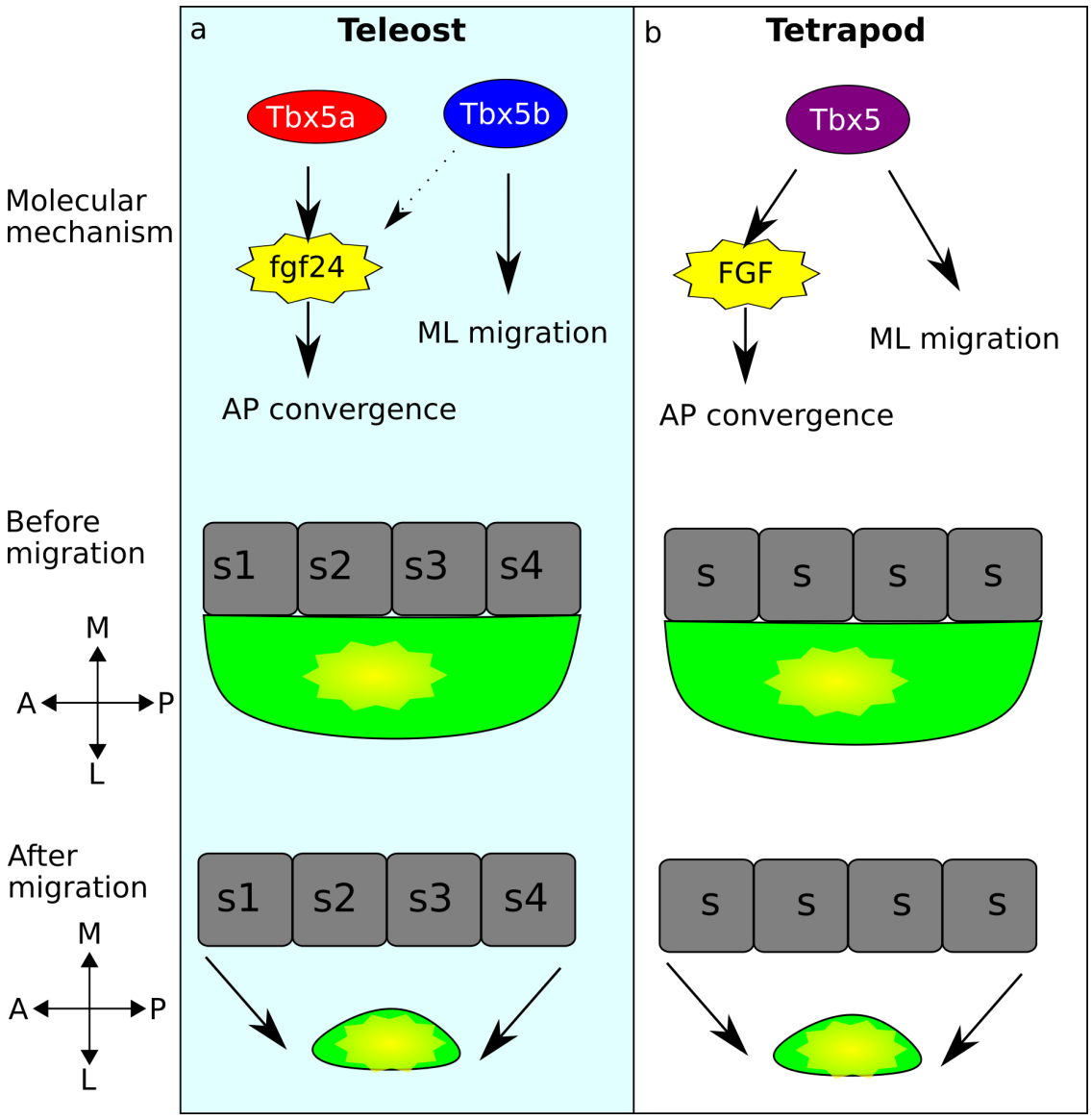

Figure 6.2: A model for the role of *Tbx5* in tetrapod limb development. (a) In teleosts, migration of the limb field is composed of two parts, AP convergence, mediated by Tbx5a via Fgf24, and ML migration, mediated by Tbx5. (b) In tetrapods, I hypothesize that both AP convergence and ML migration are controlled by Tbx5.

Although this hypothesis is not exclusive of EMT occurring in this process, the data gathered in this study does not indicate that EMT is occurring in zebrafish. Work in the zebrafish has shown that an Fgf signal is important for AP convergence, while the identification of a possible ML signal(s) is still an ongoing issue. I propose that the correct formation of a pectoral fin or forelimb could be dependent upon discrete downstream migration signals mediated separately by two T-box genes in fish but by one in tetrapods (Figure 6.2).

6.2 Future directions

In the following sections, I discuss many of the new questions posed by the findings of this dissertation. In Section 6.2.1, I propose experiments to understand the role of Tbx5b in mediating ML migration. In Section 6.2.2, I suggest methods that could be used to understand the role of enhancers and identify if subfunctionalization has occurred in the *tbx5* paralogues in zebrafish. In Section 6.2.3, I discuss the role of the *tbx5* paralogues in determining the identity of the fin field and the fate of the cells of the fin field in double-deficient embryos. In Section 6.2.4, I discuss the role of the *tbx5* paralogues in late fin development and propose experiments to understand this role.

6.2.1 How is Tbx5b regulating ML migration?

Tbx5b regulates ML migration (Figure 5.8); however, the mechanism is not understood. To identify the role of Tbx5b in ML migration, it is necessary to first identify what factors Tbx5b interacts with. From there, a putative signaling cue can be identified (or alternatively, an intrinsic molecule) which will allow determination of how Tbx5b is regulating said molecule. In Section 6.1, I proposed that ML migration could be mediated through signaling in either the somites or the YSL. In this section, I will describe experiments to identify partners that could be interacting with Tbx5b, either indirectly in the somites or YSL, or directly in the fin field.

As previously mentioned, RNA sequencing revealed genes expressed in both the somites and the YSL. To test if these genes regulate fin development, I performed a preliminary sensitized gRNA screen using transient F0 knockdowns. The embryos were sensitized with a sub-phenotypic dose of Tbx5b morpholino and screened for defects in the size and shape of the fin (for more details, see Appendix A.5). This screen found that when most of the somite genes identified in Chapter 4 were knocked down, embryos with small fins were produced (Figure A.6). This suggests that there may indeed be a link between somite patterning and fin size. This screen should be expanded to include all genes found to be misexpressed in the YSL and genes involved in the production or regulation of the extracellular matrix.

Since the screened embryos were sensitized for interactions with *tbx5b* by injection with a sub-phenotypic dose of morpholino, it is also possible that the tested genes interact with *tbx5b*, although said interaction is likely indirect. However, this screen will also identify genes that would produce small fins in a non-sensitized background. Therefore, the next step should be to repeat this screen with genes that produced small fins in a non-sensitized background. Genes that produce a significant change in the ratio of small fins between the sensitized and non-sensitized conditions may indeed be interacting with *tbx5b*, although this interaction may not be direct. Genes that produce similar ratios of small fins in the sensitized and non-sensitized conditions could be genes that can affect the size of the fin independent of interactions with Tbx5b, although this would not conclusively show that the genes do not interact with Tbx5b.

The molecules involved in mediating this ML migration through interaction with Tbx5b may also be intrinsic to the fin field. One method to identity candidates for molecules involved in ML migration specific to the fin field would be to perform a tissue-specific single cell RNA sequencing experiment. Double transgenic *Tg(tbx5a::GFP)* and *Tg(Nkx2.5::RFP)* fish would be injected with morpholinos as described in Chapter 4. However, FACS sorting would allow not only separation of the LPM from other tissues, but also separation be-

tween the heart (RFP+, GFP+) and limb field (GFP+) regions of the LPM. This would allow identification of transcriptional changes unique to the LPM, and make it more likely to identify direct targets of the *tbx5* paralogues as only cells in which the *tbx5* paralogues are expressed would be sequenced. If performed in parallel using both Tbx5a-deficient and double-deficient embryos, this method could provide a more specific look at the different transcriptional networks maintained by the *tbx5* paralogues in zebrafish, compared to the whole-embryo RNA sequencing experiments performed in Chapter 4. This would be done by comparing Tbx5a-deficient, Tbx5b-deficient and double-deficient transcriptomes to wild-type transcriptomes, as performed in Chapter 4. Because only the fin field cells would be contributing to the transcriptome, this approach would be far more likely to identify only changes in gene expression found in the fin field. As the *tbx5* paralogues are transcription factors expressed in the LPM, although *tbx5b* has no detectable expression in the fin field, this would make it more likely that differentially expressed genes are direct targets, as there would be a possibility of direct regulation. However, RNA sequencing experiments are not capable of differentiating between direct or indirect interactions.

6.2.2 What are the mechanisms of subfunctionalization in the tbx5 paralogues?

Subfunctionalization is traditionally thought to occur by division of the enhancer regions [89, 145]. The fact that *tbx5b* appears to only be expressed in the heart forming region of the LPM during early development, although it appears to still be influencing the early dynamics of fin bud formation, is suggestive of the subfunctionalization of enhancers in the *Tbx5* paralogues. However, although several conserved enhancers of *Tbx5* are known to exist in tetrapods, most of these enhancers are not conserved in the teleost genome in a sequence-specific manner, making identification difficult. For instance, the well-characterized intron 2 *Tbx5* enhancer which contains 6 HOX binding sites and RA response is not conserved in

zebrafish [20, 146].

Work done by Adachi et al. has identified one conserved noncoding region, CNS12sh, shared between gar, zebrafish and mouse, which is capable of driving expression in the pectoral fins of zebrafish that recapitulates *tbx5a* expression in the pectoral fins of zebrafish [146]. This sequence can also transiently drive expression of *tbx5a* in order to produce pectoral fins in *heartstring* -/- embryos [146], suggesting that this may be sufficient for controlling expression of *tbx5a* in the limb. However, as deletion of both the intron 2 and CNS12sh enhancer in mice results in normal forelimb growth, this suggests that there may be other enhancers necessary for expression of *Tbx5* in the mouse and that these enhancers are not necessary for limb development [147].

Further studies should seek to understand enhancer function and how they differ between the *tbx5* paralogues. One first step would be to identify if the CNS12sh enhancer or a similar enhancer exists for *tbx5b*. Using the techniques used in the Adachi paper [146], enhancer regions for both *tbx5a* and *tbx5b* could be identified and compared in order to identify if subfunctionalization has occurred among the enhancers of the *tbx5* paralogues in zebrafish. Similarly, enhancers should also be compared with tetrapods, as they contain a single copy of *Tbx5*.

6.2.3 Is tbx5 determining the identity of the fin field?

One arena left to be explored is the fate of the Tbx5+ limb cells when Tbx5 is lost. In embryos deficient in Tbx5a, these cells migrate past the site of the fin bud, but their ultimate fate is unknown. The fate map of the LPM suggests that cells posterior to somite 5 largely contribute to the peritoneum [31]. It has been a long-held assumption that when the fin field cells fail to contribute to the fin, they eventually contribute to the peritoneum [31]; however, this has never been fully tested. Initially, the role of *Tbx5* was thought to confer the identity of forelimb on the cells of the limb bud [78]. Perhaps in the absence of both *tbx5*

paralogues, these cells lose their fate as limb progenitors and are converted to another fate, such as peritoneum cells.

By 30 hpf, the Tbx5a+ cells appear to be migrating laterally even in the double-deficient embryo, at which time peritoneum cells are migrating (Figure 5.1). Could the presumptive fin field cells have converted to peritoneum cells? A challenge in identifying a fate shift to peritoneum is the lack of early genetic markers available for the peritoneum. However, the fate of the former limb field cells in both Tbx5a-deficient and double-deficient embryos could be identified by using photoconversions of embryos expressing Kaede both of the entire limb field or of smaller regions of the LPM along the AP axis in both wildtype and deficient embryos, in order to determine the fate of these cells in the mutant embryos. Performing this in smaller regions in the Tbx5b-deficient embryos would also provide information on the ultimate fate of the anterior cells that fail to contribute to the limb bud. Since previous fate map studies have identified cells as contributing to the peritoneum at 48 hpf [31], the fate would be assessed at a similar time point. If *tbx5* is necessary for the cells of the fin field to become fin and if the default fate is peritoneum, one would expect that when both copies of *tbx5* are lost, the presumptive fin field cells become peritoneum. If most photoconverted cells are present in the peritoneum at 48 hpf, this would support the hypothesis. Alternatively, the photoconverted cells may not contribute to the fin field, either due to cell death or migration to another location. If a reduced number of photoconverted cells were seen at 48 hpf, this would indicate that cell death may be occurring, which could be confirmed using cell death assays. A less clear result would be if the photoconverted cells remain scattered over the yolk at 48 hpf. If this is the case, it may not be possible to determine if presumptive fin field cells have converted fates or if instead they are lost in migration.

In my experiments, there are fewer cells in the double-deficient zebrafish embryos than in wildtype or single-deficient embryos (Figure 5.10). The small size of the fin field may be due to differences in cell proliferation or cell death. Rates of both proliferation and cell death

should be compared between wildtype and double-deficient embryos. Alternatively, work by Gros et al. has shown that in *Tbx5* -/- mutant mice, the presumptive forelimb region contains fewer mesenchymal cells that that of wildtype embryos [33]. Gros et al. show that this is not due to differences in rates of cell proliferation or cell death and instead suggest that this decrease in mesenchyme is due to failures in EMT regulated by *Tbx5*.

Could EMT be involved in the defects in either cell number or cell movement in double-deficient embryos? In order to determine this, it is necessary to first determine if EMT is occurring. In tetrapods, the LPM at the level of the limb field contains multiple layers of cells, while in zebrafish, the LPM at the level of the fin field is only a single cell layer. It is currently unknown whether the cells of the fin field are present as an epithelial tissue or as mesenchymal cells during the stages of limb field migration. Characterization of cell shape, actin dynamics in these cells, and localization of apical proteins such as N-cadherin and β-catenin should provide information on if the cells are present as a migrating epithelium or as mesenchymal cells during this time [33]. If the cells of the fin field migrate as mesenchymal cells, then characterization of earlier stages of LPM should be analyzed to determine when EMT occurs. If cell shape does change as these cells begin migration, do these changes still occur in double-deficient embryos? Analysis of cell shape and migration processes such as lamellopodia could provide insight into these questions, as well as provide information as to the structural components of how the cells of the limb field are migrating.

6.2.4 What is the role of the tbx5 paralogues in later stages of fin development?

Tetrapod *Tbx5* functions both early during limb bud initiation as well as later, with late loss of *Tbx5* in the mouse limb resulting in mispatterning of the tendons and muscles [80], as well as minor skeletal defects, particularly in the anterior region of the limb [79]. Both Parrie et al. and Pi-Roig et al. hypothesize that *tbx5b* functions primarily during late fin development

[84, 87]. Although in this work I have also shown evidence of the role of *tbx5b* early in fin development, I have not fully explored the effects of either *tbx5* paralogue during the later stages of fin development. Preliminary analysis of Tbx5b-deficient fins suggests that these fins contain muscle cells and although differentiation of the muscle cells may be delayed, the muscles appear to be present in the two stripes present in wildtype in fins (Figure A.5).

Additionally, while Parrie et al. suggest that there is a loss of the apical fold in Tbx5b-deficient embryos as seen by expression of *bmp4*, my work has shown that there may instead be a delay in formation of the apical fold (Figure 3.3). Despite this, at later stages *bmp4* shows a strong misexpression phenotype at 3 and 4 dpf in *tbx5b -/-* embryos, with very strong expression throughout the endochondral disc at a time when most expression is lost in the fins of their normally-developing siblings (Figure A.4). As Bmp4 interacts both with the Shh signaling center and with Fgf signaling, a more detailed analysis of gene expression at later stages of fin development in *tbx5b -/-* mutants could be informative in understanding the roles *tbx5b -/-* is playing late in limb development.

In order to further characterize the roles of the *tbx5* paralogues during later stages of fin development, tissue-specific CRISPRs could be generated to allow for both spatial and temporal control [148]. To drive expression of *Cas9* specifically in the fins, the CNS12sh enhancer identified by Adachi et al. could be used [146]. As these fish should be only lacking expression of either *tbx5* paralogue in the limb, this would enable study of the phenotype of adult fins of Tbx5b-deficient embryos. In order to achieve temporal clarity, this system could be coupled with the ERT2 system [148], which would allow inducible tissue-specific expression and identify if *tbx5a* is involved in fin development beyond initiation of the fin bud.

APPENDIX A

APPENDIX

A.1 Analysis of the conserved protein domains of Tbx5b

The genomic structures of the *tbx5* paralogues differ. *tbx5a* has 9 exons, while *tbx5b* contains 8 exons (Figure A.1. Furthermore, the length of both exons and introns dramatically vary between the two paralogues (Figure A.1). Previous studies has also reported that the level of sequence conservation between the two paralogues is low when comparing nucleic acid sequences; however, comparison of the protein sequences show highly conserved residues within the protein, and particularly the T-box domain [83].

The protein sequence of Tbx5a is more similar to the other TBX5 paralogues than Tbx5b is to either Tbx5a or the other TBX5 homologues [83, 84](Figure A.2). Furthermore, as previously reported, the highest level of protein conservation is in the T-box of Tbx5b (Figure A.2, yellow highlight), while the remaining parts of the protein are relatively different from both Tbx5a and the tetrapod Tbx5 proteins. However, previous work on Tbx5b has not directly discussed which protein domains or binding sites, other than the T-box are conserved between Tbx5b and other Tbx5 proteins. Of note is that Tbx5b is missing one of the two nuclear localization sequences (NLS) sites present in all other copies of Tbx5 (underlined in red, Figure A.2), and previous work has reported that both NLS sites act cooperatively for full nuclear import [150].

Tbx5b contains only one of the two conserved NLS sequences in tetrapod TBX5, while

Figure A.1: Comparison of genomic structure of *tbx5a* and *tbx5b*. This figure is derived from ENSEMBL data [149]. The black boxes represent exons while the dashed lines represents introns.

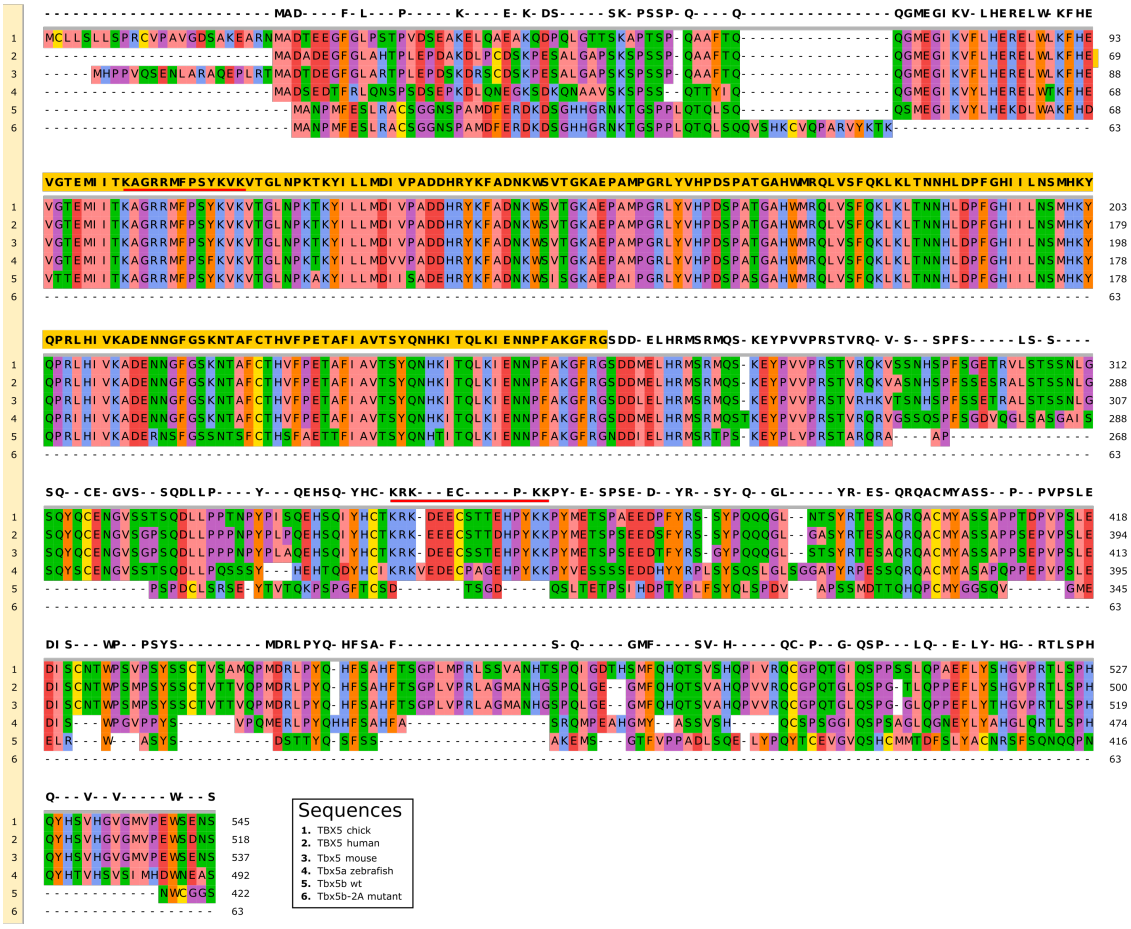

Figure A.2: Alignment of the Tbx5b mutant protein with other Tbx5 proteins reveals the mutant protein lacks conserved domains. This figure displays protein alignments using MUSCLE of TBX5 in humans, chick, mice and Tbx5a and Tbx5b in zebrafish. Also aligned is the Tbx5b mutant generated in this chapter. Yellow highlighting on the consensus sequence indicates the highly conserved T-box while the two underlined regions are the two conserved NLS sites present in Tbx5.

Tbx5a contains both of these sites (Figure A.2). This second NLS contains a lysine which is acetylated by Kat2a/b. Loss of just this lysine in TBX5 results in a severe loss of nuclear retention of TBX5, and loss of *kat2a* and *kat2b* in zebrafish produces a similar phenotype to Tbx5a knockdowns [151], suggesting that this NLS site is functional in zebrafish. Because Tbx5b is lacking one of these NLS sites, it may not be able to be maintained in the nucleus as efficiently as Tbx5a. This could be one reason why the effects of loss of Tbx5b are not as severe as loss of Tbx5a. However, at least two of the other known conserved protein binding sites are conserved in both Tbx5a and Tbx5b. In the human TBX5, P139, D150, R151 and Q151 are essential for binding with NKX2.5 [152, 11, 65, 153]. These residues are conserved in both Tbx5a and Tbx5b. Furthermore, there is also an alpha helix outside of the T-box domain, aaY255-R264, that is necessary for interaction with the NURD complex [152, 77, 154]. This domain is also conserved in both Tbx5a and Tbx5b despite the fact that Tbx5b is variable outside of the T-box domain. This suggests that Tbx5b may still be able to interact with at least some of the important cofactors involved in development that are shared with Tbx5a and the ancestral TBX5.

A.2 qPCR analysis of the *tbx5* paralogues

One initial question was if *tbx5b* was expressed in tissues in other places in the embryo. In order to test this, I performed qPCR on 24 hpf embryos divided into 3 regions. Figure A.3b shows the divisions of these embryos. The head region included the areas of known *tbx5b* expression, including both the retina and the LPM (pink). The trunk region includes the middle somites and the trunk of the embryo (green), while the tail region encompasses the more posterior region of the embryo. DNA was pooled for 10 embryos and 3 qPCRs were performed concurrently. Expression levels were normalized using the housekeeping gene *rpl13*. Analysis of this data showed that the highest levels of *tbx5b* were detected in the anterior/head region, while no expression was detected in the trunk region (Figure A.3a).

1 of the 3 reactions showed expression in the tail region, while the remaining two did not, suggesting that there may be slight levels of expression present at the tail of the developing embryo or in the most posterior somites (Figure A.3a).

qPCR analysis was also performed to detect the levels of expression of the different *tbx5* paralogues in the knockdown embryos in collaboration with Jeffrey Steimle of the Moskowitz lab. This work was performed in whole embryos at 36 hpf. At 36 hpf, expression of *tbx5a* is significantly increased in both the Tbx5a-deficient and the double-deficient embryos (Figure A.3c). This is consistent with previous work that shows the Tbx5a morpholino stabilizes the *tbx5a* transcript. Tbx5b-deficient embryos show no significant change in the levels of *tbx5a* expression at this stage (Figure A.3c). Furthermore, levels of *tbx5b* expression at 36 hpf are not altered compared to control morpholino injected embryos in either Tbx5a-deficient, Tbx5b-deficient or double-deficient embryos.

A.3 *bmp4* expression is maintained in the *tbx5b* -/- mutant fin

By 3 dpf, *bmp4* expression in the pectoral fin of the wildtype embryo has been largely lost (Figure A.4b). In the *tbx5b* -/- mutant embryos, there is still strong expression of *bmp4* in the fin mesenchyme, although this expression does not expand into the apical fold (Figure A.4b'). The fins of the *tbx5b* -/- mutant embryos are smaller both in the mesenchymal region which will form the endochondral disk and in the apical fold region. By 4 dpf, expression of *bmp4* remains in the mutant limb (Figure A.4c'), in the more central region of the limb. These *tbx5b* -/- mutant fins are still significantly smaller than the fins of their siblings at 4 dpf (Figure A.4c), and lack the clear cellular structures of the endochondral disk and apical fold (actinotrichia) that can be seen in their wildtype siblings.

This work suggests that although the early signaling centers form normally in *tbx5b* -/- mutants (Figure 1.6), there are problems with the later signaling pathways in the apical fold. Unlike in wildtype, there remains a strong mesenchymal expression of *bmp4* after 3 dpf in

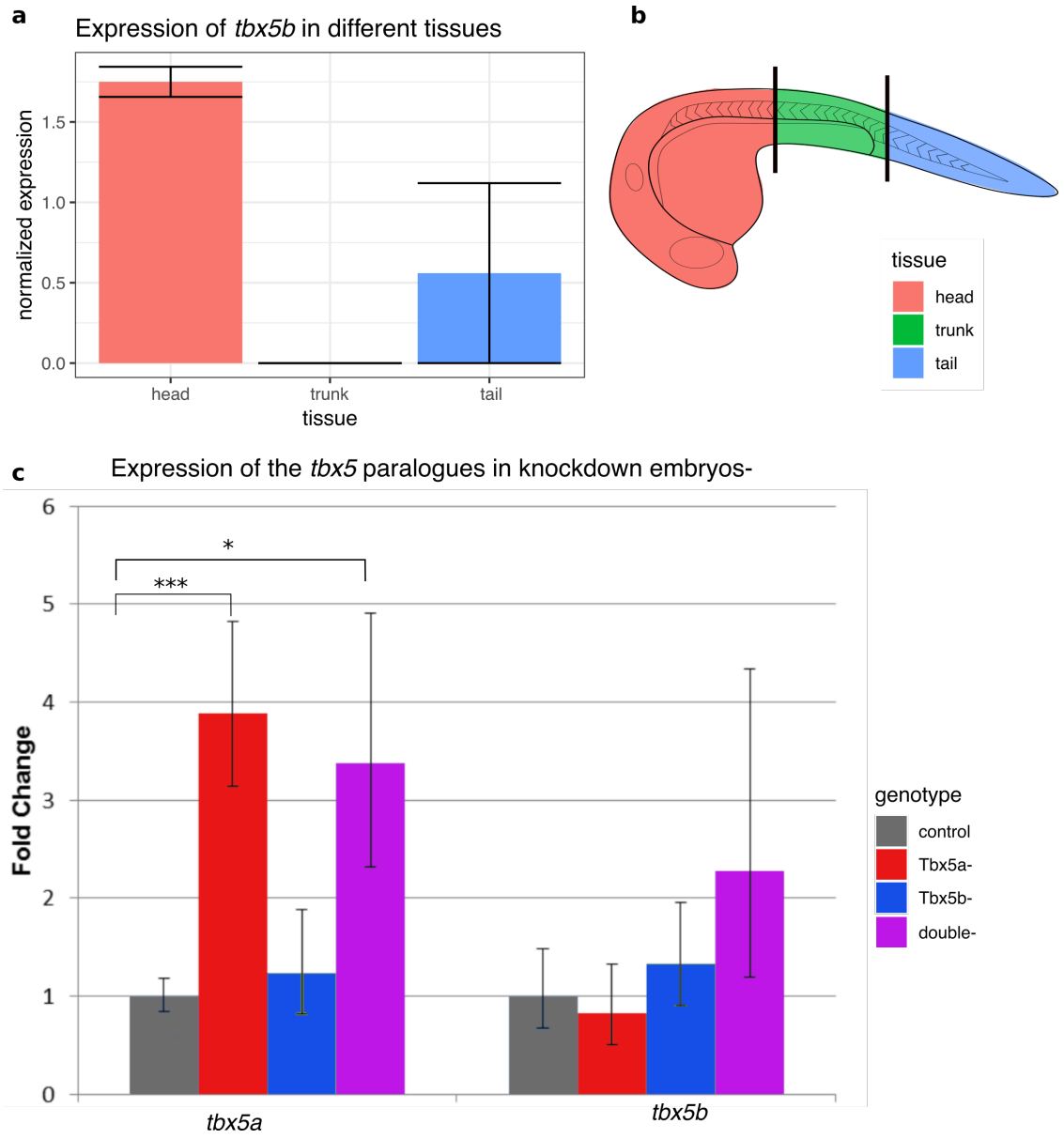

Figure A.3: qPCR analysis of *tbx5a* and *tbx5b* expression. (a) Expression of *tbx5b* throughout the different regions of the embryo at 24 hpf. (b) Schematic indicating correlation between parts of embryo and figure. (c) Relative expression levels of *tbx5a* and *tbx5b* in knockdown embryos at 36 hpf. For (c) embryos collected by EBA, qPCR analysis performed by Jeffrey Steimle * $p<0.05$, *** $p<0.001$

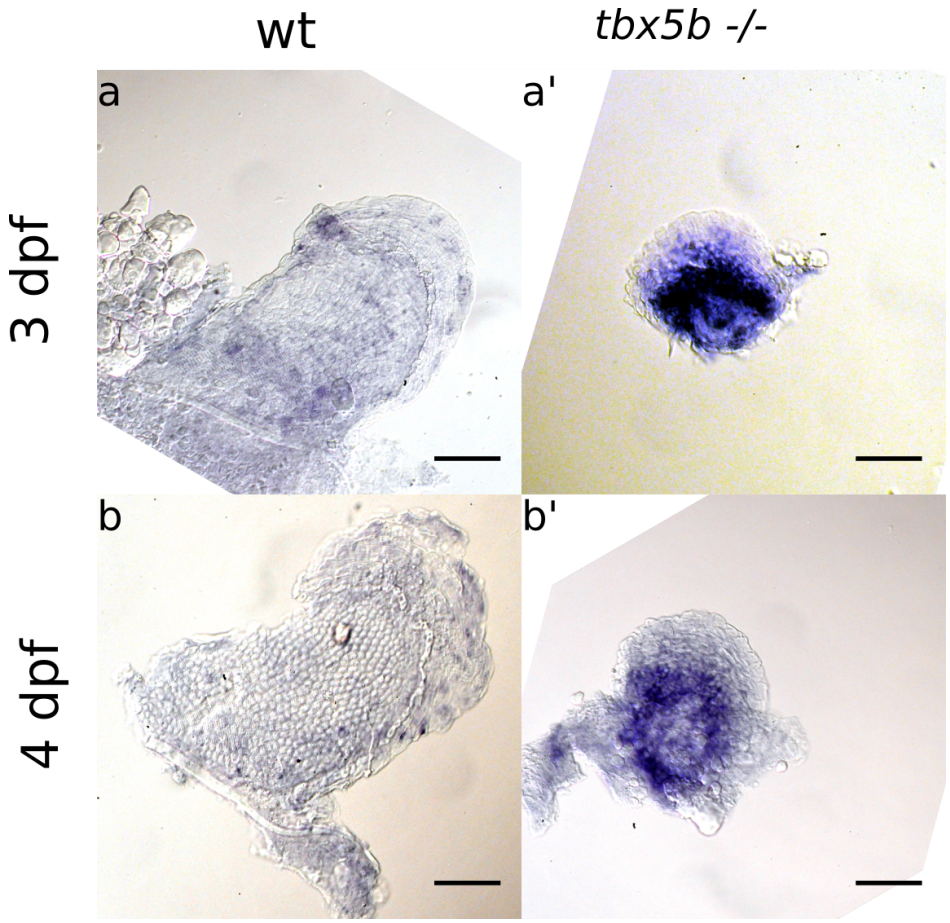

Figure A.4: *bmp4* expression in the fins of *tbx5b* -/- mutants over time. (a-a') *bmp4* expression in the fins of *tbx5b* -/- embryos (a') and wildtype siblings (a) at 3 dpf. (b-b') *bmp4* expression in the fins of *tbx5b* -/- embryos (b') and wildtype siblings (b) at 4 dpf. The anterior side of the fine is oriented to the left. Scalebars are 100 µm

tbx5b -/- mutant fins. The expanded expression of *bmp4* in the mesenchymal section of the limb bud without expression in the apical fold at 3 and 4 dpf in the *tbx5b* mutants suggest that at least part of the defects in the pectoral fins of Tbx5b-deficient embryos may be due to a failure to properly maintain signaling in the AF and the rest of the fin.

A.4 Muscle migration into the Tbx5b-deficient pectoral fins

In order to determine if defects were present in the muscle of Tbx5b-deficient fins, *Tg(a-actin:GFP)* fish were injected with Tbx5b morpholino. This transgenic line will mark muscle cells. At 48 hpf, two separate clusters of muscle cells can be seen in the wildtype fin (arrows, Figure A.5a). These will contribute to the abductor and adductor muscles of the fin. However, Tbx5b-deficient embryos at the same stage display no flourescence in the fin (Figure A.5a'). This suggests that at this time, there are no *a-actin* positive cells in the muscle, and perhaps no muscle present at all at this time, either because the cells from the somite have not migrated into the fin or because these cells are not appropriately differentiated. However, by 72 hpf, the fins of the Tbx5b-deficient embryos do contain two clusters of GFP+ cells (Figure A.5b'), suggesting that muscle development in embryos lacking Tbx5b is merely delayed, not lost.

A.5 A screen for genes with changes in expression in the somites

Because there were so many somite genes identified in the RNA sequencing study in Chapter 4, I decided to undertake a sensitized screen of genes expressed in the somites in order to detect possible effects on limb development, as well as a few other genes such as *cpt1b*, *cypb1b*, and *krt91*. All three genes were found on the list of 78 differentially expressed genes (Figure 4.3). *cpt1b* was chosen due to its expression in somites despite the lack of notable differential expression found by analysis of *in situ* hybridization, *cypb1b* was chosen due to

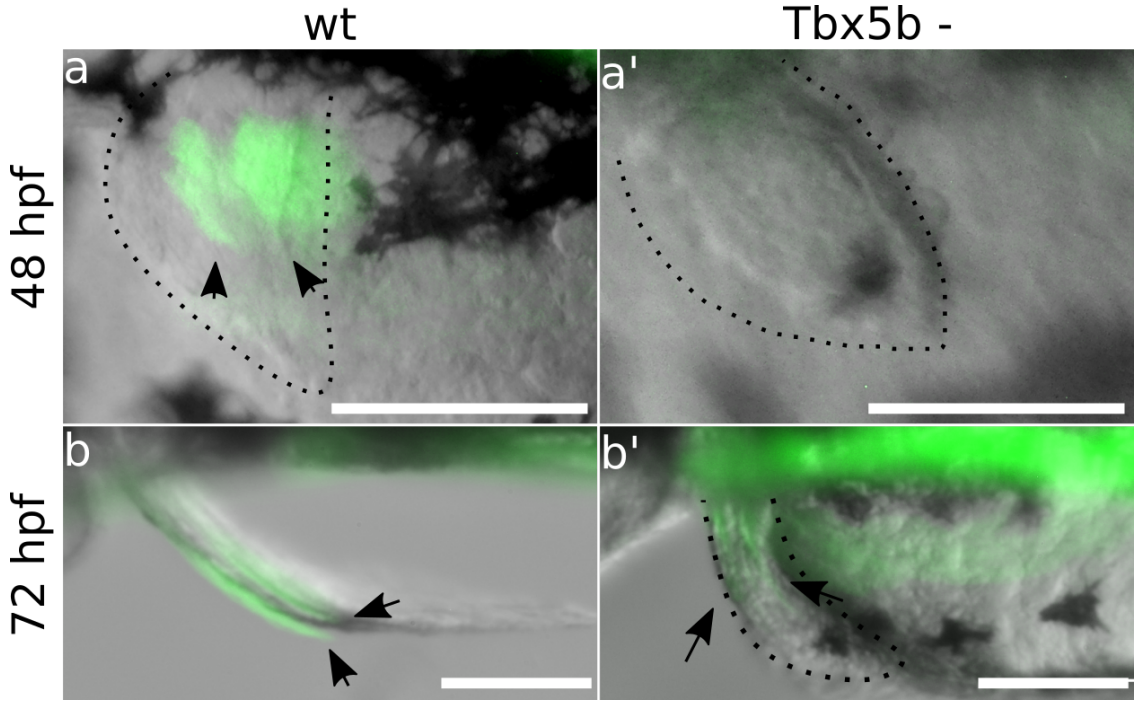

Figure A.5: Differentiation of myoblasts appears delayed in Tbx5b-deficient embryos. Fluorescence of *a-actin::GFP* in the fin. At 48 hpf, muscle cells are clearly visible in the wt (a) but not the Tbx5b-deficient fin (a'). By 72 hpf, muscle cells can be seen clearly in both wt (b) and Tbx5b-deficient (b') fins. Scale bars are 100 µm. All views are dorsal.

the role of Cyp proteins in RA signaling, and *krt91* was chosen because keratins play an important role in maintaining the apical fin fold.

Embryos were injected with a sub-phenotypic dose of Tbx5b morpholino. As can be seen in Figure A.6, the half dose of MO produced largely normal embryos, with only a small percentage of embryos having small fins. I concurrently injected gRNAs generated against each of the genes (sequences found in Table 2.1) and examined the size of the resulting fin bud at 3 dpf. 11 of the genes tested showed small fins above the sensitized dose threshold (Figure A.6). Since many of these genes affect somite development, many of them also produced embryos with twisted or shortened bodies. In order to identify small fins that were not a byproduct of an overall deformed body, I also quantified the percent of embryos with normal sized bodies and small fins. 10 of the 11 genes still showed a greater percent of small fins than the sensitized dose of morpholino alone (Figure A.6).

To test if the effect that these mostly somitic genes have on the size of the fin is independent of an interaction with Tbx5b, a secondary screen should be performed, in which these gRNAs are injected into embryos without a sensitizing dose of Tbx5b morpholino. Genes that still produce small fins may be producing these small fins independently of an interaction with *tbx5b*, while genes that only produce small fins in the sensitized embryos may be interacting with *tbx5b* to form small fins.

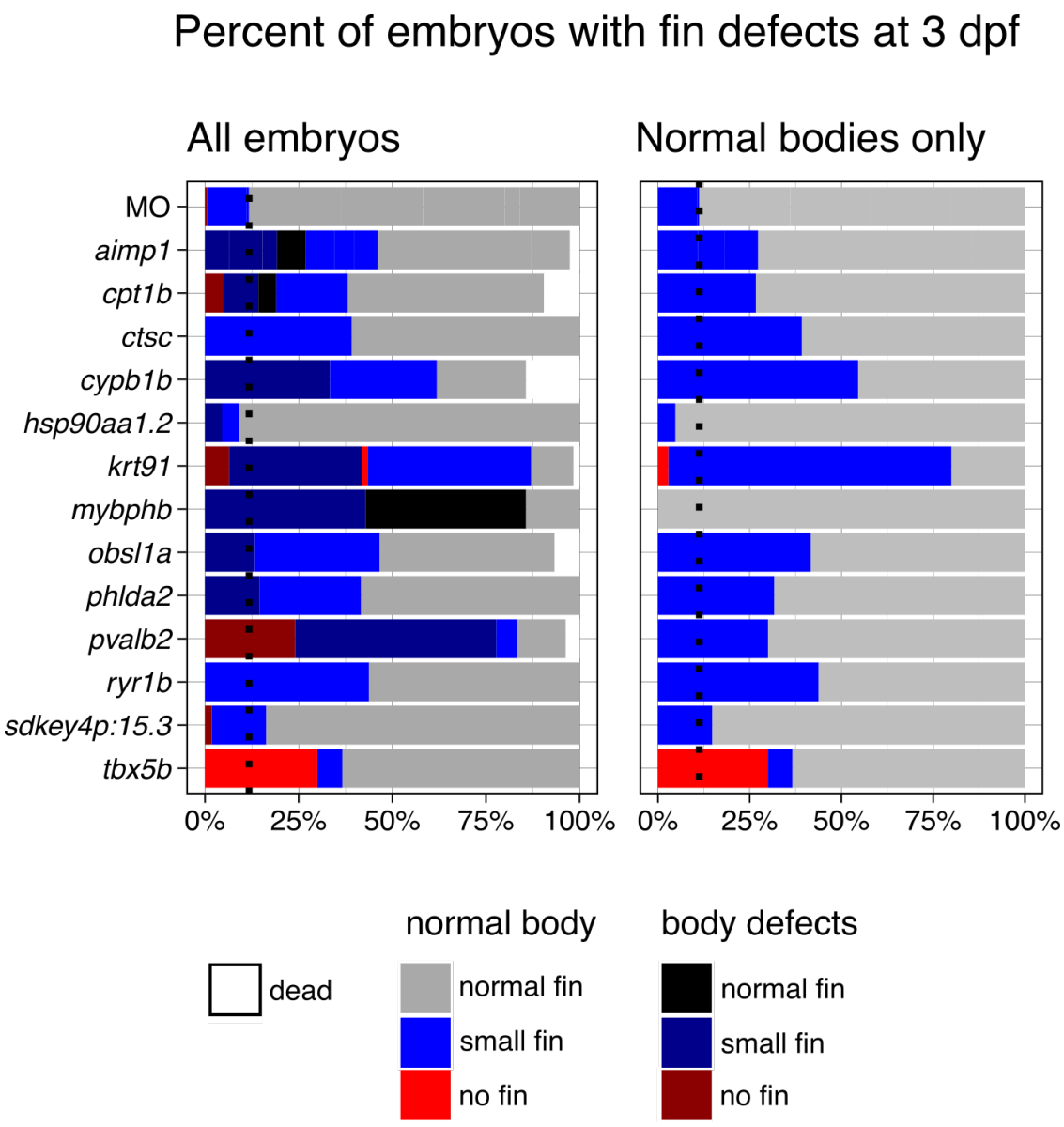

Figure A.6: a CRISPR screen for effects on the fin field of genes misregulated in embryos deficient for the Tbx5 paralogues. This graph shows the percentages of embryos at 3 dpf with the given fin phenotypes. The first graph includes all embryos, while the second graph only shows embryos that did not have other severe phenotypes, such as twisted bodies, which could be affecting fin size as a side effect rather than being the direct cause of a small fin. The dashed line represents the percent of small fins present in the half dose MO embryos.

APPENDIX B

SUPPLEMENTARY TABLES

Table B.1: Primers used to generate probes

Gene	FW sequence	RV sequence
ahcy	ATGAACACGCAGCAAAGAAA	TAATACGACTCACTATAGgg TGCTTCTCTGTCAGTTTGGT
aimp1	AGCTGAACCCCAAGAAGAAA	TAATACGACTCACTATAGgg TTCAGCACAATTGGAGAGGT
ankrd9	TGGAGGTGTTTCATTGGGAA	TAATACGACTCACTATAGgg CTGTCAGGTCCGTTACGTAA
bnip4	CTCGTGGGTAGAGCTTCATT	TAATACGACTCACTATAGgg CAGCAGTAACTTCAGCAAA
c9	CCCTGGAATGTTGGAGTTCT	TAATACGACTCACTATAGgg TATACCAAATCCAGGAGCGG
cbln11	AGAGTCCTAAAGTGGCGTTC	TAATACGACTCACTATAGgg CTCCGTTGGACATTTGATCG
cmn	GTTCCCTGTTCGCTTTTGTT	TAATACGACTCACTATAGggTCCTCCATTTGTGTTTCCCA
cox6b1	CGCATCTGTCGTTTCAATGT	TAATACGACTCACTATAGgg TGTCCCATTTCTCGATCCAG
cpt1b	GAGATTGCAAGAGGAGACGA	TAATACGACTCACTATAGgg AGGAGAGCTTTGAGGAGGTA
cryba1l1	ATAGGTTTACTCGATCCGCC	TAA TAC GAC TCA CTA TAG GGA CTC CAT GAT GTA CTG CCT G
ctsc	ATCCAGACCAACAACACTCA	TAATACGACTCACTATAGgg ATAGACCTCCAGAGCGACTC
ctslb	TGTGGGTCCTGTATCTGTTG	TAATACGACTCACTATAGgg CTCCAGTGACCTTACATT
cyp11a1	CGGTTACTTTCACACTGCTG	TAATACGACTCACTATAGgg AGAACTGATGATCACGACCC
cyp1b1	TTCACCAAAACAGTCGGAGC	TAATACGACTCACTATAGggGCTTGCCGAGTGAGAAGATG
dhrs9	GAGGACGAGCTGAAGAAGAT	TAATACGACTCACTATAGgg AGTACTGATCCTGCCGAAA
egln3	ATTCTGCACGTTTCACATGC	TAATACGACTCACTATAGggTAAATACAGGTGACGCAGC
elavl2	AACCAACCTGATCGTGAACT	TAATACGACTCACTATAGgg CGGTCAAATCGGATAAAGCC
elovl7b	AACGGCTACATCTACAGGTG	TAATACGACTCACTATAGgg CTGCATGAAGAAGAACTGGC
epd	TTCTCATCACTCTCATCGGC	TAATACGACTCACTATAGgg CAACACCGAAGAAGCTGAAG
exd1	AAGAGGACGGTGTGAGTTAC	TAATACGACTCACTATAGgg TGCTGGACTGAAGAACACAT
gins1	TTGTCCAATCAGAAAGCAGC	TAATACGACTCACTATAGgg CTAAAGGTTGGGAGATGA
gpd1a	AGAGCACGAGAATGTCAAGT	TAATACGACTCACTATAGgg AGTAGCAGGAGAAACAGAGC
gtpbp1l	GGCGATTATGGTCTGGATGA	TAATACGACTCACTATAGgg CTTTGATGACCTCTCGCAGA
hsp70l	CAGACCTTCACCACCTACTC	TAATACGACTCACTATAGggTCCCTGGTAGAGTTTGGAGA
hsp90aa1.2	TCCTCTGATGCATTGGACAA	TAATACGACTCACTATAGgg CCACGTCCAATTGATTCACC
hspb11	AAGCACAGAAGAAGCCAAAC	TAATACGACTCACTATAGgg TGAAACGTGGTCAATCTCG
krt91	TCTGCAAATGACAAAGCCAC	TAATACGACTCACTATAGgg CTCGTGGTTCTTCTTGAGGA
LOC100329294	AGAGGAGGACAGGATGAAGA	TAATACGACTCACTATAGgg AGATGTTTGGTCCGAGTCTC
LOC570474	TCAAACAGTGCTGATCCTCA	TAATACGACTCACTATAGgg TGCCTCTGTATGTGCTGTAG
lyrm1	ATGTGCTGTCTCTGTATCGG	TAATACGACTCACTATAGggAAGTACGGTGAAGTGTGTGT
malt1a	CTTCAAGCATTGTCTGTGGG	TAATACGACTCACTATAGgg TGTTTTAGGTCAGGCAGGTT
mia	TCTCCGACAAGAAGCTATGC	TAATACGACTCACTATAGgg CATTAACGCATGAGTCTC
mipa	GCTCTGCTCTACGACTTCAT	TAATACGACTCACTATAGgg TAGAAATGACAGAGGTGCCC
mir16c	GTGTGTGCGTGTGTTGTC	TAATACGACTCACTATAGgg ATGTGCTGCTTGGTGACTT
mmp2	GCCGAAATGAACATGGTGAT	TAATACGACTCACTATAGggAAGTTGTATGTGGTGGAGCA
mrpl20	TCACACACACTTGCTGAAAC	TAATACGACTCACTATAGgg TCAGCTCAGTGTAGTTGA
mrpl39	TGACCTTCAGAGATGCAGAC	TAATACGACTCACTATAGgg ATCCAGAAGCAGATCACA
mybphb	ACCAGCACCGATAAAGAAGT	TAATACGACTCACTATAGgg TCCACAACGTATCCATCCAG
ndufa4	CGCTTCATTCCTGCTGTACA	TAATACGACTCACTATAGgg CCAGCTGATTCACTAGCCTC
nots	TTGAGTCGAGCACATACACA	TAATACGACTCACTATAGgg TGGGTGTCGCTCCTATAAAC
nup54	GTCATCTTCATCCACTCCGT	TAATACGACTCACTATAGgg AACACTCCAGCTGATCAACA
obsl1a	GGATTTATCGCAGGCTGGTG	TAATACGACTCACTATAGggACCAGGGATCGAAATGTGC
p4ha1b	GCAGGTTAAAGAATGGGCAG	TAATACGACTCACTATAGgg TGGGAAGTACTGTCTCTGGA
parp3	TGCTGAGGTTCACGAGGATT	TAATACGACTCACTATAGgg TCAACTGGATGAGGCACAGT
phlda2	CCTGTTCACATCTGACTGGA	TAATACGACTCACTATAGggTGCAGGTTTATTCCGAAGAC
pnp5a	GTTCTGCACTGTTCAAGGAC	TAATACGACTCACTATAGgg AAACGCACTCCAAACCTTTC

Continued on following page

Table B.1: continued from previous page

Gene	FW sequence	RV sequence
pvalb2	TCAGGATCATACAACAGGGC	TAATACGACTCACTATAGgg CCTTCTTGATGTCATCGGGA
rn7sk	CCATTGATCGCTAGGGTTGA	TAATACGACTCACTATAGgg ATGTGTCTGAAGTCTTGG
rpph1	GTCACTCGCCAACACCTC	TAATACGACTCACTATAGgg CTCACACATCGCACTCATTC
rs1a	TGATTGCGATGATTCCTCCA	TAATACGACTCACTATAGgg ACCACTTTCACCTCCTTCAG
ryr1b	TGAACGTCTACAACACTGCT	TAATACGACTCACTATAGgg AGTGAAGTCCATCAAAGCCA
si:ch211-117m20.5	TGGGAGGACTGGTAAGATGA	TAATACGACTCACTATAGggTTGTTCTCCGTAGATCCAGC
si:dkey-204l11.1	atttacccaaagccacagga	TAATACGACTCACTATAGgg ttgtgcacttcttcctgagt
si:dkey-4p15.3	ATTGCCAATGACCAGGGTAA	TAATACGACTCACTATAGgg CCAGAGATAGTTCCAGCAT
slc25a4	CGTCTACCCTCTTGACTTCG	TAATACGACTCACTATAGgg TCCGGACTGCATCATCATAC
sox11b	GAACATTACCAAGCAGAGCG	TAATACGACTCACTATAGgg AGAGAGAGGCAAAGGTTTCC
srsf10b	AAAGTGAACAATAACCGGCG	TAATACGACTCACTATAGgg TGTGTGTTCTTCCTCTGGAC
tbx5b	TCCCAGCTACAAAGTGAAGG	TAATACGACTCACTATAGggAGACAGTCAGGAGATGGTG
tmigd1	CTCACGCAACCTTTGGATTT	TAATACGACTCACTATAGgg CGGTGGTCAGATCTAGAACC
tyrp1b	CACTACAGCACAGCAGAAAC	TAATACGACTCACTATAGggACCACGGTGATTCTCTGATC
uox	GAGAACCGGCTATGGAAAGA	TAATACGACTCACTATAGgg TTAACAGCTTTCCATGCAGC
vrk2	AAACCCTATGCCCTGTGAAA	TAATACGACTCACTATAGgg TTTCAGTCAGTCCAGAACCC
wu:fc46h12	GTCACCATGCAGACCAGAG	TAATACGACTCACTATAGgg AGGTTAAAGAGGGTGCAGT
zgc:110425	ATCATGGCAGAAACAGCAAC	TAATACGACTCACTATAGgg TTTCTTGGCTTTCTTTGGGC
zgc:113232	AGTGGAGATGCAGGGATTTC	TAATACGACTCACTATAGgg CATACTGGGAGATCTGAGCC
zgc:153405	TCGCTTAGAGAAACATGGCT	TAATACGACTCACTATAGgg TTTCTTCACCTTCTTCGGC
zgc:153713	CAGGGCAGGAGGATTATGAC	TAATACGACTCACTATAGgg AACACAAGCGGTAAACACTG
zgc:153901	TGTCACAGTGCTGAACATCT	TAATACGACTCACTATAGgg ACAGTTCATGACGTAGGGAC
zgc:158463	ACTCCGGCATGCTAAATAGT	zgc:158463rct72
zgc:194221	GACACCAATTACCGGCAATC	TAATACGACTCACTATAGgg GCGGTACTGTGAATCTACCA
zgc:195001	AATGCCCATTAGTAGCCCAA	TAATACGACTCACTATAGgg AACGTTAAGATACCGCCCAT
zgc:77398	CTGGGCAAACAACACAAAGA	TAATACGACTCACTATAGggCCACTGTCAAAGAAATC
zgc:77651	TGTTAACTGTTCAGCCCTGT	TAATACGACTCACTATAGgg CCATACTTGCAAAACCAT

Table B.2: Significant differential gene expression from the preliminary experiment at 18 hpf

gene	sample 1	sample 2	value 1	value 2	log2 FC	p value	q value
FP236171.1	starAB	tbx5a	0.456249	0	-inf	5.00E-05	0.00901062
slc2a15b	starAB	tbx5a	2.1089	9.70372	2.20205	5.00E-05	0.00901062
si:ch211-217k17.9	starAB	tbx5a	63.6349	30.7111	-1.05106	0.0004	0.0492677
grhprb	starAB	tbx5a	16.9947	45.7375	1.42829	5.00E-05	0.00901062
ncapd3	starAB	tbx5a	41.5102	20.0544	-1.04955	0.0001	0.0162912
fgg	starAB	tbx5a	18.1749	41.5798	1.19393	5.00E-05	0.00901062
si:dkey-117m1.4	starAB	tbx5a	28.2445	6.88685	-2.03605	5.00E-05	0.00901062
junba	starAB	tbx5a	75.2219	18.9749	-1.98706	5.00E-05	0.00901062
METRNL (2 of 2)	starAB	tbx5a	11.4002	1.82915	-2.63982	5.00E-05	0.00901062
ITGA2 (2 of 2)	starAB	tbx5a	14.3167	5.17175	-1.46898	5.00E-05	0.00901062
mat2al	starAB	tbx5a	80.6853	10.681	-2.91726	5.00E-05	0.00901062
spg20a	starAB	tbx5a	1.05989	0.232334	-2.18964	0.00035	0.0443614
elovl7b	starAB	tbx5a	87.2775	34.2263	-1.3505	5.00E-05	0.00901062
raf1b	starAB	tbx5a	25.6267	11.7321	-1.12719	0.0002	0.028817
FILIP1L (2 of 2)	starAB	tbx5a	13.12	4.4205	-1.56949	5.00E-05	0.00901062
prph	starAB	tbx5a	0.372718	1.42533	1.93514	0.0002	0.028817
ghrh	starAB	tbx5a	5.5541	0.229514	-4.5969	5.00E-05	0.00901062
ITPR1 (1 of 2)	starAB	tbx5a	3.74255	1.10155	-1.76449	5.00E-05	0.00901062
GPT (2 of 2)	starAB	tbx5a	6.92957	2.19757	-1.65686	5.00E-05	0.00901062
mylpfb	starAB	tbx5a	2.87322	10.8987	1.92342	0.00025	0.0337898
gch2	starAB	tbx5a	5.97287	28.3611	2.24742	5.00E-05	0.00901062
mmrn2b	starAB	tbx5a	11.5045	3.84762	-1.58016	5.00E-05	0.00901062
lsm12	starAB	tbx5a	142.821	67.8372	-1.07406	0.00025	0.0337898
PRODH2	starAB	tbx5a	4.29879	14.0388	1.70742	5.00E-05	0.00901062
ace	starAB	tbx5a	12.3795	1.25418	-3.30314	5.00E-05	0.00901062
slc16a9b	starAB	tbx5a	18.2115	5.86597	-1.63441	5.00E-05	0.00901062
zgc:173961	starAB	tbx5a	4.31077	19.0801	2.14605	5.00E-05	0.00901062
dcdc2b	starAB	tbx5a	12.4076	2.75411	-2.17157	5.00E-05	0.00901062
gins1	starAB	tbx5a	17.2015	40.4914	1.23508	0.0002	0.028817
‘march8	starAB	tbx5a	11.8695	3.55195	-1.74058	5.00E-05	0.00901062
vrk2	starAB	tbx5a	23.9988	4.92667	-2.28428	5.00E-05	0.00901062
cdhr1a	starAB	tbx5a	0.115704	0.513559	2.15009	0.00035	0.0443614
zgc:153911	starAB	tbx5a	4.2328	1.06856	-1.98594	5.00E-05	0.00901062
sb:cb252	starAB	tbx5a	180.865	82.67	-1.12947	5.00E-05	0.00901062
plp1a	starAB	tbx5a	7.79339	25.4963	1.70996	5.00E-05	0.00901062
ccng1	starAB	tbx5a	3692.32	542.087	-2.76793	5.00E-05	0.00901062
nudt6	starAB	tbx5a	7.98544	2.45273	-1.70298	5.00E-05	0.00901062
irg1l	starAB	tbx5a	23.0857	4.37961	-2.39813	5.00E-05	0.00901062
wu:fj08f03	starAB	tbx5a	15.5121	6.35776	-1.28681	5.00E-05	0.00901062
egr1	starAB	tbx5a	13.6938	5.90178	-1.2143	0.00025	0.0337898
fosl1a	starAB	tbx5a	27.9554	1.59799	-4.1288	5.00E-05	0.00901062
CABZ01047562.1	starAB	tbx5a	11.6205	3.22581	-1.84893	5.00E-05	0.00901062
gpm6aa	starAB	tbx5a	2.79643	7.57039	1.43678	0.0001	0.0162912
AL929007.2	starAB	tbx5a	0.833972	3.16384	1.92361	5.00E-05	0.00901062
RNF14 (5 of 5)	starAB	tbx5a	29.9547	1.10983	-4.75438	5.00E-05	0.00901062
RNF169	starAB	tbx5a	14.1581	2.54921	-2.4735	5.00E-05	0.00901062
her8.2	starAB	tbx5a	0.477737	2.44976	2.35835	0.00025	0.0337898
CR626907.1	starAB	tbx5a	1.06473	7.30332	2.77806	5.00E-05	0.00901062
sesn3	starAB	tbx5a	123.304	36.7271	-1.7473	5.00E-05	0.00901062
CR478286.2	starAB	tbx5a	2.00851	6.81973	1.76359	5.00E-05	0.00901062

Continued on following page

Table B.2: continued from previous page

gene	sample 1	sample 2	value 1	value 2	log2 FC	p value	q value
bbc3	starAB	tbx5a	16.1132	1.00516	-4.00275	5.00E-05	0.00901062
BX908796.1	starAB	tbx5a	0.310528	0	#NAME?	5.00E-05	0.00901062
EXO5	starAB	tbx5a	42.3752	5.05659	-3.06698	5.00E-05	0.00901062
DNAH5	starAB	tbx5a	2.44638	0.971068	-1.333	0.00035	0.0443614
tp53inp1	starAB	tbx5a	20.2537	8.79666	-1.20316	0.0003	0.0394991
rpz5	starAB	tbx5a	24.9595	5.19994	-2.26302	5.00E-05	0.00901062
nr0b2a	starAB	tbx5a	11.0034	24.4453	1.1516	0.0002	0.028817
atxn1b	starAB	tbx5a	11.6166	0.515699	-4.49351	5.00E-05	0.00901062
rspo1	starAB	tbx5a	6.8172	0.209049	-5.02727	5.00E-05	0.00901062
SH3D21	starAB	tbx5a	13.0404	33.0747	1.34274	0.0002	0.028817
azin1a	starAB	tbx5a	39.1261	10.4972	-1.89813	5.00E-05	0.00901062
CNDP1	starAB	tbx5a	76.1154	193.451	1.34571	5.00E-05	0.00901062
fabp7a	starAB	tbx5a	16.6905	51.7432	1.63234	5.00E-05	0.00901062
CABZ01073069.1	starAB	tbx5a	1.4468	0	#NAME?	0.00025	0.0337898
ankrd5b	starAB	tbx5a	0.790036	0.147316	-2.42301	0.00035	0.0443614
BX005375.2	starAB	tbx5a	4.61849	0.981974	-2.23366	5.00E-05	0.00901062
bnip4	starAB	tbx5a	100.658	37.1721	-1.43717	5.00E-05	0.00901062
CU638738.1	starAB	tbx5a	0.977146	0.151838	-2.68604	5.00E-05	0.00901062
prox2	starAB	tbx5a	3.11804	0.658798	-2.24273	5.00E-05	0.00901062
si:dkey-238c7.12	starAB	tbx5a	70.2315	220.094	1.64793	5.00E-05	0.00901062
si:ch211-264e16.1	starAB	tbx5a	0.809682	4.88346	2.59248	5.00E-05	0.00901062
fosb	starAB	tbx5a	5.05689	0.780756	-2.69531	5.00E-05	0.00901062
abcc5	starAB	tbx5a	27.4578	7.51087	-1.87017	5.00E-05	0.00901062
zbtb38	starAB	tbx5a	0.614339	0.0977788	-2.65144	0.00025	0.0337898
txnipa	starAB	tbx5a	264.838	123.834	-1.0967	5.00E-05	0.00901062
fabp3	starAB	tbx5a	362.158	748.684	1.04774	0.0002	0.028817
cica	starAB	tbx5a	4.88362	2.06545	-1.24149	0.0001	0.0162912
si:ch211-39a7.1	starAB	tbx5a	5.74328	0.106062	-5.75889	5.00E-05	0.00901062
il11b	starAB	tbx5a	0.515026	0	#NAME?	5.00E-05	0.00901062
ptp4a3	starAB	tbx5a	88.0288	35.0335	-1.32924	0.00025	0.0337898
zgc:123103	starAB	tbx5a	0	1.02519	inf	5.00E-05	0.00901062
nme2b.2	starAB	tbx5a	364.775	850.398	1.22113	5.00E-05	0.00901062
prdm1b	starAB	tbx5a	1.39319	0.301273	-2.20925	5.00E-05	0.00901062
pik3r3a	starAB	tbx5a	63.2304	17.192	-1.87888	5.00E-05	0.00901062
gadd45aa	starAB	tbx5a	38.4238	4.3314	-3.1491	5.00E-05	0.00901062
si:dkey-82k12.7	starAB	tbx5a	0.496953	0	#NAME?	5.00E-05	0.00901062
plk3	starAB	tbx5a	59.3103	24.078	-1.30056	5.00E-05	0.00901062
otomp	starAB	tbx5a	1.74334	7.59292	2.1228	5.00E-05	0.00901062
itgb1b.1	starAB	tbx5a	7.62004	22.0979	1.53604	5.00E-05	0.00901062
smarcd3a	starAB	tbx5a	8.34201	2.71872	-1.61747	5.00E-05	0.00901062
fastk	starAB	tbx5a	19.9127	6.73253	-1.56447	5.00E-05	0.00901062
APOM	starAB	tbx5a	49.812	120.561	1.2752	5.00E-05	0.00901062
CU929133.2	starAB	tbx5a	0.523679	4.67017	3.15672	5.00E-05	0.00901062
si:ch211-121a2.3	starAB	tbx5a	2.95636	0.54591	-2.43709	5.00E-05	0.00901062
rd3	starAB	tbx5a	9.17517	1.45482	-2.6569	5.00E-05	0.00901062
sox7	starAB	tbx5a	11.0522	4.70046	-1.23347	0.0004	0.0492677
lnx1	starAB	tbx5a	32.8531	2.56926	-3.6766	5.00E-05	0.00901062
slc10a1	starAB	tbx5a	0.815709	3.17244	1.95947	0.0003	0.0394991
sesn1	starAB	tbx5a	25.773	10.1458	-1.34498	5.00E-05	0.00901062
atf3	starAB	tbx5a	15.8767	1.83811	-3.11062	5.00E-05	0.00901062
jdp2	starAB	tbx5a	18.7756	5.29094	-1.82726	5.00E-05	0.00901062

Continued on following page

Table B.2: continued from previous page

gene	sample 1	sample 2	value 1	value 2	log2 FC	p value	q value
MGST3	starAB	tbx5a	40.9434	121.971	1.57484	5.00E-05	0.00901062
dhcr24	starAB	tbx5a	2.47107	7.89674	1.67612	5.00E-05	0.00901062
CRIP2	starAB	tbx5a	0.571492	2.43058	2.08849	0.0001	0.0162912
rasl11b	starAB	tbx5a	24.0515	6.68755	-1.84658	5.00E-05	0.00901062
foxo3b	starAB	tbx5a	56.3215	7.61336	-2.88708	5.00E-05	0.00901062
ptgs2b	starAB	tbx5a	26.4947	4.92681	-2.42698	5.00E-05	0.00901062
cited2	starAB	tbx5a	28.8203	11.4415	-1.33281	5.00E-05	0.00901062
fos	starAB	tbx5a	87.7227	18.7529	-2.22583	5.00E-05	0.00901062
thbs4b	starAB	tbx5a	12.1592	36.4054	1.5821	5.00E-05	0.00901062
TAF1C	starAB	tbx5a	24.5917	4.35417	-2.4977	5.00E-05	0.00901062
tbca	starAB	tbx5a	45.6387	113.561	1.31514	5.00E-05	0.00901062
hspb11	starAB	tbx5a	9.63686	26.493	1.45898	5.00E-05	0.00901062
serpinf1	starAB	tbx5a	0.774039	2.4949	1.6885	0.0002	0.028817
si:ch211-25g7.3	starAB	tbx5a	2.93068	0.785559	-1.89944	0.0001	0.0162912
f2rl1.2	starAB	tbx5a	22.7548	7.22656	-1.65479	5.00E-05	0.00901062
rb1	starAB	tbx5a	8.9125	18.8613	1.08153	0.0003	0.0394991
hoga1	starAB	tbx5a	2.81875	8.07908	1.51914	5.00E-05	0.00901062
CABZ01044356.1	starAB	tbx5a	2.91138	0.786805	-1.88763	5.00E-05	0.00901062
cdkn1a	starAB	tbx5a	51.6659	9.09483	-2.50609	5.00E-05	0.00901062
malt1a	starAB	tbx5a	3.74025	1.40656	-1.41097	0.00025	0.0337898
si:ch73-21g5.7	starAB	tbx5a	9.16424	30.2646	1.72354	5.00E-05	0.00901062
ednrab	starAB	tbx5a	19.7488	43.7736	1.14829	0.0002	0.028817
phlda3	starAB	tbx5a	81.7241	6.19749	-3.721	5.00E-05	0.00901062
si:dkey-21o19.6	starAB	tbx5a	18.5167	0.148683	-6.96044	5.00E-05	0.00901062
gdi1	starAB	tbx5a	16.6825	35.3863	1.08485	0.0002	0.028817
nr4a1	starAB	tbx5a	9.78003	1.15917	-3.07675	5.00E-05	0.00901062
FP565458.1	starAB	tbx5a	0.426495	0	#NAME?	5.00E-05	0.00901062
LAMA1	starAB	tbx5a	38.3667	20.0825	-0.933915	0.00025	0.0337898
ADARB2	starAB	tbx5a	2.3454	0.709381	-1.7252	0.00015	0.0231409
ARMC3	starAB	tbx5a	5.21694	1.8246	-1.51562	5.00E-05	0.00901062
rpl22l1	starAB	tbx5a	298.13	1025.03	1.78165	5.00E-05	0.00901062
lyrm1	starAB	tbx5a	30.4169	7.90083	-1.9448	5.00E-05	0.00901062
PTPRM (2 of 2)	starAB	tbx5a	3.04359	1.07901	-1.49607	0.00015	0.0231409
CABZ01068602.1	starAB	tbx5a	1.25622	0.323255	-1.95834	0.00025	0.0337898
BX294110.1	starAB	tbx5a	154.279	49.6135	-1.63673	5.00E-05	0.00901062
tnni2a.1	starAB	tbx5a	0.334414	0	#NAME?	5.00E-05	0.00901062
DBNDD1	starAB	tbx5a	0.245117	0.895174	1.8687	0.0001	0.0162912
ptpn9a	starAB	tbx5a	1.92159	4.38444	1.19009	0.0002	0.028817
phlda2	starAB	tbx5a	86.1543	36.5287	-1.23789	0.00015	0.0231409
RPS27L	starAB	tbx5a	1119.6	166.311	-2.75103	5.00E-05	0.00901062
kif15	starAB	tbx5a	14.4019	48.1069	1.73999	0.0001	0.0162912
RBL2	starAB	tbx5a	12.1068	0.567011	-4.41629	5.00E-05	0.00901062
si:ch1073-322p19.1	starAB	tbx5a	5.4976	2.13432	-1.36502	0.00015	0.0231409
TRIM35 (10 of 41)	starAB	tbx5a	0	0.18269	inf	5.00E-05	0.00901062
junbb	starAB	tbx5a	80.9268	25.7704	-1.65091	5.00E-05	0.00901062
gosr2	starAB	tbx5a	11.2829	36.2715	1.6847	5.00E-05	0.00901062
slc4a1a	starAB	tbx5a	1.07863	4.1214	1.93394	5.00E-05	0.00901062
baxa	starAB	tbx5a	77.1778	31.1003	-1.31126	0.0001	0.0162912
socs3a	starAB	tbx5a	5.57326	1.19831	-2.21752	5.00E-05	0.00901062
hsp90b1	starAB	tbx5a	27.7902	62.069	1.15929	5.00E-05	0.00901062
mdm2	starAB	tbx5a	476.412	91.6408	-2.37815	5.00E-05	0.00901062

Continued on following page

Table B.2: continued from previous page

gene	sample 1	sample 2	value 1	value 2	log2 FC	p value	q value
zgc:77651	starAB	tbx5a	4.29212	12.3385	1.5234	5.00E-05	0.00901062
si:ch211-199m9.3	starAB	tbx5a	0.277494	0	#NAME?	5.00E-05	0.00901062
FP015791.1	starAB	tbx5a	26.6001	1.28562	-4.37089	5.00E-05	0.00901062
BCL2L14	starAB	tbx5a	18.0606	4.22114	-2.09714	5.00E-05	0.00901062
DGKI	starAB	tbx5a	1.70109	0.482914	-1.81662	5.00E-05	0.00901062
dcn	starAB	tbx5a	12.3111	25.6688	1.06005	0.00025	0.0337898
strap	starAB	tbx5a	97.0759	48.8385	-0.991095	0.00025	0.0337898
pah	starAB	tbx5a	1.65086	5.01679	1.60355	5.00E-05	0.00901062
CR388095.1	starAB	tbx5a	0.188847	0	#NAME?	5.00E-05	0.00901062
tp53	starAB	tbx5a	551.858	103.074	-2.42061	5.00E-05	0.00901062
c9	starAB	tbx5a	10.3267	50.6364	2.2938	5.00E-05	0.00901062
aqp3a	starAB	tbx5a	0.981962	5.2306	2.41324	5.00E-05	0.00901062
thbs4a	starAB	tbx5a	0.142601	0.970108	2.76616	5.00E-05	0.00901062
si:ch211-160e1.5	starAB	tbx5a	241.133	44.0099	-2.45393	5.00E-05	0.00901062
ypel1	starAB	tbx5a	14.8537	5.67078	-1.3892	5.00E-05	0.00901062
C5H8orf4 (1 of 2)	starAB	tbx5a	31.8447	13.6403	-1.22318	0.0002	0.028817
ATF5 (1 of 2)	starAB	tbx5a	3.7721	1.30496	-1.53136	0.00025	0.0337898
si:dkey-204l11.1	starAB	tbx5a	32.246	1.39396	-4.53186	5.00E-05	0.00901062
kcmf1	starAB	tbx5a	22.4748	9.55857	-1.23345	5.00E-05	0.00901062
atf4b1	starAB	tbx5a	671.515	270.96	-1.30934	5.00E-05	0.00901062
casp8	starAB	tbx5a	47.9714	3.6754	-3.7062	5.00E-05	0.00901062
ahcy	starAB	tbx5a	168.799	360.508	1.09472	5.00E-05	0.00901062
zgc:165344	starAB	tbx5a	60.9054	29.4688	-1.04738	0.0004	0.0492677
pl10	starAB	tbx5a	149.03	54.3147	-1.45619	5.00E-05	0.00901062
ENSDARG00000006544	starAB	tbx5a	0.258901	0	#NAME?	0.00025	0.0337898
GCA	starAB	tbx5a	30.0341	70.0534	1.22185	0.0001	0.0162912
h1fx	starAB	tbx5a	73.6219	32.7894	-1.16691	5.00E-05	0.00901062
parp3	starAB	tbx5a	17.6559	4.43729	-1.9924	5.00E-05	0.00901062
soat2	starAB	tbx5a	4.91158	14.3227	1.54405	5.00E-05	0.00901062
BX470211.1	starAB	tbx5a	1.94569	0.422113	-2.20458	0.00015	0.0231409
fxr2	starAB	tbx5a	80.4962	39.2933	-1.03464	0.00015	0.0231409
arhgap1	starAB	tbx5a	6.25052	14.6202	1.22591	5.00E-05	0.00901062
tnnt3b	starAB	tbx5a	6.91452	2.16764	-1.6735	0.0001	0.0162912
CR352229.3	starAB	tbx5a	96.5527	16.8611	-2.51762	5.00E-05	0.00901062
RNF166 (1 of 2)	starAB	tbx5a	0	0.418527	inf	5.00E-05	0.00901062
zgc:113413	starAB	tbx5a	2.14965	5.98122	1.47633	0.00035	0.0443614
C7H4orf48	starAB	tbx5a	0.803682	3.72018	2.21068	0.0001	0.0162912
cilp	starAB	tbx5a	3.75396	9.14638	1.28479	0.00015	0.0231409
mmp2	starAB	tbx5a	79.4379	29.6897	-1.41987	5.00E-05	0.00901062
asic1a	starAB	tbx5a	4.69513	0.223725	-4.39137	5.00E-05	0.00901062
C8H9orf172 (2 of 2)	starAB	tbx5a	2.18185	0.811773	-1.4264	0.00015	0.0231409
EGR3	starAB	tbx5a	0.840675	0.0650695	-3.6915	0.0002	0.028817
TMCC1 (2 of 2)	starAB	tbx5a	4.52646	0.900725	-2.32922	5.00E-05	0.00901062
calrl2	starAB	tbx5a	31.1101	63.9894	1.04045	0.0002	0.028817
C8H1orf228	starAB	tbx5a	4.19101	1.07401	-1.96428	0.0001	0.0162912
acer1	starAB	tbx5a	8.53592	3.24664	-1.3946	0.0003	0.0394991
zgc:110353	starAB	tbx5a	5.02549	1.2885	-1.96358	5.00E-05	0.00901062
AL929453.1	starAB	tbx5a	1.34913	0.216348	-2.6406	5.00E-05	0.00901062
dusp2	starAB	tbx5a	1.52289	0.320809	-2.24703	0.0001	0.0162912
crfb1	starAB	tbx5a	4.90299	1.59047	-1.6242	5.00E-05	0.00901062
REV1	starAB	tbx5a	11.4117	4.47664	-1.35003	5.00E-05	0.00901062

Continued on following page

Table B.2: continued from previous page

gene	sample 1	sample 2	value 1	value 2	log2 FC	p value	q value
si:dkey-145p14.5	starAB	tbx5a	43.1311	17.5729	-1.29538	5.00E-05	0.00901062
cdca7a	starAB	tbx5a	56.6617	124.356	1.13403	0.00015	0.0231409
zak	starAB	tbx5a	7.96677	1.00326	-2.9893	5.00E-05	0.00901062
si:dkey-145p14.6	starAB	tbx5a	1.28605	0	#NAME?	0.0003	0.0394991
phgdh	starAB	tbx5a	19.0554	46.1027	1.27465	5.00E-05	0.00901062
TANC1 (1 of 2)	starAB	tbx5a	5.49617	1.15091	-2.25565	5.00E-05	0.00901062
slc2a15b	starAB	tbx5b	2.1089	10.6335	2.33405	5.00E-05	0.00901062
ednrb1a	starAB	tbx5b	0.171173	0.635701	1.8929	0.0004	0.0492677
si:dkey-117m1.4	starAB	tbx5b	28.2445	10.0053	-1.4972	5.00E-05	0.00901062
CABZ01072534.1	starAB	tbx5b	0.452156	1.14783	1.34401	0.00025	0.0337898
cxcl-c1c	starAB	tbx5b	0.357904	2.12833	2.57208	5.00E-05	0.00901062
METRNL (2 of 2)	starAB	tbx5b	11.4002	2.39206	-2.25274	5.00E-05	0.00901062
col5a3b	starAB	tbx5b	3.50943	8.29695	1.24134	0.0002	0.028817
ITGA2 (2 of 2)	starAB	tbx5b	14.3167	5.61231	-1.35104	0.00035	0.0443614
EPHA5	starAB	tbx5b	0.148659	0.702339	2.24016	5.00E-05	0.00901062
mmp13a	starAB	tbx5b	8.45992	3.15369	-1.4236	0.0002	0.028817
mat2al	starAB	tbx5b	80.6853	10.0894	-2.99947	5.00E-05	0.00901062
pcyox1	starAB	tbx5b	5.35069	13.9046	1.37777	0.00015	0.0231409
ak3	starAB	tbx5b	99.6096	48.308	-1.04402	0.0001	0.0162912
uox	starAB	tbx5b	97.4424	42.8928	-1.18381	5.00E-05	0.00901062
ENSDARG00000073699	starAB	tbx5b	0.211319	1.13997	2.43151	0.00015	0.0231409
ghrh	starAB	tbx5b	5.5541	0.233621	-4.57131	5.00E-05	0.00901062
fam43a	starAB	tbx5b	8.06584	3.29308	-1.29239	0.0001	0.0162912
ITPR1 (1 of 2)	starAB	tbx5b	3.74255	1.03618	-1.85275	5.00E-05	0.00901062
pax7a	starAB	tbx5b	2.77591	11.7826	2.08562	5.00E-05	0.00901062
CR759952.1	starAB	tbx5b	2.60899	9.90187	1.92421	5.00E-05	0.00901062
GPT (2 of 2)	starAB	tbx5b	6.92957	2.56954	-1.43126	0.00015	0.0231409
mylpfb	starAB	tbx5b	2.87322	10.0406	1.80511	0.0003	0.0394991
gch2	starAB	tbx5b	5.97287	31.7153	2.40868	5.00E-05	0.00901062
mmrn2b	starAB	tbx5b	11.5045	3.12512	-1.88021	5.00E-05	0.00901062
PTS	starAB	tbx5b	17.1924	51.5502	1.5842	5.00E-05	0.00901062
col1a1b	starAB	tbx5b	23.6477	47.1858	0.996652	0.0003	0.0394991
lsm12	starAB	tbx5b	142.821	71.0105	-1.0081	0.0003	0.0394991
PRODH2	starAB	tbx5b	4.29879	12.586	1.54982	5.00E-05	0.00901062
ace	starAB	tbx5b	12.3795	1.30496	-3.24588	5.00E-05	0.00901062
CU459092.1	starAB	tbx5b	0.251058	0	#NAME?	5.00E-05	0.00901062
slc16a9b	starAB	tbx5b	18.2115	7.17453	-1.3439	5.00E-05	0.00901062
slc2a15a	starAB	tbx5b	0.374328	2.57367	2.78145	5.00E-05	0.00901062
dcdc2b	starAB	tbx5b	12.4076	1.95615	-2.66514	5.00E-05	0.00901062
cyp1b1	starAB	tbx5b	3.1898	0.620938	-2.36094	5.00E-05	0.00901062
vrk2	starAB	tbx5b	23.9988	4.29392	-2.4826	5.00E-05	0.00901062
zgc:153911	starAB	tbx5b	4.2328	10.1129	1.25651	0.0004	0.0492677
plp1a	starAB	tbx5b	7.79339	23.21	1.57442	5.00E-05	0.00901062
ccng1	starAB	tbx5b	3692.32	498.304	-2.88943	5.00E-05	0.00901062
gpr137	starAB	tbx5b	45.0177	20.4009	-1.14186	0.0002	0.028817
nudt6	starAB	tbx5b	7.98544	2.75959	-1.53292	0.00035	0.0443614
CABZ01047562.1	starAB	tbx5b	11.6205	3.38019	-1.78149	5.00E-05	0.00901062
gpm6aa	starAB	tbx5b	2.79643	9.30939	1.7351	5.00E-05	0.00901062
RNF14 (5 of 5)	starAB	tbx5b	29.9547	1.03555	-4.85431	5.00E-05	0.00901062
RNF169	starAB	tbx5b	14.1581	2.73473	-2.37215	5.00E-05	0.00901062
her8.2	starAB	tbx5b	0.477737	2.83701	2.57008	0.0001	0.0162912

Continued on following page

Table B.2: continued from previous page

gene	sample 1	sample 2	value 1	value 2	log2 FC	p value	q value
egln2	starAB	tbx5b	9.43445	2.14464	-2.1372	5.00E-05	0.00901062
CR626907.1	starAB	tbx5b	1.06473	6.31644	2.56862	5.00E-05	0.00901062
SPA17	starAB	tbx5b	7.61691	2.51597	-1.59809	0.00015	0.0231409
sesn3	starAB	tbx5b	123.304	16.971	-2.86107	5.00E-05	0.00901062
csf1ra	starAB	tbx5b	0.192971	0.7914	2.03602	0.0003	0.0394991
CR478286.2	starAB	tbx5b	2.00851	5.14578	1.35726	0.00025	0.0337898
ADAMTS15 (2 of 2)	starAB	tbx5b	0.29969	1.28028	2.09492	5.00E-05	0.00901062
bbc3	starAB	tbx5b	16.1132	1.55796	-3.37051	5.00E-05	0.00901062
EXO5	starAB	tbx5b	42.3752	4.65983	-3.18487	5.00E-05	0.00901062
rab38a	starAB	tbx5b	1.55918	5.24132	1.74914	0.00015	0.0231409
DNAH5	starAB	tbx5b	2.44638	0.900346	-1.4421	0.0001	0.0162912
nr4a3	starAB	tbx5b	1.04937	12.8211	3.61092	5.00E-05	0.00901062
col6a6	starAB	tbx5b	0.293927	0.86169	1.55171	5.00E-05	0.00901062
tp53inp1	starAB	tbx5b	20.2537	8.51099	-1.25079	0.00035	0.0443614
rpz5	starAB	tbx5b	24.9595	5.90853	-2.07872	5.00E-05	0.00901062
nr0b2a	starAB	tbx5b	11.0034	23.0222	1.06507	0.0003	0.0394991
atxn1b	starAB	tbx5b	11.6166	0.423094	-4.77906	5.00E-05	0.00901062
slc45a4	starAB	tbx5b	11.5289	4.80485	-1.26269	5.00E-05	0.00901062
rspo1	starAB	tbx5b	6.8172	0.190413	-5.16197	5.00E-05	0.00901062
EIF2C1	starAB	tbx5b	3.40623	10.4896	1.62271	5.00E-05	0.00901062
azin1a	starAB	tbx5b	39.1261	10.0758	-1.95724	5.00E-05	0.00901062
CNDP1	starAB	tbx5b	76.1154	168.683	1.14805	5.00E-05	0.00901062
fabp7a	starAB	tbx5b	16.6905	49.6809	1.57366	5.00E-05	0.00901062
egln3	starAB	tbx5b	7.75813	1.24	-2.64537	5.00E-05	0.00901062
ankrd5b	starAB	tbx5b	0.790036	0.147275	-2.42341	0.0004	0.0492677
p4ha1b	starAB	tbx5b	114.498	36.6192	-1.64465	5.00E-05	0.00901062
BX005375.2	starAB	tbx5b	4.61849	0.665246	-2.79546	5.00E-05	0.00901062
bnip4	starAB	tbx5b	100.658	32.3813	-1.63623	5.00E-05	0.00901062
CU638738.1	starAB	tbx5b	0.977146	2.91448	1.57659	5.00E-05	0.00901062
prox2	starAB	tbx5b	3.11804	1.15443	-1.43346	0.0004	0.0492677
PARP6 (1 of 4)	starAB	tbx5b	0.653104	0.128101	-2.35004	5.00E-05	0.00901062
si:dkey-238c7.12	starAB	tbx5b	70.2315	151.943	1.11334	0.00025	0.0337898
si:ch211-264e16.1	starAB	tbx5b	0.809682	3.16814	1.96821	5.00E-05	0.00901062
abcc5	starAB	tbx5b	27.4578	9.82605	-1.48253	0.0003	0.0394991
zbtb38	starAB	tbx5b	0.614339	0.0527919	-3.54065	0.00015	0.0231409
KCNJ1 (3 of 7)	starAB	tbx5b	0.380155	1.6101	2.08249	0.00035	0.0443614
fabp3	starAB	tbx5b	362.158	749.826	1.04994	0.00015	0.0231409
eomesa	starAB	tbx5b	0.713424	3.28413	2.20268	5.00E-05	0.00901062
si:ch211-39a7.1	starAB	tbx5b	5.74328	0.169798	-5.07998	5.00E-05	0.00901062
lim2.4	starAB	tbx5b	0	0.169446	inf	5.00E-05	0.00901062
ptp4a3	starAB	tbx5b	88.0288	37.2038	-1.24252	0.00035	0.0443614
prdm1b	starAB	tbx5b	1.39319	0.393633	-1.82346	5.00E-05	0.00901062
pik3r3a	starAB	tbx5b	63.2304	16.1364	-1.9703	5.00E-05	0.00901062
gadd45aa	starAB	tbx5b	38.4238	4.30509	-3.15789	5.00E-05	0.00901062
amotl2b	starAB	tbx5b	29.5899	11.4999	-1.36349	5.00E-05	0.00901062
si:dkey-82k12.7	starAB	tbx5b	0.496953	0	-inf	5.00E-05	0.00901062
otomp	starAB	tbx5b	1.74334	10.7164	2.61989	5.00E-05	0.00901062
itgb1b.1	starAB	tbx5b	7.62004	20.8682	1.45343	5.00E-05	0.00901062
CU179656.1	starAB	tbx5b	0.307832	0.85609	1.47562	5.00E-05	0.00901062
fastk	starAB	tbx5b	19.9127	8.50069	-1.22804	5.00E-05	0.00901062
APOM	starAB	tbx5b	49.812	122.574	1.29909	5.00E-05	0.00901062

Continued on following page

Table B.2: continued from previous page

gene	sample 1	sample 2	value 1	value 2	log2 FC	p value	q value
CREB3L3 (2 of 2)	starAB	tbx5b	21.0455	9.18436	-1.19626	0.0004	0.0492677
CU929133.2	starAB	tbx5b	0.523679	4.40741	3.07318	5.00E-05	0.00901062
si:ch211-121a2.3	starAB	tbx5b	2.95636	0.485063	-2.60758	5.00E-05	0.00901062
rd3	starAB	tbx5b	9.17517	1.64672	-2.47814	0.0001	0.0162912
lnx1	starAB	tbx5b	32.8531	2.81088	-3.54694	5.00E-05	0.00901062
slc10a1	starAB	tbx5b	0.815709	3.7209	2.18952	5.00E-05	0.00901062
sesn1	starAB	tbx5b	25.773	7.61408	-1.75912	5.00E-05	0.00901062
ccdc164	starAB	tbx5b	4.90659	1.66584	-1.55847	5.00E-05	0.00901062
MGST3	starAB	tbx5b	40.9434	106.448	1.37844	0.0001	0.0162912
dhcr24	starAB	tbx5b	2.47107	8.156	1.72273	5.00E-05	0.00901062
CRIP2	starAB	tbx5b	0.571492	2.35752	2.04447	0.0001	0.0162912
rhag	starAB	tbx5b	1.31291	4.08519	1.63764	0.0001	0.0162912
rasl11b	starAB	tbx5b	24.0515	3.30685	-2.8626	5.00E-05	0.00901062
si:dkey-85n7.7	starAB	tbx5b	0.968484	0	‘-inf	5.00E-05	0.00901062
foxo3b	starAB	tbx5b	56.3215	9.58664	-2.55459	5.00E-05	0.00901062
cited2	starAB	tbx5b	28.8203	11.9795	-1.26652	5.00E-05	0.00901062
thbs4b	starAB	tbx5b	12.1592	33.7469	1.4727	5.00E-05	0.00901062
TAF1C	starAB	tbx5b	24.5917	6.11762	-2.00713	0.0002	0.028817
tbca	starAB	tbx5b	45.6387	101.535	1.15365	0.00025	0.0337898
adora2ab	starAB	tbx5b	7.79602	3.07021	-1.3444	0.0001	0.0162912
irf1b	starAB	tbx5b	0.265952	1.74513	2.7141	5.00E-05	0.00901062
klf4a	starAB	tbx5b	6.02653	16.3693	1.44159	5.00E-05	0.00901062
rb1	starAB	tbx5b	8.9125	23.9321	1.42504	5.00E-05	0.00901062
aldocb	starAB	tbx5b	21.5396	6.2301	-1.78966	5.00E-05	0.00901062
p4ha2	starAB	tbx5b	48.3355	20.8232	-1.21489	5.00E-05	0.00901062
TMEM43	starAB	tbx5b	21.5195	5.54605	-1.95611	5.00E-05	0.00901062
cdkn1a	starAB	tbx5b	51.6659	10.5056	-2.29806	5.00E-05	0.00901062
rdh5	starAB	tbx5b	0.707851	2.95893	2.06356	5.00E-05	0.00901062
ahr1b	starAB	tbx5b	0.150961	0.632868	2.06773	0.00035	0.0443614
malt1a	starAB	tbx5b	3.74025	1.3585	-1.46112	0.0001	0.0162912
PLEKHG1	starAB	tbx5b	2.92314	7.34607	1.32946	0.00025	0.0337898
si:ch211-117c9.5	starAB	tbx5b	1.61596	0.375845	-2.10419	0.00035	0.0443614
si:ch73-21g5.7	starAB	tbx5b	9.16424	29.7361	1.69813	5.00E-05	0.00901062
ednrab	starAB	tbx5b	19.7488	47.6596	1.271	5.00E-05	0.00901062
phlda3	starAB	tbx5b	81.7241	6.81406	-3.58417	5.00E-05	0.00901062
si:dkey-21o19.6	starAB	tbx5b	18.5167	0.118913	-7.28277	5.00E-05	0.00901062
gdi1	starAB	tbx5b	16.6825	36.5878	1.13302	5.00E-05	0.00901062
nr4a1	starAB	tbx5b	9.78003	31.9289	1.70695	5.00E-05	0.00901062
nlrc3	starAB	tbx5b	0.755472	0.0726941	-3.37747	0.00035	0.0443614
pck2	starAB	tbx5b	210.993	99.1705	-1.08921	0.0002	0.028817
ARMC3	starAB	tbx5b	5.21694	1.73357	-1.58945	5.00E-05	0.00901062
rpl22l1	starAB	tbx5b	298.13	810.395	1.44268	5.00E-05	0.00901062
lyrm1	starAB	tbx5b	30.4169	8.19038	-1.89287	5.00E-05	0.00901062
cox6b1	starAB	tbx5b	35.2464	5.5856	-2.65769	5.00E-05	0.00901062
ppm1h	starAB	tbx5b	37.1561	15.6746	-1.24517	5.00E-05	0.00901062
CABZ01068602.1	starAB	tbx5b	1.25622	0.277266	-2.17974	5.00E-05	0.00901062
BX294110.1	starAB	tbx5b	154.279	47.783	-1.69097	5.00E-05	0.00901062
cyp11a1	starAB	tbx5b	47.4224	21.0411	-1.17236	5.00E-05	0.00901062
gpia	starAB	tbx5b	38.3014	14.5581	-1.39558	0.0002	0.028817
DBNDD1	starAB	tbx5b	0.245117	1.04204	2.08786	5.00E-05	0.00901062
SLC6A13	starAB	tbx5b	1.5531	4.24906	1.45199	0.0002	0.028817

Continued on following page

Table B.2: continued from previous page

gene	sample 1	sample 2	value 1	value 2	log2 FC	p value	q value
CCDC135	starAB	tbx5b	4.01993	1.51572	-1.40717	0.0003	0.0394991
ptpn9a	starAB	tbx5b	1.92159	4.74949	1.30547	0.0001	0.0162912
lamb4	starAB	tbx5b	0.924794	2.90314	1.65041	5.00E-05	0.00901062
RPS27L	starAB	tbx5b	1119.6	132.894	-3.07465	5.00E-05	0.00901062
kif15	starAB	tbx5b	14.4019	42.0784	1.54682	5.00E-05	0.00901062
RBL2	starAB	tbx5b	12.1068	0.681189	-4.15162	5.00E-05	0.00901062
akt1s1	starAB	tbx5b	127.893	54.9929	-1.21762	5.00E-05	0.00901062
ABCC6 (1 of 3)	starAB	tbx5b	0.542402	0.156314	-1.79492	0.0004	0.0492677
gosr2	starAB	tbx5b	11.2829	29.1121	1.36748	5.00E-05	0.00901062
slc4a1a	starAB	tbx5b	1.07863	3.56454	1.72452	5.00E-05	0.00901062
baxa	starAB	tbx5b	77.1778	33.1328	-1.21992	0.00025	0.0337898
CU928083.1	starAB	tbx5b	3.88309	8.78701	1.17817	0.00035	0.0443614
mdm2	starAB	tbx5b	476.412	64.0293	-2.89541	5.00E-05	0.00901062
zgc:77651	starAB	tbx5b	4.29212	12.2014	1.50728	5.00E-05	0.00901062
FP015791.1	starAB	tbx5b	26.6001	0.652037	-5.35034	5.00E-05	0.00901062
ANO6	starAB	tbx5b	0.216771	0.706464	1.70445	0.0004	0.0492677
BCL2L14	starAB	tbx5b	18.0606	3.57853	-2.3354	5.00E-05	0.00901062
DGKI	starAB	tbx5b	1.70109	0.560199	-1.60245	0.00025	0.0337898
dcn	starAB	tbx5b	12.3111	27.2536	1.14648	0.0002	0.028817
strap	starAB	tbx5b	97.0759	49.4287	-0.973764	0.00025	0.0337898
pah	starAB	tbx5b	1.65086	6.00911	1.86394	5.00E-05	0.00901062
5'8S'rRNA	starAB	tbx5b	3175.75	942.968	-1.75181	5.00E-05	0.00901062
isg15	starAB	tbx5b	45.1224	1.02401	-5.46154	5.00E-05	0.00901062
tp53	starAB	tbx5b	551.858	111.843	-2.30282	5.00E-05	0.00901062
c9	starAB	tbx5b	10.3267	50.7684	2.29755	5.00E-05	0.00901062
aqp3a	starAB	tbx5b	0.981962	5.50653	2.4874	5.00E-05	0.00901062
thbs4a	starAB	tbx5b	0.142601	0.916229	2.68372	5.00E-05	0.00901062
tbx5a	starAB	tbx5b	1.1106	5.29869	2.2543	5.00E-05	0.00901062
si:ch211-160e1.5	starAB	tbx5b	241.133	31.3757	-2.94211	5.00E-05	0.00901062
ypel1	starAB	tbx5b	14.8537	6.14774	-1.27269	0.0002	0.028817
ATF5 (1 of 2)	starAB	tbx5b	3.7721	1.30305	-1.53347	0.0001	0.0162912
si:dkey-204l11.1	starAB	tbx5b	32.246	1.35614	-4.57154	5.00E-05	0.00901062
fsta	starAB	tbx5b	53.7748	22.1409	-1.28021	5.00E-05	0.00901062
atf4b1	starAB	tbx5b	671.515	249.547	-1.42811	5.00E-05	0.00901062
bcl11ab	starAB	tbx5b	0.353143	2.03718	2.52825	5.00E-05	0.00901062
casp8	starAB	tbx5b	47.9714	2.5206	-4.25033	5.00E-05	0.00901062
pck1	starAB	tbx5b	4.8226	12.0352	1.31938	0.00035	0.0443614
si:ch211-114n24.6	starAB	tbx5b	61.0377	156.084	1.35455	5.00E-05	0.00901062
h1fx	starAB	tbx5b	73.6219	27.8624	-1.40181	5.00E-05	0.00901062
parp3	starAB	tbx5b	17.6559	3.99318	-2.14454	5.00E-05	0.00901062
soat2	starAB	tbx5b	4.91158	11.9154	1.27857	0.00025	0.0337898
pnp5a	starAB	tbx5b	29.4678	62.742	1.09029	0.0002	0.028817
tspan18a	starAB	tbx5b	16.0046	6.7559	-1.24426	0.0001	0.0162912
arhgap1	starAB	tbx5b	6.25052	13.9528	1.15851	0.00015	0.0231409
tnnt3b	starAB	tbx5b	6.91452	1.59598	-2.11519	5.00E-05	0.00901062
rgs9bp	starAB	tbx5b	1.49322	0.40362	-1.88736	0.00035	0.0443614
CR352229.3	starAB	tbx5b	96.5527	12.1286	-2.9929	5.00E-05	0.00901062
igf2a	starAB	tbx5b	45.7609	10.2329	-2.1609	5.00E-05	0.00901062
TPCN2	starAB	tbx5b	17.3009	7.85885	-1.13845	0.00035	0.0443614
zgc:113413	starAB	tbx5b	2.14965	6.42977	1.58066	5.00E-05	0.00901062
mmp2	starAB	tbx5b	79.4379	27.9803	-1.50541	5.00E-05	0.00901062

Continued on following page

Table B.2: continued from previous page

gene	sample 1	sample 2	value 1	value 2	log2 FC	p value	q value
PRKDC	starAB	tbx5b	3.04913	6.53816	1.10049	0.00025	0.0337898
CABZ01056056.1	starAB	tbx5b	20.1913	41.5297	1.04041	0.0004	0.0492677
SIPA1	starAB	tbx5b	0.354026	1.18358	1.74123	0.0001	0.0162912
nefm	starAB	tbx5b	1.81613	5.20504	1.51904	0.00015	0.0231409
asic1a	starAB	tbx5b	4.69513	0.302467	-3.95632	5.00E-05	0.00901062
gpd1a	starAB	tbx5b	45.2685	12.2789	-1.88233	5.00E-05	0.00901062
C8H9orf172 (2 of 2)	starAB	tbx5b	2.18185	0.662694	-1.71914	5.00E-05	0.00901062
si:ch211-251b21.1	starAB	tbx5b	0.191946	0.953733	2.31288	5.00E-05	0.00901062
zgc:110353	starAB	tbx5b	5.02549	1.13962	-2.14071	0.0001	0.0162912
AL929453.1	starAB	tbx5b	1.34913	0.241438	-2.4823	5.00E-05	0.00901062
crfb1	starAB	tbx5b	4.90299	1.45603	-1.75162	0.00015	0.0231409
REV1	starAB	tbx5b	11.4117	4.82533	-1.24182	0.0002	0.028817
tnfaip6	starAB	tbx5b	8.06448	3.21899	-1.32497	0.0004	0.0492677
si:dkey-145p14.5	starAB	tbx5b	43.1311	14.6818	-1.5547	5.00E-05	0.00901062
ccdc173	starAB	tbx5b	9.62422	3.77878	-1.34875	0.0001	0.0162912
CABZ01088039.1	starAB	tbx5b	56.8769	23.8994	-1.25087	5.00E-05	0.00901062
cdca7a	starAB	tbx5b	56.6617	133.771	1.23932	5.00E-05	0.00901062
zak	starAB	tbx5b	7.96677	1.24613	-2.67655	5.00E-05	0.00901062
phgdh	starAB	tbx5b	19.0554	51.9071	1.44573	5.00E-05	0.00901062
TANC1 (1 of 2)	starAB	tbx5b	5.49617	1.58469	-1.79423	5.00E-05	0.00901062

Table B.3: Significant differential gene expression from the preliminary experiment at 21 hpf

gene	sample 1	sample 2	value 1	value 2	log2 FC	p value	q value
5 8S rRNA	starAB	tbx5b	187.483	3449.4	4.20151	5.00E-05	0.00827294
5S rRNA	starAB	tbx5b	0	43.9349	inf	5.00E-05	0.00827294
aaNA2	starAB	tbx5b	1.59256	5.01791	1.65574	0.0003	0.0383679
abcc5	starAB	tbx5b	32.0651	88.8024	1.46959	5.00E-05	0.00827294
ace	starAB	tbx5b	2.65742	13.1323	2.30502	5.00E-05	0.00827294
AL929007.2	starAB	tbx5b	2.89956	0.51974	-2.47997	5.00E-05	0.00827294
and2	starAB	tbx5b	13.7196	6.27541	-1.12845	0.0004	0.0478606
apoea	starAB	tbx5b	203.641	96.7588	-1.07356	5.00E-05	0.00827294
apom	starAB	tbx5b	177.722	80.5078	-1.14243	0.0001	0.0151462
asb15a	starAB	tbx5b	3.56848	0.806979	-2.14471	5.00E-05	0.00827294
atp1b4	starAB	tbx5b	19.7879	6.76241	-1.54901	5.00E-05	0.00827294
atxn1b	starAB	tbx5b	2.89143	19.0813	2.72231	5.00E-05	0.00827294
bbc3	starAB	tbx5b	2.76799	15.0393	2.44182	5.00E-05	0.00827294
bcl3	starAB	tbx5b	0.351474	1.86019	2.40396	5.00E-05	0.00827294
bmb	starAB	tbx5b	6.07048	30.6887	2.33782	5.00E-05	0.00827294
bscl2l	starAB	tbx5b	8.82339	3.0349	-1.53969	5.00E-05	0.00827294
BX296557.7	starAB	tbx5b	329.174	1310.03	1.99268	5.00E-05	0.00827294
CABZ01035189.1	starAB	tbx5a	1.81137	6.43539	1.82895	5.00E-05	0.00827294
CABZ01035189.1	starAB	tbx5b	1.81137	5.31071	1.55183	5.00E-05	0.00827294
CABZ01076094.1	starAB	tbx5b	10.8225	3.62521	-1.5779	5.00E-05	0.00827294
CABZ01113191.1	starAB	tbx5b	2.43434	0.940828	-1.37153	0.0001	0.0151462
CASKIN1 (1 of 2)	starAB	tbx5b	0.344172	4.00178	3.53944	5.00E-05	0.00827294
casq1a	starAB	tbx5b	39.5188	16.2818	-1.27928	5.00E-05	0.00827294
ccng1	starAB	tbx5b	610.705	2872.17	2.23359	5.00E-05	0.00827294
cdkn1a	starAB	tbx5b	14.707	85.4904	2.53926	5.00E-05	0.00827294
cetp	starAB	tbx5b	8.22001	2.6276	-1.64539	5.00E-05	0.00827294
chrnb3a	starAB	tbx5b	5.92244	2.41202	-1.29595	0.00035	0.043649
cica	starAB	tbx5b	4.31445	11.4843	1.41242	5.00E-05	0.00827294
cited2	starAB	tbx5b	19.2067	41.0654	1.09631	0.0002	0.0275462
col11a2	starAB	tbx5a	22.6152	55.8423	1.30407	5.00E-05	0.00827294
col11a2	starAB	tbx5b	22.6152	46.3234	1.03445	5.00E-05	0.00827294
col14a1a	starAB	tbx5b	44.4545	91.1895	1.03654	5.00E-05	0.00827294
col17a1a	starAB	tbx5b	1.93486	0.370135	-2.3861	5.00E-05	0.00827294
cpn1	starAB	tbx5b	51.7835	171.167	1.72484	5.00E-05	0.00827294
CR735107.2	starAB	tbx5a	0.339054	0	NA	5.00E-05	0.00827294
CRP	starAB	tbx5b	4.43098	0.844576	-2.39132	0.0003	0.0383679
cryba1b	starAB	tbx5b	69.4836	30.5177	-1.18703	5.00E-05	0.00827294
cryba1l1	starAB	tbx5b	69.8284	32.1944	-1.117	0.00025	0.0327245
cryba1l2	starAB	tbx5b	5.20989	1.74373	-1.57908	0.00025	0.0327245
cryba4	starAB	tbx5b	75.5535	31.3316	-1.26988	0.00015	0.0217344
crybb1l1	starAB	tbx5b	50.2467	20.0827	-1.32308	5.00E-05	0.00827294
crybb1l2	starAB	tbx5b	62.6435	25.7379	-1.28327	5.00E-05	0.00827294
crygmxl2	starAB	tbx5b	13.8249	2.32265	-2.57342	5.00E-05	0.00827294
crygn2	starAB	tbx5b	54.8229	23.6797	-1.21113	5.00E-05	0.00827294
CT956064.3	starAB	tbx5b	75.9999	196.219	1.36839	5.00E-05	0.00827294
CT990561.1	starAB	tbx5b	1.55304	0.482123	-1.68762	0.0001	0.0151462
ctsc	starAB	tbx5b	91.1839	217.312	1.25291	5.00E-05	0.00827294
CU896645.1	starAB	tbx5b	80.1742	7.72531	-3.37547	5.00E-05	0.00827294
CU929133.1	starAB	tbx5b	5.95679	1.51904	-1.97137	0.00015	0.0217344
cyp11a1	starAB	tbx5b	8.22243	31.3778	1.93211	5.00E-05	0.00827294

Continued on following page

Table B.3: continued from previous page

gene	sample 1	sample 2	value 1	value 2	log2 FC	p value	q value
CYSLTR2	starAB	tbx5b	0	0.2035	inf	5.00E-05	0.00827294
dcdc2b	starAB	tbx5b	3.47384	10.9403	1.65505	0.0004	0.0478606
ddit4	starAB	tbx5a	65.961	143.704	1.12341	5.00E-05	0.00827294
dla	starAB	tbx5b	72.1108	31.3343	-1.20247	5.00E-05	0.00827294
dld	starAB	tbx5b	69.8732	31.6462	-1.14271	5.00E-05	0.00827294
efemp2a	starAB	tbx5b	31.4616	61.8417	0.974989	0.00035	0.043649
egr1	starAB	tbx5a	15.8372	4.23892	-1.90155	5.00E-05	0.00827294
ENSDARG00000067824	starAB	tbx5b	0.587174	1.71542	1.5467	0.0002	0.0275462
ENSDARG00000079340	starAB	tbx5b	0.901646	3.59432	1.99508	5.00E-05	0.00827294
ENSDARG00000089390	starAB	tbx5b	1.07274	2.73018	1.3477	0.0002	0.0275462
ENSDARG00000092644	starAB	tbx5b	33.6061	17.2197	-0.964658	0.0004	0.0478606
EXO5	starAB	tbx5b	6.55414	36.3696	2.47226	5.00E-05	0.00827294
f2rl1.2	starAB	tbx5b	14.6827	29.434	1.00337	0.0004	0.0478606
f7	starAB	tbx5b	7.19777	2.37244	-1.60118	5.00E-05	0.00827294
fabp7a	starAB	tbx5b	253.682	82.8799	-1.61393	5.00E-05	0.00827294
fam20a	starAB	tbx5b	8.78886	2.90503	-1.59713	5.00E-05	0.00827294
fastk	starAB	tbx5b	10.0577	29.3224	1.5437	5.00E-05	0.00827294
fgg	starAB	tbx5b	72.5846	36.9831	-0.972795	0.0004	0.0478606
FILIP1L (1 of 2)	starAB	tbx5b	14.5804	36.2526	1.31406	5.00E-05	0.00827294
fos	starAB	tbx5a	57.7255	17.9184	-1.68777	5.00E-05	0.00827294
fosl1a	starAB	tbx5b	23.2626	73.9085	1.66773	5.00E-05	0.00827294
foxi1	starAB	tbx5b	7.47679	17.8032	1.25165	0.0001	0.0151462
foxo3b	starAB	tbx5b	19.7137	71.4589	1.85792	5.00E-05	0.00827294
FP102888.1	starAB	tbx5b	0	0.398009	inf	5.00E-05	0.00827294
ftcd	starAB	tbx5b	26.5681	9.88638	-1.42618	5.00E-05	0.00827294
gadd45aa	starAB	tbx5b	6.6541	26.6287	2.00066	5.00E-05	0.00827294
gch2	starAB	tbx5b	287.88	144.572	-0.993679	0.00025	0.0327245
gfap	starAB	tbx5b	146.669	75.6108	-0.955904	0.0004	0.0478606
ghrh	starAB	tbx5b	0.994086	9.0782	3.19096	5.00E-05	0.00827294
glra4a	starAB	tbx5b	6.29752	2.30358	-1.4509	0.00015	0.0217344
gosr2	starAB	tbx5b	34.9752	13.8158	-1.34001	5.00E-05	0.00827294
gpm6aa	starAB	tbx5b	57.5137	21.392	-1.42683	5.00E-05	0.00827294
gpnmb	starAB	tbx5b	1.55508	0.396246	-1.97252	5.00E-05	0.00827294
grasp	starAB	tbx5b	7.01515	19.8211	1.49849	5.00E-05	0.00827294
grk1a	starAB	tbx5b	0.19721	0.880403	2.15843	0.0002	0.0275462
GRM2 (2 of 2)	starAB	tbx5b	4.74809	1.5421	-1.62245	5.00E-05	0.00827294
gtpbp1l	starAB	tbx5b	8.28959	18.977	1.19488	5.00E-05	0.00827294
habp2	starAB	tbx5b	3.05385	0.591857	-2.36731	5.00E-05	0.00827294
helt	starAB	tbx5b	15.676	5.09737	-1.62073	5.00E-05	0.00827294
her13	starAB	tbx5b	43.1725	14.8403	-1.54059	5.00E-05	0.00827294
her4.2	starAB	tbx5b	17.9692	5.22091	-1.78315	5.00E-05	0.00827294
her4.2	starAB	tbx5b	12.552	4.68422	-1.42204	5.00E-05	0.00827294
her4.3	starAB	tbx5b	9.38591	2.75063	-1.77074	5.00E-05	0.00827294
her4.4	starAB	tbx5b	7.71778	2.66296	-1.53515	5.00E-05	0.00827294
her8.2	starAB	tbx5b	8.27292	2.6321	-1.65218	0.00015	0.0217344
hmgb1b	starAB	tbx5b	538.33	265.582	-1.01933	5.00E-05	0.00827294
hsc70	starAB	tbx5b	1.84779	0.420285	-2.13636	5.00E-05	0.00827294
irf1b	starAB	tbx5b	1.26368	4.28621	1.76207	5.00E-05	0.00827294
irg1l	starAB	tbx5b	8.76613	27.8367	1.66697	5.00E-05	0.00827294
ITPR1 (2 of 2)	starAB	tbx5b	1.36908	4.50153	1.71721	5.00E-05	0.00827294
jdp2	starAB	tbx5a	24.4767	9.33952	-1.38999	5.00E-05	0.00827294

Continued on following page

Table B.3: continued from previous page

gene	sample 1	sample 2	value 1	value 2	log2 FC	p value	q value
junba	starAB	tbx5a	52.8582	20.4145	-1.37253	5.00E-05	0.00827294
junbb	starAB	tbx5a	85.3654	33.8485	-1.33456	5.00E-05	0.00827294
KRT78	starAB	tbx5b	2.35354	0.374499	-2.6518	0.0002	0.0275462
lim2.4	starAB	tbx5b	12.2804	4.13268	-1.5712	5.00E-05	0.00827294
lmo7b	starAB	tbx5b	5.23961	11.9474	1.18916	0.0002	0.0275462
lnx1	starAB	tbx5b	7.50975	52.2827	2.7995	5.00E-05	0.00827294
lppr4b	starAB	tbx5b	0.153431	0	NA	0.0002	0.0275462
lyrm1	starAB	tbx5b	6.33174	29.5983	2.22484	5.00E-05	0.00827294
lzts2b	starAB	tbx5b	2.43741	6.30523	1.3712	0.0004	0.0478606
mat2al	starAB	tbx5b	13.0746	38.8225	1.57012	5.00E-05	0.00827294
Metazoa SRP	starAB	tbx5b	0	2.30966	inf	5.00E-05	0.00827294
Metazoa SRP	starAB	tbx5b	0	1.71487	inf	5.00E-05	0.00827294
Metazoa SRP	starAB	tbx5b	0	2.49436	inf	5.00E-05	0.00827294
Metazoa SRP	starAB	tbx5b	3.45521	38.3508	3.47241	5.00E-05	0.00827294
Metazoa SRP	starAB	tbx5b	0	1.87077	inf	5.00E-05	0.00827294
Metazoa SRP	starAB	tbx5b	0	5.30052	inf	5.00E-05	0.00827294
Metazoa SRP	starAB	tbx5b	82.7591	701.277	3.083	5.00E-05	0.00827294
METRNL (1 of 2)	starAB	tbx5b	6.28528	20.6192	1.71394	5.00E-05	0.00827294
mgst3	starAB	tbx5b	137.796	50.2899	-1.45419	5.00E-05	0.00827294
mipa	starAB	tbx5b	14.4091	4.42844	-1.70211	5.00E-05	0.00827294
mipb	starAB	tbx5b	4.92838	0.698549	-2.81868	5.00E-05	0.00827294
mmp13a	starAB	tbx5b	1.43835	5.54387	1.94648	5.00E-05	0.00827294
mmrn2b	starAB	tbx5b	8.30608	20.3665	1.29396	5.00E-05	0.00827294
mogat2	starAB	tbx5b	7.07407	16.7795	1.24609	0.00025	0.0327245
mybl1	starAB	tbx5b	6.78487	3.15634	-1.10407	0.00035	0.043649
mylpfb	starAB	tbx5b	684.574	245.325	-1.48051	5.00E-05	0.00827294
myoz1a	starAB	tbx5b	4.73032	1.67388	-1.49874	0.0004	0.0478606
ndst3	starAB	tbx5b	12.5311	5.39691	-1.2153	5.00E-05	0.00827294
NELL2A	starAB	tbx5b	4.04911	1.4921	-1.44026	0.00025	0.0327245
nes	starAB	tbx5b	42.834	20.3674	-1.07249	0.00015	0.0217344
neurod4	starAB	tbx5b	54.8038	21.7923	-1.33045	5.00E-05	0.00827294
nme2b.2	starAB	tbx5b	1366.37	595.86	-1.19731	5.00E-05	0.00827294
npas3b	starAB	tbx5b	5.53173	1.38692	-1.99584	5.00E-05	0.00827294
nr0b2a	starAB	tbx5b	46.7705	22.7584	-1.0392	0.00015	0.0217344
nr4a3	starAB	tbx5b	5.35502	16.3419	1.60961	5.00E-05	0.00827294
otpa	starAB	tbx5b	15.6048	3.46703	-2.17022	5.00E-05	0.00827294
pfkma	starAB	tbx5b	3.56267	0.694996	-2.35788	5.00E-05	0.00827294
phc3	starAB	tbx5b	0.72706	3.13276	2.10729	5.00E-05	0.00827294
phlda3	starAB	tbx5b	11.138	76.121	2.77281	5.00E-05	0.00827294
pik3r3a	starAB	tbx5b	28.1026	76.8879	1.45206	5.00E-05	0.00827294
plp1a	starAB	tbx5b	67.5945	20.0364	-1.75428	5.00E-05	0.00827294
pou2f2a	starAB	tbx5b	5.87786	2.50656	-1.22958	5.00E-05	0.00827294
pou3f1	starAB	tbx5b	69.0633	28.175	-1.2935	5.00E-05	0.00827294
prtgb	starAB	tbx5b	166.4	69.0299	-1.26937	5.00E-05	0.00827294
ptgs2b	starAB	tbx5b	9.79304	26.0867	1.41348	5.00E-05	0.00827294
PTPRD	starAB	tbx5b	2.1607	5.24355	1.27905	0.0003	0.0383679
pvalb2	starAB	tbx5b	729.143	296.802	-1.2967	5.00E-05	0.00827294
rasl11b	starAB	tbx5b	4.26476	15.0811	1.8222	5.00E-05	0.00827294
rb1	starAB	tbx5b	31.8713	13.9674	-1.19019	0.0001	0.0151462
rbl2	starAB	tbx5b	3.0464	24.8522	3.0282	5.00E-05	0.00827294
rd3	starAB	tbx5b	2.95248	8.65895	1.55227	5.00E-05	0.00827294

Continued on following page

Table B.3: continued from previous page

gene	sample 1	sample 2	value 1	value 2	log2 FC	p value	q value
rdh5	starAB	tbx5b	6.93501	1.66237	-2.06066	5.00E-05	0.00827294
RHOU (1 of 2)	starAB	tbx5b	3.48397	1.12803	-1.62692	5.00E-05	0.00827294
rhoub	starAB	tbx5b	26.5463	56.9347	1.1008	5.00E-05	0.00827294
rn7sk	starAB	tbx5b	52.8961	309.903	2.55059	5.00E-05	0.00827294
RNAeP nuc	starAB	tbx5b	1.60768	39.5859	4.62193	0.00015	0.0217344
RNF14 (3 of 5)	starAB	tbx5b	1.95938	25.0826	3.67822	5.00E-05	0.00827294
rnf169	starAB	tbx5b	6.45198	21.2829	1.72188	5.00E-05	0.00827294
rpl22l1	starAB	tbx5b	940.474	285.631	-1.71923	5.00E-05	0.00827294
rps27.2	starAB	tbx5b	173.141	840.36	2.27906	5.00E-05	0.00827294
rrm2	starAB	tbx5b	62.1255	26.754	-1.21543	5.00E-05	0.00827294
rspo1	starAB	tbx5b	0.8342	8.70939	3.38411	5.00E-05	0.00827294
rx2	starAB	tbx5b	10.0765	3.73946	-1.4301	5.00E-05	0.00827294
s1pr1	starAB	tbx5b	34.2379	16.8892	-1.01949	0.00025	0.0327245
scrt1a	starAB	tbx5b	13.5071	3.08558	-2.1301	5.00E-05	0.00827294
sesn3	starAB	tbx5b	49.7419	130.039	1.38641	5.00E-05	0.00827294
si:ch211-123n6.1	starAB	tbx5b	0	0.4152	inf	5.00E-05	0.00827294
si:ch211-145g9.5	starAB	tbx5b	0	0.288051	inf	5.00E-05	0.00827294
si:ch211-152f23.5	starAB	tbx5b	8.4355	2.90102	-1.53991	5.00E-05	0.00827294
si:ch211-155k24.9	starAB	tbx5b	4.19487	14.7245	1.81153	5.00E-05	0.00827294
si:ch211-217a12.1	starAB	tbx5b	5.73577	26.3319	2.19875	5.00E-05	0.00827294
si:ch211-39a7.1	starAB	tbx5b	0.883942	15.6019	4.14163	5.00E-05	0.00827294
si:ch211-92l17.1	starAB	tbx5b	0.584646	10.901	4.22075	5.00E-05	0.00827294
si:ch73-21g5.7	starAB	tbx5b	149.221	31.8841	-2.22654	5.00E-05	0.00827294
si:ch73-95a24.1	starAB	tbx5b	0.369403	6.00579	4.02309	5.00E-05	0.00827294
si:dkey-117j14.6	starAB	tbx5b	2.48048	19.0046	2.93766	5.00E-05	0.00827294
si:dkey-117m1.4	starAB	tbx5b	14.8075	47.7174	1.68818	5.00E-05	0.00827294
si:dkey-11n6.3	starAB	tbx5b	11.2575	2.17275	-2.3733	5.00E-05	0.00827294
si:dkey-153n9.4	starAB	tbx5b	0	1.34224	inf	0.0001	0.0151462
si:dkey-193b18.1	starAB	tbx5b	1.65469	6.81562	2.04228	5.00E-05	0.00827294
si:dkey-196j8.2	starAB	tbx5b	2.23623	6.47181	1.5331	5.00E-05	0.00827294
si:dkey-21o19.6	starAB	tbx5b	1.2269	31.2899	4.6726	5.00E-05	0.00827294
si:dkey-52d15.1	starAB	tbx5b	4.10708	1.1323	-1.85885	5.00E-05	0.00827294
si:dkey-79f11.10	starAB	tbx5b	0	0.426654	inf	5.00E-05	0.00827294
si:dkey-79f11.9	starAB	tbx5b	0	1.35218	inf	5.00E-05	0.00827294
si:dkeyp-97b10.3	starAB	tbx5b	9.32446	2.95193	-1.65936	5.00E-05	0.00827294
slc10a1	starAB	tbx5b	8.34213	1.84764	-2.17473	5.00E-05	0.00827294
slc16a9b	starAB	tbx5b	24.908	50.6334	1.02348	0.00025	0.0327245
slc22a7a	starAB	tbx5b	20.3767	9.42001	-1.11312	0.0004	0.0478606
slc25a4	starAB	tbx5b	39.1186	6.46962	-2.5961	5.00E-05	0.00827294
slc4a1a	starAB	tbx5b	38.0487	13.0138	-1.54781	5.00E-05	0.00827294
smad3b	starAB	tbx5b	9.82066	3.41734	-1.52295	5.00E-05	0.00827294
sox11b	starAB	tbx5b	234.454	105.141	-1.15698	5.00E-05	0.00827294
sox4b	starAB	tbx5b	16.2702	38.9143	1.25807	5.00E-05	0.00827294
spam1	starAB	tbx5b	6.75081	2.5883	-1.38306	0.0002	0.0275462
TAF1C	starAB	tbx5b	7.4105	28.424	1.93947	0.0002	0.0275462
tbx6	starAB	tbx5b	4.14123	14.5134	1.80926	5.00E-05	0.00827294
tmsb	starAB	tbx5b	52.8281	24.5155	-1.10761	5.00E-05	0.00827294
tpi1a	starAB	tbx5b	5.78226	1.6084	-1.84601	0.00035	0.043649
tyrp1b	starAB	tbx5b	71.9738	36.2457	-0.989663	0.0002	0.0275462
U3	starAB	tbx5b	10.7567	82.2735	2.9352	5.00E-05	0.00827294
U3	starAB	tbx5b	20.8959	241.568	3.53114	5.00E-05	0.00827294

Continued on following page

Table B.3: continued from previous page

gene	sample 1	sample 2	value 1	value 2	log2 FC	p value	q value
U4	starAB	tbx5b	41.301	383.793	3.21608	5.00E-05	0.00827294
U4atac	starAB	tbx5b	0	42.9988	inf	5.00E-05	0.00827294
uox	starAB	tbx5b	6.61693	17.0063	1.36183	0.00015	0.0217344
vrk2	starAB	tbx5b	6.14667	28.7028	2.22331	5.00E-05	0.00827294
vtnb	starAB	tbx5b	53.1437	26.9036	-0.9821	0.00035	0.043649
wu:fj08f03	starAB	tbx5b	9.91856	21.2423	1.09874	0.0003	0.0383679
zgc:158463	starAB	tbx5b	1334.05	3254.32	1.28655	5.00E-05	0.00827294
zgc:194210	starAB	tbx5b	10.104	22.8557	1.17763	0.0002	0.0275462
zgc:195001	starAB	tbx5b	3.12315	0.858493	-1.86312	0.0002	0.0275462
zgc:77650	starAB	tbx5b	189.857	73.3269	-1.3725	5.00E-05	0.00827294
zmynd11	starAB	tbx5b	38.1757	76.5577	1.00389	0.00035	0.043649

Table B.4: Significant differential gene expression of triplicate data at 18 hpf

gene	sample 1	sample 2	value 1	value 2	log2 FC	p value	q values
per3	starAB	tbx5a	2.73686	0.542804	-2.33402	5.00E-05	0.00650109
egln3	starAB	tbx5a	1.8039	8.20567	2.1855	5.00E-05	0.00650109
wu:fc46h12	starAB	tbx5a	18.6079	6.24972	-1.57405	0.00015	0.0158731
malt1a	starAB	tbx5a	2.93532	0.942157	-1.63948	5.00E-05	0.00650109
zgc:173585	starAB	tbx5a	5.6915	17.3139	1.60505	0.00015	0.0158731
zgc:158463	starAB	tbx5a	363.889	3343.77	3.1999	0.0001	0.0114918
per1b	starAB	tbx5a	2.18574	0.425303	-2.36156	5.00E-05	0.00650109
col2a1a	starAB	tbx5a	34.1632	73.4797	1.1049	0.0002	0.0196474
per3	starAB	tbx5b	2.73686	0.892317	-1.61689	5.00E-05	0.00650109
cmn	starAB	tbx5b	22.6875	62.3803	1.45919	5.00E-05	0.00650109
egln3	starAB	tbx5b	1.8039	6.4929	1.84775	5.00E-05	0.00650109
p4ha1b	starAB	tbx5b	55.4656	114.767	1.04904	0.00015	0.0158731
wu:fc46h12	starAB	tbx5b	18.6079	5.69321	-1.7086	5.00E-05	0.00650109
xirp1	starAB	tbx5b	7.73928	16.062	1.05338	5.00E-05	0.00650109
tmigd1	starAB	tbx5b	3.49303	0.779581	-2.16371	0.00015	0.0158731
vtg7	starAB	tbx5b	0.371682	1.23175	1.72857	0.0002	0.0196474
obsl1a	starAB	tbx5b	4.21618	8.32797	0.982027	0.0001	0.0114918
si:dkey-85k7.7	starAB	tbx5b	3.83401	10.1249	1.40098	5.00E-05	0.00650109
col28a1a	starAB	tbx5b	20.5367	40.3363	0.973878	0.00015	0.0158731
per3	starAB	double	2.73686	0.610119	-2.16536	5.00E-05	0.00650109
ndufa4	starAB	double	25.4134	12.2471	-1.05316	0.00055	0.0404092
chd	starAB	double	2.4845	5.48699	1.14306	0.0003	0.0264437
bnip4	starAB	double	41.7236	17.732	-1.23451	0.0001	0.0114918
hspb11	starAB	double	39.4421	16.2339	-1.28073	0.00065	0.045171
malt1a	starAB	double	2.93532	0.986618	-1.57295	5.00E-05	0.00650109
c3b.2	starAB	double	1.6939	0.698009	-1.27904	0.00045	0.0351624
zgc:173585	starAB	double	5.6915	24.5612	2.1095	5.00E-05	0.00650109
hspb9	starAB	double	44.6582	16.1851	-1.46426	0.00015	0.0158731
c9	starAB	double	9.27336	21.0227	1.18078	0.00065	0.045171
zgc:158463	starAB	double	363.889	943.913	1.37515	5.00E-05	0.00650109
per1b	starAB	double	2.18574	0.741146	-1.56029	5.00E-05	0.00650109
mir16c	starAB	double	22.3333	0	#NAME?	0.0003	0.0264437

Table B.5: Significant differential gene expression of triplicate data at 21 hpf

gene	sample 1	sample 2	value 1	value 2	log2 FC	p value	q values
cep97	starAB	tbx5a	30.9186	11.7292	-1.39837	5.00E-05	0.00650109
eed	starAB	tbx5a	74.8023	35.055	-1.09346	0.0003	0.0264437
zgc:110091	starAB	tbx5a	104.928	41.3546	-1.34328	5.00E-05	0.00650109
tfdp1b	starAB	tbx5a	73.0732	30.7664	-1.24799	5.00E-05	0.00650109
mrpl39	starAB	tbx5a	57.536	27.1162	-1.08531	0.0001	0.0114918
aimp1	starAB	tbx5a	205.959	98.6318	-1.06223	0.00055	0.0404092
zgc:77358	starAB	tbx5a	25.2666	11.6783	-1.1134	0.00035	0.029378
tmem39a	starAB	tbx5a	32.1905	15.7207	-1.03397	0.0003	0.0264437
si:dkeyp-80c12.10	starAB	tbx5a	942.959	499.255	-0.917419	0.00055	0.0404092
minal	starAB	tbx5a	37.2747	17.0337	-1.1298	0.00015	0.0158731
rs1a	starAB	tbx5a	10.2193	4.55018	-1.1673	0.0007	0.0474034
gb:kf234084	starAB	tbx5a	0.604119	1.7792	1.55832	0.00065	0.045171
per3	starAB	tbx5a	4.95651	2.16359	-1.1959	0.0003	0.0264437
ube2v1	starAB	tbx5a	193.155	89.5223	-1.10944	0.0003	0.0264437
aspscr1	starAB	tbx5a	35.4662	16.4627	-1.10724	0.00045	0.0351624
pde6c	starAB	tbx5a	0.416303	1.14914	1.46486	0.00055	0.0404092
hhex	starAB	tbx5a	24.6118	8.7173	-1.4974	5.00E-05	0.00650109
cfap36	starAB	tbx5a	32.4527	15.6801	-1.0494	0.0004	0.0323737
wu:fj16a03	starAB	tbx5a	393.39	205.978	-0.933466	0.0004	0.0323737
wdr1	starAB	tbx5a	282.829	150.166	-0.913367	0.0007	0.0474034
otop1	starAB	tbx5a	38.0378	11.7466	-1.69519	5.00E-05	0.00650109
exosc3	starAB	tbx5a	16.1739	6.10879	-1.40471	0.0001	0.0114918
si:dkey-4p15.3	starAB	tbx5a	4.03344	10.613	1.39575	5.00E-05	0.00650109
cdkal1	starAB	tbx5a	51.4027	24.3087	-1.08037	0.00025	0.0231995
zgc:113232	starAB	tbx5a	7.35118	19.1918	1.38444	5.00E-05	0.00650109
srsf10b	starAB	tbx5a	129.82	44.9214	-1.53103	5.00E-05	0.00650109
cx52.9	starAB	tbx5a	1.06082	0.25349	-2.06519	0.00055	0.0404092
crip1	starAB	tbx5a	7.39689	3.07814	-1.26486	0.00055	0.0404092
exd1	starAB	tbx5a	5.36542	1.84677	-1.53868	0.00055	0.0404092
ubl7b	starAB	tbx5a	71.5465	36.0379	-0.989366	0.00065	0.045171
dhdhl	starAB	tbx5a	90.8764	46.916	-0.953827	0.0004	0.0323737
dtwd1	starAB	tbx5a	23.9403	10.958	-1.12745	0.00065	0.045171
spata5l1	starAB	tbx5a	17.8333	9.06854	-0.975632	0.00055	0.0404092
ube2q1	starAB	tbx5a	24.7215	12.8916	-0.939335	0.00075	0.0496969
sf3b4	starAB	tbx5a	139.602	63.0531	-1.14668	0.0002	0.0196474
s100a10a	starAB	tbx5a	10.764	4.10508	-1.39073	0.00025	0.0231995
rnu11	starAB	tbx5a	26.0696	0	#NAME?	0.00065	0.045171
dnajc8	starAB	tbx5a	120.291	61.4797	-0.968342	0.00045	0.0351624
krtt1c19e	starAB	tbx5a	81.4303	42.3194	-0.944246	0.0002	0.0196474
krt91	starAB	tbx5a	225.46	92.7131	-1.28203	5.00E-05	0.00650109
utp18	starAB	tbx5a	68.8982	30.4925	-1.17601	0.0001	0.0114918
fggy	starAB	tbx5a	29.7415	15.632	-0.927974	0.0006	0.0428942
zgc:154086	starAB	tbx5a	2.33986	0.796622	-1.55446	0.00025	0.0231995
polr2d	starAB	tbx5a	305.741	140.772	-1.11895	0.0003	0.0264437
gata6	starAB	tbx5a	31.4637	16.1716	-0.960223	0.00045	0.0351624
ifi30	starAB	tbx5a	190.335	97.5303	-0.964618	0.0002	0.0196474
rpph1	starAB	tbx5a	58.8987	3.90562	-3.91461	5.00E-05	0.00650109
zgc:154006	starAB	tbx5a	3.77611	1.35077	-1.48311	0.00055	0.0404092
zgc:92789	starAB	tbx5a	15.646	6.34754	-1.30153	0.0003	0.0264437
hsd3b2	starAB	tbx5a	20.9258	10.4086	-1.00751	0.0006	0.0428942
zp3a.2	starAB	tbx5a	8.81166	3.53692	-1.31692	0.0001	0.0114918

Continued on following page

Table B.5: continued from previous page

gene	sample 1	sample 2	value 1	value 2	log2 FC	p value	q values
hsp90aa1.2	starAB	tbx5a	74.496	196.45	1.39893	5.00E-05	0.00650109
nup54	starAB	tbx5a	91.9978	40.5152	-1.18314	0.0001	0.0114918
bxdc2	starAB	tbx5a	149.391	54.5899	-1.45239	5.00E-05	0.00650109
txndc15	starAB	tbx5a	67.1714	26.6558	-1.3334	5.00E-05	0.00650109
zgc:194221	starAB	tbx5a	7.52097	2.82525	-1.41254	0.0002	0.0196474
si:dkey-169i5.4	starAB	tbx5a	1.59684	4.44618	1.47734	0.00045	0.0351624
alpi.2	starAB	tbx5a	1.54731	0.420734	-1.87878	0.00025	0.0231995
atad3b	starAB	tbx5a	51.1402	21.8766	-1.22507	5.00E-05	0.00650109
mrpl20	starAB	tbx5a	164.314	63.0306	-1.38234	5.00E-05	0.00650109
fblim1	starAB	tbx5a	18.0296	8.05706	-1.16204	0.00025	0.0231995
bysl	starAB	tbx5a	203.918	89.1679	-1.1934	0.0003	0.0264437
atp5d	starAB	tbx5a	431.159	206.553	-1.06171	0.0003	0.0264437
elavl2	starAB	tbx5a	3.06844	1.02583	-1.58071	0.0004	0.0323737
aldh8a1	starAB	tbx5a	51.998	26.5534	-0.969557	0.0003	0.0264437
pus7	starAB	tbx5a	32.2094	13.8024	-1.22256	0.0003	0.0264437
cyp11a1	starAB	tbx5a	35.9785	15.4158	-1.22273	5.00E-05	0.00650109
zgc:173552	starAB	tbx5a	1.4865	0.354032	-2.06996	0.0007	0.0474034
zgc:173585	starAB	tbx5a	6.78424	32.263	2.24962	5.00E-05	0.00650109
LOC570474	starAB	tbx5a	19.5526	6.63426	-1.55935	5.00E-05	0.00650109
pdhx	starAB	tbx5a	23.6541	10.0034	-1.24161	0.0001	0.0114918
zgc:153921	starAB	tbx5a	10.7771	3.36916	-1.67751	5.00E-05	0.00650109
ndufa6	starAB	tbx5a	553.109	274.657	-1.00993	0.0007	0.0474034
rrp7a	starAB	tbx5a	131.105	60.3405	-1.11952	0.00035	0.029378
tmem11	starAB	tbx5a	56.0251	29.1734	-0.941419	0.00035	0.029378
hsp70.1	starAB	tbx5a	3.40691	10.9688	1.68687	5.00E-05	0.00650109
zgc:109934	starAB	tbx5a	70.389	33.5325	-1.06979	0.00025	0.0231995
ddx47	starAB	tbx5a	103.674	47.1841	-1.13568	0.0006	0.0428942
slc25a38a	starAB	tbx5a	18.2093	7.76391	-1.22982	0.00015	0.0158731
nhp2l1a	starAB	tbx5a	26.4277	11.3702	-1.21679	5.00E-05	0.00650109
ngs	starAB	tbx5a	1.30446	4.26259	1.70828	0.00045	0.0351624
rab3ip	starAB	tbx5a	20.8572	10.7062	-0.9621	0.00075	0.0496969
zgc:92791	starAB	tbx5a	30.1206	13.6142	-1.14564	0.0003	0.0264437
zgc:85975	starAB	tbx5a	367.904	147.652	-1.31713	0.00065	0.045171
rnf185	starAB	tbx5a	62.6914	30.2585	-1.05093	0.0004	0.0323737
epd	starAB	tbx5a	11.8013	3.91941	-1.59023	0.0003	0.0264437
selm	starAB	tbx5a	174.579	92.9817	-0.908864	0.00035	0.029378
mia	starAB	tbx5a	208.125	102.451	-1.02252	0.00025	0.0231995
fdx1l	starAB	tbx5a	35.5473	16.5264	-1.10496	0.0004	0.0323737
aamp	starAB	tbx5a	100.824	45.5023	-1.14783	0.0001	0.0114918
cbln11	starAB	tbx5a	10.3799	2.90602	-1.83668	5.00E-05	0.00650109
zgc:110425	starAB	tbx5a	9.16002	3.40213	-1.42891	0.00025	0.0231995
polr2l	starAB	tbx5a	326.354	177.503	-0.878595	0.00065	0.045171
exosc6	starAB	tbx5a	91.986	43.8978	-1.06727	0.0007	0.0474034
gpd1a	starAB	tbx5a	27.8519	11.2052	-1.31361	5.00E-05	0.00650109
plxnd1	starAB	tbx5a	8.61282	3.48693	-1.30453	0.0003	0.0264437
pggt1b	starAB	tbx5a	75.2415	30.9508	-1.28155	5.00E-05	0.00650109
LOC100329294	starAB	tbx5a	73.8194	20.3226	-1.86091	5.00E-05	0.00650109
ubxn4	starAB	tbx5a	36.4091	15.3254	-1.24838	0.0001	0.0114918
zgc:158619	starAB	tbx5a	99.5783	43.5178	-1.19423	5.00E-05	0.00650109
dhrs9	starAB	tbx5a	17.9489	7.4321	-1.27205	0.00015	0.0158731
dnaaf2	starAB	tbx5a	1.50557	0.42732	-1.81692	0.00025	0.0231995

Continued on following page

Table B.5: continued from previous page

gene	sample 1	sample 2	value 1	value 2	log2 FC	p value	q values
ndufaf3	starAB	tbx5a	130.786	61.3925	-1.09107	0.00025	0.0231995
wdr77	starAB	tbx5a	132.197	61.166	-1.11189	0.00025	0.0231995
zgc:154064	starAB	tbx5a	76.8312	32.5866	-1.23741	0.0001	0.0114918
zgc:136826	starAB	tbx5a	914.903	356.639	-1.35915	5.00E-05	0.00650109
zgc:153713	starAB	tbx5a	484.751	178.625	-1.44031	5.00E-05	0.00650109
tmem43	starAB	tbx5a	44.0156	15.6209	-1.49454	5.00E-05	0.00650109
zgc:77398	starAB	tbx5a	13.2693	4.42487	-1.58439	0.0007	0.0474034
mif	starAB	tbx5b	58.769	27.8028	-1.07982	0.00045	0.0351624
ankrd9	starAB	tbx5b	16.5031	7.13871	-1.209	0.0004	0.0323737
egln3	starAB	tbx5b	3.75173	1.28448	-1.54638	0.0007	0.0474034
vsx2	starAB	tbx5b	1.68938	5.45376	1.69076	5.00E-05	0.00650109
rpph1	starAB	tbx5b	58.8987	3.96623	-3.8924	5.00E-05	0.00650109
zgc:194221	starAB	tbx5b	7.52097	2.88727	-1.38121	0.0002	0.0196474
rx1	starAB	tbx5b	1.45202	4.29178	1.56352	5.00E-05	0.00650109
cyp11a1	starAB	tbx5b	35.9785	13.1748	-1.44935	5.00E-05	0.00650109
zgc:153405	starAB	tbx5b	4.99623	1.1448	-2.12575	0.0004	0.0323737
anxa1a	starAB	tbx5b	204.997	104.805	-0.967891	0.00015	0.0158731
si:ch211-117m20.5	starAB	tbx5b	11.527	1.27747	-3.17365	5.00E-05	0.00650109
hsp70l	starAB	tbx5b	0.756311	2.31835	1.61605	0.00065	0.045171
dct	starAB	tbx5b	2.46323	7.44777	1.59626	5.00E-05	0.00650109
dhrs9	starAB	tbx5b	17.9489	7.65284	-1.22983	0.00015	0.0158731
zgc:153713	starAB	tbx5b	484.751	238.794	-1.02148	0.00065	0.045171
fat1a	starAB	21hpf 5a5b	5.24351	10.3094	0.97536	0.00025	0.0231995
vcanb	starAB	21hpf 5a5b	1.42343	3.67256	1.36741	0.0001	0.0114918
fezf2	starAB	21hpf 5a5b	2.23071	0.670579	-1.73402	0.0004	0.0323737
per3	starAB	21hpf 5a5b	4.95651	1.84247	-1.42768	5.00E-05	0.00650109
uox	starAB	21hpf 5a5b	61.7536	28.1567	-1.13304	0.0002	0.0196474
rasd1	starAB	21hpf 5a5b	120.119	58.6889	-1.03331	0.0002	0.0196474
pvalb2	starAB	21hpf 5a5b	34.5188	81.1526	1.23326	0.00015	0.0158731
srsf10b	starAB	21hpf 5a5b	129.82	59.5854	-1.12348	0.00045	0.0351624
ryr1b	starAB	21hpf 5a5b	1.34107	3.03902	1.18023	0.0004	0.0323737
ifi30	starAB	21hpf 5a5b	190.335	102.606	-0.891426	0.0005	0.0379421
rpph1	starAB	21hpf 5a5b	58.8987	4.9167	-3.58248	5.00E-05	0.00650109
zp3a.2	starAB	21hpf 5a5b	8.81166	3.60265	-1.29036	0.00035	0.029378
dnmt3aa	starAB	21hpf 5a5b	2.00317	4.56276	1.18763	0.0007	0.0474034
notch1a	starAB	21hpf 5a5b	5.64962	11.648	1.04386	0.0002	0.0196474
sult3st4	starAB	21hpf 5a5b	0.765464	0.131988	-2.53592	0.0005	0.0379421
zgc:153154	starAB	21hpf 5a5b	3.5621	0.954278	-1.90025	0.00015	0.0158731
ptgdsb	starAB	21hpf 5a5b	40.889	19.9671	-1.03408	0.00035	0.029378
pus7	starAB	21hpf 5a5b	32.2094	14.0778	-1.19406	0.0005	0.0379421
cyp11a1	starAB	21hpf 5a5b	35.9785	12.5047	-1.52467	5.00E-05	0.00650109
zgc:173552	starAB	21hpf 5a5b	1.4865	0.247885	-2.58417	0.0003	0.0264437
lrp5	starAB	21hpf 5a5b	2.60164	5.81807	1.16112	0.00035	0.029378
hsp70.1	starAB	21hpf 5a5b	3.40691	8.96125	1.39524	5.00E-05	0.00650109
zgc:171779	starAB	21hpf 5a5b	2.93893	1.00254	-1.55164	0.00075	0.0496969
pvalb1	starAB	21hpf 5a5b	9.61523	23.6992	1.30145	0.00075	0.0496969
cdh15	starAB	21hpf 5a5b	5.76642	12.2467	1.08665	0.00025	0.0231995
hsp70l	starAB	21hpf 5a5b	0.756311	3.13544	2.05162	5.00E-05	0.00650109
zgc:153901	starAB	21hpf 5a5b	10.6477	4.79967	-1.14954	0.0005	0.0379421
nots	starAB	21hpf 5a5b	4.40373	1.64801	-1.418	0.00075	0.0496969
prtga	starAB	21hpf 5a5b	9.43832	25.0475	1.40806	5.00E-05	0.00650109

Continued on following page

Table B.5: continued from previous page

gene	sample 1	sample 2	value 1	value 2	log2 FC	p value	q values
krtcap2	starAB	21hpf 5a5b	8.33329	2.09737	-1.99031	0.0002	0.0196474
zgc:153713	starAB	21hpf 5a5b	484.751	225.81	-1.10214	0.0003	0.0264437

Table B.6: Significant differential gene expression of genes detected with EdgeR at 18hpf

gene	MO	logFC	logCPM	LR	p value	FDR
zgc:158463	tbx5a	-3.155192924	7.588779911	22.57538744	2.02E-06	0.01494411
hbl4	tbx5a	-5.279466012	5.353637758	14.22524197	0.00016218	0.599743091
irx5a	tbx5a	-5.075177124	5.328253702	13.42745291	0.000247969	0.61132518
dsg2.1	tbx5a	-5.130726415	5.194944572	12.86984262	0.00033392	0.617417508
utp11l	tbx5a	3.60857727	5.593196885	11.55020361	0.000677418	0.744344013
zgc:158482	tbx5a	-4.966559835	4.833017356	11.34906264	0.000754861	0.744344013
dachc	tbx5a	4.934441132	5.115189709	11.16600144	0.0008331	0.744344013
zgc:162608	tbx5a	2.739204763	6.213855815	11.06693595	0.000878808	0.744344013
cpsf3l	tbx5a	5.044821511	4.762315942	11.01090755	0.000905773	0.744344013
pfdn1	tbx5a	4.569659254	4.974891965	9.535127807	0.002015761	0.850156687
sox9b	tbx5a	4.685799939	4.668288066	9.370888198	0.002204587	0.850156687
ccdc77	tbx5a	4.604065997	4.914575971	9.332892067	0.002250768	0.850156687
sdf4	tbx5a	2.90740204	5.331374727	9.202340674	0.002417059	0.850156687
wu:fa19b12	tbx5a	4.625450356	4.648270432	9.085896205	0.002575882	0.850156687
zgc:153256	tbx5a	4.658746969	4.587009924	9.005508402	0.002691671	0.850156687
maf1	tbx5a	3.364195134	5.323111124	8.995951339	0.002705784	0.850156687
lbx1b	tbx5a	4.434494469	4.623792853	8.756010275	0.003085834	0.850156687
foxp1a	tbx5a	4.462864293	5.112152114	8.719732858	0.003147842	0.850156687
erbb2ip	tbx5a	3.592769652	5.177517812	8.681728048	0.003214161	0.850156687
slc12a3	tbx5a	-4.600718472	4.839032563	8.652410401	0.00326629	0.850156687
gpc1b	tbx5a	4.651679671	4.650360027	8.59643465	0.003368218	0.850156687
ccne2	tbx5a	-3.28120224	5.249106056	8.525172782	0.003502675	0.850156687
eif2b5	tbx5a	-3.303762445	5.109004288	8.513047622	0.00352609	0.850156687
sar1ab	tbx5a	4.486739121	4.920712239	8.473243616	0.003604082	0.850156687
dusp4	tbx5a	4.481487625	4.738307374	8.43126247	0.003688242	0.850156687
cldnf	tbx5a	4.528707555	4.708770927	8.426977353	0.003696944	0.850156687
tubgcp2	tbx5a	-4.337387598	4.642287311	8.402435251	0.003747187	0.850156687
orc1	tbx5a	-4.373009512	4.937270059	8.347853977	0.003861431	0.850156687
mid1ip1l	tbx5a	4.48280062	4.84693651	8.345573112	0.003866282	0.850156687
mybl2b	tbx5a	3.18883303	5.540073359	8.18729034	0.004218489	0.850156687
pklr	tbx5a	-3.353632831	4.92729535	8.163025324	0.0042753	0.850156687
naa50	tbx5a	1.848001404	6.412201713	8.160605183	0.004281008	0.850156687
mmp9	tbx5a	4.49176575	5.16682443	8.157706913	0.004287855	0.850156687
npr3	tbx5a	4.273866252	4.978049822	8.098985273	0.004429005	0.850156687
zgc:73185	tbx5a	4.434259432	4.864925785	8.005241125	0.004664215	0.850156687
fzd8b	tbx5a	-4.354747281	4.817920871	7.888389099	0.004975316	0.850156687
fam160a2	tbx5a	3.496553646	5.657106231	7.879707049	0.004999258	0.850156687
ptena	tbx5a	4.309639781	5.296187108	7.803165019	0.00521548	0.850156687
ndufs8a	tbx5a	2.700326193	5.415316582	7.78316637	0.005273529	0.850156687
cbx6a	tbx5a	4.504034689	4.68834447	7.775232282	0.005296741	0.850156687
tagln	tbx5a	-4.379202834	4.818422053	7.75394409	0.005359537	0.850156687
mut	tbx5a	4.268910019	5.035638074	7.721856494	0.005455627	0.850156687
socs6b	tbx5a	4.312028359	4.544214243	7.719964094	0.005461348	0.850156687
cdkn1bb	tbx5a	2.23930207	5.900183973	7.668686733	0.005618734	0.850156687
gins4	tbx5a	4.526280109	4.747537881	7.660794654	0.005643364	0.850156687
ildr1b	tbx5a	4.284735593	4.564423014	7.645593275	0.005691118	0.850156687
ctsz	tbx5a	4.248023001	4.794224728	7.635310648	0.005723653	0.850156687
nudt18	tbx5a	-4.169471717	4.964922835	7.629241288	0.005742946	0.850156687
prkacaa	tbx5a	3.143197753	5.028247252	7.623606915	0.005760915	0.850156687
gatad1	tbx5a	4.292057117	4.649709882	7.582637723	0.005893314	0.850156687
nadkb	tbx5a	-3.263730445	4.867733868	7.556486548	0.005979445	0.850156687

Continued on following page

Table B.6: continued from previous page

gene	MO	logFC	logCPM	LR	p value	FDR
zgc:194508	tbx5a	4.318122807	4.729188253	7.494486794	0.006188817	0.850156687
slc35a5	tbx5a	-1.744453383	6.940941035	7.375648081	0.006611296	0.850156687
tsen15	tbx5a	4.204475051	4.620304945	7.324957848	0.006800356	0.850156687
zgc:175088	tbx5a	1.687731091	6.543115776	7.306626649	0.006870078	0.850156687
rcan3	tbx5a	-4.168655179	4.871474642	7.205320978	0.007268775	0.850156687
flrt3	tbx5a	1.741571626	6.435559649	7.204212715	0.007273265	0.850156687
fam96b	tbx5a	-4.168946649	4.852723737	7.18800374	0.007339259	0.850156687
unc50	tbx5a	4.260132705	4.796893341	7.185907354	0.007347839	0.850156687
sox7	tbx5a	-4.134256446	4.602866262	7.181432076	0.007366189	0.850156687
aste1	tbx5a	-3.283404769	4.978711455	7.174640189	0.007394128	0.850156687
b3gnt2b	tbx5a	3.192099041	5.077541641	7.174505342	0.007394683	0.850156687
si:ch73-80e1.2	tbx5a	-4.124942038	4.543610455	7.155833701	0.007472056	0.850156687
trim35-27	tbx5a	-4.143845996	4.847343224	7.130433327	0.007578641	0.850156687
dtx1	tbx5a	-4.134174896	4.62774831	7.126807818	0.007593981	0.850156687
igf2r	tbx5a	-4.115557531	4.584191158	7.117558059	0.007633261	0.850156687
si:ch211-154o6.2	tbx5a	-4.207489757	4.816174299	7.101597598	0.007701528	0.850156687
lrwd1	tbx5a	-4.157451902	4.798599311	7.037525948	0.007981922	0.868151361
ext1a	tbx5a	4.273692788	4.869890155	6.972285381	0.00827817	0.887323897
rbm42	tbx5a	2.680723374	4.996483363	6.924757477	0.008501052	0.898196866
prdx6	tbx5a	4.050082608	4.562263025	6.851543628	0.008856472	0.922569963
zgc:161969	tbx5a	1.656763649	6.473898618	6.723613227	0.009514468	0.940786441
lman2lb	tbx5a	4.040565197	4.83194645	6.719947924	0.009534041	0.940786441
sft2d1	tbx5a	4.080690224	4.810427361	6.68621295	0.009716139	0.940786441
ino80c	tbx5a	4.068972625	4.721018021	6.676412821	0.009769704	0.940786441
rock2b	tbx5a	2.988266375	5.039589981	6.629928291	0.01002793	0.940786441
dpysl3	tbx5a	4.046880368	4.798224407	6.532314668	0.010593202	0.940786441
cenpk	tbx5a	4.092096432	4.796685317	6.50987433	0.010727709	0.940786441
anks4b	tbx5a	2.096266689	5.94103839	6.497345354	0.010803568	0.940786441
tyw1	tbx5a	1.720462221	6.224384603	6.484134712	0.010884151	0.940786441
hccsa.1	tbx5a	1.770646717	7.114841536	6.47659917	0.010930392	0.940786441
plekha7a	tbx5a	4.107323024	4.608064981	6.464970455	0.011002147	0.940786441
gda	tbx5a	2.086392552	5.973071336	6.463817036	0.011009291	0.940786441
sncb	tbx5a	4.093842363	4.630354476	6.434200814	0.011194351	0.940786441
LOC796180	tbx5a	4.021839526	4.774143884	6.432348715	0.01120603	0.940786441
lrrc17	tbx5a	-2.999832263	4.946860935	6.414737522	0.011317706	0.940786441
soul3	tbx5a	-3.020684777	5.048267615	6.357228425	0.011690402	0.940786441
tead3b	tbx5a	4.095764216	4.870709882	6.347511357	0.011754608	0.940786441
atg5	tbx5a	-3.971081952	4.651271745	6.339365044	0.011808715	0.940786441
loxl2b	tbx5a	-3.899267443	5.085246067	6.289633181	0.012144618	0.940786441
snrkb	tbx5a	-4.005653676	4.876404897	6.278026094	0.012224419	0.940786441
rgl1	tbx5a	-3.924363123	4.899956506	6.276606908	0.012234213	0.940786441
snx30	tbx5a	-2.827719807	4.920027488	6.275348332	0.012242905	0.940786441
schip1	tbx5a	-3.88988101	4.478852406	6.26693446	0.012301179	0.940786441
h2afy	tbx5a	-3.880720588	4.645119747	6.26369225	0.01232371	0.940786441
stab2	tbx5a	2.518829298	5.366441222	6.246728061	0.012442293	0.940786441
fbxl8	tbx5a	4.082931697	4.705211613	6.245187089	0.012453123	0.940786441
stx11b.2	tbx5a	-3.90175879	4.545744966	6.243384669	0.012465802	0.940786441
uri1	tbx5a	1.955690618	5.864647503	6.213860489	0.012675391	0.946941354
arr3b	tbx5a	-3.892146448	4.610524596	6.172238122	0.012977033	0.955331785
zgc:101800	tbx5a	-3.861014505	4.520688759	6.137194894	0.013236713	0.955331785
polr2i	tbx5a	-3.83997238	4.954747391	6.080188764	0.013670616	0.955331785

Continued on following page

Table B.6: continued from previous page

gene	MO	logFC	logCPM	LR	p value	FDR
bfb	tbx5a	-1.903957343	6.299080086	6.070163389	0.013748424	0.955331785
aoc2	tbx5a	-3.869292142	4.566563984	6.064595799	0.013791831	0.955331785
jam3b	tbx5a	2.925056115	5.016797516	6.045493369	0.013941837	0.955331785
oxsr1b	tbx5a	2.382740046	5.714514382	6.04501082	0.013945648	0.955331785
glyctk	tbx5a	-2.271650925	6.409895081	6.043597007	0.013956819	0.955331785
wwox	tbx5a	2.871793552	5.218790356	6.02669973	0.014091055	0.955331785
fundc2	tbx5a	2.356004742	5.342086361	5.99589357	0.014339216	0.955331785
rnasekb	tbx5a	2.07204928	5.509408942	5.986011147	0.014419774	0.955331785
cul1a	tbx5a	1.796785728	5.467389431	5.971663063	0.014537564	0.955331785
tbk1	tbx5a	2.876919003	4.930818667	5.894012432	0.015192446	0.955331785
sema4c	tbx5a	3.817832587	4.433919441	5.859125074	0.015496495	0.955331785
dpm1	tbx5a	2.83910674	5.203241333	5.843587713	0.015633917	0.955331785
nfil3-5	tbx5a	3.851550839	4.546874892	5.800575406	0.016020931	0.955331785
fundc1	tbx5a	-2.825481599	5.0712276	5.792739644	0.016092492	0.955331785
pdlim1	tbx5a	-2.359416229	5.347769755	5.783931331	0.016173328	0.955331785
fam58a	tbx5a	3.801835036	4.560399188	5.758530465	0.01640879	0.955331785
chchd4	tbx5a	2.427312013	5.201681851	5.747805336	0.016509269	0.955331785
dyrk2	tbx5a	-3.889823688	4.626310561	5.745253723	0.016533267	0.955331785
lias	tbx5a	2.869673264	4.862382974	5.736551916	0.01661538	0.955331785
zgc:136472	tbx5a	2.031876167	5.689322285	5.736131526	0.016619357	0.955331785
tpst1	tbx5a	-2.853839369	4.897593207	5.732266095	0.016655976	0.955331785
kiz	tbx5a	3.833894276	4.565912806	5.713311023	0.016836754	0.955331785
slc25a4	tbx5a	3.834322149	4.726775895	5.700176766	0.016963204	0.955331785
golim4a	tbx5a	-2.925758305	4.922931821	5.697332609	0.016990715	0.955331785
dub	tbx5a	3.791044245	4.621983608	5.690437259	0.017057604	0.955331785
stoml2	tbx5a	3.821844653	4.782314697	5.67844551	0.017174578	0.955331785
slc25a44a	tbx5a	3.821974958	5.116666456	5.672264311	0.017235195	0.955331785
chmp3	tbx5a	3.822050638	4.607252146	5.66866474	0.017270597	0.955331785
upk1a	tbx5a	3.83540155	4.628745969	5.666620142	0.017290739	0.955331785
tnnc1a	tbx5a	3.844044911	4.567057689	5.653396014	0.017421602	0.955331785
vsg1	tbx5a	-1.993768052	5.782637342	5.619640029	0.017760296	0.955331785
nf2b	tbx5a	2.856458641	5.106322156	5.604696969	0.017912393	0.955331785
bcar3	tbx5a	3.810287748	4.723349585	5.593144341	0.018030901	0.955331785
pnp5a	tbx5a	2.410125602	5.155962122	5.573674598	0.01823246	0.955331785
kpna7	tbx5a	2.255141362	5.575337594	5.56170063	0.018357573	0.955331785
uqcc3	tbx5a	3.760220516	4.559269096	5.535506355	0.018634372	0.955331785
amt	tbx5a	2.89895284	5.070329137	5.528605325	0.018708012	0.955331785
rtel1	tbx5a	3.790239692	4.719062667	5.526904569	0.018726206	0.955331785
prc1b	tbx5a	-2.897904135	4.909314707	5.510205913	0.018905821	0.955331785
hnrnpr	tbx5a	-2.81218754	4.82990332	5.505964189	0.018951729	0.955331785
wdr91	tbx5a	2.858455374	4.918391916	5.502133688	0.018993285	0.955331785
acat1	tbx5a	3.82540767	4.644247187	5.501534666	0.018999792	0.955331785
si:ch211-191j22.3	tbx5a	3.834079944	4.69946736	5.490100631	0.019124442	0.955331785
fstl1a	tbx5a	1.19342927	7.201197892	5.481507164	0.019218681	0.955331785
mfsd12a	tbx5a	1.893287626	5.870544602	5.476449519	0.01927437	0.955331785
suv420h2	tbx5a	3.835224421	4.625553712	5.438485355	0.019697743	0.955331785
tbx21	tbx5a	3.811827844	4.747715066	5.426404067	0.019834481	0.955331785
gtpbp1l	tbx5a	3.82015708	4.586379109	5.425386086	0.019846047	0.955331785
nr3c1	tbx5a	2.47921256	4.964113423	5.422770344	0.019875799	0.955331785
ubn2a	tbx5a	1.530738691	6.720967645	5.41962274	0.019911662	0.955331785
immt	tbx5a	-2.167806378	5.656228226	5.408522837	0.020038666	0.955331785

Continued on following page

Table B.6: continued from previous page

gene	MO	logFC	logCPM	LR	p value	FDR
cops6	tbx5a	-2.780930475	4.792286956	5.396923735	0.020172277	0.955331785
nup160	tbx5a	-1.764979598	5.772744971	5.39250568	0.020223411	0.955331785
mpp5a	tbx5a	3.906697852	4.673603505	5.390008663	0.02025237	0.955331785
meis2b	tbx5a	2.07751061	5.29691422	5.387673827	0.020279488	0.955331785
rab24	tbx5a	3.797524952	4.625951427	5.366745826	0.020524234	0.960741982
ofd1	tbx5a	-2.370345463	5.013773512	5.292855463	0.021413082	0.985952098
nt5c2b	tbx5a	3.864012513	4.730210516	5.29191133	0.021424693	0.985952098
npc1	tbx5a	1.734953283	5.90919707	5.270081505	0.021694997	0.985952098
st14a	tbx5a	-2.338533565	5.476769979	5.269991548	0.021696118	0.985952098
mthfr	tbx5a	-3.594034064	4.569080911	5.248779781	0.021962167	0.985952098
slc1a4	tbx5a	-3.594058687	4.665318154	5.242720546	0.022038784	0.985952098
zgc:92139	tbx5a	-1.809724669	5.740855846	5.2213115	0.022311718	0.985952098
mtm1	tbx5a	3.813784643	4.72625288	5.186395403	0.022764385	0.985952098
rp2	tbx5a	-3.594462041	4.727529149	5.139067123	0.023393215	0.985952098
sp8b	tbx5a	1.904116601	5.871394816	5.135770092	0.023437687	0.985952098
plbd1	tbx5a	2.142639087	5.382445727	5.11139376	0.023769218	0.985952098
basp1	tbx5a	-3.698553329	4.591415463	5.107506107	0.02382254	0.985952098
rhbdl2	tbx5a	-3.594597093	4.672205652	5.102378819	0.023893055	0.985952098
mogs	tbx5a	-3.620167116	4.50547781	5.094953331	0.02399556	0.985952098
mrps28	tbx5a	-3.572303559	4.860808643	5.08896654	0.024078537	0.985952098
znf384l	tbx5a	-3.650205583	4.545830061	5.08485548	0.024135688	0.985952098
myoc	tbx5a	2.73684022	4.847597792	5.060797403	0.024472975	0.985952098
trove2	tbx5a	-1.857513249	5.752167303	5.041310248	0.024749764	0.985952098
cldn2	tbx5a	2.106821708	5.318136088	5.017221623	0.025096407	0.985952098
lims2	tbx5a	2.351633641	5.476126926	5.007063316	0.025244095	0.985952098
nos2b	tbx5a	2.82158436	4.824548104	4.993989112	0.025435507	0.985952098
meig1	tbx5a	-3.6072947	4.589625988	4.99362126	0.025440914	0.985952098
camk1db	tbx5a	2.734381177	5.030519222	4.989979687	0.025494508	0.985952098
timm8a	tbx5a	-3.54820399	4.663865005	4.949819968	0.026093386	0.985952098
scrib	tbx5a	1.777226943	6.189170194	4.945081398	0.026165007	0.985952098
igfbp7	tbx5a	1.98191388	5.363617383	4.941666815	0.026216743	0.985952098
col5a3a	tbx5a	-2.716162446	4.98452358	4.93917843	0.026254513	0.985952098
zgc:174680	tbx5a	1.084422886	7.586044316	4.899668638	0.026861849	0.985952098
haus6	tbx5a	2.664494156	4.965602631	4.897368743	0.02689765	0.985952098
hk2	tbx5a	2.323992818	5.226248075	4.863446829	0.02743148	0.985952098
ubac1	tbx5a	-3.543720762	4.606296014	4.843126404	0.02775653	0.985952098
prkaa1	tbx5a	-3.55486425	4.850717808	4.840722059	0.027795254	0.985952098
mybphb	tbx5a	-1.334689826	6.946444694	4.829644329	0.027974401	0.985952098
cd99l2	tbx5a	2.345034666	4.985481954	4.82766085	0.028006604	0.985952098
tpm1	tbx5a	-2.673112512	4.778969174	4.81915545	0.028145132	0.985952098
trim35-19	tbx5a	1.737749277	5.529470629	4.799320967	0.028470956	0.985952098
ntmt1	tbx5a	1.52416057	6.235032009	4.7973753	0.028503129	0.985952098
vmhc	tbx5a	3.531183799	5.304332079	4.791141961	0.028606455	0.985952098
stc1l	tbx5a	3.531256977	4.567182733	4.78977279	0.028629203	0.985952098
akt2l	tbx5a	-2.615605277	5.078329427	4.784442656	0.02871794	0.985952098
reln	tbx5a	-1.958936423	5.288954535	4.78399267	0.028725444	0.985952098
zcchc8	tbx5a	-2.700516545	4.86973819	4.776023372	0.028858689	0.985952098
map7d1b	tbx5a	1.630999781	5.810150996	4.766808	0.029013571	0.985952098
ubap2a	tbx5a	-1.252961458	6.854969804	4.765055754	0.029043119	0.985952098
wdr21	tbx5a	-3.552264274	4.622652607	4.75768187	0.029167806	0.985952098
itm2ba	tbx5a	1.350386107	6.696057689	4.756619813	0.029185811	0.985952098

Continued on following page

Table B.6: continued from previous page

gene	MO	logFC	logCPM	LR	p value	FDR
srp9	tbx5a	1.763521619	5.78018948	4.756095617	0.029194701	0.985952098
ndufa4	tbx5a	3.508794377	4.453513903	4.752271697	0.029259643	0.985952098
glmna	tbx5a	3.573091073	4.83444326	4.747373376	0.029343051	0.985952098
sox11b	tbx5a	1.262216106	6.816408241	4.744773207	0.029387427	0.985952098
snapc1a	tbx5a	3.533767102	4.477840365	4.741987397	0.029435049	0.985952098
dgcr8	tbx5a	1.208452292	7.632090392	4.73229671	0.029601332	0.985952098
tmem82	tbx5a	2.296309685	5.441630464	4.730499934	0.029632271	0.985952098
tmed1b	tbx5a	3.558548451	4.609746386	4.727638215	0.029681616	0.985952098
ccnd1	tbx5a	1.018535992	7.925944985	4.726800778	0.029696072	0.985952098
vwa8	tbx5a	3.558788439	4.588765019	4.724629356	0.029733591	0.985952098
zgc:162154	tbx5a	1.859298572	6.392163196	4.701193494	0.03014168	0.985952098
kdm5c	tbx5a	1.324808992	6.775568992	4.698247964	0.030193381	0.985952098
zgc:158263	tbx5a	1.846362313	5.582317521	4.692860309	0.030288188	0.985952098
hiat1a	tbx5a	3.522364416	4.565926035	4.692243678	0.030299059	0.985952098
dnm3a	tbx5a	1.70625237	5.962678269	4.689940701	0.030339694	0.985952098
ska2	tbx5a	3.522822899	4.811671563	4.677353433	0.0305628	0.985952098
mipa	tbx5a	3.49042874	4.793843298	4.664916863	0.030784914	0.985952098
tm9sf4	tbx5a	1.614980204	6.14629182	4.651732788	0.031022217	0.985952098
jmjd4	tbx5a	-1.432271668	6.589315304	4.649172074	0.031068529	0.985952098
prmt6	tbx5a	2.554756374	5.037682077	4.646899992	0.031109681	0.985952098
zgc:158222	tbx5a	-3.523304254	4.681490506	4.646130948	0.031123623	0.985952098
setd8b	tbx5a	1.668521394	5.698737898	4.642532509	0.031188945	0.985952098
ppp2r2bb	tbx5a	1.560119312	6.005214665	4.635238168	0.031321797	0.985952098
sord	tbx5a	-2.081838297	5.479226722	4.628266104	0.031449331	0.985952098
exoc5	tbx5a	3.549347297	4.58509831	4.623735801	0.03153249	0.985952098
appbp2	tbx5a	2.592458296	5.283958905	4.621103518	0.031580914	0.985952098
yrk	tbx5a	2.02069022	5.246160874	4.618581813	0.031627377	0.985952098
atp6v0a2b	tbx5a	3.471393017	4.520475316	4.615747649	0.031679682	0.985952098
lrrc59	tbx5a	1.294305954	6.423399213	4.614794104	0.0316973	0.985952098
veph1	tbx5a	-3.565728966	4.833059044	4.600003335	0.031971894	0.985952098
smyhc2	tbx5a	3.550709073	5.076731323	4.598683801	0.031996512	0.985952098
ccdc28a	tbx5a	3.54088935	4.742355905	4.597049201	0.032027035	0.985952098
zgc:171579	tbx5a	3.568425364	4.646341388	4.596499604	0.032037304	0.985952098
zc3hc1	tbx5a	1.815436767	5.477369024	4.58289013	0.032292705	0.985952098
zgc:162964	tbx5a	-1.812053377	5.567720455	4.58057032	0.032336451	0.985952098
stxbp5l	tbx5a	3.525860059	4.566875755	4.574833646	0.032444896	0.985952098
cacng1a	tbx5a	3.47701699	5.102455065	4.573539551	0.032469412	0.985952098
zfpl1	tbx5a	3.520201228	4.666291851	4.553768971	0.032846368	0.985952098
alg5	tbx5a	2.516843357	5.420174949	4.552295093	0.032874652	0.985952098
bhlha15	tbx5a	3.48886039	4.542145118	4.542488124	0.0330635	0.985952098
hspb11	tbx5a	3.468321846	4.877816319	4.530557025	0.033294779	0.985952098
abcf2a	tbx5a	1.253017792	6.477135985	4.527803468	0.033348395	0.985952098
taf2	tbx5a	-2.068478809	5.310426576	4.519212816	0.033516249	0.985952098
ptrh1	tbx5a	3.527561655	4.778801533	4.514251346	0.033613594	0.985952098
ech1	tbx5a	3.496857325	4.705641176	4.50436915	0.033808365	0.985952098
gstt1b	tbx5a	3.488322072	4.60591961	4.498456321	0.033925466	0.985952098
mllt3	tbx5a	2.560287194	5.242242251	4.492358426	0.034046677	0.985952098
wnt5b	tbx5a	-2.62034858	4.738232883	4.472966319	0.03443516	0.985952098
ptgfr	tbx5a	3.512171321	4.647215058	4.467985552	0.034535686	0.985952098
ide	tbx5a	1.558529303	6.136737286	4.462157671	0.034653699	0.985952098
gna15.1	tbx5a	2.627116282	4.922622453	4.461027441	0.034676634	0.985952098

Continued on following page

Table B.6: continued from previous page

gene	MO	logFC	logCPM	LR	p value	FDR
boc	tbx5a	2.209238918	5.281843589	4.457039799	0.034757681	0.985952098
ptbp1a	tbx5a	1.546777868	6.205906323	4.452786907	0.034844338	0.985952098
tnika	tbx5a	1.950926682	5.927349147	4.447471967	0.034952953	0.985952098
pygma	tbx5a	1.539334334	6.255678535	4.429105375	0.035331022	0.985952098
eif2d	tbx5a	-2.546296074	5.08671948	4.423500565	0.035447245	0.985952098
sh3rf1	tbx5a	2.235410846	5.226573139	4.421266749	0.035493677	0.985952098
myhc4	tbx5a	3.45128168	4.661796942	4.417889167	0.035564005	0.985952098
cmtm6	tbx5a	2.545499292	4.849142373	4.417030921	0.035581899	0.985952098
cdc23	tbx5a	2.201621054	5.390852746	4.415487936	0.035614092	0.985952098
mrps15	tbx5a	2.777920603	4.868894521	4.413546071	0.035654651	0.985952098
eif2b4	tbx5a	2.144925786	5.102232026	4.405117912	0.035831248	0.985952098
anapc16	tbx5a	-2.198072398	5.051743696	4.402898563	0.035877902	0.985952098
dnajc25	tbx5a	3.530609615	4.705138216	4.399496121	0.035949551	0.985952098
polr3e	tbx5a	1.963332449	5.440069297	4.397766147	0.035986038	0.985952098
ccdc90b	tbx5a	3.581945019	4.747022855	4.388953918	0.036172501	0.985952098
xpo6	tbx5a	2.515404859	4.897844908	4.385907885	0.036237188	0.985952098
sv2c	tbx5a	2.239025598	5.077598771	4.384835004	0.036260001	0.985952098
mixl1	tbx5a	1.134784676	6.971144613	4.365895885	0.036665199	0.99331799
ubr7	tbx5a	1.670090815	5.709658126	4.350006046	0.037008815	0.995263913
pcf11	tbx5a	1.571855695	6.191991025	4.338966726	0.037249523	0.995263913
nfkb2	tbx5a	2.576396684	4.761574922	4.309896186	0.037891274	0.995263913
tab3	tbx5a	2.55705858	4.979639433	4.298150188	0.038153851	0.995263913
zgc:100864	tbx5a	1.58900435	6.043217436	4.283479425	0.038484491	0.995263913
adam10b	tbx5a	2.251855817	4.759654175	4.279362398	0.038577817	0.995263913
paqr3a	tbx5a	1.748297859	5.35495739	4.278186642	0.038604513	0.995263913
emc9	tbx5a	2.532381464	4.605088801	4.277354006	0.03862343	0.995263913
tnip1	tbx5a	2.545422192	4.996624772	4.277173248	0.038627538	0.995263913
cecr5	tbx5a	-2.516262547	5.089024559	4.273226935	0.038717338	0.995263913
nebl	tbx5a	1.997541924	5.531657873	4.267885944	0.038839223	0.995263913
slmo2	tbx5a	2.488235817	5.407620944	4.240437954	0.039471984	0.995263913
tm7sf2	tbx5a	1.898955501	5.299793553	4.239018885	0.03950499	0.995263913
zgc:56525	tbx5a	1.469200139	6.078296869	4.229852519	0.039718892	0.995263913
utp3	tbx5a	1.405841807	6.112203478	4.229457456	0.039728138	0.995263913
znf865	tbx5a	1.431743453	5.843697622	4.228332153	0.039754488	0.995263913
fbxw8	tbx5a	1.930805227	5.396877539	4.226171348	0.039805135	0.995263913
clec14a	tbx5a	3.41795862	4.662585262	4.207428572	0.040247305	0.995263913
pin4	tbx5a	2.487201399	4.908570519	4.185440115	0.040772625	0.995263913
rabac1	tbx5a	1.801010954	5.374404808	4.165338191	0.041259175	0.995263913
apela	tbx5a	2.55014718	4.740663155	4.163288429	0.04130913	0.995263913
bag6	tbx5a	1.803917224	5.489924088	4.161610652	0.041350066	0.995263913
synj2bp	tbx5a	1.698109445	5.460580691	4.15537356	0.041502618	0.995263913
zgc:66014	tbx5a	1.638171771	5.857274778	4.151168952	0.041605792	0.995263913
zgc:113229	tbx5a	-1.773657865	5.413945463	4.144507403	0.041769807	0.995263913
si:ch211-286b5.5	tbx5a	1.916462473	5.131033284	4.132339898	0.042071141	0.995263913
ing5b	tbx5a	2.508050126	4.80614603	4.130250093	0.042123125	0.995263913
ufsp2	tbx5a	-1.209868519	8.042984945	4.12881756	0.042158799	0.995263913
nol10	tbx5a	-1.502653937	5.80159557	4.092265844	0.043079854	0.995263913
nol6	tbx5a	-1.703218897	5.663183994	4.092124266	0.043083462	0.995263913
b3galt2	tbx5a	-2.024720023	4.895333196	4.091173505	0.043107703	0.995263913
hgs	tbx5a	1.990729514	5.347392138	4.066337545	0.043746027	0.995263913
polr2k	tbx5a	2.18148941	4.874197774	4.058607535	0.043946724	0.995263913

Continued on following page

Table B.6: continued from previous page

gene	MO	logFC	logCPM	LR	p value	FDR
h2afx	tbx5a	1.797181942	5.169233401	4.05551107	0.04402739	0.995263913
pltp	tbx5a	2.087956159	5.305642664	4.051143057	0.044141446	0.995263913
rdh10b	tbx5a	-3.220300645	4.70593298	4.049627447	0.044181094	0.995263913
pim3	tbx5a	-3.255611132	4.725863285	4.049426731	0.044186348	0.995263913
rpz2	tbx5a	2.576103546	4.692999271	4.04758996	0.044234453	0.995263913
cetn3	tbx5a	-3.256546714	4.606974848	4.040477871	0.044421241	0.995263913
phtf2	tbx5a	-3.230825752	4.434281689	4.037430839	0.044501521	0.995263913
zgc:77650	tbx5a	-2.481304694	4.881626889	4.033009968	0.044618268	0.995263913
churc1	tbx5a	-3.211050728	4.625954432	4.032324598	0.044636397	0.995263913
lrrc47	tbx5a	1.507543902	6.357034301	4.031729447	0.044652145	0.995263913
dpydb	tbx5a	-3.257511304	4.523445629	4.03116337	0.044667129	0.995263913
lyrm1	tbx5a	1.974606594	5.59531868	4.029864197	0.044701539	0.995263913
tsn	tbx5a	1.956615915	5.183645112	4.023340168	0.044874756	0.995263913
ddx51	tbx5a	1.462184176	5.983454265	4.000630285	0.045483252	0.995263913
mgst3	tbx5a	-2.087376201	5.089450444	3.99319648	0.045684319	0.995263913
hdac8	tbx5a	-3.262191741	4.668622628	3.984650962	0.045916613	0.995263913
nucb2a	tbx5a	1.088182992	7.034508409	3.975042077	0.0461793	0.995263913
znrf3	tbx5a	-3.199270233	4.542070021	3.971469521	0.046277369	0.995263913
wipf2b	tbx5a	-2.538313228	4.812221296	3.965391425	0.046444723	0.995263913
dcun1d2a	tbx5a	-3.21037074	4.742978396	3.964412507	0.046471736	0.995263913
pnp4a	tbx5a	-3.23361994	4.457911454	3.96403225	0.046482233	0.995263913
zgc:110339	tbx5a	-1.810460999	5.211756709	3.963181615	0.046505725	0.995263913
dennd6b	tbx5a	1.964873652	5.232408312	3.959799006	0.046599267	0.995263913
rfwd2	tbx5a	2.554607435	4.798000242	3.947106729	0.046952029	0.995263913
zgc:55262	tbx5a	-3.198097861	4.501109995	3.940067894	0.047148875	0.995263913
csnk1g2b	tbx5a	1.758720779	5.56331161	3.933775154	0.047325592	0.995263913
lrpap1	tbx5a	1.633730175	5.921737878	3.930220171	0.047425735	0.995263913
ube3c	tbx5a	-3.208307378	4.58860048	3.926204415	0.047539126	0.995263913
mcamb	tbx5a	-3.235411043	4.814775759	3.914214402	0.047879388	0.995263913
zgc:158766	tbx5a	2.614368827	4.666473122	3.903663554	0.048180934	0.995263913
ahcy	tbx5a	-1.033892906	7.489424627	3.903466184	0.048186594	0.995263913
hhex	tbx5a	-3.222440612	4.564764285	3.887378406	0.048650309	0.995263913
efhc1	tbx5a	-3.209638581	4.626664775	3.884873227	0.048722941	0.995263913
vps72	tbx5a	-1.949766559	5.242842244	3.883918665	0.048750646	0.995263913
rad17	tbx5a	2.138649832	5.442502923	3.874603895	0.049021876	0.995263913
zgc:77651	tbx5a	2.549726464	4.791488166	3.863062096	0.049360165	0.995263913
znf609	tbx5a	1.870146492	5.152480981	3.843856242	0.049928564	0.995263913
npffr1l2	tbx5a	-3.209270097	4.565282726	3.841956192	0.049985171	0.995263913
hbl4	tbx5b	-5.535019125	5.353637758	16.32104858	5.35E-05	0.244637587
loxl2b	tbx5b	-5.470252753	5.085246067	15.56197476	7.98E-05	0.244637587
irx5a	tbx5b	-5.291135773	5.328253702	15.1512796	9.92E-05	0.244637587
zbtb37	tbx5b	-2.367731735	6.406297832	13.12101293	0.000292002	0.539911913
si:ch211-154o6.2	tbx5b	-5.162148374	4.816174299	12.01527368	0.000527663	0.61861445
leng1	tbx5b	5.062078795	4.954287332	11.80054022	0.000592135	0.61861445
tmem54b	tbx5b	-2.653769899	6.146795214	11.77768456	0.00059945	0.61861445
cmn	tbx5b	-2.51530912	5.994346196	11.57308234	0.000669134	0.61861445
znf207a	tbx5b	2.517146063	6.201653075	11.1657309	0.000833221	0.684722804
mrps28	tbx5b	-4.663910042	4.860808643	10.03897366	0.001532626	0.996331174
si:ch211-147a11.3	tbx5b	-2.585605031	5.479574544	9.88929828	0.001662428	0.996331174
si:dkey-284p5.3	tbx5b	-2.981955018	5.797749962	9.474691615	0.002083259	0.996331174
bfb	tbx5b	-2.284164421	6.299080086	9.28963166	0.002304545	0.996331174

Continued on following page

Table B.6: continued from previous page

gene	MO	logFC	logCPM	LR	p value	FDR
lin54	tbx5b	4.472106102	4.725187364	8.807506334	0.002999938	0.996331174
atg5	tbx5b	-4.487507919	4.651271745	8.794904401	0.003020731	0.996331174
ehmt1a	tbx5b	4.463418828	4.97688664	8.726490202	0.003136196	0.996331174
mthfr	tbx5b	-4.346362676	4.569080911	8.568784835	0.003419753	0.996331174
cd22	tbx5b	-2.418675739	5.598836455	8.552322501	0.003450817	0.996331174
emc9	tbx5b	4.429135421	4.605088801	8.536420276	0.003481096	0.996331174
ino80e	tbx5b	4.486929214	4.780313566	8.520950422	0.003510811	0.996331174
tmem177	tbx5b	-4.355692191	4.604816694	8.369470804	0.003815767	0.996331174
nexn	tbx5b	-1.554098036	7.791830397	8.364874168	0.003825431	0.996331174
nebl	tbx5b	3.279929379	5.531657873	8.344337106	0.003868913	0.996331174
mtmr2	tbx5b	-4.344031957	4.703657971	8.333725159	0.003891578	0.996331174
pim3	tbx5b	-4.328763973	4.725863285	8.260754895	0.004051128	0.996331174
orc1	tbx5b	-4.340583765	4.937270059	8.228987181	0.004122653	0.996331174
slc35a5	tbx5b	-1.831037192	6.940941035	8.226370349	0.004128602	0.996331174
polr2i	tbx5b	-4.328634748	4.954747391	8.198989265	0.004191373	0.996331174
tmem183a	tbx5b	4.487431274	4.797333168	8.096307058	0.004435554	0.996331174
eng2b	tbx5b	-2.773910025	5.351977524	7.882299598	0.004992096	0.996331174
slc40a1	tbx5b	-4.323442942	4.896683613	7.786260729	0.005264504	0.996331174
dcun1d2b	tbx5b	-3.251120042	5.058288331	7.767620384	0.005319108	0.996331174
dpysl5a	tbx5b	-2.625355872	4.937809516	7.593737946	0.005857138	0.996331174
coro1ca	tbx5b	-1.988070795	5.765093756	7.552064079	0.005994138	0.996331174
yipf6	tbx5b	4.237423201	4.775572893	7.518859517	0.006105632	0.996331174
h2afx	tbx5b	2.716541842	5.169233401	7.489015751	0.006207648	0.996331174
rnd1l	tbx5b	4.306896805	4.820201452	7.485766441	0.006218859	0.996331174
ube2q2	tbx5b	-2.489043226	5.36175703	7.403669362	0.006509097	0.996331174
rp2	tbx5b	-4.13487989	4.727529149	7.286985525	0.006945592	0.996331174
mcrs1	tbx5b	-2.279763839	5.467829039	7.272273569	0.007002711	0.996331174
arr3b	tbx5b	-4.157697621	4.610524596	7.267235222	0.007022382	0.996331174
tmem8c	tbx5b	-1.932502465	5.835439029	7.182782854	0.007360645	0.996331174
stk10	tbx5b	-4.150033967	4.671454132	7.132274485	0.007570863	0.996331174
mcamb	tbx5b	-4.160513916	4.814775759	7.102214467	0.007698878	0.996331174
frem2b	tbx5b	-4.127254919	4.66618909	7.087226093	0.007763532	0.996331174
cx36.7	tbx5b	-4.17067602	4.632167348	7.08368695	0.00777888	0.996331174
igf2r	tbx5b	-4.096573834	4.584191158	7.05690209	0.007896042	0.996331174
prkaa1	tbx5b	-4.17697682	4.850717808	7.027206982	0.008028047	0.996331174
kif7	tbx5b	-4.132519215	4.866259742	7.018446185	0.008067421	0.996331174
lppr3a	tbx5b	4.330796495	4.669351336	7.002330911	0.008140365	0.996331174
triap1	tbx5b	-4.108923404	4.720071996	6.978313644	0.008250331	0.996331174
xpc	tbx5b	-2.057236846	5.759290103	6.975227933	0.00826457	0.996331174
exosc2	tbx5b	2.646066518	5.549772592	6.96983981	0.008289492	0.996331174
znf576.2	tbx5b	-2.140680394	5.397799469	6.962440162	0.008323843	0.996331174
fzd8b	tbx5b	-4.13279276	4.817920871	6.942417196	0.008417529	0.996331174
tagln	tbx5b	-4.169288403	4.818422053	6.88328473	0.008700552	0.996331174
hnrnph1	tbx5b	-1.909508561	6.090980691	6.8405393	0.008911193	0.996331174
heatr5a	tbx5b	-4.170372429	4.706495277	6.819403876	0.009017266	0.996331174
slc12a3	tbx5b	-4.154126948	4.839032563	6.789089017	0.00917167	0.996331174
ephb4a	tbx5b	4.057473209	4.643311648	6.734036326	0.009459032	0.996331174
notch3	tbx5b	-2.12796039	5.902159647	6.703215504	0.00962392	0.996331174
gsto2	tbx5b	4.063036733	4.813817455	6.66214701	0.009848219	0.996331174
zgc:162082	tbx5b	-2.494286127	5.391374914	6.648748455	0.00992255	0.996331174
slc10a7	tbx5b	4.075767116	4.867319935	6.630696385	0.010023607	0.996331174

Continued on following page

Table B.6: continued from previous page

gene	MO	logFC	logCPM	LR	p value	FDR
zgc:153426	tbx5b	4.0339348	4.878147066	6.606919805	0.010158322	0.996331174
tm2d3	tbx5b	4.022318422	4.615421532	6.521760001	0.01065625	0.996331174
veph1	tbx5b	-4.175170356	4.833059044	6.517154376	0.010683882	0.996331174
dctn4	tbx5b	-2.955352584	4.832365446	6.503442172	0.010766585	0.996331174
six1b	tbx5b	2.919103681	5.147708269	6.48205632	0.010896885	0.996331174
pold2	tbx5b	4.078766175	4.645407733	6.472901371	0.010953157	0.996331174
smyhc1	tbx5b	-1.18008714	8.82418967	6.468041483	0.010983151	0.996331174
zgc:113090	tbx5b	-1.375224103	6.7574879	6.434311618	0.011193653	0.996331174
cx30.3	tbx5b	-2.970046913	5.040966425	6.429200884	0.011225907	0.996331174
trim33	tbx5b	1.819878441	6.323897254	6.428098391	0.011232878	0.996331174
col15a1b	tbx5b	-3.000827746	4.988717222	6.397666392	0.011427047	0.996331174
slc1a1	tbx5b	-3.884999855	4.669145732	6.376536466	0.011563888	0.996331174
ndufab1a	tbx5b	1.856593863	5.959380083	6.375626045	0.011569822	0.996331174
pqlc2	tbx5b	3.004875569	4.94842548	6.372505079	0.011590187	0.996331174
nudt18	tbx5b	-3.876884664	4.964922835	6.365863174	0.011633649	0.996331174
igsf8	tbx5b	-2.959793734	4.865173005	6.341416939	0.011795062	0.996331174
zgc:173587	tbx5b	3.990521987	4.619555553	6.334625101	0.011840314	0.996331174
fgfr2	tbx5b	2.090365903	5.548957135	6.312111184	0.011991596	0.996331174
mmp2	tbx5b	-2.229671421	5.577357062	6.262264494	0.012333645	0.996331174
guca1e	tbx5b	-3.894691292	4.915492024	6.240999049	0.012482604	0.996331174
cahz	tbx5b	4.07590862	4.764570866	6.230792588	0.012554753	0.996331174
dsg2.1	tbx5b	-3.895012205	5.194944572	6.218239852	0.012644075	0.996331174
cul1a	tbx5b	1.826568953	5.467389431	6.189069297	0.012854177	0.996331174
ube3c	tbx5b	-3.886445062	4.58860048	6.176502558	0.012945792	0.996331174
tuba4l	tbx5b	-3.916595295	4.586852395	6.149233151	0.013146909	0.996331174
cetn3	tbx5b	-3.859348588	4.606974848	6.148159814	0.013154891	0.996331174
aoc2	tbx5b	-3.89604301	4.566563984	6.14358413	0.013188972	0.996331174
mmp23bb	tbx5b	-1.557962556	6.552343838	6.105982596	0.013472502	0.996331174
c1galt1b	tbx5b	-3.876924799	4.604258245	6.103811266	0.013489065	0.996331174
mad1l1	tbx5b	-3.913229923	4.725828411	6.073921938	0.013719201	0.996331174
trim35-27	tbx5b	-3.876931206	4.847343224	6.065514384	0.01378466	0.996331174
hdac8	tbx5b	-3.872217759	4.668622628	6.034555828	0.01402848	0.996331174
cul5a	tbx5b	-2.64287984	4.990873458	6.030152092	0.014063521	0.996331174
snrkb	tbx5b	-3.914379744	4.876404897	6.022803861	0.014122193	0.996331174
anapc5	tbx5b	-3.876939358	4.685015126	6.017749983	0.014162692	0.996331174
ccne2	tbx5b	-2.848222588	5.249106056	5.978963943	0.014477504	0.996331174
zp3b	tbx5b	4.024193828	4.684422657	5.941094671	0.014791829	0.996331174
st14a	tbx5b	-2.455563425	5.476769979	5.941030713	0.014792366	0.996331174
si:ch211-286b5.5	tbx5b	2.443109561	5.131033284	5.920785189	0.014963289	0.996331174
ufsp2	tbx5b	-1.443351077	8.042984945	5.913433598	0.015025857	0.996331174
txlnbb	tbx5b	-2.010946944	6.183464823	5.897490189	0.015162476	0.996331174
si:dkey-42i9.4	tbx5b	-1.732316744	5.863001296	5.862690515	0.015465136	0.996331174
timm9	tbx5b	-2.628529684	5.059819509	5.855043673	0.015532473	0.996331174
spred2b	tbx5b	3.831080895	4.901749052	5.837175006	0.015691	0.996331174
eif2d	tbx5b	-2.829630735	5.08671948	5.830739719	0.0157485	0.996331174
wu:fa26c03	tbx5b	-2.49452664	5.468818622	5.822431307	0.015823058	0.996331174
vamp1	tbx5b	3.855594893	4.613116392	5.758539973	0.016408701	0.996331174
si:ch211-133n4.4	tbx5b	-2.814909746	5.068791345	5.75080095	0.016481141	0.996331174
zgc:65894	tbx5b	3.790905142	4.522806918	5.701824986	0.016947283	0.996331174
keap1a	tbx5b	-2.839915695	4.671095664	5.700756097	0.016957606	0.996331174
knstrn	tbx5b	3.779806631	4.678852168	5.682192258	0.017137941	0.996331174

Continued on following page

Table B.6: continued from previous page

gene	MO	logFC	logCPM	LR	p value	FDR
gsdf	tbx5b	3.08394957	4.747890464	5.675396628	0.01720445	0.996331174
usp2a	tbx5b	3.836395775	4.764463883	5.674090538	0.017217263	0.996331174
rab18b	tbx5b	2.497066446	5.096590204	5.670863225	0.017248966	0.996331174
hoxb6a	tbx5b	-1.544294273	6.451844516	5.669204659	0.017265282	0.996331174
zgc:113019	tbx5b	-2.497762594	4.643122717	5.657907373	0.017376844	0.996331174
zbtb10	tbx5b	-2.82962252	4.867666375	5.644801683	0.017507196	0.996331174
ywhae2	tbx5b	2.939604378	5.093317321	5.612879069	0.017828946	0.996331174
lycat	tbx5b	3.810603522	4.698955733	5.598866646	0.0179721	0.996331174
slco1c1	tbx5b	-2.160445978	5.183341216	5.572109707	0.018248761	0.996331174
coro1b	tbx5b	3.864706667	4.631476543	5.556338055	0.018413892	0.996331174
cdipt	tbx5b	3.850843212	4.775278631	5.488491313	0.019142054	0.996331174
soul3	tbx5b	-2.831791782	5.048267615	5.466634366	0.019382918	0.996331174
tmem161a	tbx5b	-2.856704371	5.005190159	5.466443744	0.019385032	0.996331174
zgc:113232	tbx5b	-2.845886403	5.065472546	5.444633587	0.019628532	0.996331174
selt1b	tbx5b	3.836035121	4.897681675	5.438486757	0.019697728	0.996331174
hsp90aa1.1	tbx5b	-0.987703734	9.165220044	5.423683423	0.019865408	0.996331174
rab14	tbx5b	-1.156798341	7.559495437	5.375463625	0.020421913	0.996331174
tpgs2	tbx5b	-1.982645808	5.920789393	5.319978215	0.021082275	0.996331174
zgc:153725	tbx5b	2.848626885	4.886004693	5.296056399	0.021373763	0.996331174
mob4	tbx5b	-1.260384806	6.951341009	5.282788611	0.021537227	0.996331174
rdh10b	tbx5b	-3.600114791	4.70593298	5.282682615	0.021538538	0.996331174
prc1b	tbx5b	-2.826048364	4.909314707	5.245472264	0.022003955	0.996331174
churc1	tbx5b	-3.58426474	4.625954432	5.24411542	0.022021121	0.996331174
parp3	tbx5b	-3.588610394	4.546352052	5.207905037	0.022484412	0.996331174
nedd9	tbx5b	-2.449533519	4.884937796	5.172525986	0.022946826	0.996331174
neu1	tbx5b	-2.469979987	5.079790406	5.16414591	0.023057793	0.996331174
ebag9	tbx5b	-3.567881113	4.7628704	5.161686185	0.023090469	0.996331174
hoxb5a	tbx5b	-1.189644904	7.213247753	5.152788645	0.023209071	0.996331174
med13a	tbx5b	-1.765906485	5.458950188	5.144437391	0.023320966	0.996331174
galnt2	tbx5b	-2.300890414	5.400097553	5.136987282	0.023421259	0.996331174
jmjd4	tbx5b	-1.494568627	6.589315304	5.136128259	0.023432852	0.996331174
cnpy1	tbx5b	3.823710113	4.725069568	5.131283589	0.023498344	0.996331174
stk24b	tbx5b	-2.328828528	5.476894406	5.114338587	0.02372891	0.996331174
anxa13	tbx5b	-1.826478284	5.52814494	5.099174834	0.023937228	0.996331174
nudt19	tbx5b	-3.575390928	4.585592874	5.097860207	0.023955378	0.996331174
wdr43	tbx5b	1.252789026	6.848404797	5.090950041	0.024051012	0.996331174
tradd	tbx5b	-3.552936219	4.476529827	5.05795571	0.024513137	0.996331174
galcb	tbx5b	-2.684936361	4.584056714	5.056890334	0.024528211	0.996331174
golga2	tbx5b	-2.16820132	5.233773807	5.051566202	0.024603689	0.996331174
cecr5	tbx5b	-2.688280393	5.089024559	5.047121823	0.02466688	0.996331174
pgrmc1	tbx5b	-1.847371882	5.528703334	5.04168148	0.02474446	0.996331174
cdh6	tbx5b	-1.584984826	5.868524423	5.039358141	0.024777669	0.996331174
vsg1	tbx5b	-1.901275067	5.782637342	5.027013894	0.024954889	0.996331174
micu1	tbx5b	-2.685001542	5.073691805	5.026179157	0.02496692	0.996331174
si:ch211-107n13.1	tbx5b	2.365540206	5.197887934	5.006429784	0.025253336	0.996331174
mtg1	tbx5b	2.696168413	4.621244888	4.996959965	0.025391881	0.996331174
lrwd1	tbx5b	-3.597053133	4.798599311	4.978820506	0.025659472	0.996331174
uhmk1	tbx5b	2.982975479	4.821198215	4.978055923	0.025670815	0.996331174
cox4i2	tbx5b	-2.721789482	4.68822763	4.975337805	0.025711182	0.996331174
fam96b	tbx5b	-3.569881312	4.852723737	4.973123437	0.025744117	0.996331174
fbxl14a	tbx5b	-2.137834539	5.125600216	4.963415208	0.025889028	0.996331174

Continued on following page

Table B.6: continued from previous page

gene	MO	logFC	logCPM	LR	p value	FDR
npffr1l2	tbx5b	-3.591791948	4.565282726	4.956864023	0.025987294	0.996331174
timm8a	tbx5b	-3.549775288	4.663865005	4.953695633	0.026034958	0.996331174
fundc1	tbx5b	-2.645997435	5.0712276	4.936757958	0.026291306	0.996331174
si:dkey-110k5.6	tbx5b	-2.228084222	4.900933983	4.932502788	0.026356119	0.996331174
ndufs1	tbx5b	-1.295900725	6.538917873	4.929191251	0.026406673	0.996331174
jam2a	tbx5b	-2.365308381	4.978986742	4.927938144	0.02642583	0.996331174
mia	tbx5b	2.678156679	4.992653228	4.924735469	0.026474855	0.996331174
camk2n1a	tbx5b	-3.617440328	4.667763904	4.920288909	0.026543078	0.996331174
eif4enif1	tbx5b	2.37731548	4.852528931	4.913959086	0.026640511	0.996331174
fundc2	tbx5b	2.040201616	5.342086361	4.911441426	0.026679368	0.996331174
tubg1	tbx5b	2.757112034	4.92026692	4.908009599	0.026732429	0.996331174
osgep	tbx5b	-1.521566777	5.952618615	4.903152905	0.026807708	0.996331174
rras2	tbx5b	-2.339172059	5.10872785	4.901664848	0.026830817	0.996331174
si:dkey-67c22.2	tbx5b	-1.459569943	6.072957026	4.897394669	0.026897246	0.996331174
basp1	tbx5b	-3.599679979	4.591415463	4.879104517	0.027183718	0.996331174
LOC558044	tbx5b	-1.442779449	7.201137088	4.868091527	0.02735774	0.996331174
apeh	tbx5b	-2.732896646	4.851464965	4.864142919	0.027420416	0.996331174
pdcd2	tbx5b	-2.678475372	5.001758759	4.860078902	0.027485079	0.996331174
ppp2r5cb	tbx5b	3.550412184	4.523592859	4.857695787	0.027523071	0.996331174
lrrc17	tbx5b	-2.663212812	4.946860935	4.811841812	0.02826482	0.996331174
cdo1	tbx5b	-1.467016249	6.348661511	4.79747127	0.028501541	0.996331174
tsen54	tbx5b	3.541296662	4.519906744	4.794178813	0.028556066	0.996331174
uba5	tbx5b	2.037316717	5.512376454	4.781913211	0.028760151	0.996331174
snx17	tbx5b	3.508975978	4.430995829	4.770777545	0.028946749	0.996331174
zgc:171422	tbx5b	3.542864535	4.479947379	4.768458385	0.02898577	0.996331174
gmeb1	tbx5b	3.543369688	4.568212239	4.760044865	0.029127789	0.996331174
zgc:153256	tbx5b	2.750047472	4.587009924	4.757168926	0.0291765	0.996331174
adrbk2	tbx5b	3.545483967	4.525768529	4.724139575	0.02974206	0.996331174
gtf2h4	tbx5b	3.522557936	4.60540175	4.718032661	0.029847874	0.996331174
grnb	tbx5b	3.531323428	4.68390845	4.713086873	0.029933856	0.996331174
ston2	tbx5b	3.509718918	4.523582853	4.71245755	0.029944815	0.996331174
drc1	tbx5b	-1.530374328	5.905425944	4.711870577	0.02995504	0.996331174
srp68	tbx5b	1.422700617	6.336545925	4.709817132	0.029990842	0.996331174
cyp2x12	tbx5b	3.580268436	4.647847123	4.706303	0.030052213	0.996331174
lsm12b	tbx5b	-1.463234219	6.273671023	4.684279205	0.030439832	0.996331174
ripk4	tbx5b	3.547903518	4.683481924	4.681627133	0.030486858	0.996331174
zgc:162879	tbx5b	-1.374260801	6.338130663	4.679296901	0.030528241	0.996331174
mboat1	tbx5b	3.565386387	4.664941684	4.670358939	0.030687513	0.996331174
sgut1	tbx5b	-2.225622287	5.195516783	4.65920759	0.030887443	0.996331174
slc30a9	tbx5b	2.371958458	4.871873295	4.649669267	0.031059531	0.996331174
si:ch211-255a21.1	tbx5b	-2.090439507	5.074138159	4.636665868	0.031295748	0.996331174
cltcb	tbx5b	1.429440228	6.200614687	4.636157005	0.031305029	0.996331174
cpt1b	tbx5b	3.489341969	4.865959534	4.612481107	0.031740079	0.996331174
gdpd1	tbx5b	-2.047463748	5.414145042	4.60885279	0.031807305	0.996331174
gfod2	tbx5b	3.570567507	4.780940816	4.597404973	0.032020389	0.996331174
senp3a	tbx5b	-1.401624009	6.1163736	4.587480907	0.032206316	0.996331174
cxxc1b	tbx5b	-2.418514689	4.857311236	4.575946029	0.032423838	0.996331174
pcm1	tbx5b	-1.437100824	6.334292596	4.573066295	0.032478382	0.996331174
si:dkeyp-117h8.4	tbx5b	-1.442482363	6.010553782	4.556346643	0.032796963	0.996331174
prdm8	tbx5b	3.488637438	4.625576282	4.55558683	0.032811518	0.996331174
aste1	tbx5b	-2.722683633	4.978711455	4.551661347	0.032886822	0.996331174

Continued on following page

Table B.6: continued from previous page

gene	MO	logFC	logCPM	LR	p value	FDR
zgc:153901	tbx5b	-1.174505592	6.598050121	4.545115528	0.033012794	0.996331174
zgc:123078	tbx5b	-2.648406724	4.547010504	4.519521737	0.033510198	0.996331174
kdm5ba	tbx5b	-1.507489654	5.733086421	4.517606151	0.03354774	0.996331174
bmpr1ba	tbx5b	1.328846588	6.195211423	4.490664626	0.034080426	0.996331174
si:dkey-204l11.1	tbx5b	-2.705407323	4.547841348	4.487037751	0.034152808	0.996331174
ccdc102a	tbx5b	-2.692717578	4.895299688	4.485419755	0.034185151	0.996331174
lepr	tbx5b	2.337934374	5.235183413	4.47154199	0.034463876	0.996331174
si:dkeyp-104h9.5	tbx5b	-2.555514637	4.804419678	4.467767272	0.034540098	0.996331174
prpf40a	tbx5b	-1.132866307	6.821166169	4.464921535	0.034597679	0.996331174
brd7	tbx5b	-1.617966418	5.898261294	4.463243443	0.03463168	0.996331174
zgc:66479	tbx5b	-2.183119712	5.713034031	4.459448921	0.034708693	0.996331174
nefmb	tbx5b	-2.167308585	5.660976224	4.455301953	0.034793065	0.996331174
cab39l1	tbx5b	-1.766984838	5.63759461	4.455288252	0.034793344	0.996331174
rcn3	tbx5b	-1.080744789	7.476353077	4.44132875	0.035078936	0.996331174
anapc16	tbx5b	-2.203974587	5.051743696	4.4294112	0.035324692	0.996331174
pdzk1ip1	tbx5b	-1.100752546	7.10984451	4.426103126	0.035393228	0.996331174
sh3bgr	tbx5b	-2.703581387	4.9393823	4.421008077	0.035499058	0.996331174
ccdc65	tbx5b	-2.105070272	5.25127144	4.404995577	0.035833818	0.996331174
tsn	tbx5b	2.041948349	5.183645112	4.398959597	0.035960862	0.996331174
cpsf3l	tbx5b	2.352509422	4.762315942	4.367220603	0.036636703	0.996331174
clcn7	tbx5b	-2.250999786	5.000822771	4.324292203	0.037572037	0.996331174
lrsam1	tbx5b	-0.932498788	8.487061212	4.32301617	0.037600219	0.996331174
cflara	tbx5b	-1.431928657	6.165449313	4.318903169	0.037691209	0.996331174
camk2a	tbx5b	-2.498799112	5.174654165	4.302401817	0.038058588	0.996331174
tmem19	tbx5b	2.202275108	4.926381684	4.299456536	0.038124554	0.996331174
adam10b	tbx5b	2.253043245	4.759654175	4.296865998	0.038182674	0.996331174
wdr46	tbx5b	-1.204798957	6.499716408	4.267600586	0.038845746	0.996331174
tsku	tbx5b	-2.474467906	4.565203854	4.264618461	0.038913987	0.996331174
ilk	tbx5b	-1.836352553	5.45892318	4.239237848	0.039499895	0.996331174
dusp4	tbx5b	2.56743407	4.738307374	4.233300955	0.039638279	0.996331174
ergic2	tbx5b	-2.055415152	5.073912251	4.232169315	0.039664714	0.996331174
gnrhr4	tbx5b	-2.483557441	4.569195638	4.230366725	0.03970686	0.996331174
glyctk	tbx5b	-1.922852853	6.409895081	4.206419817	0.040271248	0.996331174
zgc:174877	tbx5b	2.573951077	4.704419075	4.204003814	0.040328655	0.996331174
acer3	tbx5b	-2.514112943	4.57050573	4.192839819	0.040595042	0.996331174
sgk1	tbx5b	2.643546516	4.782206532	4.188711687	0.040694011	0.996331174
uox	tbx5b	-2.054623812	4.880507802	4.182983354	0.040831764	0.996331174
zgc:153631	tbx5b	-2.187691516	4.718681681	4.178002101	0.04095195	0.996331174
twist1a	tbx5b	1.414101368	6.016373661	4.163001884	0.041316118	0.996331174
shcbp1	tbx5b	-1.776867891	5.194383684	4.156772558	0.041468349	0.996331174
vps18	tbx5b	-2.506949074	4.707253151	4.150930889	0.041611642	0.996331174
esd	tbx5b	-1.964435243	5.234955719	4.124857932	0.042257569	0.996331174
lmo7a	tbx5b	-1.856773829	5.343985618	4.113777495	0.042535256	0.996331174
spast	tbx5b	2.32340319	4.815669088	4.105560128	0.042742431	0.996331174
rrp36	tbx5b	-1.486304493	5.674472776	4.103658487	0.042790526	0.996331174
chtopa	tbx5b	-1.052488385	7.189492477	4.075207082	0.043516932	0.996331174
auh	tbx5b	-2.49536953	4.67031143	4.074164404	0.043543798	0.996331174
lap3	tbx5b	-2.517693525	4.851572438	4.073883399	0.043551041	0.996331174
st3gal7	tbx5b	-2.485001339	4.710036739	4.0708502	0.043629309	0.996331174
polr2k	tbx5b	2.177694031	4.874197774	4.056537043	0.044000645	0.996331174
golim4a	tbx5b	-2.531231104	4.922931821	4.045556562	0.044287773	0.996331174

Continued on following page

Table B.6: continued from previous page

gene	MO	logFC	logCPM	LR	p value	FDR
farsb	tbx5b	-1.615371002	5.450669393	4.036427344	0.044527993	0.996331174
si:ch211-42i9.8	tbx5b	-2.177428433	4.722607022	4.019145834	0.044986492	0.996331174
c6	tbx5b	-1.279961822	6.61940853	4.017202951	0.045038349	0.996331174
tmx1	tbx5b	-3.201792986	4.543955823	4.016898044	0.045046493	0.996331174
ppp6c	tbx5b	-1.576416534	5.63597482	4.008866569	0.045261568	0.996331174
timm10b	tbx5b	-3.20172566	4.565159412	4.005766687	0.04534487	0.996331174
h2afy	tbx5b	-3.225247336	4.645119747	4.002350654	0.045436853	0.996331174
phtf2	tbx5b	-3.210127413	4.434281689	3.996088259	0.045605992	0.996331174
rad51ap1	tbx5b	-3.220970344	4.567862372	3.986568161	0.045864389	0.996331174
traf1	tbx5b	-3.221015663	4.62512362	3.985437009	0.045895194	0.996331174
atp1a1a.4	tbx5b	-1.5014625	5.968477745	3.982561999	0.045973587	0.996331174
dpydb	tbx5b	-3.226840545	4.523445629	3.971749281	0.046269682	0.996331174
tgm2b	tbx5b	-3.201467086	4.518935338	3.962522561	0.046523935	0.996331174
rhbdl2	tbx5b	-3.22731731	4.672205652	3.96241644	0.046526868	0.996331174
rfwd2	tbx5b	2.554268975	4.798000242	3.961074384	0.046563975	0.996331174
polr3h	tbx5b	1.943470454	5.258161804	3.960116682	0.046590474	0.996331174
cant1a	tbx5b	-2.083639887	5.188857639	3.957337574	0.04666746	0.996331174
praf2	tbx5b	-2.233312729	4.836282728	3.952866549	0.046791596	0.996331174
taf9	tbx5b	-1.935119426	5.329123737	3.945145168	0.047006798	0.996331174
alox5ap	tbx5b	-2.482819096	4.761706776	3.938587545	0.047190384	0.996331174
prkar2aa	tbx5b	-1.441302732	5.905831197	3.935663328	0.047272494	0.996331174
dgcr2	tbx5b	-3.186730197	4.476890345	3.926044613	0.047543644	0.996331174
mogs	tbx5b	-3.22922868	4.50547781	3.924156927	0.04759705	0.996331174
si:ch73-80e1.2	tbx5b	-3.211254634	4.543610455	3.923632155	0.047611908	0.996331174
bmpr1ab	tbx5b	-1.098515878	8.35712876	3.920549283	0.047699293	0.996331174
si:ch211-284b7.3	tbx5b	1.866229959	5.149653966	3.920480071	0.047701257	0.996331174
sdcbp2	tbx5b	-1.219894012	6.254872646	3.915296559	0.047848573	0.996331174
ift52	tbx5b	-2.497861502	4.681160495	3.914719373	0.047865006	0.996331174
ano10a	tbx5b	-2.493664178	4.83206757	3.912315574	0.04793351	0.996331174
phlda2	tbx5b	-3.201167095	4.742946447	3.911335596	0.047961467	0.996331174
aox5	tbx5b	-2.479134201	6.093771572	3.905487512	0.048128662	0.996331174
nol10	tbx5b	-1.46622684	5.80159557	3.90150255	0.048242943	0.996331174
ppp5c	tbx5b	-1.216148612	6.397812319	3.901300461	0.048248746	0.996331174
fntb	tbx5b	-1.959677847	5.044628316	3.896576001	0.048384623	0.996331174
tmf1	tbx5b	-2.168741891	4.961840253	3.879968045	0.048865487	0.996331174
braf	tbx5b	-1.780153885	5.397997539	3.8791725	0.048888648	0.996331174
nck2a	tbx5b	-3.211927973	4.587083212	3.878595826	0.048905443	0.996331174
chtf18	tbx5b	-1.658893297	5.240040548	3.865359354	0.049292637	0.996331174
plxnb2a	tbx5b	-2.228071111	4.869662359	3.865287199	0.049294756	0.996331174
snupn	tbx5b	2.08531659	5.161110989	3.863759908	0.049339643	0.996331174
pgm3	tbx5b	-3.206409671	4.88529402	3.863653466	0.049342773	0.996331174
eno1a	tbx5b	-2.054195562	5.408801505	3.860208268	0.04944419	0.996331174
trpv4	tbx5b	-3.206444978	4.608662156	3.855510021	0.04958285	0.996331174
ldlrad3	tbx5b	-2.020901089	5.001126169	3.849250602	0.049768223	0.996331174
tmem182a	tbx5b	-3.219754947	4.855396644	3.848866665	0.049779617	0.996331174
efhc1	tbx5b	-3.188926986	4.626664775	3.846043119	0.049863496	0.996331174
ikbkg	tbx5b	-2.450800868	4.827962203	3.84476541	0.049901502	0.996331174
atp6v1f	tbx5b	1.782206514	5.517399151	3.844538942	0.049908242	0.996331174
fbxo9	tbx5b	-1.73310206	5.435825852	3.844439405	0.049911204	0.996331174
cdr2l	tbx5b	-2.211157887	4.972716391	3.843057361	0.049952356	0.996331174
mpnd	double	2.61971738	4.760991409	4.31255904	0.037832011	0.877133387

Continued on following page

Table B.6: continued from previous page

gene	MO	logFC	logCPM	LR	p value	FDR
spon1b	double	-2.16591557	4.949442877	4.299982603	0.038112763	0.879851664
tmem88b	double	1.373741591	6.402757867	4.296665324	0.03818718	0.879851664
aldh6a1	double	-1.647689502	5.76685351	4.28955832	0.038347126	0.880792997
ska2	double	2.561962096	4.811671563	4.272660405	0.038730247	0.886838726
f10	double	-2.160408474	4.848935066	4.266552074	0.038869725	0.887285457
cdon	double	-1.477967614	5.829942176	4.249099753	0.039271143	0.893690377
zgc:113208	double	-2.655237911	4.665555165	4.225654029	0.039817271	0.894738611
dpm3	double	2.745437782	4.794917842	4.225286089	0.039825905	0.894738611
hbs1l	double	-1.647091339	5.634123542	4.22359376	0.039865641	0.894738611
melk	double	-1.815170816	5.546148568	4.218743825	0.039979748	0.894738611
plekha8	double	-2.645599765	4.58852565	4.211665591	0.040146898	0.894738611
notch3	double	-1.630489178	5.902159647	4.208604394	0.040219414	0.894738611
ptp4a2b	double	1.338132542	6.392032426	4.20623193	0.04027571	0.894738611
zic4	double	-2.613127573	4.800637914	4.203696044	0.040335974	0.894738611
zcchc24	double	-2.184235076	5.20656785	4.200754864	0.040405989	0.894738611
rap2c	double	-2.165581612	5.038355354	4.192110998	0.040612496	0.89662693
cmah	double	-2.675071879	4.908513382	4.178959302	0.040928826	0.897775652
stt3b	double	-1.800330734	5.538153313	4.173172963	0.04106882	0.897775652
abca5	double	-2.675963888	4.671962005	4.117550618	0.042440483	0.897775652
hectd3	double	-1.30057748	6.282542775	4.113751475	0.042535911	0.897775652
blf	double	-1.45496777	5.987051432	4.111312056	0.042597303	0.897775652
xpo4	double	-1.644119517	5.704388389	4.093646544	0.04304468	0.897775652
e2f7	double	-2.689271765	4.817983633	4.087745587	0.04319522	0.897775652
tmem2	double	-1.921241967	5.524169936	4.077467008	0.043458761	0.897775652
ptgr1	double	-1.583752503	5.733907447	4.055453438	0.044028893	0.897775652
mbd3b	double	-1.504303863	5.94657322	4.04814976	0.044219786	0.897775652
ppfia2	double	-2.627783448	4.836725038	4.04592664	0.044278064	0.897775652
itga3b	double	-2.104046	5.154387837	4.028656163	0.04473356	0.897775652
taf13	double	2.392681643	5.345845071	4.024820112	0.044835401	0.897775652
cmtm6	double	-2.454173907	4.849142373	4.018679514	0.044998933	0.897775652
lyrm1	double	2.07348747	5.59531868	4.014994097	0.045097381	0.897775652
sv2c	double	-2.476402097	5.077598771	4.01185809	0.045181332	0.897775652
tspo	double	-1.619555033	5.312152849	4.00794285	0.045286374	0.897775652
slc35c1	double	2.275802816	4.72083135	4.007345192	0.045302431	0.897775652
zgc:92744	double	-1.180964034	6.369763587	4.002526849	0.045432104	0.897775652
cirh1a	double	-1.636639995	5.48128112	4.00103547	0.04547232	0.897775652
acss1	double	-1.891566395	5.214619994	3.994104233	0.045659717	0.897775652
metrnl	double	-2.462751885	4.809417863	3.960050362	0.046592309	0.897775652
myoc	double	-2.475998965	4.847597792	3.955627987	0.046714885	0.897775652
rbfox1l	double	-1.200467763	6.386349397	3.950451717	0.046858788	0.897775652
igf2bp3	double	-1.645959901	5.718548869	3.950094638	0.046868732	0.897775652
stc1l	double	-2.440332076	4.567182733	3.949492546	0.046885504	0.897775652
foxc1b	double	2.575845016	4.725590236	3.948901364	0.046901979	0.897775652
snf8	double	-2.427706399	4.560567999	3.944540278	0.047023701	0.897775652
zfp36l1b	double	-1.753446411	5.386544693	3.931149527	0.047399534	0.897775652
zgc:91910	double	-1.463789318	6.034237616	3.924792489	0.047579062	0.897775652
ube2b	double	-3.203595805	4.665886607	3.92288927	0.04763295	0.897775652
rhbdl2	double	-2.479560115	4.672205652	3.922768663	0.047636367	0.897775652
ugt2a5	double	-3.220519064	4.478356327	3.921289636	0.047678292	0.897775652
ino80	double	2.253812392	5.058434922	3.921172697	0.047681608	0.897775652
hsp90aa1.2	double	-1.16514875	7.46962896	3.920281936	0.047706879	0.897775652

Continued on following page

Table B.6: continued from previous page

gene	MO	logFC	logCPM	LR	p value	FDR
rab3da	double	-3.220957109	4.458734325	3.913241213	0.047907119	0.897775652
tmem59l	double	2.566220822	4.588654737	3.903907031	0.048173953	0.897775652
sptlc3	double	-3.204431901	4.543328438	3.90267033	0.048209424	0.897775652
si:ch211-137a8.2	double	2.085143061	4.99920036	3.901315743	0.048248307	0.897775652
ttc9b	double	-3.204508699	4.388288653	3.892399862	0.048505066	0.897775652
col2a1b	double	-1.00988475	7.108060658	3.890770592	0.048552142	0.897775652
ppil3	double	-3.203770192	4.646941051	3.890660731	0.048555318	0.897775652
bag5	double	-3.220520713	4.479450488	3.887764128	0.048639136	0.897775652
parp2	double	-1.398035996	5.874820982	3.886302968	0.048681475	0.897775652
nostrin	double	-3.221822638	4.500751184	3.879680664	0.048873852	0.897775652
zbed4	double	-2.469092027	4.92006626	3.877679944	0.048932131	0.897775652
psen1	double	-2.032671627	5.392360574	3.874086282	0.049036995	0.897775652
mbtps2	double	-3.204645227	4.43478657	3.873936419	0.049041373	0.897775652
spred1	double	-2.197880877	4.853336621	3.872357237	0.049087533	0.897775652
pqbp1	double	-0.990985404	7.311064586	3.871945449	0.049099577	0.897775652
epha7	double	-3.223296553	4.629981556	3.869077191	0.049183557	0.897775652
tmem177	double	-2.434532287	4.604816694	3.868858004	0.049189981	0.897775652
ephb4a	double	-3.223377171	4.643311648	3.867518783	0.049229249	0.897775652
stab2	double	1.678081758	5.366441222	3.86091867	0.04942326	0.897775652
hells	double	-1.241396022	6.494720943	3.852231215	0.049679861	0.897775652
itpa	double	-3.203150561	4.64653994	3.851298747	0.049707486	0.897775652
pxk	double	-3.18755364	4.455247958	3.848846604	0.049780212	0.897775652
frem3	double	-1.560217956	5.949448959	3.848117039	0.049801871	0.897775652
pla2g6	double	-2.440228876	4.860676981	3.847176053	0.049829822	0.897775652
mespab	double	-2.699636005	4.855328957	3.845818215	0.049870184	0.897775652
nptxrb	double	-3.204852629	4.520337561	3.84537416	0.049883391	0.897775652
prickle2b	double	-3.224519491	4.543927807	3.845165601	0.049889595	0.897775652
dpysl5a	double	-3.204875431	4.937809516	3.842195355	0.049978042	0.897775652
rad17	double	3.00741865	5.442502923	6.463852296	0.011009072	0.940346171
slc40a1	double	-3.95789011	4.896683613	6.390954596	0.011470333	0.940346171
mob3a	double	2.954650607	5.058951185	6.386686692	0.011497945	0.940346171
vox	double	-2.978997013	4.702296535	6.37206123	0.011593086	0.940346171
crfb12	double	2.949252453	5.084791815	6.338646114	0.011813502	0.940346171
aktip	double	2.105566574	5.67426447	6.249939239	0.012419757	0.940346171
fgf2	double	-1.741675338	6.014102306	6.248246269	0.012431633	0.940346171
yipf1	double	3.807572037	4.410521519	6.229991276	0.012560436	0.940346171
itpa	double	3.836979013	4.64653994	6.215362962	0.012664638	0.940346171
ggcta	double	1.459432594	7.486195805	6.20333944	0.012750951	0.940346171
lrrc57	double	2.998051473	5.004950001	6.197121201	0.012795827	0.940346171
sirt2	double	2.936442831	4.911950025	6.182659367	0.012900824	0.940346171
rras	double	1.924997957	6.177407835	6.174804867	0.01295822	0.940346171
mmp13a	double	3.161354346	4.909080959	6.161633136	0.013055062	0.940346171
cul1a	double	1.77590304	5.467389431	6.125987423	0.013320886	0.940346171
cishb	double	1.577677598	6.29557159	6.124256254	0.013333937	0.940346171
msh6	double	1.37111717	7.008375541	6.119738686	0.013368056	0.940346171
galnt2	double	-2.456980319	5.400097553	6.088243533	0.013608431	0.940346171
rnf175	double	3.84157854	4.688988015	6.085804848	0.013627227	0.940346171
irx5a	double	-3.770306351	5.328253702	6.083573761	0.013644447	0.940346171
cxadr	double	3.841679803	4.800546582	6.082836281	0.013650144	0.940346171
ndufs5	double	-1.888074391	5.955556689	6.041082115	0.013976715	0.940346171
mob4	double	-1.334719748	6.951341009	6.032916891	0.014041511	0.940346171

Continued on following page

Table B.6: continued from previous page

gene	MO	logFC	logCPM	LR	p value	FDR
zgc:65894	double	3.790905142	4.522806918	6.028407247	0.01407743	0.940346171
ebag9	double	-3.780663993	4.7628704	6.028303842	0.014078255	0.940346171
ppm1ba	double	3.843785295	4.589553895	6.01990742	0.014145389	0.940346171
tbc1d25	double	2.576488757	4.991098521	6.017065778	0.014168184	0.940346171
knstrn	double	3.779806631	4.678852168	6.008449243	0.014237535	0.940346171
meis2b	double	2.181389385	5.29691422	6.006441116	0.014253747	0.940346171
znrf3	double	-3.781064802	4.542070021	5.999009524	0.014313912	0.940346171
zgc:66101	double	-2.256178268	5.415238735	5.998486802	0.014318154	0.940346171
kif1b	double	3.875140612	4.670262068	5.9903865	0.01438405	0.940346171
dnajb1b	double	1.754942177	6.077665852	5.963928601	0.01460147	0.940346171
dyrk1b	double	1.988389795	5.82090899	5.947013617	0.014742241	0.940346171
smtnl1	double	2.370866482	6.247221469	5.943021938	0.014775664	0.940346171
edem1	double	2.795346172	5.060260609	5.915944075	0.01500446	0.940346171
tmem176l.4	double	2.78731866	5.275735551	5.856073742	0.015523384	0.940346171
gins1	double	0.920125948	9.354773957	5.84780162	0.015596523	0.940346171
elovl6l	double	3.840437595	4.56669026	5.847215907	0.015601715	0.940346171
rbm19	double	2.103697373	5.498274908	5.826656787	0.015785094	0.940346171
lats2	double	2.550204042	5.337373886	5.826515748	0.01578636	0.940346171
anapc5	double	-3.801552963	4.685015126	5.793941332	0.016081496	0.940346171
mrps28	double	-3.737153645	4.860808643	5.790372908	0.016114171	0.940346171
abl2	double	-2.861908338	4.703365075	5.788253813	0.016133607	0.940346171
pcsk5b	double	3.820283095	4.704246409	5.755256894	0.016439392	0.940346171
sox7	double	-3.739415665	4.602866262	5.72327965	0.016741431	0.940346171
cratb	double	2.779572523	4.994011493	5.719833126	0.016774325	0.940346171
zgc:77056	double	3.719265004	4.621364215	5.714295797	0.016827313	0.940346171
fbxw5	double	1.730857546	6.086096536	5.714092098	0.016829265	0.940346171
psmd5	double	3.781652533	4.749215162	5.713180799	0.016838003	0.940346171
diablob	double	3.735148153	4.861328869	5.671251071	0.017245153	0.940346171
oc90	double	1.033298841	8.369836398	5.661984912	0.017336492	0.940346171
trim35-28	double	-3.762512279	4.568001921	5.660520292	0.017350975	0.940346171
zgc:77375	double	2.796451775	4.522279443	5.639150889	0.017563711	0.940346171
dcun1d2b	double	-2.824264706	5.058288331	5.626158358	0.017694368	0.940346171
stk24b	double	-2.39296971	5.476894406	5.597149413	0.017989725	0.940346171
cx28.8	double	3.079492656	4.894775702	5.585043311	0.018114485	0.940346171
slc5a2	double	1.671016335	6.438113737	5.570368987	0.018266911	0.940346171
tagln	double	-3.785332359	4.818422053	5.565257228	0.018320319	0.940346171
zgc:66472	double	2.798542799	5.160323591	5.524802573	0.018748719	0.940346171
sord	double	-2.218330666	5.479226722	5.513895086	0.018865987	0.940346171
slc25a33	double	2.424090948	5.083420661	5.485250782	0.019177569	0.940346171
heatr1	double	2.199440577	5.824127903	5.468886941	0.01935795	0.940346171
mis18bp1	double	2.793159724	5.071222197	5.461630359	0.019438501	0.940346171
nos2b	double	2.910684511	4.824548104	5.448021146	0.019590505	0.940346171
mfsd12a	double	1.848809787	5.870544602	5.444170043	0.019633741	0.940346171
zgc:111986	double	1.909397737	5.651911329	5.435495675	0.01973149	0.940346171
etfa	double	1.705175986	6.022180547	5.428165273	0.019814486	0.940346171
rbm39b	double	1.611247611	6.064574223	5.425650482	0.019843042	0.940346171
si:dkey-72l14.4	double	2.832476944	4.688717119	5.41495167	0.019965006	0.940346171
slc25a47b	double	1.751745729	5.956020091	5.400049915	0.020136176	0.940346171
si:dkey-284p5.3	double	-2.339972484	5.797749962	5.37014677	0.020484254	0.940346171
cald1a	double	2.467619514	5.31825972	5.305801292	0.021254521	0.940346171
flrt3	double	1.428550863	6.435559649	5.30573985	0.02125527	0.940346171

Continued on following page

Table B.6: continued from previous page

gene	MO	logFC	logCPM	LR	p value	FDR
zgc:55870	double	1.538154722	6.242372518	5.289072489	0.021459647	0.940346171
traf4a	double	2.266941993	5.652883393	5.246992755	0.021984734	0.940346171
lims1	double	2.874311957	4.953869773	5.243030251	0.022034861	0.940346171
zgc:174160	double	1.559395798	6.549658754	5.229904308	0.022201754	0.940346171
zgc:162613	double	1.307939036	6.833370609	5.229176134	0.022211051	0.940346171
wu:fa19b12	double	2.804019238	4.648270432	5.221022704	0.022315424	0.940346171
rpz4	double	1.632871577	6.538039818	5.207685115	0.022487256	0.940346171
stab2	double	2.13503061	5.366441222	5.174614044	0.022919263	0.940346171
frem1b	double	2.133794573	5.310326786	5.164525486	0.023052754	0.940346171
pura	double	3.517496032	4.542923456	5.159805778	0.023115482	0.940346171
tdp2b	double	3.517745554	4.585143692	5.151826823	0.02322193	0.940346171
gabrr3a	double	3.537296119	5.05850211	5.138988247	0.023394278	0.940346171
slc30a9	double	2.476071789	4.871873295	5.137054275	0.023420355	0.940346171
snrpb2	double	2.008799834	5.544660687	5.124061135	0.023596332	0.940346171
glt8d2	double	2.765232493	5.26981564	5.109951884	0.02378898	0.940346171
rps6kal	double	2.680244527	5.105626922	5.098148346	0.023951398	0.940346171
golga5	double	2.128045558	5.48631871	5.077977174	0.024231625	0.940346171
zgc:193812	double	3.491714693	4.517972651	5.072626346	0.02430653	0.940346171
ppp2r3c	double	0.949682134	8.627889016	5.05969395	0.024488562	0.940346171
tyw1	double	1.458789071	6.224384603	5.042751149	0.024729187	0.940346171
si:ch211-199g17.1	double	3.574349891	4.708950871	5.0378828	0.024798781	0.940346171
bbs2	double	3.534699902	4.480348453	5.029664457	0.024916725	0.940346171
tmem238	double	3.49104895	4.778775502	5.020125799	0.025054349	0.940346171
atp1b1b	double	3.53538963	4.932744251	5.014805332	0.025131455	0.940346171
tpst1l	double	3.522054856	4.52215047	5.007391224	0.025239314	0.940346171
hnrnpr	double	-2.681913602	4.82990332	5.00008831	0.025346025	0.940346171
c1ql3b	double	3.509553238	4.630233886	4.999254577	0.025358238	0.940346171
thumpd3	double	2.299396885	5.221602062	4.971483904	0.025768531	0.940346171
pcolcea	double	3.502174397	4.831660806	4.948988521	0.026105938	0.940346171
zgc:56197	double	3.523988209	4.68590915	4.938195141	0.026269454	0.940346171
si:dkey-222f8.3	double	1.502892487	6.986249068	4.927699491	0.02642948	0.940346171
rab11ba	double	1.781972286	5.66436844	4.926608947	0.026446165	0.940346171
phactr4b	double	3.510403507	4.497470449	4.923927417	0.026487239	0.940346171
rnasekb	double	1.782248898	5.509408942	4.915142631	0.026622265	0.940346171
ints7	double	-3.465078935	4.455312342	4.903148033	0.026807783	0.940346171
fcho2	double	2.687925317	5.312281656	4.898154494	0.026885413	0.940346171
pygma	double	1.602728133	6.255678535	4.896760294	0.026907129	0.940346171
nfe2	double	3.470663666	4.562122727	4.896545463	0.026910477	0.940346171
pphln1	double	-1.298797349	6.351773371	4.895476046	0.026927149	0.940346171
dcun1d2a	double	-3.491756415	4.742978396	4.892277391	0.026977078	0.940346171
dpp9	double	1.993970222	5.694919928	4.889344902	0.027022938	0.940346171
hapln1a	double	3.551141246	4.786048589	4.883126424	0.027120454	0.940346171
prmt3	double	-2.773178124	4.918152081	4.882890067	0.027124167	0.940346171
nudt18	double	-3.451366366	4.964922835	4.87968619	0.027174559	0.940346171
zgc:55262	double	-3.484177105	4.501109995	4.871684809	0.027300834	0.940346171
xpr1b	double	1.966604051	5.084288621	4.85752205	0.027525843	0.940346171
hbl4	double	-3.460760623	5.353637758	4.849186342	0.027659177	0.940346171
gpc1b	double	2.829078201	4.650360027	4.84558606	0.027716972	0.940346171
bicc2	double	2.707884079	4.836122929	4.842390474	0.027768377	0.940346171
bhlha15	double	3.48886039	4.542145118	4.836652461	0.027860928	0.940346171
uros	double	3.456990046	4.682305621	4.830111785	0.027966817	0.940346171

Continued on following page

Table B.6: continued from previous page

gene	MO	logFC	logCPM	LR	p value	FDR
mark3a	double	2.316604933	4.93631337	4.827742185	0.028005283	0.940346171
dtx1	double	-3.498818673	4.62774831	4.815135723	0.02821085	0.940346171
zgc:171480	double	2.600777451	5.021590847	4.811238896	0.028274711	0.940346171
slc35e1	double	-2.35651702	4.994467634	4.81054713	0.028286063	0.940346171
upf1	double	-2.003096125	5.343048547	4.806231104	0.028356999	0.940346171
ptrh1	double	3.527561655	4.778801533	4.802242703	0.028422715	0.940346171
bmpr1ba	double	1.359114052	6.195211423	4.786447712	0.028684526	0.940346171
znf644a	double	2.637561727	4.978906902	4.78225886	0.028754379	0.940346171
blvrb	double	-3.494820486	4.935576027	4.781462488	0.028767679	0.940346171
si:ch211-156j16.1	double	1.864770818	5.864684009	4.772200892	0.028922829	0.940346171
fgfr2	double	1.726103862	5.548957135	4.772171479	0.028923323	0.940346171
zgc:158482	double	-3.486053583	4.833017356	4.763356371	0.029071805	0.940346171
cln3	double	-3.486094754	4.501876626	4.760901325	0.029113299	0.940346171
fam96b	double	-3.486097458	4.852723737	4.760739908	0.029116029	0.940346171
cnn2	double	1.352443406	6.492572796	4.756201602	0.029192904	0.940346171
aldh18a1	double	-3.495593561	4.623517963	4.752122249	0.029262184	0.940346171
oxct1a	double	1.91619063	5.494546165	4.751058223	0.029280283	0.940346171
efhc1	double	-3.481370241	4.626664775	4.749555678	0.02930586	0.940346171
gab1	double	2.628238772	4.79313498	4.742097714	0.029433161	0.940346171
tceb1b	double	2.242689997	5.200772126	4.739744274	0.029473452	0.940346171
camk2a	double	-2.575835271	5.174654165	4.724990762	0.029727343	0.940346171
zdhhc16b	double	0.892133489	9.073401159	4.724964559	0.029727796	0.940346171
yme1l1b	double	1.153633306	7.396158344	4.72475731	0.029731379	0.940346171
atrx	double	1.309316928	6.784583207	4.721970749	0.029779594	0.940346171
ehd1a	double	-1.508161646	5.961132585	4.708804824	0.030008507	0.940346171
c3a.6	double	3.50309534	4.903172004	4.703188531	0.030106714	0.940346171
znf384l	double	-3.491466016	4.545830061	4.702221748	0.030123653	0.940346171
rp9	double	2.015598683	5.572133659	4.685053237	0.030426121	0.940346171
chchd4	double	2.039737863	5.201681851	4.682716204	0.030467538	0.940346171
cdo1	double	-1.435888166	6.348661511	4.675076702	0.030603336	0.940346171
mansc1	double	1.695652248	5.826241932	4.667876704	0.0307319	0.940346171
lrwd1	double	-3.462749975	4.798599311	4.653064895	0.030998154	0.940346171
grk7a	double	2.619051822	4.882272602	4.634307535	0.031338789	0.940346171
sepw2a	double	1.301527973	6.776745505	4.630384118	0.031410531	0.940346171
slc12a3	double	-3.498959197	4.839032563	4.617212563	0.031652636	0.940346171
mixl1	double	1.156180996	6.971144613	4.610595968	0.031774989	0.940346171
ube2v2	double	1.159642434	7.254143648	4.609009274	0.031804403	0.940346171
hmgxb4a	double	-2.587508814	4.543218196	4.608805433	0.031808184	0.940346171
zgc:103697	double	2.048558313	5.143901574	4.603822053	0.031900762	0.940346171
tecrb	double	-2.584900273	4.931210102	4.592918989	0.032104294	0.940346171
slit3	double	2.201925438	5.074768838	4.590114427	0.032156867	0.940346171
foxm1	double	1.138411478	7.418963661	4.584415002	0.032263983	0.940346171
stxbp1a	double	-2.584618126	4.604932522	4.579012242	0.032365867	0.940346171
camk2n1a	double	-3.471920514	4.667763904	4.577221007	0.03239972	0.940346171
irx1a	double	-2.368135213	4.811741868	4.577126796	0.032401501	0.940346171
slc25a1a	double	0.947313913	8.374495815	4.574808961	0.032445363	0.940346171
thap3	double	1.430655306	6.510579621	4.570361673	0.032529697	0.940346171
smyhc3	double	2.693712423	5.0491633	4.569480018	0.032546443	0.940346171
onecut1	double	1.517791357	6.362589889	4.564996265	0.032631745	0.940346171
zgc:66447	double	-2.548699635	5.031877737	4.527730492	0.033349817	0.940346171
rpl35	double	0.898920198	8.825604912	4.526834864	0.033367277	0.940346171

Continued on following page

Table B.6: continued from previous page

gene	MO	logFC	logCPM	LR	p value	FDR
phospho1	double	1.680838695	5.642554802	4.524502072	0.033412797	0.940346171
alg9	double	-3.483717827	4.724528991	4.523523464	0.033431913	0.940346171
ubn2a	double	1.366172662	6.720967645	4.507383197	0.033748836	0.940346171
anxa5b	double	2.118339121	5.575868616	4.504099202	0.033813702	0.940346171
apela	double	2.617735521	4.740663155	4.502652314	0.033842323	0.940346171
cdca4	double	1.908269212	5.676542732	4.492942055	0.034035056	0.940346171
pim1	double	1.89784164	5.355442967	4.488088879	0.034131814	0.940346171
pdcd2	double	-2.575170967	5.001758759	4.485936974	0.034174808	0.940346171
pgls	double	-3.467139146	4.776523171	4.480796959	0.034277733	0.940346171
tor1	double	2.629222354	4.719040031	4.474325334	0.034407784	0.940346171
cox17	double	2.625310956	4.945340233	4.473517959	0.034424045	0.940346171
tuba7l	double	0.904358588	8.566772254	4.469685142	0.034501349	0.940346171
rras2	double	-2.234445754	5.10872785	4.46722655	0.034551032	0.940346171
zbtb10	double	-2.553970222	4.867666375	4.467047938	0.034554644	0.940346171
ebna1bp2	double	1.352573513	6.55365742	4.458257591	0.034732909	0.940346171
zgc:136472	double	1.698747623	5.689322285	4.44748096	0.034952769	0.940346171
zgc:162154	double	1.745270637	6.392163196	4.419820011	0.035523783	0.940346171
fam175a	double	-1.357570486	6.391207963	4.413994304	0.035645285	0.940346171
snrpf	double	1.085791281	7.044025961	4.412994125	0.035666188	0.940346171
si:ch211-226m16.2	double	-2.579993315	4.868935562	4.40968047	0.035735534	0.940346171
MGC174152	double	-1.843449293	5.551601515	4.407485854	0.035781539	0.940346171
sltm	double	1.024834936	7.577956792	4.406099823	0.035810626	0.940346171
mibp	double	1.888631695	5.362962853	4.402509981	0.035886077	0.940346171
cops6	double	-2.540355194	4.792286956	4.380442288	0.036353563	0.940346171
fbxo11a	double	1.469870449	6.243549546	4.380274244	0.036357147	0.940346171
eif3i	double	0.961548308	7.468738905	4.353755554	0.036927429	0.940346171
foxh1	double	1.704768762	5.420130772	4.345609224	0.03710449	0.940346171
jtb	double	1.096386709	7.234028754	4.338944258	0.037250015	0.940346171
htr2b	double	2.710690026	4.585477434	4.320794558	0.037649338	0.940346171
ctsc	double	0.987593592	7.841304166	4.316401248	0.037746671	0.940346171
ints8	double	2.484573923	5.215977205	4.309496965	0.037900167	0.940346171
nrn1lb	double	1.137445248	7.13655775	4.308805536	0.037915575	0.940346171
jam3b	double	2.214525443	5.016797516	4.298276363	0.03815102	0.940346171
crtap	double	1.231309225	6.47631206	4.29099024	0.038314844	0.940346171
zgc:73185	double	2.605945062	4.864925785	4.276961972	0.03863234	0.940346171
mbd1a	double	2.058229322	5.163455346	4.271592558	0.038754593	0.940346171
cnot10	double	2.074609711	5.11174186	4.259633074	0.039028351	0.940346171
sigmar1	double	1.982738678	4.943550516	4.242584177	0.039422119	0.940346171
sdc4	double	-1.717542433	5.681316109	4.242029818	0.039434992	0.940346171
brpf1	double	-1.743043773	5.360447399	4.240164707	0.039478337	0.940346171
tmem17	double	1.69003921	5.97343594	4.238779418	0.039510563	0.940346171
utp3	double	1.377396252	6.112203478	4.224293154	0.039849214	0.940346171
zgc:175088	double	1.202522806	6.543115776	4.217783248	0.040002389	0.940346171
lrp6	double	-2.556523943	4.738207634	4.203808574	0.040333298	0.940346171
cp	double	-2.578188257	4.899541111	4.18366392	0.040815373	0.940346171
ahcy	double	-1.061068751	7.489424627	4.176381694	0.040991126	0.940346171
chchd7	double	1.424590091	6.291222059	4.162582931	0.041326338	0.940346171
zgc:66427	double	2.017492786	5.259254647	4.1576263	0.041447451	0.940346171
st14a	double	-2.101515028	5.476769979	4.150554342	0.041620896	0.940346171
ube2l3b	double	1.821795069	5.412194168	4.1253992	0.042244053	0.940346171
sp9	double	1.568019357	5.666605176	4.124726993	0.042260839	0.940346171

Continued on following page

Table B.6: continued from previous page

gene	MO	logFC	logCPM	LR	p value	FDR
sec61a1	double	0.887828035	7.913920895	4.119256527	0.042397707	0.940346171
ccdc24	double	0.801585918	10.55376429	4.10404931	0.042780637	0.940346171
exoc6b	double	1.770845465	5.347903307	4.099897567	0.042885812	0.940346171
zgc:56699	double	2.602724769	4.737546986	4.090167508	0.043133367	0.940346171
nucb2b	double	0.763057605	9.666752284	4.088095434	0.043186279	0.940346171
socs6b	double	2.506751712	4.544214243	4.082385596	0.043332439	0.940346171
zgc:91860	double	2.539996687	4.949811196	4.077688402	0.043453067	0.940346171
naga	double	-1.768154443	5.268447278	4.069137212	0.043673576	0.940346171
lyn	double	2.50241805	4.987254755	4.06221042	0.043853061	0.940346171
taf9	double	-1.945431143	5.329123737	4.052229141	0.044113058	0.940346171
zgc:153018	double	1.593046049	5.915521791	4.050570355	0.044156424	0.940346171
ccdc84	double	0.755150084	10.09677466	4.03639854	0.044528753	0.940346171
sass6	double	2.183084454	4.948418876	4.023504709	0.044870379	0.940346171
chmp6b	double	1.513361569	5.826206513	4.01970619	0.044971547	0.940346171
metrnl	double	2.451841392	4.809417863	3.985467324	0.045894368	0.940346171
slc26a1	double	2.518897073	4.954763753	3.982438656	0.045976953	0.940346171
ogdha	double	1.374492363	6.243704673	3.979871459	0.046047077	0.940346171
zcchc7	double	1.647747149	5.47846364	3.976833753	0.046130199	0.940346171
scg2b	double	3.148281701	4.479562171	3.969021917	0.046344685	0.940346171
cops7a	double	2.447669109	5.03688865	3.96620666	0.046422239	0.940346171
adnp2b	double	1.844445879	5.271553539	3.963887191	0.046486238	0.940346171
tyms	double	1.752986651	5.444580222	3.963226545	0.046504484	0.940346171
sox1b	double	2.447903669	4.546240451	3.961901446	0.046541103	0.940346171
med16	double	-2.206884746	4.721106882	3.956299512	0.04669625	0.940346171
optn	double	3.176870175	4.608284946	3.954390792	0.046749237	0.940346171
bzw2	double	3.162759642	4.411767255	3.948536078	0.046912162	0.940346171
hs2st1a	double	3.131291633	4.364207439	3.946289055	0.046974851	0.940346171
yif1a	double	1.762361224	5.250455002	3.940187976	0.047145509	0.940346171
mrpl39	double	-1.955824166	5.125903568	3.923432001	0.047617576	0.940346171
mtfr2	double	2.453648263	4.708466774	3.910991569	0.047971286	0.940346171
nfybb	double	3.131819694	4.478147779	3.907206525	0.048079452	0.940346171
yars	double	1.68724179	5.818251572	3.904587711	0.048154442	0.940346171
gatad1	double	2.465279751	4.649709882	3.902844308	0.048204432	0.940346171
cnot6l	double	3.167735637	4.607020344	3.900863699	0.048261291	0.940346171
sulf1	double	1.63146101	5.589342748	3.897753646	0.048350716	0.940346171
vtna	double	2.47760695	4.801552992	3.897387419	0.048361258	0.940346171
ccnf	double	1.026088832	8.321635277	3.89168928	0.048525592	0.940346171
prkar1ab	double	3.13203509	4.685401772	3.890898224	0.048548452	0.940346171
c6	double	-1.254403434	6.61940853	3.886720668	0.048669367	0.940346171
rbp7b	double	2.46010708	4.779980943	3.884857638	0.048723393	0.940346171
paip1	double	3.154038414	4.648963853	3.883120479	0.048773826	0.940346171
hdac4	double	2.442483663	4.781563339	3.882692537	0.048786258	0.940346171
tpcn2	double	3.169602125	4.691340743	3.882245133	0.04879926	0.940346171
aptx	double	1.233921281	6.389637885	3.881747259	0.048813732	0.940346171
nxpe3	double	3.170120576	4.506975354	3.87699896	0.048951984	0.940346171
zgc:123335	double	3.145194784	4.499881431	3.87454493	0.049023598	0.940346171
nr1h5	double	3.18868325	4.608923155	3.87128955	0.049118768	0.940346171
cep63	double	3.132295654	4.497404908	3.870876408	0.04913086	0.940346171
lrrc42	double	3.120681436	4.564473597	3.86955952	0.049169424	0.940346171
mrpl38	double	-1.579135706	5.451936693	3.866309446	0.049264737	0.940346171
zgc:194508	double	2.496469887	4.729188253	3.865517008	0.049288006	0.940346171

Continued on following page

Table B.6: continued from previous page

gene	MO	logFC	logCPM	LR	p value	FDR
pkma	double	3.132420956	4.60424581	3.861131234	0.049416999	0.940346171
ctdnep1b	double	3.113305389	4.49734828	3.861007035	0.049420657	0.940346171
wbscr22	double	2.443663502	5.053613351	3.859634737	0.049461095	0.940346171
twf1b	double	3.190714474	4.852843622	3.856036761	0.049567284	0.940346171
zgc:92518	double	-2.071110041	4.959446849	3.853473863	0.049643071	0.940346171
trim8a	double	3.191578602	4.947099064	3.849456096	0.049762125	0.940346171
zgc:158257	double	3.112855936	4.451890896	3.847072107	0.04983291	0.940346171

Table B.7: Significant differential gene expression of genes detected with EdgeR at 21hpf

gene	MO	logFC	logCPM	LR	p value	FDR
sri	tbx5a	-5.577137734	5.088896444	15.62509434	7.72E-05	0.459096657
ube2r2	tbx5a	-5.332640456	5.18763447	14.11513093	0.000171955	0.459096657
ighmbp2	tbx5a	-5.09369464	5.033948084	12.87222962	0.000333494	0.459096657
glyr1	tbx5a	-3.341140182	5.694117425	12.81163483	0.00034447	0.459096657
panx1a	tbx5a	-5.336296679	4.722873094	12.7853035	0.000349353	0.459096657
zgc:113229	tbx5a	-3.283251378	5.413945463	12.60002183	0.000385742	0.459096657
zfyve21	tbx5a	-5.087091751	4.850370893	12.37759922	0.000434515	0.459096657
zgc:123172	tbx5a	-5.100069335	4.856535282	11.6402172	0.000645411	0.596682159
hsp90aa1.2	tbx5a	-1.943631364	7.46962896	11.06588241	0.000879307	0.722595221
gnat2	tbx5a	-3.528006209	5.495126724	10.61348275	0.00112266	0.763522107
ftr82	tbx5a	-2.784695447	5.425444059	10.48959056	0.00120049	0.763522107
rab43	tbx5a	-3.066190374	5.658405591	10.03624441	0.001534898	0.763522107
unc5a	tbx5a	4.819679957	4.896741974	10.03171456	0.001538677	0.763522107
plxna3	tbx5a	-4.714620155	5.162244018	9.944356624	0.001613432	0.763522107
kdelr3	tbx5a	4.954865176	4.742146227	9.864890725	0.001684627	0.763522107
dpysl2b	tbx5a	-4.716196919	4.833125904	9.564477552	0.001983786	0.763522107
stmn4	tbx5a	-2.174905869	6.469334787	9.556075975	0.001992887	0.763522107
ube2v2	tbx5a	-1.64105655	7.254143648	9.547407176	0.002002321	0.763522107
aif1l	tbx5a	-2.70639072	5.44264838	8.985290882	0.002721615	0.763522107
zgc:174263	tbx5a	-4.516673348	4.830321995	8.983171275	0.002724773	0.763522107
tcf3b	tbx5a	-1.77717648	6.644966197	8.83296115	0.00295838	0.763522107
zgc:113090	tbx5a	-1.809865208	6.7574879	8.764342494	0.003071768	0.763522107
arid3c	tbx5a	-3.340733035	5.372522901	8.710269502	0.003164224	0.763522107
slc26a3.2	tbx5a	-4.560310223	4.818397695	8.685866378	0.003206871	0.763522107
siah1	tbx5a	-3.336980906	5.165042504	8.625643575	0.003314633	0.763522107
dpp7	tbx5a	-1.47096276	8.522502226	8.471507228	0.003607524	0.763522107
cdc7	tbx5a	-4.353997616	4.505541663	8.424098537	0.003702802	0.763522107
srsf10b	tbx5a	1.716637282	6.736387998	8.378422808	0.003797018	0.763522107
lepa	tbx5a	-4.362647312	4.590743222	8.338586735	0.003881178	0.763522107
ctc1	tbx5a	-4.346891219	5.0262711	8.333044207	0.003893037	0.763522107
lin7c	tbx5a	-2.558155049	5.447001415	8.320435704	0.003920152	0.763522107
slc7a7	tbx5a	-2.422484609	5.508303198	8.22498904	0.004131745	0.763522107
npc1	tbx5a	2.19456382	5.90919707	8.197201825	0.004195505	0.763522107
psen1	tbx5a	-2.744710048	5.392360574	8.08872823	0.004454141	0.763522107
smo	tbx5a	-2.081204769	6.021896027	8.036903564	0.004583382	0.763522107
plp2	tbx5a	-2.001051956	5.920575491	8.024407671	0.004615112	0.763522107
zgc:163057	tbx5a	-4.373846978	4.524084973	7.996609586	0.004686502	0.763522107
foxc1b	tbx5a	4.487143311	4.725590236	7.995477269	0.004689434	0.763522107
ube2f	tbx5a	-4.337673098	4.935838814	7.980140169	0.004729328	0.763522107
iars2	tbx5a	-4.34629808	4.826440796	7.97418997	0.004744898	0.763522107
ticrr	tbx5a	-4.374264074	4.954805889	7.948129562	0.00481371	0.763522107
igsf8	tbx5a	4.313782662	4.865173005	7.890839565	0.00496858	0.763522107
hdac8	tbx5a	-4.344876379	4.668622628	7.828451945	0.005143013	0.763522107
hpca	tbx5a	-4.345663669	4.763201758	7.822270482	0.005160632	0.763522107
raph1b	tbx5a	-4.355467593	4.908504318	7.811622774	0.005191127	0.763522107
slc35e3	tbx5a	2.130191295	6.367520455	7.723493733	0.005450682	0.763522107
rrp15	tbx5a	1.719260071	6.604652869	7.722413729	0.005453943	0.763522107
drg1	tbx5a	-2.162031906	5.826014231	7.713343823	0.005481412	0.763522107
uros	tbx5a	4.307847687	4.682305621	7.681071057	0.005580304	0.763522107
mycla	tbx5a	3.132859199	5.12653965	7.661323224	0.005641711	0.763522107
mrpl15	tbx5a	-2.48909249	5.415413348	7.589648011	0.005870441	0.763522107

Continued on following page

Table B.7: continued from previous page

gene	MO	logFC	logCPM	LR	p value	FDR
nudt22	tbx5a	-1.384102579	7.771353817	7.570484332	0.005933184	0.763522107
usp25	tbx5a	-3.090951818	5.088631427	7.5519292	0.005994586	0.763522107
scrn2	tbx5a	4.308372461	4.64430018	7.535411782	0.006049791	0.763522107
pola1	tbx5a	-2.747993066	5.527854294	7.523324228	0.006090518	0.763522107
zgc:158343	tbx5a	3.142817784	5.109564408	7.47100564	0.006270052	0.763522107
zgc:63882	tbx5a	-1.399287765	8.313379368	7.44952742	0.006345311	0.763522107
phb2a	tbx5a	-2.729862892	5.086017571	7.441447194	0.006373862	0.763522107
neu1	tbx5a	-3.251311515	5.079790406	7.401429393	0.006517207	0.763522107
tmem238	tbx5a	3.133986386	4.778775502	7.401063492	0.006518533	0.763522107
zgc:85858	tbx5a	-4.312709042	4.797129789	7.297866614	0.006903653	0.763522107
mob1bb	tbx5a	-4.140951441	4.700890348	7.285875472	0.006949885	0.763522107
apool	tbx5a	-1.17101227	8.34158819	7.282795912	0.00696181	0.763522107
nfil3	tbx5a	-3.335042971	4.712552443	7.271841968	0.007004394	0.763522107
zgc:123284	tbx5a	-3.103212765	5.026749983	7.269991054	0.007011615	0.763522107
idh3a	tbx5a	2.469396471	5.633724682	7.26451285	0.007033034	0.763522107
zgc:110269	tbx5a	-4.132482462	4.896604311	7.254161656	0.007073689	0.763522107
zcchc24	tbx5a	-2.746569992	5.20656785	7.24683832	0.007102596	0.763522107
asrgl1	tbx5a	-4.150262819	4.995294544	7.241642658	0.007123178	0.763522107
dap3	tbx5a	-3.09063806	4.914609823	7.160585663	0.007452286	0.765934848
pcdh19	tbx5a	-2.114684754	5.819596245	7.121943819	0.00761461	0.765934848
nfil3-5	tbx5a	-4.140716076	4.546874892	7.07486316	0.007817279	0.765934848
tinagl1	tbx5a	-4.150702379	4.649211183	7.037524396	0.007981929	0.765934848
chchd3a	tbx5a	-4.122138946	4.500495552	7.031288399	0.008009771	0.765934848
tmem2	tbx5a	-2.425367442	5.524169936	7.029426966	0.008018101	0.765934848
zgc:158482	tbx5a	-4.16185158	4.833017356	7.000423961	0.008149041	0.765934848
zgc:66474	tbx5a	-4.141617575	4.778091756	6.95628306	0.008352538	0.765934848
yeats4	tbx5a	-1.580973629	6.376394865	6.947073736	0.008395645	0.765934848
map2k6	tbx5a	-1.377307097	6.891148587	6.932748157	0.008463155	0.765934848
tor1	tbx5a	-4.121004188	4.719040031	6.863863763	0.008795616	0.765934848
tuba1c	tbx5a	1.959228616	5.845828226	6.849644773	0.00886589	0.765934848
chchd1	tbx5a	3.02781643	4.996794143	6.817339894	0.009027694	0.765934848
twsg1a	tbx5a	4.088710191	4.678969141	6.803250179	0.009099208	0.765934848
mapre2	tbx5a	-2.406351949	5.383147562	6.797748081	0.009127292	0.765934848
eps8	tbx5a	-4.130439921	4.738266007	6.786224541	0.009186399	0.765934848
yars2	tbx5a	-1.31283101	7.702065062	6.776338211	0.009237421	0.765934848
ldb1b	tbx5a	-4.130380591	4.776593549	6.771565076	0.009262158	0.765934848
st5	tbx5a	-4.152625322	4.69079218	6.766030535	0.009290926	0.765934848
pla2g6	tbx5a	-3.074881809	4.860676981	6.760782978	0.009318287	0.765934848
slc29a1a	tbx5a	-4.13078354	4.778603524	6.760366434	0.009320462	0.765934848
ldlrap1a	tbx5a	-4.152355246	4.604546759	6.725569646	0.009504037	0.768742034
pllp	tbx5a	-1.342364291	7.000445468	6.638587185	0.009979304	0.768742034
zgc:103508	tbx5a	4.09397393	4.846836444	6.598475742	0.010206611	0.768742034
kank3	tbx5a	-2.642972272	5.502413908	6.540644811	0.010543713	0.768742034
sox19b	tbx5a	-2.612144644	5.19414874	6.522787211	0.010650097	0.768742034
vimp	tbx5a	-2.439992889	5.244248467	6.514790073	0.010698095	0.768742034
pdzrn3b	tbx5a	-2.629069207	4.850190064	6.488062359	0.010860129	0.768742034
uqcc2	tbx5a	4.094354608	4.755685954	6.475845129	0.01093503	0.768742034
cpt2	tbx5a	-2.330192621	5.354953586	6.458975749	0.011039326	0.768742034
hoxc5a	tbx5a	-2.320601109	5.776224485	6.409479432	0.011351269	0.768742034
slc39a10	tbx5a	-2.094097369	5.669361194	6.405252132	0.011378327	0.768742034
romo1	tbx5a	-1.05454223	9.838514356	6.402615255	0.011395238	0.768742034

Continued on following page

Table B.7: continued from previous page

gene	MO	logFC	logCPM	LR	p value	FDR
arl8a	tbx5a	-2.407934068	5.364226854	6.401096121	0.011404993	0.768742034
ttc14	tbx5a	-1.563138175	8.019481288	6.393580619	0.011453377	0.768742034
unc119b	tbx5a	-3.891226367	5.008503071	6.346873878	0.011758833	0.768742034
gpsm2	tbx5a	-2.958711085	4.998525137	6.33565709	0.011833427	0.768742034
ehmt1a	tbx5a	-2.969726599	4.97688664	6.327881963	0.011885418	0.768742034
tsku	tbx5a	-3.899295403	4.565203854	6.32261661	0.01192076	0.768742034
rint1	tbx5a	-2.969422496	5.305636988	6.320113632	0.011937598	0.768742034
cerkl	tbx5a	-1.961076181	5.864008016	6.289504664	0.012145499	0.768742034
mut	tbx5a	-2.954928074	5.035638074	6.27394467	0.012252607	0.768742034
tmem180	tbx5a	-3.883268584	4.832690996	6.269766094	0.012281535	0.768742034
cenpa	tbx5a	-2.118963531	5.566028717	6.261092553	0.012341807	0.768742034
rer1	tbx5a	-2.226905667	5.831627061	6.249104694	0.01242561	0.768742034
glcci1	tbx5a	-2.963161518	5.390744703	6.231482164	0.012549865	0.768742034
sptlc3	tbx5a	-3.883212185	4.543328438	6.230480113	0.012556969	0.768742034
foxh1	tbx5a	-2.316867942	5.420130772	6.224181522	0.012601715	0.768742034
mrpl20	tbx5a	2.669114899	5.104069752	6.220883648	0.012625209	0.768742034
mgrn1a	tbx5a	-3.890605268	4.603608113	6.21411862	0.012673543	0.768742034
znf513	tbx5a	-3.899794132	4.460887111	6.189013722	0.012854581	0.768742034
gb:bc139872	tbx5a	-2.531948329	5.024716669	6.16028528	0.013065014	0.768742034
rgl1	tbx5a	-2.623505082	4.899956506	6.113487193	0.013415418	0.768742034
foxred2	tbx5a	-3.90066564	4.623780314	6.112571058	0.013422374	0.768742034
epha7	tbx5a	-3.900666894	4.629981556	6.112369581	0.013423904	0.768742034
slc43a1b	tbx5a	-2.933878616	5.07010614	6.10648725	0.013468656	0.768742034
usf2	tbx5a	-1.640713017	6.353129809	6.102197631	0.013501388	0.768742034
cyb5d2	tbx5a	1.762370448	6.768135776	6.093789661	0.013565782	0.768742034
slco1d1	tbx5a	-3.881478592	4.521504241	6.085678181	0.013628204	0.768742034
reps1	tbx5a	-3.901110209	4.690060896	6.040032745	0.013985025	0.768742034
dusp4	tbx5a	-3.901701559	4.738307374	6.016078585	0.014176112	0.768742034
tbl1xr1b	tbx5a	-3.912627326	4.543749986	6.000155029	0.014304621	0.768742034
mus81	tbx5a	-3.880669611	4.850468043	5.99811351	0.014321184	0.768742034
pdcd4b	tbx5a	-3.880971834	4.582352383	5.985346388	0.014425209	0.768742034
kif3b	tbx5a	-3.901014304	4.691852803	5.979073666	0.014476604	0.768742034
ccnb2	tbx5a	-2.932675184	5.068922619	5.977080897	0.014492971	0.768742034
kat5b	tbx5a	-3.913456538	4.626613207	5.974553985	0.014513752	0.768742034
si:rp71-45k5.4	tbx5a	-1.028272233	8.383133646	5.970469338	0.014547408	0.768742034
ube2q2	tbx5a	2.470344151	5.36175703	5.952537929	0.014696113	0.768742034
syngr2a	tbx5a	-2.217994082	5.241958426	5.92586596	0.014920204	0.768742034
slc39a13	tbx5a	-3.880442821	4.623196792	5.924005077	0.014935969	0.768742034
ralba	tbx5a	-3.901386064	4.546927469	5.911111613	0.015045675	0.768742034
vps18	tbx5a	3.860730925	4.707253151	5.898058463	0.015157584	0.768742034
slc39a6	tbx5a	-1.955637663	5.462068614	5.862143816	0.01546994	0.768742034
klf18	tbx5a	-3.914073128	4.667981114	5.850843887	0.015569583	0.768742034
mybl2a	tbx5a	-3.890309841	4.65902454	5.848280985	0.015592275	0.768742034
src	tbx5a	-3.915186889	4.647227721	5.845343894	0.015618321	0.768742034
traf6	tbx5a	-3.879259418	4.813305616	5.838322466	0.01568077	0.768742034
flot2b	tbx5a	-3.889785933	4.828319451	5.82582934	0.015792521	0.768742034
cks2	tbx5a	3.8419164	4.627671891	5.805848336	0.01597296	0.768742034
dph1	tbx5a	3.848418423	4.579336285	5.805794441	0.01597345	0.768742034
egfl7	tbx5a	3.854625944	4.584771809	5.804148617	0.015988407	0.768742034
actn3b	tbx5a	-2.242542147	5.472207434	5.783167905	0.016180353	0.768742034
nr1d2b	tbx5a	-3.878791233	4.649525725	5.783123674	0.016180761	0.768742034

Continued on following page

Table B.7: continued from previous page

gene	MO	logFC	logCPM	LR	p value	FDR
slit3	tbx5a	-2.422564195	5.074768838	5.768925746	0.016312003	0.768742034
tmco1	tbx5a	-2.103792765	5.639033509	5.766365625	0.016335785	0.768742034
cab39l1	tbx5a	-1.79455878	5.63759461	5.762294329	0.016373678	0.768742034
rab39bb	tbx5a	-1.294920252	7.346999225	5.749022565	0.016497834	0.768742034
jph1b	tbx5a	-3.867293989	4.810785376	5.748626307	0.016501555	0.768742034
gga1	tbx5a	1.896637378	5.563297147	5.724416686	0.016730593	0.768742034
LOC100535586	tbx5a	-3.915208483	4.770055061	5.709846144	0.016870018	0.768742034
asb2b	tbx5a	-2.824688449	5.239559327	5.702232528	0.016943348	0.768742034
tubgcp4	tbx5a	3.862442841	4.587210814	5.69835262	0.016980844	0.768742034
foxj1a	tbx5a	3.851555929	5.001052746	5.683338868	0.017126746	0.768742034
faf2	tbx5a	2.157169899	5.635323846	5.682251042	0.017137367	0.768742034
gtf2b	tbx5a	-1.911642719	5.891029093	5.677979834	0.017179137	0.768742034
ampd3b	tbx5a	3.863361318	4.566448678	5.659672558	0.017359364	0.768742034
asb12a	tbx5a	2.903051549	4.798544984	5.64549846	0.017500241	0.768742034
ccdc106a	tbx5a	-2.431044645	4.886579211	5.631357375	0.017641965	0.768742034
ccdc9	tbx5a	-1.311046388	6.888098325	5.62287091	0.017727587	0.768742034
yy1b	tbx5a	1.619123588	6.131266332	5.620257956	0.017754036	0.768742034
timd4	tbx5a	-1.557104885	5.909341241	5.610473607	0.017853437	0.768742034
sall4	tbx5a	-2.049272061	5.899896733	5.60809174	0.017877722	0.768742034
si:ch211-5k11.12	tbx5a	2.105509016	5.038964332	5.57989704	0.018167791	0.770771824
nom1	tbx5a	-2.430553925	4.965662632	5.579865803	0.018168115	0.770771824
dusp23a	tbx5a	-3.91671708	4.743201692	5.57318383	0.01823757	0.770771824
zgc:92606	tbx5a	2.225110574	5.238646186	5.527904586	0.018715506	0.781769654
zgc:194202	tbx5a	3.847864759	4.65995539	5.515211971	0.018851789	0.781769654
hsf2	tbx5a	-2.819520415	4.923858065	5.514089081	0.018863895	0.781769654
sec63	tbx5a	-1.757978721	5.799303546	5.50666696	0.018944115	0.781769654
tcp11l1	tbx5a	-2.812103939	4.58814691	5.493629215	0.019085885	0.781769654
tram1	tbx5a	-1.239368432	7.257757937	5.489409408	0.019132005	0.781769654
si:ch211-275j6.5	tbx5a	2.142697098	5.379572209	5.44101103	0.019669281	0.78765068
obsl1a	tbx5a	-2.821417615	5.126767919	5.437824426	0.019705199	0.78765068
nup155	tbx5a	-2.125795595	5.727737174	5.434557381	0.019742093	0.78765068
zeb1b	tbx5a	-1.795345147	6.114823131	5.40023115	0.020134085	0.78765068
tomm22	tbx5a	-1.801660383	5.937303375	5.394077508	0.020205203	0.78765068
znrf2a	tbx5a	2.751293425	4.953142197	5.372919603	0.020451717	0.78765068
chst14	tbx5a	-2.821982451	4.743427834	5.368499173	0.020503612	0.78765068
ndc80	tbx5a	-2.132773152	5.440436205	5.35663081	0.020643619	0.78765068
acss1	tbx5a	-2.147941949	5.214619994	5.345484164	0.020776013	0.78765068
pole	tbx5a	-2.143341289	5.704392108	5.343556175	0.020799002	0.78765068
papss1	tbx5a	-2.803746471	4.884394051	5.335686196	0.020893114	0.78765068
trap1	tbx5a	-1.752271715	5.503651735	5.326539999	0.021003041	0.78765068
anks4b	tbx5a	1.906882832	5.94103839	5.290146066	0.021446421	0.78765068
flot2a	tbx5a	-1.468927912	6.623449337	5.278418281	0.021591354	0.78765068
zbed4	tbx5a	-2.795318482	4.92006626	5.258325692	0.021842021	0.78765068
nebl	tbx5a	1.90709952	5.531657873	5.251463563	0.02192832	0.78765068
timm10	tbx5a	-2.313039596	5.425879825	5.23445178	0.022143786	0.78765068
eif4ebp3l	tbx5a	-1.639750686	5.880597219	5.214083695	0.022404651	0.78765068
polr2h	tbx5a	2.363658395	5.211678887	5.181021525	0.022834895	0.78765068
decr2	tbx5a	-2.816408383	4.743494211	5.137673014	0.023412009	0.78765068
naa15b	tbx5a	1.823733578	5.948985866	5.136570999	0.023426876	0.78765068
grhl2b	tbx5a	-3.608523066	4.49939578	5.121536669	0.023630682	0.78765068
aldh6a1	tbx5a	-1.781813872	5.76685351	5.119583611	0.023657293	0.78765068

Continued on following page

Table B.7: continued from previous page

gene	MO	logFC	logCPM	LR	p value	FDR
ppil3	tbx5a	-3.598490603	4.646941051	5.114047903	0.023732885	0.78765068
cry-dash	tbx5a	-3.609152745	4.564154681	5.090047578	0.024063531	0.78765068
trpm4a	tbx5a	2.148227205	5.599519401	5.087956692	0.024092562	0.78765068
rnasen	tbx5a	-3.599112206	4.582876791	5.071170911	0.024326946	0.78765068
serpinc1	tbx5a	-0.918048722	8.853569864	5.067848042	0.024373624	0.78765068
bcap29	tbx5a	-2.661640996	5.195961948	5.062263469	0.024452282	0.78765068
nostrin	tbx5a	-3.600125754	4.500751184	5.041725408	0.024743833	0.78765068
cops8	tbx5a	-2.156599058	5.027106446	5.036092139	0.02482443	0.78765068
dpysl5a	tbx5a	-3.599755239	4.937809516	5.032280072	0.024879125	0.78765068
idi1	tbx5a	-1.364728095	6.522684349	5.029265062	0.024922472	0.78765068
h2afy	tbx5a	-3.589063107	4.645119747	5.027982339	0.024940938	0.78765068
chpt1	tbx5a	-1.547070289	6.030891808	5.026890207	0.024956671	0.78765068
znf207b	tbx5a	-1.538361205	5.783945976	5.025225606	0.024980671	0.78765068
ccdc85b	tbx5a	-2.660969168	5.073814943	5.016357959	0.025108928	0.78765068
nup205	tbx5a	1.545332437	6.192097685	5.015724803	0.025118112	0.78765068
sin3aa	tbx5a	-3.610272772	5.01515906	5.007395305	0.025239254	0.78765068
zgc:165507	tbx5a	-3.610433343	4.502608168	4.998567029	0.025368314	0.78765068
coro2a	tbx5a	2.104563875	5.201973243	4.995594475	0.025411923	0.78765068
cblc	tbx5a	-3.599082145	4.762947566	4.992875397	0.025451882	0.78765068
ier2	tbx5a	-2.658400362	5.22816007	4.992300405	0.02546034	0.78765068
kdm6al	tbx5a	-3.599557428	4.885813214	4.988459961	0.025516909	0.78765068
haus3	tbx5a	-3.589154632	4.703233484	4.98529265	0.025563661	0.78765068
aimp1	tbx5a	1.39570914	6.263813044	4.980500222	0.02563457	0.78765068
dennd2db	tbx5a	2.728291732	4.807340558	4.979740924	0.025645823	0.78765068
zgc:92027	tbx5a	-1.723615926	5.917974174	4.972653857	0.025751107	0.78765068
adprh	tbx5a	-3.600590809	4.523406625	4.969432946	0.025799104	0.78765068
acsl4b	tbx5a	-3.599209223	4.628516797	4.965712917	0.025854655	0.78765068
tyrp1b	tbx5a	-3.589436885	4.54228666	4.963296969	0.025890799	0.78765068
rab11fip4a	tbx5a	-3.588535891	4.833370319	4.960657273	0.02593035	0.78765068
vps33a	tbx5a	-1.545989765	5.953520205	4.959487746	0.025947893	0.78765068
kctd13	tbx5a	-3.578455198	4.453343254	4.959205183	0.025952133	0.78765068
wdr91	tbx5a	-3.599713347	4.918391916	4.958560994	0.025961803	0.78765068
rcc1	tbx5a	-1.942940044	5.744181064	4.947496884	0.026128472	0.78765068
zic4	tbx5a	-2.803303964	4.800637914	4.947019894	0.026135683	0.78765068
sp2	tbx5a	-3.599330002	4.524430922	4.939504535	0.02624956	0.78765068
hcfc2	tbx5a	-0.924358807	8.374055561	4.937373127	0.02628195	0.78765068
maf1	tbx5a	-2.121117653	5.323111124	4.936902485	0.026289108	0.78765068
zgc:113944	tbx5a	-3.588805943	4.580785788	4.936631836	0.026293225	0.78765068
sox9b	tbx5a	-3.600329417	4.668288066	4.933243335	0.026344827	0.78765068
prph2l	tbx5a	-3.600888396	4.744722653	4.921620864	0.026522623	0.78765068
zgc:195001	tbx5a	-3.589077055	4.632053792	4.908313912	0.026727719	0.78765068
si:dkey-15d12.2	tbx5a	-3.589065284	4.724963748	4.906488974	0.026755975	0.78765068
inhbb	tbx5a	-2.80531088	4.688209395	4.905438751	0.02677225	0.78765068
trim55a	tbx5a	-3.588585615	4.699792667	4.905259023	0.026775036	0.78765068
wdr6	tbx5a	-3.60058879	4.790070204	4.886670513	0.027064832	0.78765068
ugt2a6	tbx5a	-3.576816134	4.682862299	4.874575235	0.027255148	0.78765068
hif1an	tbx5a	-3.566295011	4.842556488	4.871931775	0.027296927	0.78765068
nr1h3	tbx5a	-3.601190442	4.587570355	4.871786678	0.027299222	0.78765068
acss2	tbx5a	-1.80898833	5.778791376	4.870733608	0.027315886	0.78765068
tmcc3	tbx5a	-1.716792422	5.817082786	4.868665888	0.027348636	0.78765068
acvr2b	tbx5a	-2.647305597	4.608758467	4.86328744	0.027434014	0.78765068

Continued on following page

Table B.7: continued from previous page

gene	MO	logFC	logCPM	LR	p value	FDR
mboat7	tbx5a	-2.318250938	5.379445385	4.862180474	0.027451621	0.78765068
rgcc	tbx5a	-3.588779914	4.644564766	4.861721395	0.027458926	0.78765068
elovl1b	tbx5a	1.944261932	5.275078814	4.852079952	0.027612816	0.78765068
golt1b	tbx5a	-2.224290164	5.037082676	4.846295771	0.027705569	0.78765068
emc6	tbx5a	1.862105855	5.795786115	4.844845514	0.027728876	0.78765068
znf143b	tbx5a	3.554413962	4.776765293	4.840695842	0.027795677	0.78765068
rab40c	tbx5a	-3.600347835	4.708546416	4.831509598	0.027944152	0.788418149
fzd1	tbx5a	-3.576030032	4.726835324	4.80622324	0.028357128	0.788418149
si:ch211-196f5.2	tbx5a	-1.306824415	6.519821195	4.804927589	0.028378459	0.788418149
sdha	tbx5a	-1.594663383	5.917395791	4.797062889	0.028508298	0.788418149
gpr160	tbx5a	3.557751805	4.763139683	4.792133198	0.028589998	0.788418149
dact2	tbx5a	-2.659126397	5.047576366	4.777433116	0.028835072	0.788418149
xrcc6bp1	tbx5a	3.553947519	4.496359959	4.77647256	0.028851162	0.788418149
msxd	tbx5a	3.557835556	4.683884107	4.776056898	0.028858127	0.788418149
ddx43	tbx5a	3.565402532	4.685191291	4.771154616	0.02894041	0.788418149
pole2	tbx5a	3.561346722	4.525661526	4.767298996	0.029005297	0.788418149
kalrnb	tbx5a	-2.646945833	4.77772696	4.76360699	0.029067572	0.788418149
hrasb	tbx5a	-2.813937154	4.727958129	4.760275529	0.029123886	0.788418149
fmo5	tbx5a	-1.947495485	5.32397682	4.755278339	0.029208569	0.788418149
serpinf2b	tbx5a	-2.647432445	4.952494521	4.744002974	0.029400586	0.788994711
nde1	tbx5a	-2.795213528	4.829779168	4.741506028	0.029443286	0.788994711
ubxn8	tbx5a	3.562299312	4.563669659	4.728523239	0.029666346	0.791683096
nrxn3b	tbx5a	3.553958184	4.68551372	4.715508869	0.029891717	0.791683096
pif1	tbx5a	3.542989698	4.536375885	4.711640386	0.029959052	0.791683096
asf1bb	tbx5a	3.566316769	4.850182955	4.706789072	0.030043716	0.791683096
abhd17aa	tbx5a	3.550368	4.543550087	4.699516771	0.030171099	0.791683096
foxg1c	tbx5a	2.568612661	5.387421141	4.694312769	0.030262599	0.791683096
gtpbp10	tbx5a	3.554561611	4.567072674	4.685941464	0.030410395	0.791683096
dmd	tbx5a	3.550289609	4.542448269	4.679036389	0.030532871	0.791683096
atp1b2b	tbx5a	-2.64700414	5.136708399	4.666880962	0.030749724	0.791683096
polr2gl	tbx5a	-1.355204984	6.203434781	4.66312658	0.030817026	0.791683096
tfam	tbx5a	-1.502121972	6.050483666	4.660692098	0.03086075	0.791683096
znf292b	tbx5a	-2.088906956	5.413695155	4.654928494	0.030964522	0.791683096
nploc4	tbx5a	-2.655511085	4.687120854	4.653674316	0.030987152	0.791683096
ca2	tbx5a	-1.491952099	5.776479284	4.637046328	0.03128881	0.791683096
hrasls	tbx5a	-1.42277376	6.353978313	4.636703594	0.031295059	0.791683096
dhps	tbx5a	3.554608887	4.546489127	4.634435281	0.031336456	0.791683096
sav1	tbx5a	-2.303848943	4.917780125	4.632964676	0.031363324	0.791683096
kansl3	tbx5a	-2.022784792	5.437926166	4.62304714	0.031545152	0.792649544
vrk2	tbx5a	-0.967526934	7.990281289	4.618746409	0.031624342	0.792649544
zgc:158640	tbx5a	-1.44467087	6.094596632	4.613397153	0.031723129	0.792649544
tada2b	tbx5a	-2.175230457	5.185409645	4.581387391	0.032321036	0.804038957
adam17a	tbx5a	-1.659967117	5.771311579	4.563066547	0.03266853	0.804038957
sptlc2a	tbx5a	3.545774579	4.775599611	4.55807066	0.032763963	0.804038957
gpr186	tbx5a	3.537076878	4.92577929	4.549919247	0.032920299	0.804038957
lta4h	tbx5a	-2.051207586	5.2010532	4.548622277	0.032945245	0.804038957
zdhhc20a	tbx5a	-2.320464977	4.906397502	4.545553777	0.033004345	0.804038957
naa20	tbx5a	-2.290582597	5.095703405	4.54046745	0.033102551	0.804038957
u2af2b	tbx5a	-1.116473383	7.327270989	4.539497491	0.033121314	0.804038957
itgb1b	tbx5a	-2.053985084	5.34724024	4.529581795	0.033313758	0.804038957
zdhhc15b	tbx5a	-2.662912492	4.778942864	4.52555591	0.033392225	0.804038957

Continued on following page

Table B.7: continued from previous page

gene	MO	logFC	logCPM	LR	p value	FDR
psme1	tbx5a	-2.665481129	4.726883683	4.522719351	0.033447628	0.804038957
slc43a1a	tbx5a	-1.441955373	5.799608888	4.517572332	0.033548403	0.804038957
gpm6bb	tbx5a	-2.654197064	4.869760773	4.515339583	0.033592217	0.804038957
bcs1l	tbx5a	-2.638374182	4.625875519	4.509587175	0.033705375	0.804145007
apela	tbx5a	-2.634260944	4.740663155	4.496812679	0.033958093	0.805076451
mir451a	tbx5a	-2.621542074	5.01291691	4.496526757	0.033963772	0.805076451
ube2nb	tbx5a	-1.618281276	5.768550744	4.491138772	0.034070975	0.805076451
tlk1b	tbx5a	-2.049888051	5.318859711	4.474516557	0.034403934	0.807997328
abhd17c	tbx5a	-2.320239837	5.055427494	4.471812106	0.034458428	0.807997328
crygm3	tbx5a	3.54440662	4.609067724	4.468646398	0.03452233	0.807997328
ddx1	tbx5a	-2.032258795	5.102996152	4.451962618	0.03486116	0.811867536
dixdc1a	tbx5a	-1.634104428	5.625500436	4.449707243	0.03490723	0.811867536
hbl4	tbx5a	2.229618109	5.353637758	4.441947363	0.035066228	0.813008845
tbl3	tbx5a	1.410091101	6.017429345	4.435040435	0.035208386	0.813366818
rad17	tbx5a	-1.965151768	5.442502923	4.430526559	0.035301616	0.813366818
si:ch211-119o8.6	tbx5a	1.653044997	5.960713097	4.412245198	0.035681849	0.817075641
aagab	tbx5a	2.234296005	5.146716551	4.409098511	0.035747728	0.817075641
rdh8a	tbx5a	2.571765695	4.607813618	4.406891411	0.035794011	0.817075641
cs	tbx5a	-1.219309969	6.696722787	4.398797047	0.03596429	0.818436588
apmap	tbx5a	2.578122151	5.165730068	4.384023814	0.03627726	0.823026431
ap2b1	tbx5a	-1.93293533	5.411717274	4.372180178	0.036530225	0.825669229
cyp51	tbx5a	-2.309025055	4.954240223	4.368136111	0.036617024	0.825669229
idh3b	tbx5a	-1.849515759	5.64208504	4.352043397	0.036964569	0.830972511
sde2	tbx5a	-2.181665969	5.02797062	4.339462788	0.037238671	0.834096713
gtf3c6	tbx5a	-1.062234542	7.603754684	4.335333676	0.037329098	0.834096713
mycbp	tbx5a	2.569004339	5.066208762	4.322350301	0.037614934	0.835746194
tmem203	tbx5a	-2.635102159	4.664758588	4.321717757	0.037628919	0.835746194
spon1b	tbx5a	-2.168613426	4.949442877	4.313507509	0.037810925	0.836097814
fitm1	tbx5a	-2.311571113	4.846562289	4.310813628	0.037870845	0.836097814
tdg.1	tbx5a	-1.236975427	6.885143972	4.298306458	0.038150345	0.839761765
tspan31	tbx5a	-2.127802088	5.044533459	4.241526475	0.039446685	0.865720127
cnbpa	tbx5a	-0.919008861	7.995559207	4.214309676	0.040084374	0.876853925
matr3l	tbx5a	-1.313412377	6.378181934	4.209101269	0.040207635	0.876853925
acp1	tbx5a	-2.17627874	5.158694288	4.204375381	0.040319821	0.876853925
zgc:123096	tbx5a	-2.655162526	4.901843343	4.198973016	0.040448468	0.876853925
notum1b	tbx5a	-1.288430015	6.296688866	4.194856373	0.040546788	0.876853925
topbp1	tbx5a	-2.189986451	4.780115104	4.188261839	0.040704811	0.877410337
tspan7b	tbx5a	-2.168946358	4.763734285	4.183896052	0.040809783	0.877410337
cacng1a	tbx5a	-1.94458496	5.102455065	4.165085272	0.041265336	0.881581433
nenf	tbx5a	-2.183039588	5.089452508	4.161813546	0.041345113	0.881581433
zgc:110699	tbx5a	-0.747436915	11.73766889	4.155322991	0.041503858	0.881581433
trip11	tbx5a	-1.883805063	5.343802381	4.139409894	0.041895772	0.881581433
ddx19	tbx5a	-1.403838327	6.175079168	4.133440757	0.042043784	0.881581433
slc5a2	tbx5a	-1.426496067	6.438113737	4.131809404	0.04208433	0.881581433
ppfia2	tbx5a	-2.654672088	4.836725038	4.130059592	0.042127867	0.881581433
smad6a	tbx5a	2.558830199	4.848586278	4.128742077	0.042160679	0.881581433
arcn1a	tbx5a	-1.361263017	5.931332833	4.116221874	0.042473833	0.881581433
atf6b	tbx5a	1.016508457	8.043597027	4.111356324	0.042596189	0.881581433
hagh	tbx5a	-1.919983551	5.104686792	4.108600033	0.042665666	0.881581433
cyp1b1	tbx5a	-1.887203242	5.643421283	4.105116578	0.042753644	0.881581433
senp3b	tbx5a	-1.7638045	5.430346049	4.099017207	0.042908149	0.881581433

Continued on following page

Table B.7: continued from previous page

gene	MO	logFC	logCPM	LR	p value	FDR
scfd1	tbx5a	-2.18368702	5.330972515	4.084054459	0.043289666	0.881581433
mapk12b	tbx5a	-2.282409999	4.685833973	4.079445883	0.043407892	0.881581433
mcrs1	tbx5a	-1.77443891	5.467829039	4.072240748	0.04359341	0.881581433
ormdl1	tbx5a	-2.036066505	5.200883619	4.070885885	0.043628388	0.881581433
senp3a	tbx5a	1.315996775	6.1163736	4.063854177	0.043810398	0.881581433
aktip	tbx5a	-1.749926739	5.67426447	4.056036321	0.044013696	0.881581433
zgc:158463	tbx5a	1.245712573	7.588779911	4.04992366	0.044173342	0.881581433
stam2	tbx5a	-2.175915876	4.970906119	4.04743218	0.044238588	0.881581433
trove2	tbx5a	-1.450460953	5.752167303	4.045437323	0.044290902	0.881581433
igf2bp3	tbx5a	-1.664857582	5.718548869	4.043747915	0.044335256	0.881581433
vcp	tbx5a	-0.922560041	7.814856023	4.038994027	0.044460317	0.881581433
hnrnpr	tbx5a	-2.476374321	4.82990332	3.994372225	0.045652456	0.881581433
socs5a	tbx5a	-3.219958508	4.4781074	3.978807	0.046076186	0.881581433
arf2	tbx5a	-1.017330742	7.118888967	3.967550163	0.046385211	0.881581433
si:dkey-94e7.2	tbx5a	1.718979195	5.279269786	3.966055861	0.046426397	0.881581433
ivns1abpa	tbx5a	-1.307563494	6.508280066	3.964902013	0.046458226	0.881581433
wrnip1	tbx5a	-1.77067236	5.386511423	3.963811512	0.046488328	0.881581433
psip1	tbx5a	-2.495894301	4.666305294	3.963523967	0.046496269	0.881581433
htr5al	tbx5a	-2.476862614	4.542492531	3.959852086	0.046597798	0.881581433
lmx1bb	tbx5a	-3.220001818	4.497464115	3.956355484	0.046694697	0.881581433
arid2	tbx5a	2.220006427	5.318225979	3.955363629	0.046722223	0.881581433
smcr8b	tbx5a	-0.787543209	10.10437351	3.954487773	0.046746543	0.881581433
hemk1	tbx5a	-2.451458375	4.499397115	3.951503651	0.046829506	0.881581433
rhbdl2	tbx5a	-2.486178706	4.672205652	3.946128452	0.046979335	0.881581433
hoxc10a	tbx5a	-0.939555054	8.370266891	3.942979664	0.04706734	0.881581433
ube2b	tbx5a	-3.21136567	4.665886607	3.941798975	0.047100383	0.881581433
ahcyl2	tbx5a	-1.831160931	5.37784797	3.939815899	0.047155938	0.881581433
ube2g2	tbx5a	-2.175739741	4.774891377	3.937856288	0.047210903	0.881581433
polr1c	tbx5a	-1.765612212	5.088010744	3.936298433	0.047254648	0.881581433
znf750	tbx5a	-3.230544172	4.456006017	3.925381898	0.047562386	0.881581433
pygma	tbx5a	-1.543607162	6.255678535	3.924032748	0.047600566	0.881581433
nup98	tbx5a	-1.460079629	6.00424363	3.921153655	0.047682149	0.881581433
prrc1	tbx5a	2.107572602	5.18789149	3.908261354	0.048049282	0.881581433
acer3	tbx5a	-3.230593265	4.57050573	3.907567327	0.04806913	0.881581433
carhsp1	tbx5a	1.558034252	5.549221671	3.904102763	0.048168342	0.881581433
lin37	tbx5a	-2.486295736	4.740635319	3.902225858	0.048222179	0.881581433
znf503	tbx5a	1.135606031	6.543357531	3.898451595	0.048330632	0.881581433
grtp1b	tbx5a	-1.910363093	5.218053426	3.897640123	0.048353983	0.881581433
nr2c2	tbx5a	-2.191276345	4.706888651	3.896559791	0.04838509	0.881581433
ctssb.2	tbx5a	-2.468707884	4.758333059	3.89043721	0.04856178	0.881581433
fkbp4	tbx5a	-1.035260698	6.892727624	3.888572966	0.048615715	0.881581433
cmn	tbx5a	-1.310954991	5.994346196	3.886989681	0.048661571	0.881581433
smad1	tbx5a	-3.209617789	4.521970551	3.882042557	0.048805148	0.881581433
psmd10	tbx5a	-3.231928388	4.608365481	3.876870175	0.04895574	0.881581433
actl6a	tbx5a	-1.100348222	6.748043051	3.863671517	0.049342242	0.881581433
ccnd2a	tbx5a	-2.478232027	4.662270917	3.859615602	0.049461659	0.881581433
nfkb2	tbx5a	-2.455293318	4.761574922	3.844996347	0.04989463	0.881581433
plxna3	tbx5b	-5.105429528	5.162244018	12.47240823	0.000413007	0.987649759
itpa	tbx5b	-4.868623608	4.64653994	11.21410894	0.000811778	0.987649759
nup155	tbx5b	-2.7922614	5.727737174	10.52891643	0.001175211	0.987649759
glyr1	tbx5b	-3.036152096	5.694117425	10.24633962	0.001369561	0.987649759

Continued on following page

Table B.7: continued from previous page

gene	MO	logFC	logCPM	LR	p value	FDR
pgam2	tbx5b	4.789983482	4.795825395	9.993120571	0.001571261	0.987649759
ttc8	tbx5b	-4.737783228	4.89841886	9.945616225	0.001612329	0.987649759
use1	tbx5b	4.654361351	4.885233615	9.938653126	0.001618439	0.987649759
zgc:123172	tbx5b	-4.734065645	4.856535282	9.695848888	0.001846847	0.987649759
asrgl1	tbx5b	-4.593594785	4.995294544	9.612976852	0.001932072	0.987649759
sri	tbx5b	-4.593824825	5.088896444	9.352376075	0.002226966	0.987649759
gnat2	tbx5b	-3.322619672	5.495126724	9.208670561	0.002408716	0.987649759
zc3h10	tbx5b	-4.590301738	4.621317842	9.207243604	0.002410594	0.987649759
unc119b	tbx5b	-4.427854186	5.008503071	9.113173745	0.002537752	0.987649759
tmem180	tbx5b	-4.429081514	4.832690996	9.010959955	0.002683654	0.987649759
flot2b	tbx5b	-4.593335459	4.828319451	8.881921901	0.002880082	0.987649759
cds2	tbx5b	4.482936755	4.909946844	8.760739203	0.003077843	0.987649759
timm10	tbx5b	-2.815631695	5.425879825	8.596281403	0.003368501	0.987649759
g0s2	tbx5b	2.343424686	6.111416538	8.560367742	0.0034356	0.987649759
iars2	tbx5b	-4.427433137	4.826440796	8.464554587	0.003621339	0.987649759
reps1	tbx5b	-4.426244047	4.690060896	8.442386645	0.003665748	0.987649759
wdr91	tbx5b	-4.427071772	4.918391916	8.419871373	0.00371142	0.987649759
slc39a13	tbx5b	-4.428128345	4.623196792	8.340049353	0.003878054	0.987649759
ier2	tbx5b	-3.224539041	5.22816007	8.253166215	0.004068098	0.987649759
gtf2b	tbx5b	-2.230642574	5.891029093	8.220763668	0.004141377	0.987649759
notch1a	tbx5b	-2.520379751	5.728918434	8.163456373	0.004274284	0.987649759
dedd	tbx5b	-3.212868718	5.247857478	8.126205079	0.004362997	0.987649759
robo3	tbx5b	-2.173043961	5.908806955	8.093290857	0.004442942	0.987649759
hiat1a	tbx5b	4.302357476	4.565926035	8.087708846	0.004456647	0.987649759
csnk1db	tbx5b	-2.173216449	5.833815163	7.997464759	0.004684289	0.987649759
mgrn1a	tbx5b	-4.247127755	4.603608113	7.915293095	0.004901864	0.987649759
zgc:110269	tbx5b	-4.247469935	4.896604311	7.896896413	0.004951969	0.987649759
hoxb2a	tbx5b	4.318850134	4.711245823	7.786708944	0.005263198	0.987649759
epb41l5	tbx5b	4.315205365	4.886314752	7.769690736	0.005313014	0.987649759
zgc:77398	tbx5b	-2.724149471	5.410634272	7.694950858	0.005537552	0.987649759
bcap29	tbx5b	-3.11103109	5.195961948	7.646443046	0.005688437	0.987649759
sin3aa	tbx5b	-4.244603254	5.01515906	7.611674862	0.005799159	0.987649759
mus81	tbx5b	-4.24584426	4.850468043	7.610746409	0.005802146	0.987649759
dpp7	tbx5b	-1.390184502	8.522502226	7.580568805	0.005900082	0.987649759
hif1an	tbx5b	-4.247517337	4.842556488	7.552585676	0.005992403	0.987649759
tdp2b	tbx5b	4.095191847	4.585143692	7.456976492	0.006319106	0.987649759
hpca	tbx5b	-4.243800881	4.763201758	7.452099473	0.00633625	0.987649759
ralba	tbx5b	-4.24887957	4.546927469	7.392773302	0.006548644	0.987649759
fzd1	tbx5b	-4.247715663	4.726835324	7.351796206	0.006699579	0.987649759
cyp4t8	tbx5b	4.282510231	4.671045414	7.296287832	0.006909722	0.987649759
znf143a	tbx5b	4.103957773	4.932093603	7.282159329	0.006964277	0.987649759
jph1b	tbx5b	-4.247781844	4.810785376	7.282080618	0.006964582	0.987649759
nipa2	tbx5b	4.103123686	4.849122385	7.261553135	0.007044634	0.987649759
rint1	tbx5b	-3.10083273	5.305636988	7.15038981	0.00749477	0.987649759
ing5b	tbx5b	4.088569841	4.80614603	7.134286835	0.007562371	0.987649759
pimr136	tbx5b	4.10061242	4.850889052	7.12085236	0.007619247	0.987649759
akirin2	tbx5b	2.113713916	5.982395326	7.07958731	0.007796696	0.987649759
elovl5	tbx5b	4.114803545	4.905003326	7.064196687	0.007863957	0.987649759
isl2a	tbx5b	4.097674579	4.755854161	7.050168192	0.007925781	0.987649759
ube2b	tbx5b	-4.036623499	4.665886607	7.047710567	0.007936663	0.987649759
psmd9	tbx5b	4.094636349	4.77970877	7.043867514	0.00795371	0.987649759

Continued on following page

Table B.7: continued from previous page

gene	MO	logFC	logCPM	LR	p value	FDR
pole	tbx5b	-2.389829146	5.704392108	7.004194088	0.008131897	0.987649759
sptlc3	tbx5b	-4.035283012	4.543328438	6.9746588	0.008267198	0.987649759
ctc1	tbx5b	-4.037066634	5.0262711	6.947541081	0.008393452	0.987649759
ighmbp2	tbx5b	-4.039236419	5.033948084	6.935033742	0.008452347	0.987649759
abi1a	tbx5b	4.084295105	4.802099143	6.888637306	0.008674537	0.987649759
mpp1	tbx5b	-4.037169561	4.848242606	6.869955854	0.008765682	0.987649759
dmbx1a	tbx5b	-4.037170656	4.540397717	6.869118373	0.008769791	0.987649759
zgc:92591	tbx5b	3.100727591	4.915979471	6.863797123	0.008795944	0.987649759
mrpl36	tbx5b	-2.984274998	5.097658319	6.837875286	0.008924493	0.987649759
ttc14	tbx5b	-1.614546357	8.019481288	6.837736137	0.008925188	0.987649759
nptxrb	tbx5b	-4.032958478	4.520337561	6.788550587	0.009174437	0.987649759
zfyve21	tbx5b	-4.034920497	4.850370893	6.771067999	0.009264738	0.987649759
pcsk5b	tbx5b	4.106039719	4.704246409	6.731158931	0.009474302	0.987649759
ube2e3	tbx5b	-1.601880723	6.385153997	6.729082866	0.009485336	0.987649759
p2rx2	tbx5b	4.113945966	4.786712989	6.719082115	0.009538671	0.987649759
mysm1	tbx5b	-4.035681992	4.765739091	6.685708823	0.009718887	0.987649759
zgc:66474	tbx5b	-4.03269303	4.778091756	6.597348936	0.010213072	0.987649759
ticrr	tbx5b	-4.031274625	4.954805889	6.5755064	0.010339158	0.987649759
dpysl2b	tbx5b	-4.031589184	4.833125904	6.524389181	0.010640509	0.987649759
traf6	tbx5b	-4.038047754	4.813305616	6.505721597	0.010752792	0.987649759
flot2a	tbx5b	-1.606863419	6.623449337	6.490139296	0.010847448	0.987649759
nr1h3	tbx5b	-4.033836496	4.587570355	6.489849914	0.010849214	0.987649759
si:dkey-13i19.8	tbx5b	-2.987361439	5.212559133	6.486175958	0.010871659	0.987649759
lias	tbx5b	-2.985579793	4.862382974	6.402376168	0.011396773	0.987649759
tdg.1	tbx5b	-1.481479389	6.885143972	6.399418993	0.011415772	0.987649759
sos1	tbx5b	-2.63353943	4.980994313	6.392383304	0.011461105	0.987649759
ldlrap1a	tbx5b	-4.038867333	4.604546759	6.371372975	0.011597583	0.987649759
ube2t	tbx5b	-4.035763087	4.662492213	6.348417619	0.011748605	0.987649759
zgc:113090	tbx5b	-1.535911105	6.7574879	6.177326915	0.012939762	0.987649759
fam84b	tbx5b	3.851481667	4.562327479	6.148812987	0.013150033	0.987649759
psen1	tbx5b	-2.430857383	5.392360574	6.101108817	0.013509709	0.987649759
brd4	tbx5b	-2.297204373	5.474768796	6.09892914	0.013526383	0.987649759
fanca	tbx5b	3.854157236	4.868864094	6.094578603	0.013559726	0.987649759
pef1	tbx5b	3.869708597	4.71935328	6.079459062	0.013676264	0.987649759
pdxp	tbx5b	-4.041914532	4.68407944	6.066226253	0.013779105	0.987649759
pbdc1	tbx5b	-1.878362985	5.989602969	6.05905446	0.013835174	0.987649759
zgc:65873	tbx5b	-2.532037273	5.267362224	6.009360968	0.01423018	0.987649759
mrpl46	tbx5b	-2.528012612	4.965100712	5.997282689	0.01432793	0.987649759
klhl11	tbx5b	3.841076032	4.500319266	5.994578855	0.014349906	0.987649759
lin7c	tbx5b	-2.214188405	5.447001415	5.989106713	0.01439449	0.987649759
zgc:123284	tbx5b	-2.851597273	5.026749983	5.979319401	0.014474587	0.987649759
kdelr3	tbx5b	3.123207505	4.742146227	5.928751204	0.014895794	0.987649759
eno3	tbx5b	1.620405277	6.029719686	5.92325543	0.014942325	0.987649759
scfd1	tbx5b	-2.541719734	5.330972515	5.914821153	0.015014027	0.987649759
pxk	tbx5b	-3.791261938	4.455247958	5.893684015	0.01519528	0.987649759
rab3da	tbx5b	-3.789331847	4.458734325	5.888695731	0.015238382	0.987649759
wdyhv1	tbx5b	3.851598903	4.646721708	5.884947548	0.015270853	0.987649759
grhl2b	tbx5b	-3.787404588	4.49939578	5.883557547	0.015282912	0.987649759
dido1	tbx5b	-2.086068096	5.903494456	5.87856591	0.0153263	0.987649759
fam117bb	tbx5b	-2.862855075	5.191159718	5.86605228	0.015435629	0.987649759
stt3b	tbx5b	-2.083322664	5.538153313	5.86551867	0.015440309	0.987649759

Continued on following page

Table B.7: continued from previous page

gene	MO	logFC	logCPM	LR	p value	FDR
npm2	tbx5b	3.847963	4.72692797	5.862146517	0.015469917	0.987649759
ehmt1a	tbx5b	-2.861004822	4.97688664	5.856733303	0.015517568	0.987649759
gda	tbx5b	-2.298131324	5.973071336	5.85556183	0.0155279	0.987649759
wtap	tbx5b	-1.871211393	5.763156814	5.840086844	0.015665053	0.987649759
idh3b	tbx5b	-2.089080504	5.64208504	5.818767333	0.015856053	0.987649759
edc4	tbx5b	-2.294864961	5.515490244	5.813462848	0.015903948	0.987649759
her7	tbx5b	3.83562781	4.624392557	5.806490301	0.01596713	0.987649759
zgc:194202	tbx5b	3.847864759	4.65995539	5.803596017	0.015993432	0.987649759
toe1	tbx5b	-2.848077674	5.070518647	5.78347694	0.016177509	0.987649759
ppa1b	tbx5b	1.904010551	5.851347834	5.780484977	0.016205069	0.987649759
haus3	tbx5b	-3.789289423	4.703233484	5.769453593	0.016307104	0.987649759
ube2f	tbx5b	-3.791896347	4.935838814	5.748326127	0.016504375	0.987649759
gorab	tbx5b	-3.79335615	4.609582252	5.729524703	0.016681997	0.987649759
clk4b	tbx5b	-3.791943273	4.697026309	5.722631413	0.016747613	0.987649759
mthfd1l	tbx5b	-1.4767019	6.512760531	5.718461642	0.016787433	0.987649759
ptbp2b	tbx5b	2.432583451	5.171703234	5.706359962	0.016903554	0.987649759
zgc:113944	tbx5b	-3.787414918	4.580785788	5.699860824	0.016966258	0.987649759
znf207a	tbx5b	-1.671753244	6.201653075	5.67729089	0.017185884	0.987649759
polr2j	tbx5b	2.439554583	4.992804292	5.674950889	0.017208822	0.987649759
mtf2	tbx5b	3.874915453	4.667719316	5.655422002	0.017401487	0.987649759
zgc:158482	tbx5b	-3.791623852	4.833017356	5.6542873	0.01741275	0.987649759
eif4a1a	tbx5b	-1.010745253	8.287708605	5.633101969	0.017624417	0.987649759
med16	tbx5b	-3.78681749	4.721106882	5.614119044	0.017816335	0.987649759
chrm5a	tbx5b	-1.895258646	5.924598717	5.602273558	0.017937186	0.987649759
wdr6	tbx5b	-3.78968777	4.790070204	5.60216602	0.017938287	0.987649759
znf410	tbx5b	-2.122457874	5.553264331	5.595349177	0.018008221	0.987649759
mri1	tbx5b	-3.791715593	4.704831915	5.589425732	0.018069219	0.987649759
vcp	tbx5b	-1.074246354	7.814856023	5.565110811	0.018321851	0.987649759
dvl2	tbx5b	-3.784198167	4.542546546	5.554563079	0.018432573	0.987649759
slc29a1a	tbx5b	-3.784602261	4.778603524	5.537785358	0.018610119	0.987649759
ccz1	tbx5b	-2.431487968	5.224300306	5.525225851	0.018744183	0.987649759
csrp2bp	tbx5b	-3.787081012	4.796341146	5.506485697	0.018946078	0.987649759
cebpz	tbx5b	-1.355635749	6.778863281	5.486016916	0.019169166	0.987649759
srebf2	tbx5b	-1.852868116	5.810240438	5.480220235	0.019232836	0.987649759
zgc:152774	tbx5b	3.876951628	4.731391106	5.467066984	0.01937812	0.987649759
rarab	tbx5b	-2.44041528	5.421073691	5.461651304	0.019438269	0.987649759
cdk2	tbx5b	-2.42838063	5.045019928	5.445378481	0.019620163	0.987649759
skib	tbx5b	-1.815860211	5.774048906	5.442828733	0.019648823	0.987649759
mrpl37	tbx5b	-1.719585578	5.853042286	5.421708884	0.019887886	0.987649759
ahrra	tbx5b	2.128259682	5.27662251	5.418211123	0.019927767	0.987649759
ddx23	tbx5b	-1.420859133	6.526317905	5.389169821	0.020262108	0.987649759
LOC100535586	tbx5b	-3.792520531	4.770055061	5.380857678	0.020358867	0.987649759
heatr3	tbx5b	2.154934351	5.368474986	5.367085984	0.020520231	0.987649759
si:dkey-31g6.6	tbx5b	-2.44202145	5.016331145	5.346866186	0.02075955	0.987649759
mtss1	tbx5b	2.818842841	4.912770099	5.344509854	0.020787627	0.987649759
tmem119b	tbx5b	-2.851069511	4.641685883	5.324984829	0.021021792	0.987649759
cdh6	tbx5b	-1.866190905	5.868524423	5.323412931	0.021040762	0.987649759
mgst3	tbx5b	-2.1290864	5.089450444	5.322460445	0.021052266	0.987649759
inpp5e	tbx5b	-2.309308378	5.347170517	5.320461318	0.021076431	0.987649759
si:dkey-4p15.3	tbx5b	-3.793382192	4.623669337	5.31661406	0.021123017	0.987649759
acss2	tbx5b	-1.864042006	5.778791376	5.279958518	0.021572262	0.987649759

Continued on following page

Table B.7: continued from previous page

gene	MO	logFC	logCPM	LR	p value	FDR
ndfip1	tbx5b	-2.123478678	5.170945807	5.262495563	0.021789753	0.987649759
bcor	tbx5b	-2.713512265	5.049493551	5.254669833	0.021887954	0.987649759
acss2l	tbx5b	2.837226116	5.080069376	5.252314991	0.021917593	0.987649759
arid3c	tbx5b	-2.706519635	5.372522901	5.226940089	0.022239624	0.987649759
zzz3	tbx5b	-2.848573464	4.661204396	5.22522099	0.022261618	0.987649759
ctxn1	tbx5b	1.967457521	5.994727883	5.207713898	0.022486884	0.987649759
ube2v2	tbx5b	-1.217293948	7.254143648	5.161300867	0.023095592	0.987649759
cstf2	tbx5b	-1.537171351	6.077061499	5.160057924	0.023112127	0.987649759
slc43a1b	tbx5b	-2.714025998	5.07010614	5.093642552	0.024013702	0.987649759
pop5	tbx5b	3.561494838	4.583960385	5.067721509	0.024375403	0.987649759
rer1	tbx5b	-2.024340477	5.831627061	5.061609457	0.024461511	0.987649759
zgc:153990	tbx5b	3.553947013	4.814649494	5.038043801	0.024796476	0.987649759
foxa3	tbx5b	-2.709799093	4.834141315	5.031117693	0.024895827	0.987649759
atp1b2b	tbx5b	-2.712515094	5.136708399	5.023423503	0.025006681	0.987649759
zgc:92027	tbx5b	-1.718231211	5.917974174	5.010024414	0.025200952	0.987649759
pnp4a	tbx5b	3.553404249	4.457911454	5.00526714	0.025270303	0.987649759
aoc2	tbx5b	3.562125395	4.566563984	5.001315061	0.025328067	0.987649759
sema3d	tbx5b	3.540123666	4.885902144	4.99639022	0.025400241	0.987649759
elovl7b	tbx5b	3.565922466	4.897777192	4.989075904	0.025507827	0.987649759
sf3a1	tbx5b	-1.541872496	6.519397746	4.983654032	0.025587883	0.987649759
si:ch211-5k11.12	tbx5b	1.918156826	5.038964332	4.983200568	0.02559459	0.987649759
lepr	tbx5b	2.451104138	5.235183413	4.978692744	0.025661367	0.987649759
pex3	tbx5b	3.562413395	4.604242631	4.970199832	0.025787668	0.987649759
socs5a	tbx5b	-3.494322197	4.4781074	4.925318241	0.026465927	0.987649759
atp6v0cb	tbx5b	3.566832879	4.564283671	4.918412902	0.026571916	0.987649759
arl8	tbx5b	-1.597780522	5.789887442	4.893134151	0.026963695	0.987649759
nadl1.1	tbx5b	3.56746572	4.976317921	4.867643928	0.027364837	0.987649759
tspan33	tbx5b	3.563341357	4.693084872	4.866391	0.027384714	0.987649759
rheb	tbx5b	1.668180847	5.776351306	4.860983105	0.027470678	0.987649759
ppil3	tbx5b	-3.494067444	4.646941051	4.842331657	0.027769324	0.987649759
siah2l	tbx5b	2.316006846	5.028288524	4.833470159	0.027912395	0.987649759
otud3	tbx5b	3.573273894	4.642676067	4.81262046	0.028252053	0.987649759
rabl2	tbx5b	-3.494868305	4.608641168	4.810429895	0.028287988	0.987649759
rnasen	tbx5b	-3.495830081	4.582876791	4.805466202	0.02836959	0.987649759
sfr1	tbx5b	-1.375694969	6.479332655	4.795623287	0.028532131	0.987649759
glmna	tbx5b	-2.703400363	4.83444326	4.786194779	0.028688739	0.987649759
zgc:113229	tbx5b	-2.20099241	5.413945463	4.782885692	0.028743914	0.987649759
shha	tbx5b	2.055235947	4.950188849	4.7812007	0.028772052	0.987649759
serinc5	tbx5b	3.554694643	4.645425025	4.778423855	0.028818486	0.987649759
zgc:153631	tbx5b	-3.492327413	4.718681681	4.776516029	0.028850434	0.987649759
eps8l1	tbx5b	3.568577292	4.652177688	4.774972699	0.028876304	0.987649759
h2afy	tbx5b	-3.490157013	4.645119747	4.774890207	0.028877688	0.987649759
LOC570474	tbx5b	-3.495980085	4.452409647	4.759779337	0.029132283	0.987649759
ephb4a	tbx5b	-3.49184666	4.643311648	4.743512824	0.029408963	0.987649759
efhc2	tbx5b	-3.494142378	4.518802136	4.737953628	0.029504146	0.987649759
tyrp1b	tbx5b	-3.49652026	4.54228666	4.728830957	0.029661039	0.987649759
alpi.1	tbx5b	-3.492224143	4.474481836	4.719294444	0.029825979	0.987649759
kdm6al	tbx5b	-3.490298195	4.885813214	4.715092094	0.029898964	0.987649759
mrpl41	tbx5b	-3.497088759	4.519534898	4.699313628	0.030174666	0.987649759
dusp4	tbx5b	-3.494633373	4.738307374	4.689393372	0.03034936	0.987649759
actn3b	tbx5b	-2.033400672	5.472207434	4.676827375	0.030572161	0.987649759

Continued on following page

Table B.7: continued from previous page

gene	MO	logFC	logCPM	LR	p value	FDR
gtf3c6	tbx5b	-1.095699329	7.603754684	4.674361697	0.030616078	0.987649759
trim55a	tbx5b	-3.492131897	4.699792667	4.666589692	0.03075494	0.987649759
nfkbie	tbx5b	-3.497711849	4.520841531	4.665052077	0.03078249	0.987649759
tomm22	tbx5b	-1.674729637	5.937303375	4.656069512	0.03094395	0.987649759
hs6st1b	tbx5b	2.663070967	4.818424445	4.648002122	0.031089712	0.987649759
tor1	tbx5b	-3.489550952	4.719040031	4.647827848	0.031092869	0.987649759
raph1b	tbx5b	-3.497324351	4.908504318	4.642948578	0.031181384	0.987649759
snx18a	tbx5b	-2.714698446	4.66192986	4.632515625	0.031371534	0.987649759
ache	tbx5b	3.534797491	4.709371737	4.626783275	0.031476525	0.987649759
eftud2	tbx5b	-1.07955809	7.19525357	4.622100644	0.031562562	0.987649759
isoc1	tbx5b	2.668613539	5.066829557	4.601041894	0.031952532	0.987649759
ydjc	tbx5b	-3.489798428	4.645095039	4.592690818	0.032108568	0.987649759
med24	tbx5b	-2.196813635	5.367038498	4.57883324	0.032369248	0.987649759
panx1a	tbx5b	-3.498113802	4.722873094	4.57764465	0.03239171	0.987649759
nr1d2b	tbx5b	-3.489705499	4.649525725	4.569008236	0.032555407	0.987649759
actn2b	tbx5b	2.433433326	4.914542972	4.555235245	0.032818255	0.987649759
pdxka	tbx5b	-3.496074932	4.590966939	4.553718428	0.032847338	0.987649759
mrpl32	tbx5b	-2.194179953	4.897764065	4.540605791	0.033099876	0.987649759
smtnl	tbx5b	-1.479222147	5.969144292	4.509741001	0.033702344	0.987649759
zgpat	tbx5b	2.316865087	5.024774474	4.50113629	0.033872338	0.987649759
pola1	tbx5b	-2.201516812	5.527854294	4.496190324	0.033970456	0.987649759
zgc:63882	tbx5b	-1.086439627	8.313379368	4.490279702	0.0340881	0.987649759
siah1	tbx5b	-2.551479167	5.165042504	4.488475994	0.034124085	0.987649759
pdlim5b	tbx5b	-2.54350124	4.929169397	4.487331665	0.034146936	0.987649759
asb2b	tbx5b	-2.544251024	5.239559327	4.483834768	0.034216864	0.987649759
si:dkeyp-120h9.1	tbx5b	-2.54921353	5.12206978	4.474342055	0.034407448	0.987649759
nfe2l3	tbx5b	-1.679872118	5.578111317	4.439525374	0.035116009	0.987649759
rap2c	tbx5b	-2.199512458	5.038355354	4.417726184	0.035567402	0.987649759
igf2bp3	tbx5b	-1.716722485	5.718548869	4.408968118	0.03575046	0.987649759
limk2	tbx5b	1.749429831	5.321268569	4.407598901	0.035779168	0.987649759
trpm4b.2	tbx5b	-3.49823851	4.74708742	4.405368641	0.035825981	0.987649759
exd1	tbx5b	2.676173481	4.738758736	4.403372339	0.035867937	0.987649759
ppig	tbx5b	-0.842852401	8.828693829	4.397941613	0.035982335	0.987649759
chd8	tbx5b	-1.443520785	6.244245634	4.391808277	0.036111993	0.987649759
irf2bp2b	tbx5b	-1.479873942	5.926996968	4.38596733	0.036235925	0.987649759
zgc:111986	tbx5b	-1.603160357	5.651911329	4.38416173	0.036274325	0.987649759
itsn1	tbx5b	-1.918646427	5.417202813	4.37493105	0.036471306	0.987649759
dbt	tbx5b	-1.426916282	6.245989883	4.370140454	0.036573977	0.987649759
six1a	tbx5b	-2.553939942	4.877226822	4.365689136	0.036669648	0.987649759
usf2	tbx5b	-1.395286973	6.353129809	4.348081834	0.037050654	0.987649759
sf1	tbx5b	-1.148510692	6.715853215	4.336611689	0.037301086	0.987649759
tmem54a	tbx5b	-2.19315272	4.754277421	4.318769474	0.037694171	0.987649759
atp5s	tbx5b	-2.543735745	4.894752322	4.302310816	0.038060624	0.987649759
ccnb2	tbx5b	-2.549394722	5.068922619	4.29645933	0.038191806	0.987649759
papss1	tbx5b	-2.54622911	4.884394051	4.28167523	0.03852536	0.987649759
hspa4a	tbx5b	-1.155039705	6.754674744	4.275531791	0.038664863	0.987649759
anapc15	tbx5b	-2.19200852	5.040784514	4.252388415	0.03919517	0.987649759
med21	tbx5b	2.192140883	5.100861937	4.245820291	0.039347057	0.987649759
api5	tbx5b	-0.976605258	7.546651462	4.225933332	0.039810718	0.987649759
lhx2a	tbx5b	-2.539711549	4.582001713	4.217495802	0.040009167	0.987649759
rab18b	tbx5b	-2.197365417	5.096590204	4.21311713	0.040112561	0.987649759

Continued on following page

Table B.7: continued from previous page

gene	MO	logFC	logCPM	LR	p value	FDR
golga7	tbx5b	-1.702541434	5.589008462	4.209567258	0.04019659	0.987649759
mrpl34	tbx5b	-1.435231291	6.017024707	4.207002348	0.04025742	0.987649759
foxn4	tbx5b	-2.544920882	5.027374857	4.200675853	0.040407872	0.987649759
hoxc5a	tbx5b	-1.920822765	5.776224485	4.184224765	0.04080187	0.987649759
stk25b	tbx5b	2.185450648	5.176449117	4.180670298	0.040887526	0.987649759
fkbp7	tbx5b	-1.923607298	5.095522121	4.168116533	0.041191566	0.987649759
mibp	tbx5b	1.752408954	5.362962853	4.153591722	0.041546309	0.987649759
aldh4a1	tbx5b	-1.470619756	5.919484875	4.153138411	0.041557431	0.987649759
hormad1	tbx5b	1.915784611	5.125791831	4.14349254	0.041794853	0.987649759
glo1	tbx5b	1.584407521	5.532556965	4.133764886	0.042035732	0.987649759
ccnb3	tbx5b	-2.303192677	5.052679844	4.117997641	0.042429269	0.987649759
pus7l	tbx5b	-2.540440026	4.667699751	4.106219083	0.042725779	0.987649759
zgc:85944	tbx5b	1.320037048	6.393728471	4.100420673	0.042872545	0.987649759
slmapa	tbx5b	-1.544957928	5.692643657	4.088635438	0.043172483	0.987649759
rragcb	tbx5b	-2.195199706	5.153758547	4.084546162	0.043277072	0.987649759
jag1b	tbx5b	1.384495863	6.264392841	4.075411235	0.043511673	0.987649759
jmjd4	tbx5b	-1.184981988	6.589315304	4.062938193	0.043834166	0.987649759
blvrb	tbx5b	2.066224185	4.935576027	4.049744963	0.044178019	0.987649759
apool	tbx5b	-0.874955736	8.34158819	4.045669899	0.044284799	0.987649759
elf2b	tbx5b	-2.03136912	5.361474746	4.045565964	0.044287526	0.987649759
pcbp2	tbx5b	-1.179746107	6.588005204	4.043505946	0.044341612	0.987649759
soul3	tbx5b	2.188514722	5.048267615	4.042291456	0.044373532	0.987649759
skilb	tbx5b	2.188328224	5.033484913	4.041261669	0.044400616	0.987649759
zgc:101723	tbx5b	-2.534104366	4.735300202	4.023237671	0.044877483	0.987649759
hk1	tbx5b	-1.15954726	6.513493197	4.021868309	0.044913933	0.987649759
ndufa12	tbx5b	1.937892058	5.093247884	4.015501468	0.045083814	0.987649759
eif2ak1	tbx5b	-2.207798973	4.915263059	4.012518228	0.045163647	0.987649759
atp2a2a	tbx5b	2.475753291	4.850441106	4.005611158	0.045349053	0.987649759
tfam	tbx5b	-1.389599851	6.050483666	3.988781259	0.045804184	0.987649759
desma	tbx5b	-1.000399216	7.222066614	3.983356831	0.0459519	0.987649759
cyp2y3	tbx5b	-1.374518182	6.027907036	3.97947809	0.046057832	0.987649759
zgc:153018	tbx5b	1.44438378	5.915521791	3.978882704	0.046074115	0.987649759
rqcd1	tbx5b	1.6729428	5.445846913	3.966098395	0.046425224	0.987649759
pdhb	tbx5b	-1.464848545	5.809709968	3.965208334	0.046449774	0.987649759
galnt6	tbx5b	-2.366425434	5.343235024	3.960770118	0.046572392	0.987649759
slc5a12	tbx5b	3.182947951	4.433034512	3.957418623	0.046665213	0.987649759
cdkn1bb	tbx5b	1.389583052	5.900183973	3.949867591	0.046875056	0.987649759
tpd52	tbx5b	3.183162305	4.504551161	3.935529509	0.047276255	0.987649759
si:dkey-6a5.3	tbx5b	3.183200756	4.643857184	3.931565945	0.047387799	0.987649759
glmp	tbx5b	3.172564319	4.542046995	3.929974096	0.047432675	0.987649759
dcun1d2b	tbx5b	3.190911136	5.058288331	3.924591061	0.047584762	0.987649759
dennd5b	tbx5b	-1.628816751	5.711284772	3.923052453	0.047628327	0.987649759
pip5k1bb	tbx5b	3.179380909	4.498425687	3.922293536	0.047649831	0.987649759
rasgrp4	tbx5b	-1.627794574	5.900223076	3.919250928	0.047736146	0.987649759
ptrh2	tbx5b	2.475938063	4.582036408	3.917236122	0.047793394	0.987649759
gys2	tbx5b	3.179385161	4.647895806	3.915104761	0.047854033	0.987649759
tmem160	tbx5b	3.175518609	4.455992439	3.911344134	0.047961223	0.987649759
mtg1	tbx5b	3.176021912	4.621244888	3.910617887	0.047981953	0.987649759
ssrp1a	tbx5b	-0.830835153	8.143600389	3.909574195	0.04801176	0.987649759
slc6a11a	tbx5b	-2.188538853	4.869701863	3.907148544	0.048081111	0.987649759
zgc:65894	tbx5b	3.179391754	4.522806918	3.903886577	0.048174539	0.987649759

Continued on following page

Table B.7: continued from previous page

gene	MO	logFC	logCPM	LR	p value	FDR
tsen15	tbx5b	3.183565425	4.620304945	3.89339827	0.048476243	0.987649759
tmem206	tbx5b	3.187494912	4.585923482	3.881409435	0.048823554	0.987649759
raraa	tbx5b	-1.758640804	5.260122726	3.877826412	0.048927862	0.987649759
nudt22	tbx5b	-0.997293365	7.771353817	3.866804942	0.049250194	0.987649759
lnx2b	tbx5b	2.486215673	4.766535819	3.866156159	0.049269237	0.987649759
tmco1	tbx5b	-1.7551904	5.639033509	3.866071336	0.049271728	0.987649759
cdon	tbx5b	-1.409452656	5.829942176	3.864316911	0.049323268	0.987649759
fam49ba	tbx5b	1.668989815	5.26721342	3.862243391	0.049384255	0.987649759
erbb2	tbx5b	3.175679429	4.569899389	3.860038692	0.049449188	0.987649759
l3mbtl2	tbx5b	1.598184679	5.580413524	3.85891349	0.049482362	0.987649759
cnpy1	tbx5b	2.684310715	4.725069568	3.85441336	0.049615275	0.987649759
wdr36	tbx5b	1.673244636	5.418367385	3.852624795	0.049668205	0.987649759
arl4d	tbx5b	1.44554869	5.644265898	3.851961072	0.049687862	0.987649759
mt2	tbx5b	3.175615645	4.719502841	3.850409231	0.049733855	0.987649759
agps	tbx5b	3.174993098	4.703651948	3.845782121	0.049871257	0.987649759
ret	tbx5b	3.175578322	4.58515956	3.844743132	0.049902165	0.987649759
actn3b	double	-3.189699398	5.472207434	13.23079814	0.000275387	0.571039858
obsl1a	double	-4.039047183	5.126767919	13.12338074	0.000291633	0.571039858
kank3	double	-3.513978651	5.502413908	12.81706071	0.000343473	0.571039858
limk2	double	3.879504061	5.321268569	12.7766444	0.000350974	0.571039858
orc3	double	5.048738315	5.188518174	12.59854859	0.000386046	0.571039858
ube2f	double	-5.062934572	4.935838814	12.05863773	0.00051553	0.609217698
unc119b	double	-4.812100858	5.008503071	11.40772409	0.000731394	0.609217698
jph1b	double	-5.048813874	4.810785376	11.19116236	0.000821878	0.609217698
ctdsplb	double	-4.959837373	4.986038072	10.98220499	0.000919909	0.609217698
dynll2a	double	3.766160935	5.29493067	10.97771675	0.00092214	0.609217698
asrgl1	double	-4.834720041	4.995294544	10.93031272	0.000946035	0.609217698
ahsa1a	double	4.793913858	4.963423654	10.82986867	0.000998757	0.609217698
ube2j1	double	-4.846976557	4.608611846	10.70091411	0.001070826	0.609217698
gga1	double	2.812001536	5.563297147	10.16630016	0.00143031	0.737080823
shha	double	3.638764943	4.950188849	10.08490241	0.001494891	0.737080823
pimr110	double	4.659509546	4.64623133	9.670438039	0.001872567	0.741306715
fam117bb	double	-3.491702949	5.191159718	9.530731667	0.002020595	0.741306715
ugt2a6	double	-4.641900218	4.682862299	9.370959639	0.002204501	0.741306715
tcta	double	4.495943921	5.103608897	9.310539693	0.002278394	0.741306715
slc5a2	double	-2.090868616	6.438113737	9.31020931	0.002278804	0.741306715
traf6	double	-4.641001433	4.813305616	9.171905824	0.002457585	0.741306715
mboat7	double	-3.008863117	5.379445385	9.050874583	0.002625692	0.741306715
nrp2b	double	-2.712759988	5.602135117	9.02968388	0.002656304	0.741306715
mysm1	double	-4.543897798	4.765739091	8.94126428	0.002787997	0.741306715
coro2a	double	3.042805681	5.201973243	8.772728757	0.003057677	0.741306715
raph1b	double	-4.56137223	4.908504318	8.766475051	0.003068178	0.741306715
ticrr	double	-4.531458297	4.954805889	8.730029368	0.003130115	0.741306715
hpca	double	-4.532290273	4.763201758	8.706821012	0.003170216	0.741306715
flot2a	double	-1.846626071	6.623449337	8.694064416	0.003192479	0.741306715
polr1e	double	4.503513069	5.03980373	8.689538114	0.003200417	0.741306715
pbdc1	double	-2.215212914	5.989602969	8.682789866	0.003212289	0.741306715
kif3b	double	-4.515569181	4.691852803	8.679835351	0.003217501	0.741306715
bre	double	4.503369211	4.684680672	8.607788424	0.003347285	0.741306715
trim55a	double	-4.484767586	4.699792667	8.575135527	0.003407846	0.741306715
tmem180	double	-4.338894905	4.832690996	8.411566992	0.003728412	0.747959233

Continued on following page

Table B.7: continued from previous page

gene	MO	logFC	logCPM	LR	p value	FDR
pdlim5b	double	-3.283062533	4.929169397	8.396387632	0.003759674	0.747959233
sptssa	double	4.494586217	4.907389269	8.388994197	0.003774997	0.747959233
zgc:163061	double	4.503807333	4.73563406	8.34913797	0.003858704	0.747959233
zgc:113090	double	-1.753165058	6.7574879	8.187579332	0.004217817	0.747959233
ercc8	double	4.512385665	4.707281412	8.130568384	0.00435251	0.747959233
pola1	double	-2.837635453	5.527854294	8.126788386	0.004361594	0.747959233
med24	double	-2.797416647	5.367038498	8.105604492	0.00441286	0.747959233
jph2	double	-3.313101003	4.74446491	8.077389719	0.004482096	0.747959233
zfyve21	double	-4.326885545	4.850370893	8.020591376	0.004624847	0.747959233
bcap29	double	-3.166570268	5.195961948	7.93902751	0.004837983	0.747959233
dedd	double	-3.199240016	5.247857478	7.936420314	0.004844958	0.747959233
si:ch211-206k20.5	double	-3.208914617	5.000242518	7.848344734	0.005086726	0.747959233
fzd1	double	-4.375383704	4.726835324	7.802723741	0.005216754	0.747959233
mri1	double	-4.359816742	4.704831915	7.770060394	0.005311927	0.747959233
usp16	double	2.519184197	5.573464612	7.740490067	0.005399614	0.747959233
prph2l	double	-4.310235018	4.744722653	7.70677099	0.005501407	0.747959233
zgc:158482	double	-4.308753297	4.833017356	7.704016533	0.005509808	0.747959233
camk1db	double	3.258751851	5.030519222	7.685898628	0.005565396	0.747959233
nadkb	double	4.305502127	4.867733868	7.680801963	0.005581136	0.747959233
ydjc	double	-4.323748087	4.645095039	7.610542285	0.005802803	0.747959233
cyb5d2	double	1.997001127	6.768135776	7.573245406	0.005924102	0.747959233
wdr47b	double	3.25145702	5.181573589	7.569163966	0.005937532	0.747959233
henmt1	double	-2.202980251	5.915323447	7.550521716	0.00599927	0.747959233
st8sia1	double	4.311947397	4.567175451	7.532364042	0.006060034	0.747959233
socs5a	double	-4.136293954	4.4781074	7.474263952	0.006258715	0.747959233
sox4a	double	-2.251607076	5.602436774	7.355432697	0.006686042	0.747959233
dpp7	double	-1.369652194	8.522502226	7.320002444	0.006819132	0.747959233
ighmbp2	double	-4.138655342	5.033948084	7.28369382	0.006958331	0.747959233
ube2r2	double	-4.155010408	5.18763447	7.195151944	0.00731008	0.747959233
ahi1	double	-4.125297079	4.480472377	7.193167672	0.007318168	0.747959233
rprd2a	double	-2.702419693	5.23926763	7.167757629	0.00742255	0.747959233
zgc:174263	double	-4.140422424	4.830321995	7.130943624	0.007576484	0.747959233
sri	double	-4.158244806	5.088896444	7.11314042	0.007652094	0.747959233
haus3	double	-4.140002341	4.703233484	7.101045504	0.0077039	0.747959233
mpdu1b	double	-2.638355855	5.119295413	7.024465905	0.008040345	0.747959233
fbxo3	double	-4.140177036	4.58857541	7.008725383	0.008111341	0.747959233
sin3aa	double	-4.126547517	5.01515906	7.000099724	0.008150518	0.747959233
keap1a	double	4.09806319	4.671095664	6.9684267	0.008296041	0.747959233
hif1an	double	-4.12671425	4.842556488	6.942240517	0.00841836	0.747959233
eapp	double	4.113204332	4.863439178	6.941298242	0.008422796	0.747959233
clk4b	double	-4.109422174	4.697026309	6.922071026	0.008513832	0.747959233
uck2a	double	4.088991704	5.11169842	6.91948812	0.008526138	0.747959233
acsl4b	double	-4.110140391	4.628516797	6.91774899	0.008534434	0.747959233
sfxn4	double	4.088979908	4.845308345	6.917168878	0.008537203	0.747959233
rab43	double	-2.629554436	5.658405591	6.915047154	0.008547339	0.747959233
lysmd3	double	4.098106846	4.755695501	6.895167257	0.008642908	0.747959233
zgc:66474	double	-4.123665172	4.778091756	6.89452252	0.008646025	0.747959233
snx2	double	4.297137314	4.788370482	6.890274167	0.008666597	0.747959233
zgc:123172	double	-4.158188205	4.856535282	6.888924986	0.008673141	0.747959233
stx3a	double	4.09140368	4.664195257	6.835260684	0.008937565	0.747959233
ryr1b	double	-3.29043453	4.887239397	6.806994718	0.009080146	0.747959233

Continued on following page

Table B.7: continued from previous page

gene	MO	logFC	logCPM	LR	p value	FDR
mut	double	-3.046787898	5.035638074	6.806103326	0.00908468	0.747959233
dpy30	double	2.025780886	5.829076778	6.771350125	0.009263273	0.747959233
chchd10	double	4.097690179	4.725414277	6.694093157	0.009673286	0.747959233
st5	double	-4.12742042	4.69079218	6.684200735	0.009727113	0.747959233
prdm1a	double	-2.643525766	5.26661093	6.67994435	0.009750367	0.747959233
phactr3b	double	4.093472487	4.667388282	6.674047656	0.009782677	0.747959233
notch1a	double	-2.327939203	5.728918434	6.651310179	0.009908294	0.747959233
ufm1	double	2.265377238	5.428673222	6.62238892	0.010070467	0.747959233
klf18	double	-4.107687844	4.667981114	6.620894521	0.01007892	0.747959233
rps6ka4	double	4.105527603	5.073806466	6.593264206	0.010236531	0.747959233
dcps	double	4.084145773	4.699142601	6.579121037	0.010318183	0.747959233
rbl1	double	4.105724007	4.818632753	6.541745204	0.010537193	0.747959233
mrpl36	double	-2.949337002	5.097658319	6.541159736	0.010540661	0.747959233
ldb1b	double	-4.054336637	4.776593549	6.53223606	0.01059367	0.747959233
rarab	double	-2.635555895	5.421073691	6.471043412	0.010964614	0.747959233
mgaa	double	-2.647166743	5.047797744	6.469654102	0.010973189	0.747959233
si:dkeyp-120h9.1	double	-2.979791052	5.12206978	6.463919909	0.011008653	0.747959233
si:ch211-191j22.3	double	4.079290796	4.69946736	6.430951916	0.011214846	0.747959233
siah1	double	-2.966808136	5.165042504	6.416171025	0.011308573	0.747959233
zgc:92591	double	3.024494151	4.915979471	6.415460151	0.011313101	0.747959233
slc30a4	double	4.08931481	4.705274784	6.360035084	0.011671924	0.747959233
gnai2a	double	2.199988789	5.620259383	6.301228077	0.012065436	0.747959233
tbl3	double	1.729248617	6.017429345	6.293605524	0.012117431	0.747959233
timeless	double	-1.738933523	5.95833515	6.281942951	0.01219743	0.747959233
agpat3	double	-2.241170755	5.556682584	6.273984704	0.01225233	0.747959233
cyb561d2	double	-3.110286231	4.816038186	6.256551864	0.012373481	0.747959233
tuba1c	double	1.833854965	5.845828226	6.241252586	0.012480817	0.747959233
clic2	double	3.025458643	4.757667025	6.237221351	0.012509259	0.747959233
rer1	double	-2.223158056	5.831627061	6.224321956	0.012600715	0.747959233
gins4	double	4.124133113	4.747537881	6.215563268	0.012663206	0.747959233
mpp1	double	-3.903502139	4.848242606	6.199262864	0.012780353	0.747959233
rragcb	double	-2.63840359	5.153758547	6.172174364	0.012977501	0.747959233
zgc:65851	double	2.898404699	5.280248484	6.168885826	0.013001647	0.747959233
sh3bp5la	double	-3.859011942	4.479000008	6.16372225	0.013039653	0.747959233
atp1b2b	double	-2.966503584	5.136708399	6.158161338	0.013080711	0.747959233
ctc1	double	-3.859105728	5.0262711	6.128530172	0.013301741	0.747959233
tomm22	double	-1.901066472	5.937303375	6.110705656	0.013436547	0.747959233
rcc1	double	-2.132813778	5.744181064	6.109272321	0.013447448	0.747959233
zgc:110269	double	-3.858741595	4.896604311	6.103415429	0.013492087	0.747959233
bmp7b	double	-2.281815803	5.510861141	6.100242993	0.013516329	0.747959233
cblc	double	-3.906389984	4.762947566	6.090473372	0.013591267	0.747959233
sall4	double	-2.120475879	5.899896733	6.073182198	0.013724947	0.747959233
dmbx1a	double	-3.858184137	4.540397717	6.064499017	0.013792587	0.747959233
ythdf2	double	-2.542228715	5.239911493	6.061973921	0.013812322	0.747959233
pde6d	double	3.857065315	5.02777658	6.05833858	0.013840784	0.747959233
slco1d1	double	-3.872193183	4.521504241	6.054864535	0.013868039	0.747959233
rasgrp4	double	-1.977217439	5.900223076	6.04558877	0.013941083	0.747959233
zgc:153631	double	-3.857681327	4.718681681	6.02890116	0.014073492	0.747959233
taf1	double	-1.90814193	5.870299309	6.023701312	0.014115014	0.747959233
plrg1	double	2.324577961	5.437404391	6.014585398	0.014188112	0.747959233
gtpbp2	double	-3.872109427	4.481205977	6.013759928	0.01419475	0.747959233

Continued on following page

Table B.7: continued from previous page

gene	MO	logFC	logCPM	LR	p value	FDR
reps1	double	-3.888811489	4.690060896	6.001257742	0.014295684	0.747959233
zgc:55781	double	-3.873610709	4.585421325	5.972591579	0.014529912	0.747959233
adprh	double	-3.871986849	4.523406625	5.952350053	0.014697679	0.747959233
tinagl1	double	-3.872775221	4.649211183	5.941231432	0.014790681	0.747959233
inip	double	3.850990455	4.451216802	5.941167859	0.014791215	0.747959233
gata3	double	-2.49173853	5.171734376	5.941091689	0.014791854	0.747959233
gnat2	double	-2.818606335	5.495126724	5.936949009	0.014826663	0.747959233
mier1b	double	2.896758961	5.02656525	5.92591609	0.01491978	0.747959233
mtif2	double	-2.984531354	4.793714413	5.898834449	0.015150908	0.747959233
fli1b	double	-3.892710904	4.505923927	5.888241968	0.01524231	0.747959233
zgc:153317	double	-1.619732173	6.641225828	5.869633001	0.015404263	0.747959233
slc26a3.2	double	-3.891159391	4.818397695	5.862825387	0.015463951	0.747959233
pycr1b	double	-2.925621825	4.892287583	5.85373084	0.015544063	0.747959233
irx1a	double	-3.871755801	4.811741868	5.832336139	0.015734216	0.747959233
dusp4	double	-3.837823117	4.738307374	5.831864623	0.015738433	0.747959233
pgrmc1	double	2.059030596	5.528703334	5.812582818	0.015911908	0.747959233
zgc:113229	double	-2.39609609	5.413945463	5.807949506	0.015953886	0.747959233
adssl	double	-2.044291371	5.735719973	5.805836337	0.015973069	0.747959233
smarcd1	double	-1.5249098	6.42756599	5.755571581	0.016436447	0.747959233
ptpreb	double	3.848191553	4.606374413	5.741808519	0.016565727	0.747959233
rad17	double	-2.205176376	5.442502923	5.731324287	0.016664911	0.747959233
myca	double	2.184311486	5.445554958	5.718658511	0.01678555	0.747959233
scamp2	double	-2.931584285	4.969631242	5.714738977	0.016823066	0.747959233
eps8	double	-3.834536267	4.738266007	5.699178171	0.016972858	0.747959233
crabp2b	double	2.891333797	5.033577012	5.688824369	0.017073289	0.747959233
twist2	double	3.871602848	4.774903857	5.687687506	0.017084354	0.747959233
ing5a	double	3.863547185	4.743913725	5.687159011	0.0170895	0.747959233
atp2a1	double	-1.163838007	7.928618533	5.675437827	0.017204046	0.747959233
dio3b	double	-3.815895161	4.563890874	5.668291066	0.017274277	0.747959233
si:ch211-154o6.2	double	3.863915959	4.816174299	5.642429793	0.017530895	0.747959233
bmp5	double	3.867851398	4.816433346	5.628679318	0.017668939	0.747959233
tob1a	double	-2.396292203	5.241807979	5.628008921	0.017675697	0.747959233
si:ch211-39i2.2	double	3.855923689	4.568615525	5.619651457	0.017760181	0.747959233
hoxa2b	double	3.840155571	4.816261162	5.609645945	0.017861872	0.747959233
itga6b	double	-2.562700468	4.956767308	5.609096977	0.017867468	0.747959233
nr1d4b	double	-3.831459289	4.778406388	5.607558914	0.017883159	0.747959233
creb1a	double	-2.41904562	5.148120338	5.606050733	0.017898558	0.747959233
fkbp10b	double	2.049536695	5.476761128	5.596693324	0.017994409	0.747959233
pmp22b	double	-2.084544339	5.571281917	5.59085742	0.018054457	0.747959233
sra1	double	3.843630315	4.682528176	5.589101066	0.018072569	0.747959233
glyctk	double	1.923013515	6.409895081	5.588311708	0.018080715	0.747959233
zgc:113210	double	3.864369555	4.702242906	5.586220707	0.018102312	0.747959233
pik3r2	double	-3.850762927	4.669744599	5.56772416	0.018294524	0.751701664
aox5	double	-1.782650248	6.093771572	5.545681437	0.018526342	0.754149261
slc35a4	double	2.185778686	5.400774877	5.535713101	0.018632171	0.754149261
ube2t	double	-3.81116418	4.662492213	5.533102078	0.018659994	0.754149261
zgc:123284	double	-2.761719523	5.026749983	5.475843901	0.019281049	0.771500654
pfdn1	double	-2.399065797	4.974891965	5.474312704	0.019297948	0.771500654
dcun1d2b	double	-2.28263847	5.058288331	5.460803672	0.0194477	0.773307469
fam207a	double	-2.015246177	5.386403219	5.430646578	0.019786352	0.782566091
p2rx4a	double	2.90750727	4.885520862	5.407654853	0.020048632	0.786189603

Continued on following page

Table B.7: continued from previous page

gene	MO	logFC	logCPM	LR	p value	FDR
fuom	double	-1.797109606	5.903802514	5.398835714	0.020150189	0.786189603
dusp23a	double	-3.847618924	4.743201692	5.394797709	0.020196866	0.786189603
znf292b	double	-2.228982512	5.413695155	5.368494829	0.020503663	0.793901685
sh3d21	double	2.055668985	5.332939778	5.358204901	0.020624993	0.793901685
tk2	double	-2.410729669	5.34751173	5.350442478	0.020717013	0.793901685
zeb1b	double	-1.783656969	6.114823131	5.32702171	0.020997236	0.800492575
pltp	double	-2.140672436	5.305642664	5.307466583	0.021234213	0.805375574
sox11a	double	-1.264577159	6.921064343	5.295801937	0.021376886	0.806633089
tada2b	double	-2.281274674	5.185409645	5.166800652	0.023022579	0.806633089
galnt6	double	-2.647578793	5.343235024	5.156776889	0.023155831	0.806633089
glcci1	double	-2.728892227	5.390744703	5.155052976	0.023178829	0.806633089
foxn4	double	-2.780939144	5.027374857	5.144975461	0.02331374	0.806633089
pcbp2	double	-1.325613916	6.588005204	5.139298123	0.023390103	0.806633089
lgi2a	double	-2.736880939	5.243908473	5.139212449	0.023391257	0.806633089
trim35-7	double	-2.818195261	4.937538537	5.136678664	0.023425423	0.806633089
usp25	double	-2.652325931	5.088631427	5.100175899	0.023923417	0.806633089
dab2ipb	double	-3.569944474	4.474044162	5.084302203	0.024143391	0.806633089
zdhhc20a	double	-2.434263305	4.906397502	5.083814819	0.024150178	0.806633089
acer3	double	-3.602095674	4.57050573	5.055484778	0.024548114	0.806633089
smad1	double	-3.586208713	4.521970551	5.040569767	0.024760345	0.806633089
has2	double	-3.569389907	4.477607527	5.035940613	0.024826601	0.806633089
elovl1b	double	1.979776567	5.275078814	5.035632322	0.02483102	0.806633089
ier2	double	-2.669765495	5.22816007	5.032295274	0.024878906	0.806633089
notch2	double	-1.975368129	5.433750786	5.030841628	0.024899796	0.806633089
cry-dash	double	-3.584073036	4.564154681	5.024700493	0.024988247	0.806633089
csnk1db	double	-1.783602749	5.833815163	5.02011222	0.025054545	0.806633089
rab11fip4a	double	-3.604208073	4.833370319	4.995030915	0.025420199	0.806633089
rnasen	double	-3.56891338	4.582876791	4.993392807	0.025444273	0.806633089
znf574	double	3.560008892	4.58687499	4.990666097	0.025484397	0.806633089
mus81	double	-3.604462594	4.850468043	4.987567871	0.025530068	0.806633089
golga7	double	-1.843012064	5.589008462	4.987558802	0.025530202	0.806633089
pank2	double	3.557070789	4.516674025	4.963558624	0.025886882	0.806633089
bbs2	double	-3.584735017	4.480348453	4.954669763	0.026020294	0.806633089
col9a1b	double	-1.782593731	5.928830376	4.952482702	0.026053229	0.806633089
rnmt	double	2.077273803	5.472516078	4.939674813	0.026246974	0.806633089
zmp:0000000768	double	-2.80926298	4.701527543	4.93473813	0.026322051	0.806633089
tyr	double	-3.56818847	4.545293202	4.926825073	0.026442857	0.806633089
wdr91	double	-3.586792411	4.918391916	4.924164245	0.026483609	0.806633089
si:ch211-89p3.3	double	-3.585912444	4.567179297	4.923050009	0.026500693	0.806633089
dpysl2b	double	-3.608092667	4.833125904	4.908465263	0.026725377	0.806633089
dcaf13	double	1.883329288	5.674215786	4.902909185	0.026811491	0.806633089
npr3	double	2.239765893	4.978049822	4.899400455	0.026866021	0.806633089
ints10	double	-3.587114953	4.736613913	4.89513941	0.026932399	0.806633089
gorab	double	-3.567827697	4.609582252	4.892831012	0.02696843	0.806633089
ldlrb	double	-3.585332038	4.503704443	4.888797775	0.027031503	0.806633089
srrt	double	-1.118198039	7.271626543	4.886617036	0.02706567	0.806633089
slc7a6	double	-3.567741531	4.545942047	4.884624173	0.027096933	0.806633089
ilkap	double	3.557040248	4.979383733	4.877411981	0.027210388	0.806633089
bcor	double	-2.649906199	5.049493551	4.875341812	0.027243045	0.806633089
kdm6al	double	-3.550455715	4.885813214	4.867356523	0.027369395	0.806633089
tyrp1b	double	-3.550431788	4.54228666	4.866557884	0.027382066	0.806633089

Continued on following page

Table B.7: continued from previous page

gene	MO	logFC	logCPM	LR	p value	FDR
rab40c	double	-3.610977582	4.708546416	4.853059248	0.027597144	0.806633089
sox9b	double	-3.567400768	4.668288066	4.851829026	0.027616833	0.806633089
prkcbb	double	3.54767971	4.478037798	4.847433532	0.027687299	0.806633089
csrp2bp	double	-3.610349968	4.796341146	4.838966665	0.027823563	0.806633089
clptm1	double	-1.651975739	5.986201045	4.83554848	0.027878771	0.806633089
kat5b	double	-3.567058604	4.626613207	4.818342135	0.028158416	0.806633089
pdxka	double	-3.608802312	4.590966939	4.817932322	0.028165112	0.806633089
mycn	double	-1.315181263	6.676952548	4.81757243	0.028170994	0.806633089
sp2	double	-3.548962047	4.524430922	4.816964033	0.02818094	0.806633089
nedd9	double	3.5618738	4.884937796	4.81419471	0.028226257	0.806633089
katna1	double	3.540639999	4.812399025	4.813822184	0.028232359	0.806633089
tram1	double	-1.165794924	7.257757937	4.812767316	0.028249645	0.806633089
slc29a1a	double	-3.586005978	4.778603524	4.811112196	0.02827679	0.806633089
mmp2	double	1.975561612	5.577357062	4.803078397	0.028408932	0.806633089
pigx	double	-3.547707047	4.613292541	4.802508353	0.028418333	0.806633089
tac1	double	-1.295238783	6.515594554	4.802469724	0.02841897	0.806633089
cldn11b	double	-3.609288151	4.670147819	4.801221419	0.028439568	0.806633089
serpinf2b	double	-2.662788614	4.952494521	4.796280492	0.028521248	0.806633089
mrps24	double	3.549989581	4.870811253	4.784832376	0.028711442	0.806633089
vgll4b	double	-2.825595987	4.668318278	4.78141898	0.028768406	0.806633089
coa5	double	3.558039328	4.600704177	4.779364566	0.028802747	0.806633089
sec23b	double	1.895989327	5.72426793	4.779145442	0.028806412	0.806633089
rab39bb	double	-1.182570219	7.346999225	4.773889021	0.028894484	0.806633089
hic1l	double	3.562394068	4.607295097	4.76167197	0.029100267	0.806633089
pex3	double	3.562413395	4.604242631	4.759690945	0.029133779	0.806633089
nup54	double	-1.618568494	5.703928036	4.757469109	0.029171412	0.806633089
ino80db	double	-2.268255	5.10217346	4.756527154	0.029187382	0.806633089
cerkl	double	-1.739059354	5.864008016	4.756207751	0.029192799	0.806633089
wdr83	double	3.554543124	4.516243955	4.748458446	0.029324553	0.806633089
tor1	double	-3.528479138	4.719040031	4.747666002	0.029338061	0.806633089
rnaseh2b	double	2.246750281	5.536046581	4.734226371	0.029568143	0.809948104
zbtb8b	double	3.554573314	4.702029788	4.715437442	0.029892959	0.814200313
trappc6b	double	3.542463227	4.601605442	4.711876691	0.029954934	0.814200313
prc1b	double	3.538867255	4.909314707	4.705696623	0.030062816	0.814200313
syvn1	double	-1.949013227	5.269327233	4.691225522	0.030317017	0.814200313
tonsl	double	3.554599675	4.605547305	4.686272975	0.030404528	0.814200313
col11a1a	double	-1.239180877	7.023111846	4.68138162	0.030491216	0.814200313
mybl2a	double	-3.525361106	4.65902454	4.681225808	0.030493981	0.814200313
fbxl22	double	3.563354056	4.738758558	4.660567641	0.030862987	0.817806444
aif1l	double	-2.046434207	5.44264838	4.65741375	0.030919731	0.817806444
ptrh1	double	2.763855287	4.778801533	4.655136922	0.030960763	0.817806444
pdxp	double	-3.613792738	4.68407944	4.636759992	0.031294031	0.823667804
six1a	double	-2.623806511	4.877226822	4.611775386	0.031753143	0.8318988
pfklb	double	-2.777959071	4.817188531	4.607537356	0.031831715	0.8318988
ppp2r5eb	double	2.609850132	5.024709584	4.591749281	0.03212621	0.834573318
syncripl	double	-1.943945957	5.21239889	4.569888175	0.032538689	0.834573318
tmem168a	double	-3.591626079	4.71420783	4.569644636	0.032543316	0.834573318
stam2	double	-2.288693309	4.970906119	4.566819811	0.032597025	0.834573318
brd4	double	-2.042373773	5.474768796	4.56562096	0.032619847	0.834573318
mrpl44	double	2.601689219	4.899360671	4.562033807	0.032688234	0.834573318
gspt1	double	-2.332868641	4.942924771	4.556006212	0.032803483	0.834573318

Continued on following page

Table B.7: continued from previous page

gene	MO	logFC	logCPM	LR	p value	FDR
ncor1	double	-1.549854352	5.827877927	4.554268831	0.032836781	0.834573318
dido1	double	-1.879310424	5.903494456	4.54601675	0.032995421	0.835607908
eral1	double	3.554732244	4.651085746	4.534616374	0.033215901	0.835607908
slc23a1	double	-1.521627954	5.875366407	4.531202533	0.033282223	0.835607908
ndufb6	double	-2.275675006	4.865817264	4.528777833	0.033329412	0.835607908
elf2b	double	-2.145453247	5.361474746	4.510715982	0.033683138	0.841623279
scrib	double	-1.35085185	6.189170194	4.498664802	0.03392133	0.842657937
zgc:101663	double	-2.627215715	4.726062112	4.490422883	0.034085245	0.842657937
siah2l	double	2.243860661	5.028288524	4.4819817	0.034253981	0.842657937
hrsp12	double	-2.073771606	5.023873943	4.47936693	0.034306426	0.842657937
epb41l4a	double	-2.308278789	4.930645391	4.471617303	0.034462357	0.842657937
tmem161a	double	-2.313443601	5.005190159	4.469508933	0.034504907	0.842657937
nansb	double	1.519066215	6.100913466	4.467027933	0.034555048	0.842657937
rhbdd1	double	-2.60025313	4.622051012	4.463029316	0.034636021	0.842657937
pigl	double	0.925871364	8.632927219	4.455434917	0.034790356	0.843058821
sh3bgrl	double	-1.621910645	5.824700434	4.444078175	0.035022493	0.843058821
wnt11r	double	-2.159326375	5.273254008	4.44313386	0.035041868	0.843058821
rcan3	double	-2.150383007	4.871474642	4.439382132	0.035118955	0.843058821
tagln2	double	-1.418265339	6.287267253	4.434359113	0.035222441	0.843058821
zgc:92360	double	-1.620748514	5.526431376	4.422343399	0.03547129	0.84440603
pank1b	double	-2.274765188	5.030300958	4.420248433	0.035514865	0.84440603
sec24d	double	-1.817028788	5.666059382	4.415145597	0.035621239	0.84440603
mrpl18	double	-2.608415253	4.933643413	4.393913216	0.03606744	0.852251714
mdm4	double	-2.042412914	5.259921417	4.363429369	0.036718317	0.86486839
tdg.1	double	-1.245335968	6.885143972	4.354385818	0.036913767	0.865981929
insm1a	double	-2.584541395	4.928300741	4.346482903	0.037085458	0.865981929
tdo2a	double	-2.153885017	5.309993498	4.340901395	0.03720722	0.865981929
trip11	double	-1.917921114	5.343802381	4.33967892	0.037233944	0.865981929

Table B.8: Significant differential gene expression as detected by the HOLT method at 18 hpf

gene	starAB FPKM	Tbx5a FPKM	Tbx5b FPKM	starAB/ Tbx5a	starAB/ Tbx5b	Tbx5a/ Tbx5b	Tbx5b/ Tbx5a	Downregulated
mir16c	22.3333	6.58916	9.91553	3.389400166	2.252355648	0.664529279	1.504824591	Tbx5a &Tbx5b
wu:fc46h12	18.6079	6.24972	5.69321	2.977397387	3.268437314	1.097749776	0.910954411	Tbx5a &Tbx5b
tnni2a.4	5.16209	1.8932	1.65607	2.726648003	3.117072346	1.143188392	0.874746461	Tbx5a &Tbx5b
lect2l	4.90337	1.61454	2.40227	3.037007445	2.041140255	0.672089316	1.487897482	Tbx5a &Tbx5b
zgc:123068	3.13416	1.43313	1.05002	2.186933495	2.984857431	1.364859717	0.732676031	Tbx5a &Tbx5b
c25h12orf75	2.97406	1.31882	1.32108	2.255091673	2.251233839	0.998289278	1.001713653	Tbx5a &Tbx5b
hsbp1l1	2.78673	1.30013	1.15512	2.143424119	2.412502597	1.125536741	0.888465	Tbx5a &Tbx5b
per3	2.73686	0.542804	0.892317	5.042077803	3.067138696	0.608308482	1.643902772	Tbx5a &Tbx5b
pvalb4	2.54362	0.959339	0.587923	2.651429787	4.326450913	1.631742592	0.612841759	Tbx5a &Tbx5b
crygs1	2.3605	1.17423	0.729507	2.010253528	3.235746881	1.609621292	0.621264148	Tbx5a &Tbx5b
per1b	2.18574	0.425303	1.03786	5.139253662	2.10600659	0.409788411	2.440283751	Tbx5a &Tbx5b
zgc:194981	1.94252	0.912569	0.851222	2.128628082	2.282036883	1.072069331	0.932775494	Tbx5a &Tbx5b
pkmb	1.62891	0.75862	0.727445	2.147201497	2.239220835	1.042855474	0.958905644	Tbx5a &Tbx5b
ccl27a	1.42659	0.505802	0.563687	2.820451481	2.530819409	0.897310032	1.114442015	Tbx5a &Tbx5b
malt1a	2.93532	0.942157	2.3082	3.1155317	1.271692228	0.408178234	2.449910153	Tbx5a only
arnt	2.6206	1.2941	2.89462	2.025036705	0.905334724	0.447070773	2.23678232	Tbx5a only
map2k7	2.55302	1.19879	3.13724	2.129664078	0.81377899	0.382116128	2.617005481	Tbx5a only
kitlgb	2.36276	1.02927	2.42292	2.295568704	0.975170455	0.424805606	2.354017896	Tbx5a only
per1b	2.18574	0.425303	1.03786	5.139253662	2.10600659	0.409788411	2.440283751	Tbx5a only
aspa	2.0384	0.773269	1.7379	2.636081364	1.172909834	0.444944473	2.247471449	Tbx5a only
ankrd52a	2.02683	1.00295	2.22796	2.020868438	0.909724591	0.450165174	2.22140685	Tbx5a only
tll1	1.69786	0.751135	1.54136	2.260392606	1.10153371	0.48731964	2.052041244	Tbx5a only
si:dkey-15j16.3	1.28098	0.428318	1.06608	2.990721847	1.201579619	0.401769098	2.488991824	Tbx5a only
nitr11a	1.25015	0.354472	1.29962	3.526794782	0.961935027	0.272750496	3.666354465	Tbx5a only
mir144	114.523	94.6476	26.3345	1.209993703	4.348782016	3.594053428	0.278237377	Tbx5b only
mir429b	9.97397	23.5812	4.55429	0.422962784	2.190016446	5.177799394	0.193132241	Tbx5b only
tmigd1	3.49303	1.8993	0.779581	1.839114411	4.480650503	2.436308735	0.41045701	Tbx5b only
ebi3	1.79355	1.27602	0.593302	1.405581417	3.02299672	2.150709082	0.464962932	Tbx5b only

Table B.9: Significant differential gene expression as detected by HOLT at 21 hpf

gene	starAB FPKM	Tbx5a FPKM	Tbx5b FPKM	starAB/ Tbx5a	starAB/ Tbx5b	Tbx5a/ Tbx5b	Tbx5b/ Tbx5a	Downregulated
zgc:158463	3093.13	604.276	610.353	5.118737133	5.067772256	0.990043467	1.010056663	Tbx5a &Tbx5b
zgc:153713	484.751	178.625	238.794	2.713791463	2.029996566	0.748029682	1.336845346	Tbx5a &Tbx5b
rn7sk	512.402	41.3144	52.5911	12.40250373	9.743131442	0.785577788	1.272948415	Tbx5a &Tbx5b
cox6b1	52.5649	24.2115	17.3153	2.171071598	3.035748731	1.398272048	0.715168412	Tbx5a &Tbx5b
cyp11a1	35.9785	15.4158	13.1748	2.333871742	2.730857394	1.170097459	0.854629666	Tbx5a &Tbx5b
mir15a-2	35.525	13.632	14.2333	2.606000587	2.495907485	0.957753999	1.044109448	Tbx5a &Tbx5b
hhex	24.6118	8.7173	11.319	2.823328324	2.174379362	0.77014754	1.298452502	Tbx5a &Tbx5b
ankrd9	16.5031	7.84319	7.13871	2.1041311	2.311776217	1.098684496	0.910179404	Tbx5a &Tbx5b
dhrs9	17.9489	7.4321	7.65284	2.415050928	2.345390731	0.971155806	1.029700892	Tbx5a &Tbx5b
LOC570474	19.5526	6.63426	9.19774	2.947216419	2.125804817	0.721292404	1.386400292	Tbx5a &Tbx5b
si:ch211-117m20.5	11.527	4.96089	1.27747	2.323575004	9.023303874	3.883371038	0.257508229	Tbx5a &Tbx5b
rpph1	58.8987	3.90562	3.96623	15.08049938	14.85004652	0.984718486	1.015518663	Tbx5a &Tbx5b
zgc:92041	8.97265	3.75746	3.68451	2.387956226	2.435235622	1.019799105	0.980585289	Tbx5a &Tbx5b
wu:fa10h04	7.56511	3.6086	3.5554	2.096411351	2.127780278	1.014963155	0.985257441	Tbx5a &Tbx5b
zgc:110425	9.16002	3.40213	4.28989	2.692436797	2.135257547	0.793057631	1.26094241	Tbx5a &Tbx5b
cbln11	10.3799	2.90602	4.9084	3.571861171	2.114721702	0.592050363	1.689045499	Tbx5a &Tbx5b
zgc:194221	7.52097	2.82525	2.88727	2.662054685	2.604872423	0.978519501	1.02195204	Tbx5a &Tbx5b
insb	5.3857	2.61967	2.44597	2.055869632	2.201866744	1.071014771	0.933693939	Tbx5a &Tbx5b
exd1	5.36542	1.84677	2.14946	2.905299523	2.496171131	0.859178584	1.163902381	Tbx5a &Tbx5b
nots	4.40373	1.76893	2.00196	2.489487996	2.199709285	0.883599073	1.131735004	Tbx5a &Tbx5b
zgc:123068	4.07197	1.74724	1.58933	2.330515556	2.562067035	1.099356333	0.909623177	Tbx5a &Tbx5b
mir219-3	4.23764	1.40834	1.4085	3.008960904	3.008619098	0.999886404	1.000113609	Tbx5a &Tbx5b
zgc:153405	4.99623	1.34407	1.1448	3.717239429	4.364281971	1.174065339	0.851741353	Tbx5a &Tbx5b
zp2.2,zp2.5,zp2.6	3.29061	1.22108	1.6326	2.694835719	2.015564131	0.747935808	1.337013136	Tbx5a &Tbx5b
zgc:114046	3.24474	1.20646	1.09091	2.689471677	2.974342521	1.105920745	0.904223928	Tbx5a &Tbx5b
elavl2	3.06844	1.02583	1.07476	2.991177875	2.855000186	0.954473557	1.047697962	Tbx5a &Tbx5b
krt91	225.46	92.7131	248.839	2.431803057	0.906047685	0.372582674	2.683968069	Tbx5a only
LOC100329294	73.8194	20.3226	41.8941	3.632379715	1.762047639	0.48509456	2.061453751	Tbx5a only
mir203a	37.5348	18.0698	56.3186	2.077211701	0.666472533	0.320849595	3.116725144	Tbx5a only
rs1a	10.2193	4.55018	10.5642	2.245911151	0.967352	0.43071695	2.32171035	Tbx5a only
ift122	9.55203	4.43722	9.00719	2.152705974	1.060489453	0.492630887	2.029917381	Tbx5a only
epd	11.8013	3.91941	9.64138	3.010988899	1.224026021	0.406519606	2.459905955	Tbx5a only
per3	4.95651	2.16359	4.46939	2.29087304	1.108990265	0.48409067	2.065728719	Tbx5a only
cryba1l1	3.71096	1.44153	3.98502	2.57432034	0.931227447	0.361737206	2.764437785	Tbx5a only
si:ch211-117m20.5	11.527	4.96089	1.27747	2.323575004	9.023303874	3.883371038	0.257508229	Tbx5b only
egln3	3.75173	4.51631	1.28448	0.830706927	2.920816206	3.516060974	0.284409175	Tbx5b only
cxl34b.11	1.36764	0.61223	0.281894	2.233866357	4.851610889	2.171844736	0.460438071	Tbx5b only

SUPPLEMENTAL FILES

This is a list of the Supplemental Files submitted with my thesis. All files are available online.

Tbx5b-deficient movie

The embryo displayed is a Tbx5b-deficient embryo. This movie takes place from 18 hpf to approximately 23 hpf. Anterior is to the left, the midline is at the top. There are 40 minutes between each frame. The first 40 frames are *Tg)hand2::eGFP*, the last 40 frames are *Tg(histone2::mcherry)* with an overlay displaying the cell tracks. Scale bars are 50 µm.

Double-deficient movie

The embryo shown is a double-deficient embryo. This movie takes place from 18 hpf to approximately 23 hpf. Anterior is to the left, the midline is at the top. There are 40 minutes between each frame. The first 40 frames are *Tg)hand2::eGFP*, the last 40 frames are *Tg(histone2::mcherry)* with an overlay displaying the cell tracks. Scale bars are 50 µm.

Cell tracking analysis R script

This file includes all scripts used to analyze the cell tracking data for this paper.

References

[1] Michael I Coates. The origin of vertebrate limbs. *Development*, 1994(Supplement):169–180, January 1994.

[2] Peter Forey and Philippe Janvier. Agnathans and the origin of jawed vertebrates. *Nature*, 361(6408):129–134, January 1993.

[3] I Ruvinsky and J J Gibson-Brown. Genetic and developmental bases of serial homology in vertebrate limb evolution. *Development*, 127(24):5233–5244, December 2000.

[4] S I Agulnik, N Garvey, S Hancock, I Ruvinsky, D L Chapman, I Agulnik, R Bollag, V Papaioannou, and L M Silver. Evolution of mouse T-box genes by tandem duplication and cluster dispersion. *Genetics*, 144(1):249–254, September 1996.

[5] I Ruvinsky, A C Oates, L M Silver, and R K Ho. The evolution of paired appendages in vertebrates: T-box genes in the zebrafish. *Development genes and evolution*, 210(2):82–91, February 2000.

[6] Amy C Horton, Navin R Mahadevan, Carolina Minguillon, Kazutoyo Osoegawa, Daniel S Rokhsar, Ilya Ruvinsky, Pieter J de Jong, Malcolm P Logan, and Jeremy J Gibson-Brown. Conservation of linkage and evolution of developmental function within the Tbx2/3/4/5 subfamily of T-box genes: implications for the origin of vertebrate limbs. *Wilhelm Roux's archives of developmental biology*, 218(11-12):613–628, December 2008.

[7] Koh Onimaru, Eiichi Shoguchi, Shigeru Kuratani, and Mikiko Tanaka. Development and evolution of the lateral plate mesoderm: comparative analysis of amphioxus and lamprey with implications for the acquisition of paired fins. *Developmental biology*, 359(1):124–136, November 2011.

[8] Nobuhiro Kokubo, Manami Matsuura, Koh Onimaru, Eva Tiecke, Shigehiro Kuraku, Shigeru Kuratani, and Mikiko Tanaka. Mechanisms of heart development in the Japanese lamprey, Lethenteron japonicum. *Evolution & development*, 12(1):34–44, January 2010.

[9] D L Chapman, N Garvey, S Hancock, M Alexiou, S I Agulnik, J J Gibson-Brown, J Cebra-Thomas, R J Bollag, L M Silver, and V E Papaioannou. Expression of the T-box family genes, Tbx1-Tbx5, during early mouse development. *Developmental Dynamics*, 206(4):379–390, August 1996.

[10] Daegwon Ahn, Matthew J Kourakis, Laurel A Rohde, Lee M Silver, and Robert K Ho. T-box gene tbx5 is essential for formation of the pectoral limb bud. *Nature*, 417(6890):754–758, June 2002.

[11] B G Bruneau, G Nemer, J P Schmitt, F Charron, L Robitaille, S Caron, D A Conner, M Gessler, M Nemer, C E Seidman, and J G Seidman. A murine model of Holt-Oram syndrome defines roles of the T-box transcription factor Tbx5 in cardiogenesis and disease. *Cell*, 106(6):709–721, September 2001.

[12] C Rodríguez-Esteban, T Tsukui, S Yonei, J Magallon, K Tamura, and J C Izpisúa-Belmonte. The T-box genes Tbx4 and Tbx5 regulate limb outgrowth and identity. *Nature*, 398(6730):814–818, April 1999.

[13] H Grandel and S Schulte-Merker. The development of the paired fins in the zebrafish (Danio rerio). *Mechanisms of development*, 79(1-2):99–120, December 1998.

[14] Michael I Coates, Jonathan E Jeffery, and Marcello Rut. Fins to limbs: what the fossils say. *Evolution & development*, 4(5):390–401, September 2002.

[15] P Sordino, F van der Hoeven, and D Duboule. Hox gene expression in teleost fins and the origin of vertebrate digits. *Nature*, 375(6533):678–681, June 1995.

[16] Tetsuya Nakamura, Andrew R Gehrke, Justin Lemberg, Julie Szymaszek, and Neil H Shubin. Digits and fin rays share common developmental histories. *Nature*, August 2016.

[17] Thomas A Stewart, Ramray Bhat, and Stuart A Newman. The evolutionary origin of digit patterning. *EvoDevo*, 8(1):21, 2017.

[18] Andrew R Gehrke, Igor Schneider, Elisa de la Calle-Mustienes, Juan J Tena, Carlos Gomez-Marin, Mayuri Chandran, Tetsuya Nakamura, Ingo Braasch, John H Postlethwait, José Luis Gómez-Skarmeta, and Neil H Shubin. Deep conservation of wrist and digit enhancers in fish. *Proceedings of the National Academy of Sciences*, 112(3):803–808, January 2015.

[19] Satoko Nishimoto, Susan M Wilde, Sophie Wood, and Malcolm P O Logan. RA Acts in a Coherent Feed-Forward Mechanism with Tbx5 to Control Limb Bud Induction and Initiation. *CellReports*, 12(5):879–891, August 2015.

[20] Carolina Minguillon, Satoko Nishimoto, Sophie Wood, Elisenda Vendrell, Jeremy J Gibson-Brown, and Malcolm P O Logan. Hox genes regulate the onset of Tbx5 expression in the forelimb. *Development*, 139(17):3180–3188, September 2012.

[21] Satoko Nishimoto, Carolina Minguillon, Sophie Wood, and Malcolm P O Logan. A combination of activation and repression by a colinear Hox code controls forelimb-restricted expression of Tbx5 and reveals Hox protein specificity. *PLoS genetics*, 10(3):e1004245, March 2014.

[22] Felix A Mic, I Ovidiu Sirbu, and Gregg Duester. Retinoic acid synthesis controlled by Raldh2 is required early for limb bud initiation and then later as a proximodistal signal during apical ectodermal ridge formation. *The Journal of biological chemistry*, 279(25):26698–26706, June 2004.

[23] Heiner Grandel and Michael Brand. Zebrafish limb development is triggered by a retinoic acid signal during gastrulation. *Developmental Dynamics*, 240(5):1116–1126, May 2011.

[24] Thomas J Cunningham, Xianling Zhao, Lisa L Sandell, Sylvia M Evans, Paul A Trainor, and Gregg Duester. Antagonism between Retinoic Acid and Fibroblast Growth Factor Signaling during Limb Development. *CellReports*, 3(5):1503–1511, May 2013.

[25] Nadia Mercader, Sabine Fischer, and Carl J Neumann. Prdm1 acts downstream of a sequential RA, Wnt and Fgf signaling cascade during zebrafish forelimb induction. *Development*, 133(15):2805–2815, August 2006.

[26] Y Kawakami, J Capdevila, D Büscher, T Itoh, C Rodríguez-Esteban, and J C Izpisúa-Belmonte. WNT signals control FGF-dependent limb initiation and AER induction in the chick embryo. *Cell*, 104(6):891–900, March 2001.

[27] Jun K Takeuchi, Kazuko Koshiba-Takeuchi, Takayuki Suzuki, Mika Kamimura, Keiko Ogura, and Toshihiko Ogura. Tbx5 and Tbx4 trigger limb initiation through activation of the Wnt/Fgf signaling cascade. *Development*, 130(12):2729–2739, June 2003.

[28] Jun K Takeuchi, Makoto Ohgi, Kazuko Koshiba-Takeuchi, Hidetaka Shiratori, Ichiro Sakaki, Keiko Ogura, Yukio Saijoh, and Toshihiko Ogura. Tbx5 specifies the left/right ventricles and ventricular septum position during cardiogenesis. *Development*, 130(24):5953–5964, December 2003.

[29] Jennifer K Ng, Yasuhiko Kawakami, Dirk Büscher, Angel Raya, Tohru Itoh, Christopher M Koth, Concepción Rodríguez Esteban, Joaquín Rodríguez-León, Deborah M Garrity, Mark C Fishman, and Juan Carlos Izpisúa Belmonte. The limb identity gene Tbx5 promotes limb initiation by interacting with Wnt2b and Fgf10. *Development*, 129(22):5161–5170, November 2002.

[30] Florian Witte, Janine Dokas, Franziska Neuendorf, Stefan Mundlos, and Sigmar Stricker. Comprehensive expression analysis of all Wnt genes and their major secreted antagonists during mouse limb development and cartilage differentiation. *Gene expression patterns : GEP*, 9(4):215–223, April 2009.

[31] Qiyan Mao, Haley K Stinnett, and Robert K Ho. Asymmetric cell convergence-driven zebrafish fin bud initiation and pre-pattern requires Tbx5a control of a mesenchymal Fgf signal. *Development*, 142(24):4329–4339, December 2015.

[32] Sabine Fischer, Bruce W Draper, and Carl J Neumann. The zebrafish fgf24 mutant identifies an additional level of Fgf signaling involved in vertebrate forelimb initiation. *Development*, 130(15):3515–3524, August 2003.

[33] Jerome Gros and Clifford J Tabin. Vertebrate limb bud formation is initiated by localized epithelial-to-mesenchymal transition. *Science (New York, N.Y.)*, 343(6176):1253–1256, March 2014.

[34] Laurie A Wyngaarden, Kevin M Vogeli, Brian G Ciruna, Mathew Wells, Anna-Katerina Hadjantonakis, and Sevan Hopyan. Oriented cell motility and division underlie early limb bud morphogenesis. *Development*, 137(15):2551–2558, August 2010.

[35] H Ohuchi, T Nakagawa, A Yamamoto, A Araga, T Ohata, Y Ishimaru, H Yoshioka, T Kuwana, T Nohno, M Yamasaki, N Itoh, and S Noji. The mesenchymal factor, FGF10, initiates and maintains the outgrowth of the chick limb bud through interaction with FGF8, an apical ectodermal factor. *Development (Cambridge, England)*, 124(11):2235–2244, June 1997.

[36] Rolf Zeller, Javier Lopez-Rios, and Aimée Zuniga. Vertebrate limb bud development: moving towards integrative analysis of organogenesis. *Nature reviews. Genetics*, 10(12):845–858, December 2009.

[37] Cliff Tabin and Lewis Wolpert. Rethinking the proximodistal axis of the vertebrate limb in the molecular era. *Genes & Development*, 21(12):1433–1442, June 2007.

[38] R D Riddle, R L Johnson, E Laufer, and C Tabin. Sonic hedgehog mediates the polarizing activity of the ZPA. *Cell*, 75(7):1401–1416, December 1993.

[39] Basile Tarchini, Denis Duboule, and Marie Kmita. Regulatory constraints in the evolution of the tetrapod limb anterior-posterior polarity. *Nature*, 443(7114):985–988, October 2006.

[40] Pascal te Welscher, Marian Fernandez-Teran, Marian A Ros, and Rolf Zeller. Mutual genetic antagonism involving GLI3 and dHAND prepatterns the vertebrate limb bud mesenchyme prior to SHH signaling. *Genes & development*, 16(4):421–426, February 2002.

[41] L Niswander, S Jeffrey, G R Martin, and C Tickle. A positive feedback loop coordinates growth and patterning in the vertebrate limb. *Nature*, 371(6498):609–612, October 1994.

[42] E Laufer, C E Nelson, R L Johnson, B A Morgan, and C Tabin. Sonic hedgehog and Fgf-4 act through a signaling cascade and feedback loop to integrate growth and patterning of the developing limb bud. *Cell*, 79(6):993–1003, December 1994.

[43] Amitabha Bandyopadhyay, Kunikazu Tsuji, Karen Cox, Brian D Harfe, Vicki Rosen, and Clifford J Tabin. Genetic analysis of the roles of BMP2, BMP4, and BMP7 in limb patterning and skeletogenesis. *PLoS genetics*, 2(12):e216, December 2006.

[44] Jennifer Selever, Wei Liu, Mei-Fang Lu, Richard R Behringer, and James F Martin. Bmp4 in limb bud mesoderm regulates digit pattern by controlling AER development. *Developmental biology*, 276(2):268–279, December 2004.

[45] Jean-Denis Bénazet, Mirko Bischofberger, Eva Tiecke, Alexandre Gonçalves, James F Martin, Aimée Zuniga, Felix Naef, and Rolf Zeller. A self-regulatory system of interlinked signaling feedback loops controls mouse limb patterning. *Science (New York, N.Y.)*, 323(5917):1050–1053, February 2009.

[46] K Ahn, Y Mishina, M C Hanks, R R Behringer, and E B Crenshaw. BMPR-IA signaling is required for the formation of the apical ectodermal ridge and dorsal-ventral patterning of the limb. *Development*, 128(22):4449–4461, November 2001.

[47] Jerome Gros, Jimmy Kuang-Hsien Hu, Claudio Vinegoni, Paolo Fumene Feruglio, Ralph Weissleder, and Clifford J Tabin. WNT5A/JNK and FGF/MAPK Pathways Regulate the Cellular Events Shaping the Vertebrate Limb Bud. *Current biology*, 20(22):1993–2002, November 2010.

[48] Jeffery Barrow. Wnt/planar cell polarity signaling: an important mechanism to coordinate growth and patterning in the limb. *Organogenesis*, 7(4):260–266, October 2011.

[49] Par Marie-Paule Pautou. Etablissement de l'axe dorso-ventral dans le pied de l'embryon de poulet. *Development*, 42(1):177–194, December 1977.

[50] Jeffrey A MacCabe, Janice Errick, and John W Saunders Jr. Ectodermal control of the dorsoventral axis in the leg bud of the chick embryo,. *Developmental biology*, 39(1):69–82, July 1974.

[51] B A Parr and A P McMahon. Dorsalizing signal Wnt-7a required for normal polarity of D-V and A-P axes of mouse limb. *Nature*, 374(6520):350–353, March 1995.

[52] C A Loomis, E Harris, J Michaud, W Wurst, M Hanks, and A L Joyner. The mouse Engrailed-1 gene and ventral limb patterning. *Nature*, 382(6589):360–363, July 1996.

[53] Chi-Kuang Leo Wang, Minoru Omi, Deborah Ferrari, Hsu-Chen Cheng, Gail Lizarraga, Hsian-Jean Chin, William B Upholt, Caroline N Dealy, and Robert A Kosher. Function of BMPs in the apical ectoderm of the developing mouse limb. *Developmental biology*, 269(1):109–122, May 2004.

[54] Tohru Yano, Gembu Abe, Hitoshi Yokoyama, Koichi Kawakami, and Koji Tamura. Mechanism of pectoral fin outgrowth in zebrafish development. *Development*, 139(16):2916–2925, August 2012.

[55] A Wood and P Thorogood. An analysis of in vivo cell migration during teleost fin morphogenesis. *Journal of Cell Science*, 66:205–222, March 1984.

[56] Sarah C Rothschild, Charles A Easley, Ludmila Francescatto, James A Lister, Deborah M Garrity, and Robert M Tombes. Tbx5-mediated expression of Ca(2+)/calmodulin-dependent protein kinase II is necessary for zebrafish cardiac and pectoral fin morphogenesis. *Developmental biology*, 330(1):175–184, June 2009.

[57] I Durán, M Marí-Beffa, J A Santamaría, J Becerra, and L Santos-Ruiz. Actinotrichia collagens and their role in fin formation. *Developmental biology*, 354(1):160–172, June 2011.

[58] Jing Zhang, Purva Wagh, Danielle Guay, Luis Sanchez-Pulido, Bhaja K Padhi, Vladimir Korzh, Miguel A Andrade-Navarro, and Marie-Andrée Akimenko. Loss of fish actinotrichia proteins and the fin-to-limb transition. *Nature*, 466(7303):234–237, July 2010.

[59] Wouter Masselink, Nicholas J Cole, Fruzsina Fenyes, Silke Berger, Carmen Sonntag, Alasdair Wood, Phong D Nguyen, Naomi Cohen, Franziska Knopf, Gilbert Weidinger, Thomas E Hall, and Peter D Currie. A somitic contribution to the apical ectodermal ridge is essential for fin formation. *Nature*, 535(7613):542–546, July 2016.

[60] Raymond Teck Ho Lee, Ela W Knapik, Jean Paul Thiery, and Thomas J Carney. An exclusively mesodermal origin of fin mesenchyme demonstrates that zebrafish trunk neural crest does not generate ectomesenchyme. *Development*, 140(14):dev.093534–2932, January 2013.

[61] Erika Kague, Michael Gallagher, Sally Burke, Michael Parsons, Tamara Franz-Odendaal, and Shannon Fisher. Skeletogenic fate of zebrafish cranial and trunk neural crest. *PloS one*, 7(11):e47394, 2012.

[62] Christian U Stirnimann, Denis Ptchelkine, Clemens Grimm, and Christoph W Müller. Structural basis of TBX5-DNA recognition: the T-box domain in its DNA-bound and -unbound form. *Journal of molecular biology*, 400(1):71–81, July 2010.

[63] T K Ghosh, E A Packham, A J Bonser, T E Robinson, S J Cross, and J D Brook. Characterization of the TBX5 binding site and analysis of mutations that cause Holt-Oram syndrome. *Human Molecular Genetics*, 10(18):1983–1994, September 2001.

[64] Lagnajeet Pradhan, Sunil Gopal, Shichang Li, Shayan Ashur, Saai Suryanarayanan, Hideko Kasahara, and Hyun-Joo Nam. Intermolecular Interactions of Cardiac Transcription Factors NKX2.5 and TBX5. *Biochemistry*, 55(12):1702–1710, March 2016.

[65] Y Hiroi, S Kudoh, K Monzen, Y Ikeda, Y Yazaki, R Nagai, and I Komuro. Tbx5 associates with Nkx2-5 and synergistically promotes cardiomyocyte differentiation. *Nature Genetics*, 28(3):276–280, July 2001.

[66] Vidu Garg, Irfan S Kathiriya, Robert Barnes, Marie K Schluterman, Isabelle N King, Cheryl A Butler, Caryn R Rothrock, Reenu S Eapen, Kayoko Hirayama-Yamada, Kunitaka Joo, Rumiko Matsuoka, Jonathan C Cohen, and Deepak Srivastava. GATA4 mutations cause human congenital heart defects and reveal an interaction with TBX5. *Nature*, 424(6947):443–447, July 2003.

[67] Meenakshi Maitra, Marie K Schluterman, Haley A Nichols, James A Richardson, Cecilia W Lo, Deepak Srivastava, and Vidu Garg. Interaction of Gata4 and Gata6 with

Tbx5 is critical for normal cardiac development. *Developmental biology*, 326(2):368–377, February 2009.

[68] Daniel D Brown, Shauna N Martz, Olav Binder, Sarah C Goetz, Brenda M J Price, Jim C Smith, and Frank L Conlon. Tbx5 and Tbx20 act synergistically to control vertebrate heart morphogenesis. *Development*, 132(3):553–563, February 2005.

[69] Chunbo Wang, Dongsun Cao, Qing Wang, and Da-Zhi Wang. Synergistic activation of cardiac genes by myocardin and Tbx5. *PloS one*, 6(8):e24242, 2011.

[70] Kazuko Koshiba-Takeuchi, Jun K Takeuchi, Eric P Arruda, Irfan S Kathiriya, Rong Mo, Chi-chung Hui, Deepak Srivastava, and Benoit G Bruneau. Cooperative and antagonistic interactions between Sall4 and Tbx5 pattern the mouse limb and heart. *Nature Genetics*, 38(2):175–183, February 2006.

[71] Ange Krause, William Zacharias, Troy Camarata, Barbara Linkhart, Evelyn Law, Antje Lischke, Erik Miljan, and Hans-Georg Simon. Tbx5 and Tbx4 transcription factors interact with a new chicken PDZ-LIM protein in limb and heart development. *Developmental biology*, 273(1):106–120, September 2004.

[72] Troy Camarata, Benjamin Bimber, Andre Kulisz, Teng-Leong Chew, Jennifer Yeung, and Hans-Georg Simon. LMP4 regulates Tbx5 protein subcellular localization and activity. *The Journal of cell biology*, 174(3):339–348, July 2006.

[73] Margaret P Adam, Holly H Ardinger, Roberta A Pagon, Stephanie E Wallace, Lora JH Bean, Karen Stephens, Anne Amemiya, Deborah A McDermott, Jamie C Fong, and Craig T Basson. Holt-Oram Syndrome. 1993.

[74] Ingeborg Barisic, Ljubica Boban, Ruth Greenlees, Ester Garne, Diana Wellesley, Elisa Calzolari, Marie-Claude Addor, Larraitz Arriola, Jorieke Eh Bergman, Paula Braz, Judith Ls Budd, Miriam Gatt, Martin Haeusler, Babak Khoshnood, Kari Klungsoyr, Bob McDonnell, Vera Nelen, Anna Pierini, Annette Queisser-Wahrendorf, Judith Rankin, Anke Rissmann, Catherine Rounding, David Tucker, Christine Verellen-Dumoulin, and Helen Dolk. Holt Oram syndrome: a registry-based study in Europe. *Orphanet journal of rare diseases*, 9(1):156, October 2014.

[75] Q Y Li, R A Newbury-Ecob, J A Terrett, D I Wilson, A R Curtis, C H Yi, T Gebuhr, P J Bullen, S C Robson, T Strachan, D Bonnet, S Lyonnet, I D Young, J A Raeburn, A J Buckler, D J Law, and J D Brook. Holt-Oram syndrome is caused by mutations in TBX5, a member of the Brachyury (T) gene family. *Nature Genetics*, 15(1):21–29, January 1997.

[76] C T Basson, T Huang, R C Lin, D R Bachinsky, S Weremowicz, A Vaglio, R Bruzzone, R Quadrelli, M Lerone, G Romeo, M Silengo, A Pereira, J Krieger, S F Mesquita, M Kamisago, C C Morton, M E Pierpont, C W Müller, J G Seidman, and C E Seidman. Different TBX5 interactions in heart and limb defined by Holt-Oram syndrome

mutations. *Proceedings of the National Academy of Sciences of the United States of America*, 96(6):2919–2924, March 1999.

[77] Anna-Marie E Brassington, Sandy S Sung, Reha M Toydemir, Trung Le, Amy D Roeder, Ann E Rutherford, Frank G Whitby, Lynn B Jorde, and Michael J Bamshad. Expressivity of Holt-Oram syndrome is not predicted by TBX5 genotype. *American journal of human genetics*, 73(1):74–85, July 2003.

[78] Jun K Takeuchi, Kazuko Koshiba-Takeuchi, Ken Matsumoto, Astrid Vogel-Höpker, Mayumi Naitoh-Matsuo, Keiko Ogura, Naoki Takahashi, Kunio Yasuda, and Toshihiko Ogura. Tbx5 and Tbx4 genes determine the wing/leg identity of limb buds. *Nature*, 398(6730):810–814, April 1999.

[79] Peleg Hasson, Joanne Del Buono, and Malcolm P O Logan. Tbx5 is dispensable for forelimb outgrowth. *Development*, 134(1):85–92, January 2007.

[80] Peleg Hasson, April DeLaurier, Michael Bennett, Elena Grigorieva, L A Naiche, Virginia E Papaioannou, Timothy J Mohun, and Malcolm P O Logan. Tbx4 and tbx5 acting in connective tissue are required for limb muscle and tendon patterning. *Developmental Cell*, 18(1):148–156, January 2010.

[81] Victoria E Prince and F Bryan Pickett. Splitting pairs: the diverging fates of duplicated genes. *Nature reviews. Genetics*, 3(11):827–837, November 2002.

[82] A Amores, A Force, Y L Yan, L Joly, C Amemiya, A Fritz, R K Ho, J Langeland, V Prince, Y L Wang, M Westerfield, M Ekker, and J H Postlethwait. Zebrafish hox clusters and vertebrate genome evolution. *Science (New York, N.Y.)*, 282(5394):1711–1714, November 1998.

[83] Ricard Albalat, Mireia Baquero, and Carolina Minguillon. Identification and characterisation of the developmental expression pattern of tbx5b, a novel tbx5 gene in zebrafish. *Gene expression patterns : GEP*, 10(1):24–30, January 2010.

[84] Lindsay E Parrie, Erin M Renfrew, Aimee Vander Wal, Rachel LOCKRIDGE Mueller, and Deborah M Garrity. Zebrafish tbx5 paralogs demonstrate independent essential requirements in cardiac and pectoral fin development. *Developmental Dynamics*, 242(5):485–502, May 2013.

[85] G Begemann and P W Ingham. Developmental regulation of Tbx5 in zebrafish embryogenesis. *Mechanisms of development*, 90(2):299–304, February 2000.

[86] Deborah M Garrity, Sarah Childs, and Mark C Fishman. The heartstrings mutation in zebrafish causes heart/fin Tbx5 deficiency syndrome. *Development*, 129(19):4635–4645, October 2002.

[87] Aina Pi-Roig, Enrique Martin-Blanco, and Carolina Minguillon. Distinct tissue-specific requirements for the zebrafish tbx5 genes during heart, retina and pectoral fin development. *Open biology*, 4(4):140014–140014, 2014.

[88] Hideki Innan and Fyodor Kondrashov. The evolution of gene duplications: classifying and distinguishing between models. *Nature reviews. Genetics*, 11(2):97–108, February 2010.

[89] A E Bruce, A C Oates, V E Prince, and R K Ho. Additional hox clusters in the zebrafish: divergent expression patterns belie equivalent activities of duplicate hoxB5 genes. *Evolution & development*, 3(3):127–144, May 2001.

[90] Monte Westerfield. *The Zebrafish Book*. A Guide for the Laboratory Use of Zebrafish (Danio Rerio). 2007.

[91] A Nasevicius and S C Ekker. Effective targeted gene 'knockdown' in zebrafish. *Nature Genetics*, 26(2):216–220, October 2000.

[92] Héctor Sánchez-Iranzo, María Galardi-Castilla, Carolina Minguillon, Andrés Sanz-Morejón, Juan Manuel González-Rosa, Anastasia Felker, Alexander Ernst, Gabriela Guzmán-Martínez, Christian Mosimann, and Nadia Mercader. Tbx5a lineage tracing shows cardiomyocyte plasticity during zebrafish heart regeneration. *Nature communications*, 9(1):428, January 2018.

[93] Johannes Schindelin, Ignacio Arganda-Carreras, Erwin Frise, Verena Kaynig, Mark Longair, Tobias Pietzsch, Stephan Preibisch, Curtis Rueden, Stephan Saalfeld, Benjamin Schmid, Jean-Yves Tinevez, Daniel James White, Volker Hartenstein, Kevin Eliceiri, Pavel Tomancak, and Albert Cardona. Fiji: an open-source platform for biological-image analysis. *Nature Methods*, 9(7):676–682, July 2012.

[94] Antonia Borovina, Simone Superina, Daniel Voskas, and Brian Ciruna. Vangl2 directs the posterior tilting and asymmetric localization of motile primary cilia. *Nature cell biology*, 12(4):407–412, April 2010.

[95] Hadley Wickham. *ggplot2: Elegant Graphics for Data Analysis*. Springer-Verlag New York, 2016.

[96] Zhiyin Dai, Julie M Sheridan, Linden J Gearing, Darcy L Moore, Shian Su, Sam Wormald, Stephen Wilcox, Liam O'Connor, Ross A Dickins, Marnie E Blewitt, and Matthew E Ritchie. edgeR: a versatile tool for the analysis of shRNA-seq and CRISPR-Cas9 genetic screens. *F1000Research*, 3:95, 2014.

[97] Steven D Briscoe, Caroline B Albertin, Joanna J Rowell, and Clifton W Ragsdale. Neocortical Association Cell Types in the Forebrain of Birds and Alligators. *Current biology : CB*, 28(5):686–696.e6, March 2018.

[98] Enis Afgan, Dannon Baker, Bérénice Batut, Marius van den Beek, Dave Bouvier, Martin Cech, John Chilton, Dave Clements, Nate Coraor, Björn A Grüning, Aysam Guerler, Jennifer Hillman-Jackson, Saskia Hiltemann, Vahid Jalili, Helena Rasche, Nicola Soranzo, Jeremy Goecks, James Taylor, Anton Nekrutenko, and Daniel Blankenberg. The Galaxy platform for accessible, reproducible and collaborative biomedical analyses: 2018 update. *Nucleic Acids Research*, 46(W1):W537–W544, July 2018.

[99] Ron Edgar, Michael Domrachev, and Alex E Lash. Gene Expression Omnibus: NCBI gene expression and hybridization array data repository. *Nucleic Acids Research*, 30(1):207–210, January 2002.

[100] Tessa G Montague, José M Cruz, James A Gagnon, George M Church, and Eivind Valen. CHOPCHOP: a CRISPR/Cas9 and TALEN web tool for genome editing. *Nucleic Acids Research*, 42(Web Server issue):W401–7, July 2014.

[101] Li-En Jao, Susan R Wente, and Wenbiao Chen. Efficient multiplex biallelic zebrafish genome editing using a CRISPR nuclease system. *Proceedings of the National Academy of Sciences*, 110(34):13904–13909, August 2013.

[102] James A Gagnon, Eivind Valen, Summer B Thyme, Peng Huang, Laila Ahkmetova, Andrea Pauli, Tessa G Montague, Steven Zimmerman, Constance Richter, and Alexander F Schier. Efficient Mutagenesis by Cas9 Protein-Mediated Oligonucleotide Insertion and Large-Scale Assessment of Single-Guide RNAs. *PloS one*, 9(5):e98186, May 2014.

[103] Matthew R Swift, Van N Pham, Daniel Castranova, Kameha Bell, Richard J Poole, and Brant M Weinstein. SoxF factors and Notch regulate nr2f2 gene expression during venous differentiation in zebrafish. *Developmental biology*, 390(2):116–125, June 2014.

[104] Jin Xu, Jiaxi Cui, Aranzazu Del Campo, and Chong Hyun Shin. Four and a Half LIM Domains 1b (Fhl1b) Is Essential for Regulating the Liver versus Pancreas Fate Decision and for β-Cell Regeneration. *PLoS genetics*, 12(2):e1005831, February 2016.

[105] M Walker and C B Kimmel. Kimmel Lab no acid bone & cartilage stain for larval fish, November 2009.

[106] Didier Y R Stainier, Erez Raz, Nathan D Lawson, Stephen C Ekker, Rebecca D Burdine, Judith S Eisen, Philip W Ingham, Stefan Schulte-Merker, Deborah Yelon, Brant M Weinstein, Mary C Mullins, Stephen W Wilson, Lalita Ramakrishnan, Sharon L Amacher, Stephan C F Neuhauss, Anming Meng, Naoki Mochizuki, Pertti Panula, and Cecilia B Moens. Guidelines for morpholino use in zebrafish. *PLoS genetics*, 13(10):e1007000, October 2017.

[107] Andrea Rossi, Zacharias Kontarakis, Claudia Gerri, Hendrik Nolte, Soraya Hölper, Marcus Krüger, and Didier Y R Stainier. Genetic compensation induced by deleterious mutations but not gene knockdowns. *Nature*, 524(7564):230–233, August 2015.

[108] J W SAUNDERS. The proximo-distal sequence of origin of the parts of the chick wing and the role of the ectoderm. *The Journal of experimental zoology*, 108(3):363–403, August 1948.

[109] Emanuele Pignatti, Rolf Zeller, and Aimée Zuniga. To BMP or not to BMP during vertebrate limb bud development. *Seminars in Cell & Developmental Biology*, 32:119–127, August 2014.

[110] Jeffrey D Steimle, Scott A Rankin, Christopher E Slagle, Jenna Bekeny, Ariel B Rydeen, Sunny Sun-Kin Chan, Junghun Kweon, Xinan H Yang, Kohta Ikegami, Rangarajan D Nadadur, Megan Rowton, Andrew D Hoffmann, Sonja Lazarevic, William Thomas, Erin A T Boyle Anderson, Marko E Horb, Luis Luna-Zurita, Robert K Ho, Michael Kyba, Bjarke Jensen, Aaron M Zorn, Frank L Conlon, and Ivan P Moskowitz. Evolutionarily conserved Tbx5-Wnt2/2b pathway orchestrates cardiopulmonary development. *Proceedings of the National Academy of Sciences*, 3:201811624, October 2018.

[111] Qin Pu, Ketan Patel, and Ruijin Huang. The lateral plate mesoderm: a novel source of skeletal muscle. *Results and problems in cell differentiation*, 56(Chapter 7):143–163, 2015.

[112] Jeffrey J Schoenebeck, Brian R Keegan, and Deborah Yelon. Vessel and blood specification override cardiac potential in anterior mesoderm. *Developmental cell*, 13(2):254–267, August 2007.

[113] Noelle Paffett-Lugassy, Natasha Novikov, Spencer Jeffrey, Maryline Abrial, Burcu Guner-Ataman, Srinivasan Sakthivel, Caroline E Burns, and C Geoffrey Burns. Unique developmental trajectories and genetic regulation of ventricular and outflow tract progenitors in the zebrafish second heart field. *Development (Cambridge, England)*, 144(24):4616–4624, December 2017.

[114] J N Chen, P Haffter, J Odenthal, E Vogelsang, M Brand, F J van Eeden, M Furutani-Seiki, M Granato, M Hammerschmidt, C P Heisenberg, Y J Jiang, D A Kane, R N Kelsh, M C Mullins, and C Nüsslein-Volhard. Mutations affecting the cardiovascular system and other internal organs in zebrafish. *Development*, 123:293–302, December 1996.

[115] Amy J Sehnert, Anja Huq, Brant M Weinstein, Charline Walker, Mark Fishman, and Didier Y R Stainier. Cardiac troponin T is essential in sarcomere assembly and cardiac contractility. *Nature Genetics*, 31(1):106–110, May 2002.

[116] John P Incardona, Tracy K Collier, and Nathaniel L Scholz. Defects in cardiac function precede morphological abnormalities in fish embryos exposed to polycyclic aromatic hydrocarbons. *Toxicology and applied pharmacology*, 196(2):191–205, April 2004.

[117] Charles A Goldfarb and Lindley B Wall. Holt-Oram syndrome. *The Journal of hand surgery*, 39(8):1646–1648, August 2014.

[118] J A Hurst, C M Hall, and M Baraitser. The Holt-Oram syndrome. *Journal of medical genetics*, 28(6):406–410, June 1991.

[119] Charalampos Rallis, Benoit G Bruneau, Jo Del Buono, Christine E Seidman, J G Seidman, Sahar Nissim, Clifford J Tabin, and Malcolm P O Logan. Tbx5 is required for forelimb bud formation and continued outgrowth. *Development*, 130(12):2741–2751, June 2003.

[120] Douglas G Howe, Yvonne M Bradford, Tom Conlin, Anne E Eagle, David Fashena, Ken Frazer, Jonathan Knight, Prita Mani, Ryan Martin, Sierra A Taylor Moxon, Holly Paddock, Christian Pich, Sridhar Ramachandran, Barbara J Ruef, Leyla Ruzicka, Kevin Schaper, Xiang Shao, Amy Singer, Brock Sprunger, Ceri E Van Slyke, and Monte Westerfield. ZFIN, the Zebrafish Model Organism Database: increased support for mutants and transgenics. *Nucleic Acids Research*, 41(Database issue):D854–60, January 2013.

[121] Franck Rapaport, Raya Khanin, Yupu Liang, Mono Pirun, Azra Krek, Paul Zumbo, Christopher E Mason, Nicholas D Socci, and Doron Betel. Comprehensive evaluation of differential gene expression analysis methods for RNA-seq data. *Genome Biol*, 14(9):R95, 2013.

[122] W Liao, C Y Ho, Y L Yan, J Postlethwait, and D Y Stainier. Hhex and scl function in parallel to regulate early endothelial and blood differentiation in zebrafish. *Development*, 127(20):4303–4313, October 2000.

[123] Solei Cermenati, Silvia Moleri, Simona Cimbro, Paola Corti, Luca Del Giacco, Roberta Amodeo, Elisabetta Dejana, Peter Koopman, Franco Cotelli, and Monica Beltrame. Sox18 and Sox7 play redundant roles in vascular development. *Blood*, 111(5):2657–2666, March 2008.

[124] Nathan D Lawson and Brant M Weinstein. In vivo imaging of embryonic vascular development using transgenic zebrafish. *Developmental biology*, 248(2):307–318, August 2002.

[125] C B Kimmel, W W Ballard, S R Kimmel, B Ullmann, and T F Schilling. Stages of embryonic development of the zebrafish. *Developmental Dynamics*, 203(3):253–310, July 1995.

[126] Shane P Herbert and Didier Y R Stainier. Molecular control of endothelial cell behaviour during blood vessel morphogenesis. *Nature Reviews Molecular Cell Biology*, 12(9):551–564, August 2011.

[127] Dorien M A Hermkens, Andreas van Impel, Akihiro Urasaki, Jeroen Bussmann, Henricus J Duckers, and Stefan Schulte-Merker. Sox7 controls arterial specification in conjunction with hey2 and efnb2 function. *Development*, 142(9):1695–1704, May 2015.

[128] Hélène Pendeville, Marie Winandy, Isabelle Manfroid, Olivier Nivelles, Patrick Motte, Vincent Pasque, Bernard Peers, Ingrid Struman, Joseph A Martial, and Marianne L Voz. Zebrafish Sox7 and Sox18 function together to control arterial-venous identity. *Developmental biology*, 317(2):405–416, May 2008.

[129] Sven A Lang, Dagmar Klein, Christian Moser, Andreas Gaumann, Gabriel Glockzin, Marc H Dahlke, Wolfgang Dietmaier, Ulrich Bolder, Hans J Schlitt, Edward K Geissler, and Oliver Stoeltzing. Inhibition of heat shock protein 90 impairs epidermal growth

factor-mediated signaling in gastric cancer cells and reduces tumor growth and vascularization in vivo. *Molecular cancer therapeutics*, 6(3):1123–1132, March 2007.

[130] Valentina Charlotte Jackson, Sarah Dewilde, Alessandra Giuliano Albo, Katarzyna Lis, Davide Corpillo, and Barbara Canepa. The activity of aminoacyl-tRNA synthetase-interacting multi-functional protein 1 (AIMP1) on endothelial cells is mediated by the assembly of a cytoskeletal protein complex. *Journal of cellular biochemistry*, 112(7):1857–1868, July 2011.

[131] Oscar H Ocaña, Hakan Coskun, Carolina Minguillon, Prayag Murawala, Elly M Tanaka, Joan Galcerán, Ramón Muñoz-Chápuli, and M Angela Nieto. A right-handed signalling pathway drives heart looping in vertebrates. *Nature*, 549(7670):86–90, September 2017.

[132] Qiyan Mao. *Spatial Dynamics and Regulation of the Zebrafish Limb Morphogenetic Field*. PhD thesis, University of Chicago, November 2013.

[133] Amy R Barker, Kate V McIntosh, and Helen R Dawe. Centrosome positioning in non-dividing cells. *Protoplasma*, 253(4):1007–1021, July 2016.

[134] Crystal F Davey and Cecilia B Moens. Planar cell polarity in moving cells: think globally, act locally. *Development*, 144(2):187–200, January 2017.

[135] Giuseppe Chiapparo, Xionghui Lin, Fabienne Lescroart, Samira Chabab, Catherine Paulissen, Lorenzo Pitisci, Antoine Bondue, and Cédric Blanpain. Mesp1 controls the speed, polarity, and directionality of cardiovascular progenitor migration. *The Journal of cell biology*, 213(4):463–477, May 2016.

[136] Bo Gao, Rieko Ajima, Wei Yang, Chunyu Li, Hai Song, Matthew J Anderson, Robert R Liu, Mark B Lewandoski, Terry P Yamaguchi, and Yingzi Yang. Coordinated directional outgrowth and pattern formation by integration of Wnt5a and Fgf signaling in planar cell polarity. *Development*, 145(8):dev163824, April 2018.

[137] S Lin. *Wnt5b signaling in zebrafish development and disease*. PhD thesis, University of Iowa, 2010.

[138] Michal Reichman-Fried, Sofia Minina, and Erez Raz. Autonomous modes of behavior in primordial germ cell migration. *Developmental Cell*, 6(4):589–596, April 2004.

[139] M Starz-Gaiano, N K Cho, A Forbes, and R Lehmann. Spatially restricted activity of a Drosophila lipid phosphatase guides migrating germ cells. *Development*, 128(6):983–991, March 2001.

[140] Azadeh Paksa, Jan Bandemer, Burkhard Hoeckendorf, Nitzan Razin, Katsiaryna Tarbashevich, Sofia Minina, Dana Meyen, Antonio Biundo, Sebastian A Leidel, Nadine Peyrieras, Nir S Gov, Philipp J Keller, and Erez Raz. Repulsive cues combined with physical barriers and cell-cell adhesion determine progenitor cell positioning during organogenesis. *Nature communications*, 7(1):11288, April 2016.

[141] N Zhang, J Zhang, K J Purcell, Y Cheng, and K Howard. The Drosophila protein Wunen repels migrating germ cells. *Nature*, 385(6611):64–67, January 1997.

[142] Takuya Sakaguchi, Yutaka Kikuchi, Atsushi Kuroiwa, Hiroyuki Takeda, and Didier Y R Stainier. The yolk syncytial layer regulates myocardial migration by influencing extracellular matrix assembly in zebrafish. *Development*, 133(20):4063–4072, October 2006.

[143] Hajime Fukui, Kenta Terai, Hiroyuki Nakajima, Ayano Chiba, Shigetomo Fukuhara, and Naoki Mochizuki. S1P-Yap1 signaling regulates endoderm formation required for cardiac precursor cell migration in zebrafish. *Developmental Cell*, 31(1):128–136, October 2014.

[144] Nikolay Popgeorgiev, Benjamin Bonneau, Karine F Ferri, Julien Prudent, Julien Thibaut, and Germain Gillet. The apoptotic regulator Nrz controls cytoskeletal dynamics via the regulation of Ca2+ trafficking in the zebrafish blastula. *Developmental Cell*, 20(5):663–676, May 2011.

[145] Imogen A Hurley, Jean-Luc Scemama, and Victoria E Prince. Consequences of hoxb1 duplication in teleost fish. *Evolution & development*, 9(6):540–554, November 2007.

[146] Noritaka Adachi, Molly Robinson, Aden Goolsbee, and Neil H Shubin. Regulatory evolution of Tbx5 and the origin of paired appendages. *Proceedings of the National Academy of Sciences*, 113(36):10115–10120, September 2016.

[147] Thomas J Cunningham, Joseph J Lancman, Marie Berenguer, P Duc Si Dong, and Gregg Duester. Genomic Knockout of Two Presumed Forelimb Tbx5 Enhancers Reveals They Are Nonessential for Limb Development. *CellReports*, 23(11):3146–3151, June 2018.

[148] J Ablain and L I Zon. Tissue-specific gene targeting using CRISPR/Cas9. *Methods in cell biology*, 135:189–202, 2016.

[149] Daniel R Zerbino, Premanand Achuthan, Wasiu Akanni, M Ridwan Amode, Daniel Barrell, Jyothish Bhai, Konstantinos Billis, Carla Cummins, Astrid Gall, Carlos García Girón, Laurent Gil, Leo Gordon, Leanne Haggerty, Erin Haskell, Thibaut Hourlier, Osagie G Izuogu, Sophie H Janacek, Thomas Juettemann, Jimmy Kiang To, Matthew R Laird, Ilias Lavidas, Zhicheng Liu, Jane E Loveland, Thomas Maurel, William McLaren, Benjamin Moore, Jonathan Mudge, Daniel N Murphy, Victoria Newman, Michael Nuhn, Denye Ogeh, Chuang Kee Ong, Anne Parker, Mateus Patricio, Harpreet Singh Riat, Helen Schuilenburg, Dan Sheppard, Helen Sparrow, Kieron Taylor, Anja Thormann, Alessandro Vullo, Brandon Walts, Amonida Zadissa, Adam Frankish, Sarah E Hunt, Myrto Kostadima, Nicholas Langridge, Fergal J Martin, Matthieu Muffato, Emily Perry, Magali Ruffier, Dan M Staines, Stephen J Trevanion, Bronwen L Aken, Fiona Cunningham, Andrew Yates, and Paul Flicek. Ensembl 2018. *Nucleic Acids Research*, 46(D1):D754–D761, January 2018.

[150] Anita Collavoli, Cathy J Hatcher, Jie He, Daniel Okin, Rahul Deo, and Craig T Basson. TBX5 nuclear localization is mediated by dual cooperative intramolecular signals. *Journal of molecular and cellular cardiology*, 35(10):1191–1195, October 2003.

[151] Tushar K Ghosh, José J Aparicio-Sánchez, Sarah Buxton, Ami Ketley, Tasabeeh Mohamed, Catrin S Rutland, Siobhan Loughna, and J David Brook. Acetylation of TBX5 by KAT2B and KAT2A regulates heart and limb development. *Journal of molecular and cellular cardiology*, 114:185–198, November 2017.

[152] J D Steimle and I P Moskowitz. TBX5: A Key Regulator of Heart Development. *Current topics in developmental biology*, 122:195–221, 2017.

[153] Luis Luna-Zurita, Christian U Stirnimann, Sebastian Glatt, Bogac L Kaynak, Sean Thomas, Florence Baudin, Md Abul Hassan Samee, Daniel He, Eric M Small, Maria Mileikovsky, Andras Nagy, Alisha K Holloway, Katherine S Pollard, Christoph W Müller, and Benoit G Bruneau. Complex Interdependence Regulates Heterotypic Transcription Factor Distribution and Coordinates Cardiogenesis. *Cell*, 164(5):999–1014, February 2016.

[154] Lauren Waldron, Jeffrey D Steimle, Todd M Greco, Nicholas C Gomez, Kerry M Dorr, Junghun Kweon, Brenda Temple, Xinan Holly Yang, Caralynn M Wilczewski, Ian J Davis, Ileana M Cristea, Ivan P Moskowitz, and Frank L Conlon. The Cardiac TBX5 Interactome Reveals a Chromatin Remodeling Network Essential for Cardiac Septation. *Developmental Cell*, 36(3):262–275, February 2016.